The fire regimes of the Brazilian Cerrado under large-scale agricultural expansion and climate change

A thesis presented for the degree of Doctor of Philosophy

School of Geography and the Environment

University of Oxford

Carlota Segura García

St Catherine's College

Supervised by Dr Imma Oliveras Menor

Trinity 2024

I dedicate this thesis to my grandmothers, Chati and Josefina,
who encouraged me to explore the world further,
blurring the boundaries they had to endure.

Acknowledgements

First and foremost, I would like to thank my supervisor Imma Oliveras Menor. Imma, thank you so much for being so enthusiastic about this thesis from the very first email I sent you back in 2018. I am immensely grateful for your guidance throughout these years, and for the positivity you have always shown towards my work. Thank you for giving me the freedom to explore ideas and for all the opportunities that you have offered me. I am particularly thankful for your support through personal difficulties and during Covid-19. The Oxford-Montpellier supervision was never a problem, instead you managed to make it a great opportunity for me to grow as a scientist. *Moltes gràcies!!*

Special thanks to Ane Alencar, Vera L. S. Arruda, Wallace Silva, Dhemerson Conciani and the rest of the science team at the Insituto de Pesquisa Amazônica for welcoming me to Brasília and for showing me the Chapada dos Veadeiros, where I met the Cerrado and its fires. I am also immensely grateful to David Bauman, thank you for generously offering your time and for encouraging me to take the statistical analyses of this thesis a few steps further, they certainly enriched this thesis. Finally, I would also like to thank my collaborators, Matthew Jones, Sander Veraverbeke and Renata Libonati, for readily sharing the data that enabled the last chapter of this thesis. And, along with them, Thomas Janssen, Guilherme Mataveli and Lucas Menezes, thank you all for your keen interest in the project and all the useful insights you provided.

It has been an immense pleasure to be part of the DISturbance eCOlogy (DISCOLab) research group, such an encouraging environment to share experiences and develop academically. To Manoela Machado, Paco Navarro-Rosales, Gian Luca Spadoni, and Tash Lutz, thank you so much for your support, advice, friendship and all the fun. During these years, I have always enjoyed my visits to the AMAP research group in Montpellier, where I was warmly welcomed and always had a really attentive audience. And special thanks to Prof. Maria Antonia Carniello, Wesley Jonatar, Janeide and all the field assistants for guiding me on my first fieldtrip to Serra das Araras and generously sharing their love for, and knowledge about, the Cerrado.

I am immensely grateful to have been a member of the Oxford Ecosystems Lab, a vibrant community of scientists from whom I have learned a great deal and with whom I have so enjoyed my time at Oxford. To Yadvinder Malhi, for welcoming me to his research group, I never felt like I was missing a scientific community during Covid-19 or when my supervisor moved to a new position, and I am really grateful. I would like to thank Jesús Aguirre-Gutiérrez, Nikki Stevens, Erika Berenguer, Felipe Martello, Milton Bar-

bosa, Eleanor Thomson and Sruthi Krishna Moorthy for sharing with me their advice and experience to navigate the academic world. To my fellow PhD students, Renata Maia, Kendall Jefferys, Jed Soleiman, Xiongjie Deng, and Kerry-Anne Grey, it's been great to have such friendly and kind company in our gloomy mezzanine. Finally, special thanks to my dear 'during-covid' PhD friends, Tina Christmann, Trisha Gopalakrishna, Laura Picot, and Huanyuan Zhang-Zheng. It was marvelous to have such a supportive group to lean on. It's been wonderful to see you all get through to the end of your PhDs and then embarking in new exciting projects. Way to go!

To all my friends and colleagues at the Environmental Change Institute, I do cherish all the good moments and the affection you showed me during the last months of this thesis. Special thanks to Fred Thomas, acting rubber duck debugger, for his advice to speed up my code and showing me the *parquet* file format, it revolutionised the timings of this thesis.

Among other things, this thesis has been a journey out of depression. A heck of a journey of there and back again. This journey, and therefore this thesis, would not have been possible without my various families and a good bunch of good friends. The *tortuga* people, Blas, Leo, Rodri and Santi. You rescued me from my sinking ship offering a sweet and caring friendship filled with fun programming sessions, quesadillas, facturitas, mezcal and tequila, *muchas gracias chachos*. To the inhabitants of 11 Leander Way through the ages, Sofia, Manu, Isma, Giulia, Claire, Paola and Sapphô the Parisian cat. Your many creative talents and hobbies have made this journey more enjoyable and fun. Thank you so much for putting up with me, cheering me up, celebrating, dancing and eating. Joris, I am so lucky we met again in Oxford, that I could enjoy your friendship and we could drown our sorrows in tea. To Fabián, you were there during the toughest moments, lovingly holding my hand tight. For this and for all the fun and love, for all the things I learnt with you, I am forever grateful. Thank you to my dear friends in Oxford, Rocey, Fernando, Emilia, Rolland, Mark, Michael, Catherine... and the ones in London, Edgar, Vicky, Sergio, Sofia, Magda, Elena, Zahra, Jazmín - and so many others. In the blink of an eye it seems, but the journeys we've all been through!! My friends in Barcelona, thanks for hanging on there with me. I'm coming back, can't wait to see you more often.

Finally, huge thanks to my parents, for you have always supported me, even when you were puzzled by my choices and did not fully understand what all the fuss was about. To you and to all my family, thank you so much for all your love and encouragement, for always being there. To Guille and Lucas, can't wait to have you so close again and go see you play hockey.

Special thanks to my psychologist, thank you for giving me your hand softly and firmly at the same time. It has been wonderful to have your guiding advice and active listening, and I have learned so much. *Gràcies!*

Last but not least, this thesis was written in Python and R, using QGIS and Inkscape, and abusing Stack Exchange and others. All of the data used in this thesis was open to the public, or will be made open to the public as much as it is possible. I owe a great deal to open data and open software. Many thanks to the community of people around the world who put their time and effort in developing and improving resources and the programming skills of others without necessarily being economically rewarded - you are a stepping stone of Science.

Funding acknowledgements

This thesis would not have been possible without the financial support from the Environmental Research DTP (award NE/S007474/1) and the UK Natural Environment Research Council. I would also like to thank the Environmental Change Institute and St Catherine's College for funding part of my attendance to conferences and workshops. Finally, I would like to thank St Catherine's College and the Leatherseller's Company for partially funding three of my years at the University of Oxford.

Abstract

Over the past few decades, the Brazilian Cerrado has experienced profound changes as a consequence of rapid large-scale agricultural expansion and climate change. These processes, coupled with inadequate fire management policies, are altering the fire regimes of these neotropical savannas. In this region of fire-adapted ecosystems, with unique species and extraordinary biodiversity, changes in the patterns of fire could result in ecosystem degradation and irreversible transformations of the native vegetation.

In this context, understanding how fire occurs in different areas of the Cerrado, how it has changed over time, and how these patterns are affected by humans and the climate, is essential to identify the challenges the Cerrado faces, and to design landscape and fire management strategies that are effective at conserving the unique ecosystems and heterogeneity of this region. This thesis aims to contribute to such understanding by studying in detail different aspects of the Cerrado's fire regimes that remain as major outstanding questions in the literature. This thesis has three objectives, each of which are addressed through a research article.

In **Chapter 3 (Research Paper 1)**, titled *'Human land occupation regulates the effects of the climate on the burned area of the Brazilian Cerrado'*, the objective was to determine how land use area and the climate interact to affect the burned area of the Cerrado's native vegetation. To address this objective, we used geospatial data on burned area, land use categories and various climatic variables covering the period 1985 to 2020, summarised to a 0.2^{o} grid covering the whole Cerrado. Using a causal inference framework to design statistical models, this work found that, first, a larger anthropic land use area in the landscape reduces the proportion of Cerrado native vegetation that burns. Further, we showed that landscapes dominated by human land uses ($\geq$40% land use area) limit the responsiveness of burned area to climatic effects. Therefore, hotter and drier climatic conditions cause noticeable increases in burned area only in the least converted landscapes. Finally, we showed that changes in burned area over the study period took place in those regions of the Cerrado that were mostly unconverted in 1985. In these regions, agricultural expansion caused reductions in burned area over time, while increases in

burned area in relation to climate change took place in those areas of the Cerrado that remained more intact.

The objective of **Chapter 4 (Research Paper 2)**, titled *'The fire regimes of the Brazilian Cerrado and their changes through time'*, was to explore the geographical variation in the patterns of fire across the Cerrado, their temporal evolution, and their relation to the climate and human activities. Based again on geospatial burned area data and a 30 km grid cell over the Cerrado, this study used a spatially constrained hierarchical clustering algorithm to identify the different regions of the Cerrado presenting different fire regimes in four consecutive 9-year periods between 1985 and 2020. Focusing on the first (1985-1993) and last (2012-2020) periods, we found that there were considerable differences in the number and geographical limits of the regions identified in each period, with the exception of a region in the north of the Cerrado that was identified in both periods. In addition, in both periods the overall factor differentiating the fire regime regions was their level of fire activity, with some regions presenting large, frequent and numerous fires, while other regions presented intermediate and low levels of these fire characteristics. Further, over time, some regions increased or maintained high levels of fire activity, while other regions experienced striking reductions in their fire activity. Finally, results showed that the level of fire activity was inversely related to the level of human activities in the landscape, and directly related to climatic flammability conditions.

Finally, the objective of **Chapter 5 (Research Paper 3)**, titled *'Decoupling natural and human-caused fires in the Brazilian Cerrado'*, was to investigate the contribution of lightning and human-ignited fires to the Cerrado's patterns of fire, and compare the fire regimes created by each type of ignition. In this last study, we used a well-established ignition attribution method to identify those fires most likely caused by lightning and by humans. This study found that, between 2019 and 2023, 7.5% (95% confidence interval, CI, [6.7, 8.3]%) of fires were ignited by lightning, 89.1% (95% CI, [86.9, 91.3]%) were ignited by humans, and 3.4% (95% CI, [2.7, 4.1]%) did not have a clear ignition cause. Further, humans were the main cause of fire across the Cerrado, particularly in the regions with larger remnants of native vegetation. In addition, results showed that humans extend three-fold the fire season by creating ignitions throughout the dry season, while lightning-ignited fires were concentrated in the transition period from the

dry to the wet seasons. In addition, we found that humans tend to start fires in more flammable conditions than lightning, even when comparing fires occurring in the same month. Finally, we also found humans to cause the most extreme fires observed in this period, about one order of magnitude larger or two times more intense than the most extreme lightning-caused fires. Still, a small but relevant fraction of fires were ignited by lightning, and this type of ignition also caused large and intense fires, even if less so than the human-caused counterparts.

In this thesis, we conclude that humans are the main factor shaping the current fire regimes of the Brazilian Cerrado, both modifying the fuel continuity in relation to land use activities, and through the patterns of fire ignition. Particularly remarkable are the human controls on fire through land use area that limit both fire activity and its responsiveness to climatic effects. In addition, this thesis highlights the opposing directions of change in fire activity undergoing different areas of the Cerrado, both directly related to human activities: agricultural expansion brings about decreases in fire activity, while human ignitions during the dry season may be coupling with climate change giving rise to intensified fire activity in the largest remnants of native vegetation. Finally, this thesis also presents a range of innovative methodologies to harness the possibilities offered by the increasing wealth of data products describing different Earth system factors and processes, particularly satellite-derived datasets.

Table of Contents

Acknowledgements **i**

Abstract **ii**

Table of Contents **v**

List of Figures **x**

List of Abbreviations **xxi**

1 Introduction **1**

1.1 Thesis rationale 1

1.1.1 The changing fire regimes of tropical savannas and grasslands, a general perspective 1

1.1.2 The Brazilian Cerrado as a case study 3

1.1.3 Knowledge gaps 6

1.2 Thesis aims and objectives 8

1.3 Thesis structure 9

1.4 References 11

2 Literature Review **17**

2.1 The Brazilian Cerrado 17

2.1.1 Brief overview of the evolution of the Cerrado in the Holocene (since circa 12,000 yrs BP) 20

2.1.2 Recent patterns of land use expansion 23

2.1.3 Current climate 25

2.1.4 Current vegetation 26
2.1.5 Fire 29
2.2 On humans and the climate as main drivers of the burned area of tropical savannas 34
2.3 On the quantification of fire regimes and their changes through time . . . 37
2.4 On the causes of fire ignitions and their associated fire regimes 40
2.5 Satellite remote sensing and ancillary data products to study large-scale dynamics of fire 43
2.5.1 Burned area products 44
2.5.2 Mapping individual fire events 47
2.5.3 Other ancillary data products 48
2.6 References 57

3 Human land occupation regulates the effect of the climate on the burned area of the Brazilian Cerrado (Research Paper 1) 69
3.1 Abstract 71
3.2 Introduction 71
3.3 Results 74
3.3.1 Limited burned natural area in human-dominated landscapes . . . 74
3.3.2 Climate effects on burned natural area are conditional on human landscape dominance 75
3.3.3 Trends in burned natural area, climate change and anthropic expansion 78
3.4 Discussion 81
3.5 Methods 84
3.5.1 Study area 84
3.5.2 Land use data 85
3.5.3 Burned area data 86
3.5.4 Climate reanalysis data 86
3.5.5 Protected area data 87

3.5.6 Data analysis . . . 87
3.6 Data availability . . . 95
3.7 Code availability . . . 95
3.8 Acknowledgements . . . 95
3.9 Author contributions . . . 96
3.10 References . . . 96
3.11 Supplementary Information . . . 101
3.11.1 Supplementary Methods . . . 101
3.11.2 Supplementary Figures . . . 110
3.12 Supplementary Information References . . . 124

4 The fire regimes of the Brazilian Cerrado and their changes through time (Research Paper 2) 125

4.1 Abstract . . . 126
4.2 Introduction . . . 126
4.3 Methods . . . 129
4.3.1 Study area . . . 129
4.3.2 Data sources and processing . . . 130
4.3.3 Analysis . . . 134
4.4 Results . . . 137
4.4.1 The fire regime regions of the Cerrado . . . 137
4.4.2 Environmental characteristics of the fire regime regions . . . 141
4.4.3 Changes of fire regime regions over time . . . 145
4.5 Discussion . . . 148
4.6 Conclusion . . . 155
4.7 Data and code availability statement . . . 156
4.8 Acknowledgements . . . 156
4.9 References . . . 156
4.10 Supplementary Information . . . 163

5 Decoupling natural and human-caused fires in the Brazilian Cerrado (Research Paper 3) 179

5.1 Abstract . . . 180
5.2 Introduction . . . 181
5.3 Methods . . . 184
5.3.1 The study area . . . 184
5.3.2 Data sources . . . 185
5.3.3 Data analysis . . . 189
5.4 Results . . . 196
5.4.1 Quantifying lightning fires . . . 196
5.4.2 Spatial patterns of lightning-caused and human-caused fires across the Cerrado . . . 198
5.4.3 The spatiotemporal patterns of lightning . . . 200
5.4.4 The fire frequencies of lightning and human-caused fires . . . 202
5.4.5 Comparing weather conditions and landscape characteristics . . . 203
5.4.6 Comparing fire behaviour in relation to ignition cause . . . 204
5.5 Discussion . . . 205
5.6 Conclusions . . . 212
5.7 Data and code availability statement . . . 213
5.8 Acknowledgements . . . 213
5.9 References . . . 214
5.10 Supplementary Information . . . 221

6 Synthesis and Conclusions 229

6.1 Summary of key findings . . . 229
6.1.1 Objective 1: Determine how land use area and the climate interact to affect the burned area of the Cerrado . . . 229
6.1.2 Objective 2: Characterising the fire regime regions of the Cerrado and their changes through time . . . 231

6.1.3 Objective 3: Quantifying and comparing the fire regimes ignited by lightning and humans 232
6.2 Thesis synthesis and conclusions 234
6.3 Future research directions 239
6.4 References 243

List of Figures

2.1 The location and limits of the Cerrado used in this thesis, defined by the Instituto Brasileiro de Geografia e Estatística (IBGE, Brazil's Geography and Statistics Institute) in 2019. Colours represent the different land use and land cover categories identified by the MapBiomas project (Collection 8.0 (Souza et al., 2020)). Black lines represent the different ecoregions of the Cerrado (Sano et al., 2019), identified with numbers: 1, Alto Parnaíba; 2, Alto São Francisco; 3, Araguaia Tocantins; 4, Bananal; 5, Basaltos do Paraná; 6, Bico do Papagaio; 7, Centro-norte Piauiense; 8, Chapada dos Parecis; 9, Chapadão do São Francisco; 10, Complexo Bodoquena; 11, Costeiro; 12, Depressão Cárstica do São Francisco; 13, Depressão Cuiabana; 14, Floresta de Cocais; 15, Jequitinhonha; 16, Paracatu; 17, Paraná Guimarães; 18, Parnaguá; 19, Planalto Central; 20, Vão do Paranã. Source: Silva Arruda et al. (2024). 19

2.2 The different vegetation physiognomies of the Cerrado. Adapted from Ferreira et al. (2023), in turn adapted from Ribeiro et al. (2008). 26

2.3 **a** Average annual burned area and, **b** trends in burned area between 1998 and 2015. Maps showing the highest levels of burned area in tropical savannas and grasslands, as well as decreases in burned area in some of these savannas (e.g. in the African northern hemisphere). Maps derived using data from the Global Fire Emissions Database version 4 (Werf et al., 2017). Source: Andela et al. (2017). . 35

2.4 Distribution of different fire regimes at a global scale by a pioneering study mapping fire regimes using a clustering algorithm (Archibald et al., 2013). The map highlights five different fire regimes depending on the characteristics of the fires in each 0.5º grid cell in the period 1997 to 2010. Classification used data from the Global Fire Emissions Database version 3.1 (Werf et al., 2017), and the Moderate-resolution Imaging Spectroradiometer (MODIS) MCD45A1 (Araújo et al., 2015). The names of the fire regimes indicate their main characteristics: FIL, frequent-intense-large fires; FCS, frequent-cool-small fires; RIL, rare-intense-large fires; RCS, rare-cool-small fires; ICS, intermediate-cool-small fires. Source: Archibald et al. (2013). 38

3.1 **Posterior distributions of the covariate slopes from multilevel regression models M2 and M3.** These models use a focal climatic variable of interest as predictor to explain percentage of burned natural area, while allowing the climate effect (x-axis) to vary by decile of anthropic area percentage (y-axis). Predictor variables: **a** temperature, **b** vapour pressure deficit (VPD), **c** same year dry season precipitation, and **d** previous-year total precipitation. As calculated, natural area percentage and anthropic area percentage add to 100%. Green shaded areas indicate the regions of the posterior distributions falling outside the 90% HPDI, which we use as credibility interval. Red dashed lines are drawn as a reference to indicate whether 0 (i.e. no clear effect) is a likely outcome of the posterior distributions. 76

3.2 **Spatial distribution of the trends in time (slope coefficients) obtained from model M4 for each cell in a 0.2º grid over the Cerrado using the year as the predictor over the period 1985-2020.** Trends for **a** burned natural area percentage, **b** anthropic area percentage, and **c** temperature. Grey indicates cells with no evidence of clear trends - the 95% HPDI encompasses 0. 78

3.3 **Predicted temporal trends in burned natural area (tBA) from model M5 for those cells that were mostly intact in 1985, with 0 - 20% of anthropic area (80 - 100% of natural area).** These predictions are generated by fixing one predictor and exploring the effects of varying the other. **a** The effects of trends in temperature (tT) on tBA for two fixed values of trends in anthropic area (tA) corresponding to the 10th percentile (0.00 % year^{-1}) and 90th percentile (1.36 % year^{-1}, or 48.96 % in the period) of the range of tA values observed in this group of cells. **b** The effects of tA after fixing tT at the 10th (0.027 ºC year $^{-1}$, or 0.97 ºC in the period) and 90th (0.039 ºC year $^{-1}$, or 1.40 ºC in the period) percentiles of its observed data values for this group of cells. Grey shaded areas correspond to the 80% HPDI. 79

4.1 Fire regime regions obtained for (a) the first period (1985-1993) and (c) the last period (2012-2020) corresponding to the different clusters identified by the spatially constrained clustering algorithm performed on a 30 km grid over the Cerrado. Plots (b) and (d) present, for each period respectively, the first two axes (PC1_fire and PC2_fire) resulting from the Principal Component Analysis performed on the six fire variables (PCA_fire): the median and 99th percentile fire sizes, the burned area and the number of fires, the 99th percentile of the fire frequency distribution, and the median (peak) of the fire season. Each point in the PCAs represents a 30 km grid cell in the period coloured depending on the fire regime region it was classified into. Overall, in both periods, the PC1_fire captures a gradient of fire activity (see Results) and the fire regime regions appear ordered along this axis. In the first period, five different fire regime regions were identified: one in the north characterised by small numerous fires and a later peak of the fire season (LS_P1), a region in the centre-west with comparatively higher fire activity (HFA_P1), another region in the centre-east with intermediate fire activity (IFA_P1), and two regions with lower fire activity, one in the south (sLFA_P1) and another one in the western-most tip of the Cerrado (wLFA_P1). In the fourth and last period, three regions were identified: one in the north presenting a later peak of the fire season (LS_P4), one in the centre with higher fire activity (HFA_P4), and another one in the south with comparatively lower fire activity (LFA_P4). Note that even though the same colour scheme was used in both periods to denote analogous fire regime regions, neither the geographical limits nor the overall fire characteristics of the equally-coloured fire regime regions between periods are necessarily the same. 138

4.2 The two major axes of variation obtained from the PCA performed on each set of explanatory variables, anthropic and climatic variables. The anthropic variables (PCA_anth) used in the first (a) and last periods (b) were anthropic area percentage, livestock density, population density, and change in anthropic area percentage within the period. The climatic variables (PCA_clim) used in the first (c) and last (d) periods were the total annual precipitation, total precipitation in the dry season, average temperature in the dry season, and peak of the dry season. Points represent a 30 km grid cell in the corresponding period coloured according to the fire regime region they were classified into (see Figure 4.1). Note that even though the same colour scheme was used in both periods to denote analogous fire regime regions, neither the geographical limits nor the overall nor the fire, anthropic or climatic characteristics of the equally-coloured fire regime regions are necessarily the same. 142

4.3 Relation between the first component of the PCA performed on the anthropic variables (PC1_anth), (a) and (b) in the first and last periods respectively, or the climatic variables (PC1_clim), (c) and (d) in each period respectively, and the first component of the PCA performed on the fire variables (PC1_fire). PC1_fire in each period represents a gradient of increase in burned area, frequency, and the size and number of fires (Figure 4.1 a, Supplementary Information, Table S1), capturing a gradient of fire activity. PC1_anth in both periods represents a gradient of increase in anthropic area, population and livestock density (Figures 4.2 a and b, Supplementary Information, Table S4), that is, an increase in the presence of human activities and land use area in the landscape. Finally, PC1_clim represents a gradient of flammability conditions, with an increase in dry season temperature and in annual precipitation (contributing to vegetation growth (Krawchuk et al., 2011; Pausas et al., 2013)), and a decrease in dry season precipitation, when most fires occur (Silva et al., 2019) (Figures 4.2 c and d, Supplementary Information, Table S6). Points represent a 30 km grid cell in the corresponding period coloured according to the fire regime region they were classified into (see Figure 4.1). Note that even though the same colour scheme was used in both periods to denote analogous fire regime regions, neither the geographical limits, nor the fire, anthropic or climatic characteristics of the equally-coloured fire regime regions are necessarily the same. 143

4.4 Bivariate maps showing the PCA_fire coordinates of each 30 km grid cell in the first and last periods projected on the PCA_fire-space obtained for the first period PCA_fire. Map (a) shows the PCA_fire scores directly obtained from the fire variables in the first period (1985-1993). Map (b) shows the projection of the fire variables of the last period (2012-2020) on the PCA_fire-space of the first period. In this manner, the fire regimes (6-dimensional) are summarised into two dimensions, and the values of the grid cells in each period can be compared. PC1_fire (x-axis of the colour map) represents an increase in fire activity (larger burned area, frequency, and larger fire sizes) from white to blue, while PC2_fire (y-axis) represents the direction of a later fire season, an increase in the number of fires and a decrease in median fire size from white to yellow. 145

4.5 Relation between PC1_fire obtained in the first period, 1985-1993, (x-axis), and the projection of PC1_fire obtained for the last period, 2012-2020, projected on the PCA_fire of the first period (y-axis). (a) subset of 30 km grid cells classified into the northern fire regime region in the last period with small numerous fires and a later peak of the fire season, LS_P4; (b) subset of grid cells classified into the high fire activity region of the last period, in the centre of the Cerrado, HFA_P4; and (c) cells classified into the lower fire activity region of the last period, in the south, LFA_P4. Points represent 30 km grid cells and are coloured depending on the fire regime region they were classified into in the first period if they present clear trends in time in PC1_fire (with 80% confidence interval), or coloured in grey if they do not present clear trends in time. The dashed black lines represent the one-on-one correspondence between PC1_fire in the first period and the projection of PC1_fire in the last. Thus, points above the dashed black line represent an increase in fire activity over time, while data points below the line represent a decrease. Dashed gray lines represent the 0 values of PC1_fire and are included for reference. 146
4.6 Trends in time (slope coefficients) obtained by fitting a linear regression (using Ordinary Least Squares) to the time series of each of the six fire variables, for each 30 km grid cell over the Cerrado. Plots show the median fire size (a), the 99th percentile fire size (b), burned area (c), the number of fires (d), and the median fire season (f). The time series for these five variables comprised the annual values for each year in the period 1985-2020. The time series for the 99th percentile of the fire frequency distribution (e) comprised the frequency value in each of the four periods, since this value expresses the largest number of times the pixels in a cell burned in 9 years. Pink indicates decreases in the fire variable over time, green indicates increases, and grey indicates no clear trends in time with 80% confidence interval. 147
S4.1 Bayesian Information Criteria index calculated for each clustering solution with an increasing number of clusters between 2 and 25 for the first (a) and last (b) periods. 163
S4.2 Distribution of each of the six fire variables for each fire regime region in the first (1985-1993, shaded in blue) and last (2012-2020, shaded in orange) periods. Plots show the median fire size (a), the 99th percentile fire size (b), the burned area (c), the number of fires (d), the 99th percentile fire frequency (e), and median fire season (f), expressed in months. 164
S4.3 Distribution of each anthropic variable for each fire regime region in the first (1985-1993, shaded in blue) and last (2012-2020, shaded in orange) periods. Plots show the anthropic area percentage (a), the change in anthropic area percentage within the period (b), the patch density (c), the population density (d), and the livestock density (e). 165

S4.4 Distribution of each climatic variable for each fire regime region in the first (1985-1993, shaded in blue) and last (2012-2020, shaded in orange) periods. Plots show the mean annual precipitation (a), mean annual temperature (b), dry-season length (c), precipitation in the dry season (d), the mean annual temperature in the dry season (e), and the peak of the dry season (f). 166
S4.5 Distribution of the percentage area covered by different vegetation and land use categories (as per MapBiomas Collection 8.0 categories, see Methods) for each fire regime region in the first (1985-1993, shaded in blue) and last (2012-2020, shaded in orange) periods. Plots show savanna (a), forest (b), grassland (c), wetland (seasonally flooded savanna) (d), pasture (e), and cropland (f) land use categories. 167
S4.6 Results of the redundancy analysis (RDA) performed using each set of anthropic (top row) and climatic parameters (bottom row) as explanatory variables and the six fire characteristics as response variables, for the first (1985-1993, left column) and last (2012-2020, right column) periods. The anthropic variables comprise anthropic area percentage, livestock density, population density, and change in anthropic area percentage within the period. The climatic variables comprise the total annual precipitation, total precipitation in the dry season, mean temperature in the dry season and the peak of the dry season. The projection used to represent the RDA results is such that the angles between the explanatory and response variables represent the correlation between the variables. The data points are projected in the space of the response variables and coloured according to the fire regime region they were classified in for each period (see Methods). Note that even though the same colour scheme was used in both periods to denote analogous fire regime regions, neither the geographical limits, nor the fire, anthropic or climatic characteristics of the equally-coloured fire regime regions are necessarily the same. All variables in all cases had a p-value < 0.001. 168
S4.7 Trends in time (slope coefficients) over the four 9-year periods of fire activity (see Methods) for each 30 km grid cell in the Cerrado. The time series of fire activity comprised the PC1_fire values for each period projected on the PCA_fire space of the first period (see main, Figure 1) so that these consecutive values are comparable. The time series was calculated as a linear regression and fitted using Ordinary Least Squares. Pink indicates decreases in fire activity over time, green indicates increases, and grey indicates no clear trends in time with 80% confidence interval. 169
S4.8 Maps showing the fire regime regions identified by the spatially constrained hierarchical algorithm (see Methods) accompanied by plots of the two main axes of variation of the PCA_fire for the period 1985-1993 (a-b), 1994-2002 (c-d), 2003-2011 (e-f), and 2012-2020 (g-h). Percentage values indicate the explanatory power of each PCA axis. 170

S4.9 Maps (a and c) showing the alternative fire regime regions obtained in the first and last periods respectively when the peak of the fire season is not included as a fire variable when running the spatially constrained clustering algorithm. Figures (b) and (d) show the first two axes of the PCA_fire used to classify the grid cells. These maps and PCAs were generated to explore whether regions LS_P1 and LS_P4 in each period would present any distinct characteristic in addition to the later peak of the fire season, and would hence be delineated when running the clustering algorithm without this variable. In this case, the Bayesian Information Criteria (BIC) suggests that four regions in the first period and two regions in the last period are the clustering solutions optimising data partition. In the first period, the four-clusters solution does identify a region equivalent to LS_P1, confirming the distinct fire regime of this region compared to HFA_P1 (and its $HFA_P1_{alt.}$ equivalent alternative), with an overall lower fire activity and overall small and numerous fires. In the last period, the equivalent LS_P4 region is not identified in the two-cluster solution suggested by the BIC, suggesting that the increases in fire activity experienced by this area over time resulted in fire regimes closer to those of region HFA_P4 (and its $HFA_P4_{alt.}$ equivalent). Nevertheless, this northern area is identified in the four-clusters solution for the last period when leaving the peak of the fire season out (outlined in green in c and d, $LS_P4_{alt.}$), suggesting this area presents characteristics relevant to data classification. Moreover, despite the fire characteristics of the northern region being closer to those of $HFA_P4_{alt.}$, we can observe these cells are still clearly clustered in the PCA_fire with numerous and medium-sized fires. 171

S4.10 Map showing the limits of the Cerrado (orange), the limits of the different Cerrado ecoregions (green), and the different Brazilian states (grey) that intersect the Cerrado. Ecoregions: 1, Chapada dos Parecis; 2, Depressão Cuiabana; 3, Paraná Guimarães; 4, Complexo Bodoquena; 5, Bananal; 6, Araguaia Tocantins; 7, Planalto Central; 8, Basaltos do Paraná; 9, Alto São Francisco; 10, Vão do Paraná; 11, Paracatu; 12, Chapadão do São Francisco; 13, Bico do Papagaio; 14, Alto Parnaíba; 15, Floresta de Cocais; 16, Centro-norte Piauiense; 17, Costeiro; 18, Parnaguá; 19, Jequitinhona; 20, Depressão Cárstica do São Francisco. PA, Pará; MT, Mato Grosso; MS, Mato Grosso do Sul; GO, Goiás; DF, Distrito Federal; PR, Paraná; SP, São Paulo; MG, Minas Gerais; MA, Maranhão; TO, Tocantins; PI, Piauí; BA, Bahía. 172

5.1 Location of the study area (left panel), the Brazilian Cerrado (red), within Brazil (yellow) in South America. The Brazilian Cerrado is coloured according to the natural area percentage of each 30 km grid cell in the year 2022 (right panel). We used the land use data from the MapBiomas Collection 8.0 (Souza et al., 2020) dataset, considering as natural all MapBiomas subcategories under "Forest" (which includes savannas) along with "Wetlands" and "Grassland". Values range from 0-10% natural area (orange), indicating cells mostly converted to human land uses, to 90-100% natural area (green), indicating mostly unconverted landscapes. Grey lines represent the limits of the Brazilian states, and the labels refer to those states with some area within the Cerrado: MT, Mato Grosso; MS, Mato Grosso do Sul; GO, Goiás; DF, Distrito Federal; SP, São Paulo; PR, Paraná; MG, Minas Gerais; MA, Maranhão; TO, Toncantins; PI, Piauí; BA, Bahía. . . . 185

5.2 Inter-annual variability throughout the study period (2019-2023) of the number of fires, **a**, caused by humans (brown) and lightning (green), or with no clear cause of ignition (grey), and the corresponding annual burned areas, **b**. Numbers indicate the percentage of fires ignited by lightning in the year (**a**), and the percentage of burned area from lightning fires (**b**). Fires were considered to be ignited by lightning if their attribution score was $B \geq 0.8$, ignited by humans if $B \leq 0.2$, and the remaining fires were not considered to have a clear ignition cause. Given these attribution score thresholds, the different values shown by the coloured bars were obtained as the average out of those numbers of fires, or average burned areas, obtained when using different combinations of spatial and temporal windows in the attribution method, $\{(\Delta t_{\text{max}}, \Delta x_{\text{max}}),\ \Delta t_{\text{max}} \in [3, 7]$ days and $\Delta x_{\text{max}} \in [6, 12]$ km$\}$ (see Methods). Error bars indicate the 95% confidence interval (CI) around these averages when using the different window combinations and were obtained using bootstrapping. 197

5.3 **a** Average number of human-caused (brown) and lightning-caused (green) fires per month in the study period, 2019-2023. The numbers indicate the average number of fires per month and type of ignition and are included for reference. In each year and month, a number of fires may have no clear ignition cause (not represented in this figure). **b** Average monthly percentage of fires for each type of ignition. Lightning and human-caused fire percentages in each month do not necessarily add up to 100% as there can be fires with no clear ignition cause (see Methods). **c** Average number of lightning strikes per month (pink), average monthly precipitation (blue) and vapour pressure deficit (VPD, red). **d** Lightning ignition efficiency, the number of lightning strikes igniting fires divided by the total number of lightning strikes. **e** Ratio of the number of total lightning strikes to precipitation per month and grid cell. Error bars were obtained from the standard deviation and represent the 95% confidence interval (CI). 199

5.4 Average annual number of **a** lightning and **b** human-caused fires, and **c** lightning density in each 30 km cell over the Cerrado in the period 2019-2023. Note that maps **a** and **b** have different scales so that the spatial variation in the number of lightning-caused fires is visible despite its numbers being overall much smaller than those of human-caused fires. **d** map showing the grid cells dominated by lightning (green) or human ignitions (yellow and oranges), that is, where one of the two causes of ignitions accounts for 50% or more of the ignitions in a grid cell. Grid cells coloured in pink do not have an ignition cause accounting for more than 50% of fires (as there are fires with no clear ignition cause). Cells with less than 10 fires on average in the period appear in grey. Areas and numeric labels highlighted in red correspond to the Cerrado ecoregions referred to in the text: 1, Alto Parnaíba; 2, Araguaia Tocantins; 3, Bananal; 4, Planalto Central. Grey labels indicated the Brazilian states intersecting the Cerrado: MT, Mato Grosso; MS, Mato Grosso do Sul; GO, Goiás; DF, Distrito Federal; SP, São Paulo; PR, Paraná; MG, Minas Gerais; MA, Maranhão; TO, Tocantins; PI, Piauí; BA, Bahía. 201

5.5 Fire frequency distributions for lightning-caused (green) and human-caused (brown) fires in the period 2019-2023. Bars represent the areas burned by each type of ignition a certain number of times in the study period divided by the total area affected at least once by that ignition cause. Here, we identified lightning ($B \geq 0.8$) and human ($B \leq 0.2$) caused fires using $\Delta t_{\text{max}} = 5$ days and $\Delta x_{\text{max}} = 9$ km. The fires with intermediate attribution scores, B between 0.2 and 0.8, were considered as having no clear cause of ignition and were excluded from this analysis. 202

5.6 **a**, distribution of the precipitation accumulated over the 10 days prior to the fire start per month for lightning (green) and human-caused (brown) fires, and, **b**, over the study period 2019-2023. **c**, distribution of vapour pressure deficit (VPD) values on the day of ignition per month, and, **d**, over the whole period, per ignition cause. Here, we identified lightning ($B \geq 0.8$) and human ($B \leq 0.2$) caused fires using $\Delta t_{\text{max}} = 5$ days and $\Delta x_{\text{max}} = 9$ km. The fires with intermediate attribution scores, B between 0.2 and 0.8, were considered as having no clear cause of ignition and were excluded from this analysis. 204

5.7 Distribution of the fire sizes and median fire radiative power (FRP) of lightning (green) and human-caused (brown) fires. The distributions are shown as a strip-plot of the observations - that is, each brown or green dot in the graph represents a fire event. The white dots represent the median value of each distribution, and the black box-and-whisker show the quartiles of the distributions. **a** and **c** show the distributions per month for fire size and median FRP respectively. **b** and **d** show the fire size and median FRP distributions over the period 2019-2023 respectively. We identified lightning ($B \geq 0.8$) and human ($B \leq 0.2$) caused fires using $\Delta t_{\text{max}} = 5$ days and $\Delta x_{\text{max}} = 9$ km. The fires with intermediate attribution scores, B between 0.2 and 0.8, were considered as having no clear cause of ignition and were excluded from this analysis. 206

5.8 Weather conditions (y-axis) and natural area percentage (x-axis) of the ignition points of the largest ($\geq$ 150 km^2) fires (top row) and for those with the highest median fire radiative power (FRP) values ($\geq$ 100 MW) (bottom row). Each dot represents a fire observation coloured by the type of ignition, either human-caused (brown) or lightning-caused (green). The size of the dot represents the size (top row) or the median FRP value (bottom row) of the fire. **a** and **c**, show the relation between the precipitation accumulated in the 10 days prior to ignition and the percentage of natural area of the cell where the fire took place for the largest and most intense fires respectively. **b** and **d**, show the relation between the VPD conditions on the day of ignition and the percentage of natural area for the largest fires and most intense fires respectively. We identified lightning ($B \geq 0.8$) and human ($B \leq 0.2$) caused fires using $\Delta t_{\text{max}} = 5$ days and $\Delta x_{\text{max}} = 9$ km. The fires with intermediate attribution scores, B between 0.2 and 0.8, were considered as having no clear cause of ignition and were excluded from this analysis. 207

List of Abbreviations

AF ..... Active Fire
BP ..... Before Present
BIC ..... Bayesian Information Criteria
CG ..... Cloud-to-Ground (lightning stirkes)
CHIRPS ..... Climate Hazards Group InfraRed Precipitation with Station
CI ..... Confidence Interval
CWD ..... Climatological Water Deficit
DAG ..... Directed Acyclic Graph
ECMW ..... European Centre for Medium-range Weather Forecasts
EM ..... Electromagnetic
ERA5 ..... Fifth generation European ReAnalysis (climate dataset)
ERA5-Land ... Land component of ERA5
FRP ..... Fire Radiative Power
GFA ..... Global Fire Atlas
GLD360 ..... Vaisala Global Lightning Detection Network
HPDI ..... Highest Posterior Density Interval
IBGE ..... Instituto Brasileiro de Geografia e Estatística
ICMBio ..... Instituto Chico Mendes de Conservação da Biodiversidade
IFM ..... Integrated Fire Management
IPCC ..... Intergovernmental Panel on Climate Change
ITCZ ..... Intertropical Convergence Zone
LF ..... Low Frequency
LLS ..... Lightning Location System
MCWD ..... Maximum Climatological Water Deficit
MF ..... Medium Frequency
MODIS ..... Moderate-Resolution Imaging Spectroradiometer
PARNA ..... Parque Nacional (National Park in Portuguese)
PCA ..... Principal Component Analysis
PET ..... Potential Evapotranspiration
RDA ..... Redundancy Analysis

RCP . . . . . Representative Concentration Pathway

sECDF . . . . . smoothed Empirical Cumulative Distribution Function

TRMM . . . . . Tropical Rainfall Measuring Mission

UAV . . . . . Unmanned Aerial Vehicle

VHF . . . . . Very High Frequency

VIIRS . . . . . Visible Infrared Imaging Radiometer Suite

VLF . . . . . Very Low Frequency

VPD . . . . . Vapour Pressure Deficit

1 | Introduction

1.1 Thesis rationale

1.1.1 The changing fire regimes of tropical savannas and grasslands, a general perspective

Changes in fire dynamics have become a major concern because of environmental, societal, health and economic impacts (Bowman, Kolden, et al., 2020; Shlisky et al., 2007). In recent years, there has been an increase in the occurrence of large and uncontrollable fires in some areas of the world (Jones, Kelley, et al., 2024; Lapola et al., 2023), with devastating consequences for humans and ecosystems (Brando et al., 2020; Jones, Kelley, et al., 2024). This has added to the already common negative perception about fire occurrence of the general public, as well as to the notion that fire activity overall is being exacerbated by climate change (Doerr et al., 2016). These perceptions have often reinforced zero-fire policies that already existed in many areas of the world as blanket solutions to dealing with fires (Durigan, 2020), which implement active suppression as fire management practices (Moritz et al., 2014). However, fire is a recurrent natural disturbance agent that has been occurring for millions of years (Glasspool et al., 2004), it plays fundamental roles in the Earth system (Bowman, Balch, et al., 2009), and many ecosystems depend on it for their functioning and continuity (Shlisky et al., 2007). In addition, perhaps paradoxically, global burned area has actually declined over the past two decades driven by decreases in burned area of tropical savannas and grasslands (Andela, Morton, et al., 2017; Jones, Abatzoglou, et al., 2022; Wu et al., 2021), which otherwise are the most flammable ecosystems concentrating around 70% of total burned area (Giglio et al., 2013).

Tropical savannas are heterogeneous ecosystems with open canopies and a continuous understory layer of shade-intolerant C_4 grasses (Sankaran et al., 2005). In these ecosystems, most vegetation species have co-evolved with fire developing adaptation strategies

to resist or even thrive with periodic fires (Bond and Keeley, 2005). In fact, fire is a crucial factor maintaining their characteristic open canopies by preventing tree overgrowth (Bond, Woodward, et al., 2005; Oliveras et al., 2016; Pausas et al., 2020). However, the patterns of fire in savannas across the tropics are undergoing profound changes not only in their burned area, but also in their frequency, typical sizes and seasonality (Archibald, Nickless, et al., 2010; Arruda et al., 2021) - that is, their fire regimes are changing as a whole. Moreover, at regional scales, both increases and decreases in burned area and fire frequency over time are being reported (Andela and Werf, 2014; Silva, Nogueira, et al., 2021), pointing at the complexity of processes underpinning these changes. In these ecosystems, departures from the historical fire dynamics in either direction can have damaging effects (Pivello et al., 2021) including changes in ecosystem composition, structure or function (Stevens, Lehmann, et al., 2017; Rosan, Aragão, et al., 2019) and biodiversity losses (Durigan and Ratter, 2016). Such impacts on these ecosystems are particularly relevant because tropical savannas and grasslands are ancient and highly biodiverse ecosystems (Veldman et al., 2015; Williams et al., 2017), they are the second most productive biome (Beer et al., 2010), are home to about one fifth of the human population (Scholes et al., 1997), and support local livelihoods (Rekow, 2019; Ryan et al., 2016) and the production of agricultural commodities and livestock (Putz et al., 2010; Rekow, 2019). Thus, understanding how savanna fire regimes are changing in relation to humans and the climate is instrumental to better address their conservation, quantify their carbon emissions, and predict how these regimes may be in the future and their impacts on ecosystems and human populations (Wu et al., 2021).

The two main drivers of changes of the fire regimes of tropical savannas and grasslands, and globally, are climate change and human activities (Jones, Abatzoglou, et al., 2022). On the one hand, climate change is increasing the frequency of droughts and heatwaves and lengthening the duration of the dry season (Jolly et al., 2015), thus increasing the flammability conditions of vegetation (Simpson et al., 2016; Zanzarini et al., 2022) and creating longer windows of opportunity for fires to start and spread (Flannigan et al., 2013). Thus, under climate change, some studies predict increases in fire incidence over

some savannas (Silva, Bastos, Libonati, et al., 2019; Silva, Bastos, DaCamara, et al., 2016). Human activities, however, have a more complex relation with changes in savannas' fire regimes. Overall, the expansion of human activities brings about landscape fragmentation, argued to reduce savannas' burned area by creating fuel discontinuities (Archibald, 2016; Andela and Werf, 2014). However, this expansion has sometimes been accompanied by the introduction of alien species, which can increase fuel load and flammability (Hoffmann et al., 2004; Setterfield et al., 2010). Further, humans also increase the number of ignitions during the dry season (Archibald, Staver, et al., 2012; Menezes et al., 2022), in contrast to wet season lightning fires (Ramos-Neto et al., 2000; Menezes et al., 2022), potentially enhancing fire occurrence and their intensity. Finally, inadequate fire management policies enforcing fire suppression have been common across tropical savannas (Durigan and Ratter, 2016; Stevens, Bond, et al., 2022), contributing to woody encroachment and fuel buildup (Stevens, Lehmann, et al., 2017; Durigan and Ratter, 2016), processes that can eventually lead to large and intense fires in some areas (Fidelis et al., 2018).

1.1.2 The Brazilian Cerrado as a case study

The Brazilian Cerrado is a remarkable example of the confluence of these processes and a notable case study to understand many aspects of contemporary savanna fire regimes and their changes in recent times. Extending over 2 million km^2, the Cerrado is the most biodiverse savanna in the world (Klink et al., 2005), with high levels of endemism. Despite its ecological importance, the Cerrado is highly threatened by agricultural expansion and is thus considered to be a biodiversity hotspot for conservation (Myers et al., 2000). One of the most remarkable characteristics of this region is the heterogeneity of its vegetation (Sano, Rosa, et al., 2010), emphasised by the multiple ecoregions identified within the Cerrado (Sano, Rodrigues, et al., 2019). In fact, the Cerrado is more often described as a mosaic of open grasslands and savannas with different levels of tree cover, intermingled with patches of dry and gallery forests (Ribeiro et al., 2008). Fire plays a crucial role maintaining these characteristic mosaicking patterns of vegetation (Miranda et al., 2002)

and their biodiversity (Durigan, Pilon, et al., 2020).

In the Cerrado, fire occurs naturally because of lightning as well as in relation to human activities. Among the human uses of fire there is a wide variety of different practices, including traditional uses by indigenous peoples (Pivello, 2011; Mistry, Bilbao, et al., 2016) and pastoral communities (Eloy et al., 2019), the use of fire as part of fire management practices (Schmidt, Moura, et al., 2018), or the use of fire associated with modern agricultural activities (Pivello, 2011). All these human practices create fire regimes that differ from the naturally ignited ones, particularly in terms of frequency and seasonality (Miranda et al., 2002). The extent to which these different regimes contribute to maintaining the Cerrado or act as degrading agents is a matter of active research. In fact, until recently, the use of fire was prohibited across Brazil regardless of the type of ecosystem (Schmidt and Eloy, 2020; Durigan, 2020). These policies were the result of a mix of colonial legacies (Miranda, 2010; Pivello, 2011), the extended use of fire as a deforestation tool in fire-sensitive ecosystems (Barlow et al., 2020; Lapola et al., 2023; Pivello, 2011), and misunderstandings about the ecology of savannas (Durigan, 2020). Over the last few decades, however, there has been a push to (re)introduce the use of fire as a conservation and fire management tool (Miranda, 2010; Schmidt, Moura, et al., 2018; Mistry, Schmidt, et al., 2019; Mistry, Bilbao, et al., 2016; Durigan, 2020; Durigan and Ratter, 2016), primarily after the observation of degrading woody encroachment processes (Rosan, Sitch, et al., 2022; Stevens, Lehmann, et al., 2017; Durigan and Ratter, 2016), the occurrence of devastating fires in some protected areas as a consequence of fuel build up (Fidelis et al., 2018; Batista et al., 2018), and the increasing recognition of indigenous and traditional knowledge about Cerrado's ecology and their uses of fire (Eloy et al., 2019; Mistry, Schmidt, et al., 2019; Welch et al., 2013). These processes and efforts have recently materialised in a Brazilian National Policy on Integrated Fire Management (Lei 14,944 from 31st July 2024) promoting the use of fire to manage fire-adapted ecosystems for conservation, as well as regulating its use in private lands. Still, the use of fire associated with industrial agriculture is considered to be the main cause of fire in the Cerrado (Pivello, 2011), with complex effects on fire dynamics (Silva, Rodrigues, et al., 2020; Silva,

Nogueira, et al., 2021).

Indeed, over the past five to six decades, the Cerrado has undergone a rapid conversion to agricultural land uses, totalling a loss of around 50% of its original native vegetation (Sano, Rosa, et al., 2010; Alencar et al., 2020). This expansion has brought about widespread increases in landscape fragmentation (Rosan, Sitch, et al., 2022; Silva Arruda et al., 2024) and nowadays only a handful of regions with continuous Cerrado vegetation remain - including the areas with some degree of protection, about 12% of the Cerrado (Carranza et al., 2014). Simultaneously, the Cerrado has also experienced a warming and drying process in relation to climate change (Hofmann, Cardoso, et al., 2021; Hofmann, Silva, et al., 2023; Oliveira et al., 2014). These changes have been particularly acute during the dry season (Hofmann, Cardoso, et al., 2021; Hofmann, Silva, et al., 2023), when most Cerrado fires take place (Mataveli et al., 2018; Silva, Nogueira, et al., 2021; Silva Arruda et al., 2024).

Concomitantly, the fire regimes of the Cerrado have also changed over the past few decades (Mataveli et al., 2018; Silva, Nogueira, et al., 2021; Silva Arruda et al., 2024). When considering the Cerrado as a whole, no clear trends in burned area are observed over the past four decades, while fire size seems to have increased over this period (Silva Arruda et al., 2024). However, when exploring changes at smaller scales, a wealth of different patterns become apparent (Mataveli et al., 2018; Silva, Nogueira, et al., 2021; Silva Arruda et al., 2024). In particular, many studies report opposing trends in burned area, increases and decreases, in different parts of the Cerrado (Mataveli et al., 2018; Silva, Nogueira, et al., 2021; Silva Arruda et al., 2024). In addition, there are remarkable differences among Cerrado's ecoregions in terms of fire size and intensity (Silva, Nogueira, et al., 2021) or fire frequency (Silva Arruda et al., 2024). These observations stress the need to characterise the Cerrado's fire regimes at small scales to prevent the fire dynamics of a particular area from dominating the overall signal of the Cerrado. Further, these regional differences also suggest a complex interplay between the two drivers of fire, humans and the climate, and other landscape characteristics like the type of vegetation (Silva, Rodrigues, et al., 2020).

Overall, the current state-of-the-art indicates that the ongoing alteration of Cerrado's fire regimes are associated with the large-scale conversion of Cerrado's native vegetation to croplands and pastures in confluence with climate change (Mataveli et al., 2018; Silva, Nogueira, et al., 2021; Silva Arruda et al., 2024), putting further pressures on this highly threatened region. There remain, however, many open questions regarding the mechanisms by which humans and the climate are altering the Cerrado's fire regimes, the extent of the human footprint on the patterns of fire across the Cerrado, and how the current patterns of fire may differ from naturally ignited ones. The fire regimes of the Cerrado and the processes they are undergoing in relation to modern human activities and the climate are the focus of the present thesis.

1.1.3 Knowledge gaps

Several studies across savannas indicate that the patterns of decreases in burned area observed in some regions are related to the expansion of agricultural area and the concomitant fuel discontinuities and fire controls it brings about (Andela and Werf, 2014; Rosan, Sitch, et al., 2022). On the other hand, increasing temperatures or changes in precipitation are argued to be driving increases in burned area in other areas (Andela and Werf, 2014; Silva, Rodrigues, et al., 2020), especially where most savanna vegetation remains (Mataveli et al., 2018). Further, it is suggested that, in general, human controls on fire activity through landscape fragmentation are stronger than climatic effects, both in the Cerrado (Conciani et al., 2021) and other savannas (Andela and Werf, 2014; Archibald, Nickless, et al., 2010). However, the interaction between these two drivers of fire has not yet been quantified.

Disentangling the effects of land use and the climate appears key to understanding the mechanisms underpinning the puzzle of spatial and temporal patterns of burned area observed in the Cerrado and other savannas. In addition, a better comprehension of whether these two determinants of fire are really pushing burned area in opposite directions and how their effects combine can also help the interpretation of changes in other characteristics of fires in the Cerrado. Quantifying the effects and the interaction between land use

area and various climatic variables on Cerrado's burned area will be the focus of **Chapter 3 (Research Paper 1)**.

The fire regimes of the Cerrado have been previously characterised for each of its different ecoregions (Silva, Nogueira, et al., 2021; Silva Arruda et al., 2024), finding a striking heterogeneity of fire frequencies, sizes, intensities and burned areas (Silva, Nogueira, et al., 2021; Silva Arruda et al., 2024). However, these ecoregions may not correspond to the actual areas of the Cerrado presenting similar characteristics of fire. Moreover, studying fire regimes based on pre-established regions can hamper the analysis of the environmental factors that may explain the patterns of fire (Archibald, Lehmann, et al., 2013). In contrast, methods to identify and delineate regions with common fire regimes based solely on the spatial patterns of fire characteristics can overcome these limitations (Archibald, Lehmann, et al., 2013; Pais et al., 2023; Chuvieco et al., 2008), but have not been used to study the Cerrado's fire regimes. Further, the profound changes the Cerrado has experienced over the last four decades may imply that the geographical configuration of its fire regimes may have changed over this period, something that has also not yet been explored. Identifying the different regions of the Cerrado with different fire regimes and their changes in time will be the focus of **Chapter 4 (Research Paper 2)**.

Finally, there is a major outstanding question in the study of fires in the Cerrado regarding the cause of fire ignitions. The fact that humans are currently the main cause of ignitions in the Cerrado and other savannas is a commonly held perception (Archibald, Roy, et al., 2009) stemming from expert's knowledge about modern uses of fire (Pivello, 2011), and the temporal mismatch observed between the fire and lightning seasons (Schumacher, 2022). However, studies in some Cerrado protected areas reported the occurrence of lightning fires and suggested that these may be more frequent than usually assumed (Ramos-Neto et al., 2000; Pereira et al., 2005; Medeiros et al., 2004; Fiedler et al., 2006).

Identifying whether lightning or humans are the ignition cause of fires would represent a major advance in the study of Cerrado's fire regimes. First, it would allow to quantify by how much the number of fires ignited by humans exceeds that of fires caused by lightning

strikes, as well as comparing the timing, location and behaviour of the fires caused by each type of ignition. In short, the identification of fires by ignition cause would contribute to understanding how much human-caused fire regimes differ from those naturally ignited. At the same time, it would shed light on the causes of high fire occurrences in the more intact areas of the Cerrado, with implications for fire management policies beyond the Cerrado's protected areas. The quantification of lightning and human-caused fires and the analysis of the corresponding fire regimes will be the focus of **Chapter 5 (Research Paper 3)**.

1.2 Thesis aims and objectives

The overarching aim of this thesis is to improve our understanding of how fire has been occurring across the Cerrado over the past few decades shaped by human activities and the climate, the two main drivers of fire. This research aim is addressed through three guiding objectives, each corresponding to a research article:

Objective 1: Determine how land use area and the climate interact to affect the burned area of the Cerrado.

This objective is the main aim of **Chapter 3 (Research Paper 1)**, and was addressed through the following research questions:

1) In the Cerrado, what is the causal effect of the extent of land use area in a landscape on the percentage of burned natural area?

2) How does land use area percentage interact with the climate to affect the burned natural area of the Cerrado?

3) What are the burned natural area trends across the Cerrado? Are these trends caused by land use expansion and climate change?

Objective 2: Explore the geographical variation in the patterns of fire across the Brazilian Cerrado, their temporal evolution, and their relation to the climate and human activities.

This objective is the main aim of **Chapter 4 (Research Paper 2)**, and was addressed through the following research questions:

1) What are the regions of the Cerrado presenting different fire regimes?

2) What are the environmental variables that characterise these spatial patterns of fire?

3) How have these fire regimes changed through time?

Objective 3: Investigate the contribution of lightning and human-ignited fires to the Cerrado's current patterns of fire and compare the fire regimes created by each type of ignition.

This objective is the main aim of **Chapter 5 (Research Paper 3)**, and was addressed through the following research questions:

1) What proportion of fires in the Cerrado are ignited by lightning strikes and by humans? Do these proportions change throughout the year?

2) How does the balance between lightning and human-ignited fires change across the Cerrado?

3) What are the differences in fire behaviour and fire frequency between lightning and human-caused fires?

1.3 Thesis structure

This thesis is presented according to the requirements for the University of Oxford's Doctor of Philosophy in Geography and the Environment and follows the article-based format. This thesis is organised into 6 chapters. This chapter (**Chapter 1**) introduces the thesis background and sets out the main overarching research aim, and the specific objectives and research questions formulated to address the general aim. **Chapter 2** contextualises this thesis by first introducing the Brazilian Cerrado, the study area on which this thesis is focused, and then providing the background knowledge needed to understand the context and interpret the results of this thesis, and identifying the research gaps that motivate the

research questions addressed in this thesis.

Chapter 3 (Research Paper 1) focuses on the question of how the extent of land use area and the climate interact to explain burned area and the heterogeneous patterns of increases and decreases in burned area across the Cerrado in the period 1985 to 2020. This objective is addressed using a causal inference framework and a Bayesian multilevel modelling approach using geospatial data on burned area and various climatic variables on a 0.2^{o} grid over the Cerrado.

Once we have gained an understanding about the interplay between the climate and the extent of human land uses in the landscape, we expand our view by quantifying fire regimes as a whole - that is, including measures of frequency, fire size and seasonality, apart from burned area. Thus, in **Chapter 4 (Research Paper 2)**, we identify the different regions of the Cerrado presenting different fire regimes focusing on two different periods, 1985-1993 and 2012-2020, with the aim of understanding how the patterns of fire vary across the Cerrado, as well as through time. We delineate the different regions using a clustering algorithm with a spatial contiguity constrain on a 30 km grid over the Cerrado. Then, we use statistical ordination methods to explore the characteristics of these regions in terms of fire, climatic and anthropic characteristics, and how they have changed through time.

Then, in **Chapter 5 (Research Paper 3)**, we use an ignition-cause attribution method to identify those Cerrado fires most likely caused by lightning in the period 2019-2023 . The aim is to determine the contribution of lightning-caused fires to the Cerrado's current fire regimes. As well, we investigate whether and how the patterns and behaviour of fires ignited by humans may differ from those ignited by lightning.

Finally, **Chapter 6** concludes this thesis by presenting a synthesis of results and the implications of this research, and briefly discusses future research avenues and outstanding questions identified by the thesis.

1.4 References

Alencar, Ane et al. (2020). "Mapping Three Decades of Changes in the Brazilian Savanna Native Vegetation Using Landsat Data Processed in the Google Earth Engine Platform". In: *Remote Sensing* 12.6, p. 924.

Andela, N., D. C. Morton, et al. (2017). "A human-driven decline in global burned area". In: *Science* 356.6345, pp. 1356–1362.

Andela, Niels and Guido R. van der Werf (2014). "Recent trends in African fires driven by cropland expansion and El Niño to La Niña transition". In: *Nature Climate Change* 4.9, pp. 791–795.

Archibald, S., A. Nickless, et al. (2010). "Climate and the inter-annual variability of fire in southern Africa: a meta-analysis using long-term field data and satellite-derived burnt area data: Fire-climate interactions". In: *Global Ecology and Biogeography* 19.6, pp. 794–809.

Archibald, Sally (2016). "Managing the human component of fire regimes: lessons from Africa". In: *Philosophical Transactions of the Royal Society B: Biological Sciences* 371.1696, p. 20150346.

Archibald, Sally, Caroline E. R. Lehmann, et al. (2013). "Defining pyromes and global syndromes of fire regimes". In: *Proceedings of the National Academy of Sciences* 110.16, pp. 6442–6447.

Archibald, Sally, David P. Roy, et al. (2009). "What limits fire? An examination of drivers of burnt area in Southern Africa". In: *Global Change Biology* 15.3, pp. 613–630.

Archibald, Sally, A. Carla Staver, and Simon A. Levin (2012). "Evolution of human-driven fire regimes in Africa". In: *Proceedings of the National Academy of Sciences* 109.3, pp. 847–852.

Arruda, Vera L.S. et al. (2021). "An alternative approach for mapping burn scars using Landsat imagery, Google Earth Engine, and Deep Learning in the Brazilian Savanna". In: *Remote Sensing Applications: Society and Environment* 22, p. 100472.

Barlow, Jos et al. (2020). "Clarifying Amazonia's burning crisis". In: *Global Change Biology* 26.2, pp. 319–321.

Batista, Eugênia Kelly Luciano et al. (2018). "An evaluation of contemporary savanna fire regimes in the Canastra National Park, Brazil: Outcomes of fire suppression policies". In: *Journal of Environmental Management* 205, pp. 40–49.

Beer, Christian et al. (2010). "Terrestrial Gross Carbon Dioxide Uptake: Global Distribution and Covariation with Climate". In: *Science* 329.5993, pp. 834–838.

Bond, W and J Keeley (2005). "Fire as a global 'herbivore': the ecology and evolution of flammable ecosystems". In: *Trends in Ecology & Evolution* 20.7, pp. 387–394.

Bond, W. J., F. I. Woodward, and G. F. Midgley (2005). "The global distribution of ecosystems in a world without fire". In: *New Phytologist* 165.2, pp. 525–538.

Bowman, David M. J. S., Jennifer K. Balch, et al. (2009). "Fire in the Earth System". In: *Science* 324.5926, pp. 481–484.

Bowman, David M. J. S., Crystal A. Kolden, et al. (2020). "Vegetation fires in the Anthropocene". In: *Nature Reviews Earth & Environment* 1.10, pp. 500–515.

Brando, P. M. et al. (2020). “The gathering firestorm in southern Amazonia”. In: *Science Advances* 6.2, eaay1632.

Carranza, Tharsila et al. (2014). “Protected Area Effectiveness in Reducing Conversion in a Rapidly Vanishing Ecosystem: The Brazilian Cerrado: Protected area effectiveness in Cerrado”. In: *Conservation Letters* 7.3, pp. 216–223.

Chuvieco, Emilio, Louis Giglio, and Chris Justice (2008). “Global characterization of fire activity: toward defining fire regimes from Earth observation data”. In: *Global Change Biology* 14.7, pp. 1488–1502.

Conciani, Dhemerson E. et al. (2021). “Human-climate interactions shape fire regimes in the Cerrado of São Paulo state, Brazil”. In: *Journal for Nature Conservation* 61, p. 126006.

Doerr, Stefan H. and Cristina Santín (2016). “Global trends in wildfire and its impacts: perceptions versus realities in a changing world”. In: *Philosophical Transactions of the Royal Society B: Biological Sciences* 371.1696, p. 20150345.

Durigan, Giselda (2020). “Zero-fire: Not possible nor desirable in the Cerrado of Brazil”. In: *Flora* 268, p. 151612.

Durigan, Giselda, Natashi A. L. Pilon, et al. (2020). “No Net Loss of Species Diversity After Prescribed Fires in the Brazilian Savanna”. In: *Frontiers in Forests and Global Change* 3, p. 13.

Durigan, Giselda and James A. Ratter (2016). “The need for a consistent fire policy for Cerrado conservation”. In: *Journal of Applied Ecology* 53.1. Ed. by Jeremy James, pp. 11–15.

Eloy, Ludivine et al. (2019). “Seasonal fire management by traditional cattle ranchers prevents the spread of wildfire in the Brazilian Cerrado”. In: *Ambio* 48.8, pp. 890–899.

Fidelis, Alessandra et al. (2018). “The Year 2017: Megafires and Management in the Cerrado”. In: *Fire* 1.3, p. 49.

Fiedler, Nilton César, Daniela Araújo Merlo, and Marcelo Brilhante de Medeiros (2006). “Ocorrência de incêndios florestais no Parque Nacional da Chapada dos Veadeiros, Goiás.” In: *Ciência Florestal* 16.2, pp. 153–161.

Flannigan, Mike et al. (2013). “Global wildland fire season severity in the 21st century”. In: *Forest Ecology and Management* 294, pp. 54–61.

Giglio, Louis, James T. Randerson, and Guido R. van der Werf (2013). “Analysis of daily, monthly, and annual burned area using the fourth-generation global fire emissions database (GFED4)”. In: *Journal of Geophysical Research: Biogeosciences* 118.1, pp. 317–328.

Glasspool, I.J., D. Edwards, and L. Axe (2004). “Charcoal in the Silurian as evidence for the earliest wildfire”. In: *Geology* 32.5, p. 381.

Hoffmann, William A. et al. (2004). “Impact of the invasive alien grass *Melinis minutiflora* at the savanna-forest ecotone in the Brazilian Cerrado”. In: *Diversity and Distributions* 10.2, pp. 99–103.

Hofmann, G. S., R. C. Silva, et al. (2023). “Changes in atmospheric circulation and evapotranspiration are reducing rainfall in the Brazilian Cerrado”. In: *Scientific Reports* 13.1, p. 11236.

Hofmann, Gabriel S., Manoel F. Cardoso, et al. (2021). “The Brazilian Cerrado is becoming hotter and drier”. In: *Global Change Biology* 27.17, pp. 4060–4073.

Jolly, W. Matt et al. (2015). “Climate-induced variations in global wildfire danger from 1979 to 2013”. In: *Nature Communications* 6.1, p. 7537.

Jones, Matthew W, Douglas I Kelley, et al. (2024). “State of Wildfires 2023–2024”. In: *Earth System Science Data* 16.8. Publisher: Copernicus Publications Göttingen, Germany, pp. 3601–3685.

Jones, Matthew W., John T. Abatzoglou, et al. (2022). “Global and Regional Trends and Drivers of Fire Under Climate Change”. In: *Reviews of Geophysics* 60.3, e2020RG000726.

Klink, Carlos A. and Ricardo B. Machado (2005). “Conservation of the Brazilian Cerrado”. In: *Conservation Biology* 19.3, pp. 707–713.

Lapola, David M. et al. (2023). “The drivers and impacts of Amazon forest degradation”. In: *Science* 379.6630. _eprint: https://www.science.org/doi/pdf/10.1126/science.abp8622, eabp8622.

Mataveli, Guilherme Augusto Verola et al. (2018). “Satellite observations for describing fire patterns and climate-related fire drivers in the Brazilian savannas”. In: *Natural Hazards and Earth System Sciences* 18.1, pp. 125–144.

Medeiros, Marcelo Brilhante de and Nilton Cezar Fiedler (2004). “Incêndios florestais no parque nacional da Serra da Canastra: desafios para a conservação da biodiversidade.” In: *Ciência Florestal* 14.2, pp. 157–168.

Menezes, Lucas S et al. (2022). “Lightning patterns in the Pantanal: Untangling natural and anthropogenic-induced wildfires”. In: *Science of the Total Environment*.

Miranda, Heloisa S, Mercedes MC Bustamante, and Antonio C Miranda (2002). “The fire factor”. In: *The cerrados of Brazil: ecology and natural history of a neotropical savanna*. Columbia University Press, pp. 51–68.

Miranda, Heloisa Sinátora, ed. (2010). *Efeitos do regime de fogo sobre a estrutura de comunidades de Cerrado: Projeto Fogo*. Brasília: Ibama MMA. 144 pp.

Mistry, Jayalaxshmi, Bibiana A. Bilbao, and Andrea Berardi (2016). “Community owned solutions for fire management in tropical ecosystems: case studies from Indigenous communities of South America”. In: *Philosophical Transactions of the Royal Society B: Biological Sciences* 371.1696, p. 20150174.

Mistry, Jayalaxshmi, Isabel Belloni Schmidt, et al. (2019). “New perspectives in fire management in South American savannas: The importance of intercultural governance”. In: *Ambio* 48.2, pp. 172–179.

Moritz, Max A. et al. (2014). “Learning to coexist with wildfire”. In: *Nature* 515.7525, pp. 58–66.

Myers, Norman et al. (2000). “Biodiversity hotspots for conservation priorities”. In: *Nature* 403.6772, pp. 853–858.

Oliveira, Paulo Tarso S. et al. (2014). “Trends in water balance components across the Brazilian Cerrado”. In: *Water Resources Research* 50.9, pp. 7100–7114.

Oliveras, Immaculada and Yadvinder Malhi (2016). “Many shades of green: the dynamic tropical forest–savannah transition zones”. In: *Philosophical Transactions of the Royal Society B: Biological Sciences* 371.1703, p. 20150308.

Pais, Cristobal et al. (2023). “Global scale coupling of pyromes and fire regimes”. In: *Communications Earth & Environment* 4.1, p. 267.

Pausas, Juli G. and William J. Bond (2020). “Alternative Biome States in Terrestrial Ecosystems”. In: *Trends in Plant Science* 25.3, pp. 250–263.

Pereira, Alfredo and Helena França (2005). “Identificação de queimadas naturais ocorridas no período chuvoso de 2003-2004 no Parque Nacional das Emas, Brasil, por meio de imagens dos sensores do satélite CBERS-2”. In: *Anais XII Simpósio Brasileiro de Sensoriamento Remoto, Goiânia, Brasil, INPE*, pp. 3245–3252.

Pivello, Vânia R. (2011). “The Use of Fire in the Cerrado and Amazonian Rainforests of Brazil: Past and Present”. In: *Fire Ecology* 7.1, pp. 24–39.

Pivello, Vânia R. et al. (2021). “Understanding Brazil’s catastrophic fires: Causes, consequences and policy needed to prevent future tragedies”. In: *Perspectives in Ecology and Conservation* 19.3, pp. 233–255.

Putz, Francis E. and Kent H. Redford (2010). “The Importance of Defining ‘Forest’: Tropical Forest Degradation, Deforestation, Long-term Phase Shifts, and Further Transitions: Importance of Defining ‘Forest’”. In: *Biotropica* 42.1, pp. 10–20.

Ramos-Neto, Mário Barroso and Vânia Regina Pivello (2000). “Lightning Fires in a Brazilian Savanna National Park: Rethinking Management Strategies”. In: *Environmental Management* 26.6, pp. 675–684.

Rekow, Lea (2019). “Socio-Ecological Implications of Soy in the Brazilian Cerrado”. In: *Challenges in Sustainability* 7.1, pp. 7–29.

Ribeiro, J.F. and B.M.T. Walter (2008). “Cerrado Ecologia e Flora”. In: *As principais fitofisionomias do Bioma Cerrado*. Embrapa, pp. 152–212.

Rosan, Thais M., Luiz E.O.C. Aragão, et al. (2019). “Extensive 21st-Century Woody Encroachment in South America’s Savanna”. In: *Geophysical Research Letters* 46.12, pp. 6594–6603.

Rosan, Thais M., Stephen Sitch, et al. (2022). “Fragmentation-Driven Divergent Trends in Burned Area in Amazonia and Cerrado”. In: *Frontiers in Forests and Global Change* 5, p. 801408.

Ryan, Casey M. et al. (2016). “Ecosystem services from southern African woodlands and their future under global change”. In: *Philosophical Transactions of the Royal Society B: Biological Sciences* 371.1703, p. 20150312.

Sankaran, Mahesh et al. (2005). “Determinants of woody cover in African savannas”. In: *Nature* 438.7069, pp. 846–849.

Sano, Edson E., Ariane A. Rodrigues, et al. (2019). “Cerrado ecoregions: A spatial framework to assess and prioritize Brazilian savanna environmental diversity for conservation”. In: *Journal of Environmental Management* 232, pp. 818–828.

Sano, Edson E., Roberto Rosa, et al. (2010). “Land cover mapping of the tropical savanna region in Brazil”. In: *Environmental Monitoring and Assessment* 166.1, pp. 113–124.

Schmidt, Isabel B., Lívia C. Moura, et al. (2018). “Fire management in the Brazilian savanna: First steps and the way forward”. In: *Journal of Applied Ecology* 55.5. Ed. by Rafael Zenni, pp. 2094–2101.

Schmidt, Isabel Belloni and Ludivine Eloy (2020). “Fire regime in the Brazilian Savanna: Recent changes, policy and management”. In: *Flora* 268, p. 151613.

Scholes, Robert J and Steven R Archer (1997). “Tree-grass interactions in savannas”. In: *Annual review of Ecology and Systematics* 28.1. Publisher: Annual Reviews 4139 El Camino Way, PO Box 10139, Palo Alto, CA 94303-0139, USA, pp. 517–544.

Schumacher, Vanúcia (2022). “Characteristics of lightning-caused wildfires in central Brazil in relation to cloud-ground and dry lightning”. In: *Agricultural and Forest Meteorology*.

Setterfield, Samantha A. et al. (2010). “Turning up the heat: the impacts of *Andropogon gayanus* (gamba grass) invasion on fire behaviour in northern Australian savannas”. In: *Diversity and Distributions* 16.5, pp. 854–861.

Shlisky, Ayn et al. (2007). “Fire, ecosystems and people: threats and strategies for global biodiversity conservation”. In: *Arlington: The Nature Conservancy*, pp. 1–17.

Silva, P S, J A Rodrigues, et al. (2020). “Drivers of burned area patterns in Cerrado: the case of MATOPIBA region”. In: *2020 IEEE Latin American GRSS & ISPRS Remote Sensing Conference (LAGIRS)*.

Silva, Patrícia, Ana Bastos, Carlos C. DaCamara, et al. (2016). “Future Projections of Fire Occurrence in Brazil Using EC-Earth Climate Model”. In: *Revista Brasileira de Meteorologia* 31.3, pp. 288–297.

Silva, Patrícia S., Ana Bastos, Renata Libonati, et al. (2019). “Impacts of the 1.5 °C global warming target on future burned area in the Brazilian Cerrado”. In: *Forest Ecology and Management* 446, pp. 193–203.

Silva, Patrícia S., Joana Nogueira, et al. (2021). “Putting fire on the map of Brazilian savanna ecoregions”. In: *Journal of Environmental Management* 296, p. 113098.

Silva Arruda, Vera Laísa da et al. (2024). “Assessing four decades of fire behavior dynamics in the Cerrado biome (1985 to 2022)”. In: *Fire Ecology* 20.1, p. 64.

Simpson, Kimberley J. et al. (2016). “Determinants of flammability in savanna grass species”. In: *Journal of Ecology* 104.1. Ed. by Hans Cornelissen, pp. 138–148.

Stevens, Nicola, William Bond, et al. (2022). “Grassy Ecosystems in the Anthropocene”. In: *Annual Review of Environment and Resources* 47.1, pp. 261–289.

Stevens, Nicola, Caroline E. R. Lehmann, et al. (2017). “Savanna woody encroachment is widespread across three continents”. In: *Global Change Biology* 23.1, pp. 235–244.

Veldman, Joseph W et al. (2015). “Toward an old-growth concept for grasslands, savannas, and woodlands”. In: *Frontiers in Ecology and the Environment* 13.3. Publisher: Wiley Online Library, pp. 154–162.

Welch, James R. et al. (2013). “Indigenous Burning as Conservation Practice: Neotropical Savanna Recovery amid Agribusiness Deforestation in Central Brazil”. In: *PLoS ONE* 8.12. Ed. by Brock Fenton, e81226.

Williams, RJ et al. (2017). “Australia’s tropical savannas: vast, ancient and rich landscapes”. In: *Australian vegetation*. Publisher: Cambridge University Press Cambridge, pp. 368–388.

Wu, Chao et al. (2021). “Historical and future global burned area with changing climate and human demography”. In: *One Earth* 4.4, pp. 517–530.

Zanzarini, Vagner, Alan N. Andersen, and Alessandra Fidelis (2022). “Flammability in tropical savannas: Variation among growth forms and seasons in Cerrado”. In: *Biotropica* 54.4, pp. 979–987.

2 | Literature Review

In this chapter, I start by introducing the Brazilian Cerrado, a brief introduction to its recent history, and its ecological, climatic and landscape characteristics, providing the necessary information and context to support this thesis. Then, in the next three sections, I elaborate on the state of knowledge and research gaps that have been addressed in each of the three research papers of this thesis (**Chapter 3 (Research Paper 1)**, **Chapter 4 (Research Paper 2)** and **Chapter 5 (Research Paper 3)**). In each of these three sections, I introduce the subject addressed and the necessary concepts with a general perspective and then focus on the Brazilian Cerrado, detailing the scholarship and unresolved questions. Finally, I give a brief overview of the main methodologies and sources of data used in this thesis.

2.1 The Brazilian Cerrado

Cerrado is the name given to a Neotropical region comprising a wealth of different ecosystems, often referred to as a tropical savanna because this is the dominant vegetation type (Gottsberger et al., 2006). Most of this region of savanna-like ecosystems is found within Brazil (Figure 2.1), which constitutes the study area of this thesis, although a small extension is also found within Bolivia and Paraguay (Ribeiro and Walter, 2008).

The Brazilian Cerrado is a complex and heterogeneous region at many different levels, its vegetation composition and rich biodiversity, its topography and soils, its patterns of land use area, its patterns of fire, and the varied human communities and economic activities - indigenous groups, traditional pastoral or *quilombola* communities, small and extensive agricultural properties, and some large urban centres. In addition, the Cerrado encompasses the headwaters of three major South American river basins as well as large aquifers, providing important hydrological resources to this continent (Oliveira, Nearing, et al., 2014). The geographical patterns of the vegetation, landscape and environmental characteristics of the Cerrado have been studied and classified into nineteen ecoregions

(Sano, Rodrigues, et al., 2019) (Figure 2.1).

The official geographical limits of the Cerrado have varied through time and within the literature (Vieira et al., 2022). In this thesis, we use the official geographical limits defined by the Instituto Brasileiro de Geografia e Estatística (IBGE, Brazil's Geography and Statistics Institute) in 2019 (Biomas, 2019), as this is the most recent official version (Figure 2.1).

The Brazilian Cerrado has a marked seasonal climate that shapes the phenological cycle of this region (Oliveras et al., 2013), which is dominated by C_4 grasses: during the wet season, rainfall enables vegetation growth; during the dry season, vegetation is in general subject to hydric stress, and perennial plants dry out while some tree species shed their leaves (Oliveras et al., 2013). As a consequence, particularly in the more open forms of Cerrado vegetation, there is a general accumulation of dry dead biomass - or alive but with little moisture content - over the dry season that can easily burn (Simon, Grether, et al., 2009). In turn, fire favours the establishment of grasses and shrubs against the proliferation of trees and fire-sensitive species (Mistry, 1998). These synergies between fire and certain vegetation types that allow to maintain the open ecosystems of the Cerrado are mediated by the fact that most vegetation species endemic to the Cerrado are adapted to fire (Simon, Grether, et al., 2009; Gottsberger et al., 2006).

It has been estimated that the majority of Cerrado vegetation lineages diversified less than 4 million (M) years before present (yrs BP) (Simon, Grether, et al., 2009). This indicates that Cerrado vegetation started evolving and expanding around this time, coinciding with the global expansion of the savanna biome dominated by C_4 grasses (Simon, Grether, et al., 2009). Further, phylogenetic studies indicate that endemic Cerrado species seem to have evolved in situ through rapid and frequent adaptive shifts to resist fire, evolving from nearby fire-free ecosystems' species and lineages (Simon, Grether, et al., 2009; Simon and Pennington, 2012). Indeed, paleo-pollen and charcoal records evidence the presence of fire in Cerrado from 32,000 yrs BP (Salgado-Labouriau et al., 1997) mediated by climatic fluctuations and the corresponding shifts in vegetation (Cassino, Sabino, et al., 2023), as well as by the presence of large herbivores (Dantas et al., 2020; Doughty et al., 2016).

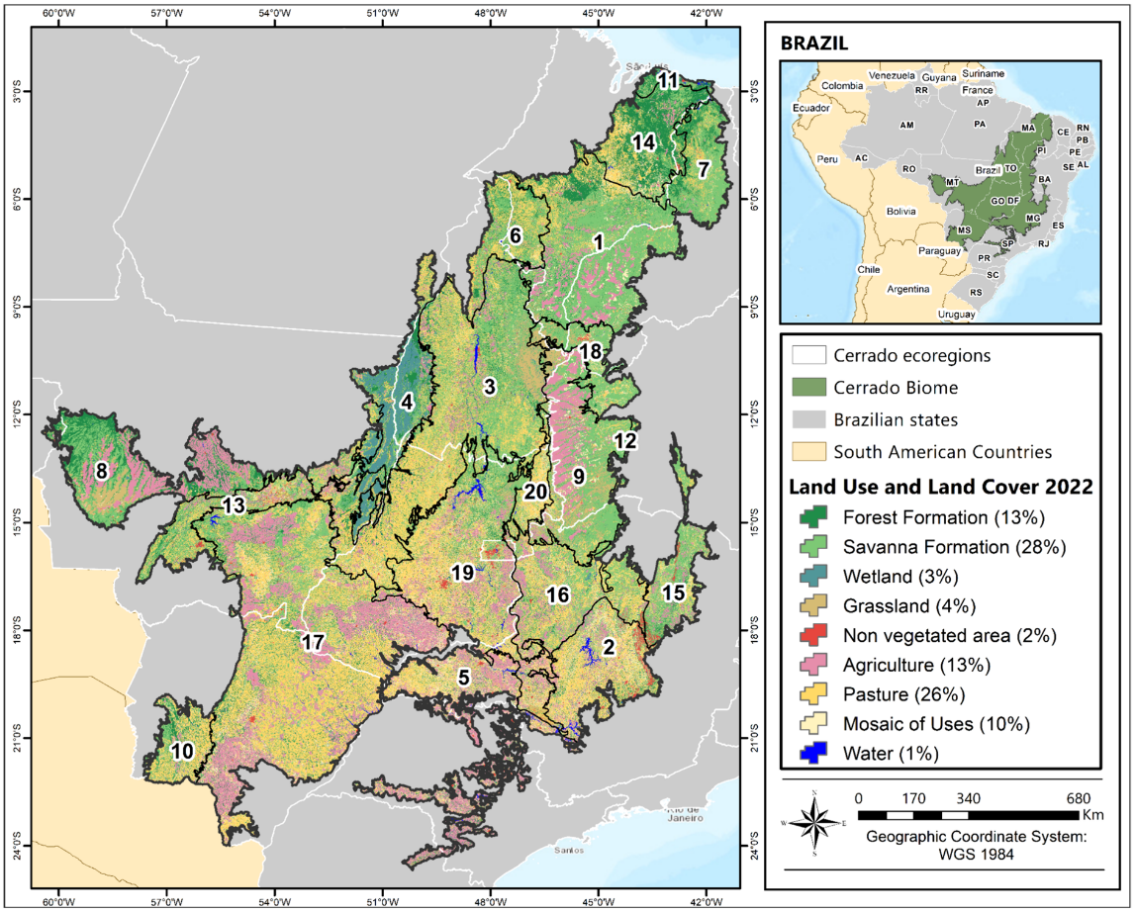

Figure 2.1: The location and limits of the Cerrado used in this thesis, defined by the Instituto Brasileiro de Geografia e Estatística (IBGE, Brazil's Geography and Statistics Institute) in 2019. Colours represent the different land use and land cover categories identified by the MapBiomas project (Collection 8.0 (Souza et al., 2020)). Black lines represent the different ecoregions of the Cerrado (Sano, Rodrigues, et al., 2019), identified with numbers: 1, Alto Parnaíba; 2, Alto São Francisco; 3, Araguaia Tocantins; 4, Bananal; 5, Basaltos do Paraná; 6, Bico do Papagaio; 7, Centro-norte Piauiense; 8, Chapada dos Parecis; 9, Chapadão do São Francisco; 10, Complexo Bodoquena; 11, Costeiro; 12, Depressão Cárstica do São Francisco; 13, Depressão Cuiabana; 14, Floresta de Cocais; 15, Jequitinhonha; 16, Paracatu; 17, Paraná Guimarães; 18, Parnaguá; 19, Planalto Central; 20, Vão do Paranã. Source: Silva Arruda et al. (2024).

Historically, fire was ignited by lightning and, later on, as human populations proliferated in South America, it was also ignited by humans (Cassino, Sabino, et al., 2023).

2.1.1 Brief overview of the evolution of the Cerrado in the Holocene (since circa 12,000 yrs BP)

Over 10,000 yrs BP, the extent of savannas and grasslands in eastern South America was much larger than present-day Cerrado. This larger extension is confirmed by evidence in the paleological records indicating the presence of savannas and grasslands in areas that are currently dominated by forests (Dantas et al., 2020), and by the presence of pockets of savannas and grasslands within currently forested areas (Dantas et al., 2020). This larger extension is also inferred from the evidence in the fossil record showing the presence of megafauna (mammals of very large dimensions, generally over 50 Kg (Dantas et al., 2020)) across South America (Dantas et al., 2020; Doughty et al., 2016).

Megafauna, and particularly mega-herbivores, have a big impact on ecosystems as they consume biomass and shape vegetation structure (Dantas et al., 2020). These large mammals can maintain the open structure of grassy ecosystems in regions that could otherwise sustain forests, playing a similar role to fire as biomass consumers (Bond and Keeley, 2005). Around 12,000-10,000 yrs BP, however, megafauna was in the process of extinction across South America, with archaeological evidence pointing at humans as a major cause (Prates et al., 2021). Humans have been present in South America since at least 15,000 yrs BP (Vialou et al., 2017), and population densities in central Brazil show a peak between 12,700 yrs BP and 8,800 yrs BP (Araujo, Correa, et al., 2025; Prates et al., 2021). Some authors relate this peak in human population precisely to their hunting of megafauna, whose extinction would have also prompted the decrease in human population (Prates et al., 2021).

Importantly, before their extinction, the densities of megafauna in present-day central Brazil has been estimated to have been larger than in Africa (Doughty et al., 2016). Different authors argue that, consequently, such drastic extinctions would have prompted profound transformations on the vegetation of the herbivory-maintained savannas (Dantas et al., 2020; Doughty et al., 2016; Johnson, 2009). Indeed, fossil records indicate increases in arboreal vegetation in many sites in South America following megafauna ex-

tinction (Behling, 2003). On the other hand, rather immediate surges in fire activity could have also followed megafauna extinction, as fire occurrence would have no longer been limited by megafauna vegetation consumption (Johnson, 2009; Dantas et al., 2020). Indeed, some studies have found evidence of no fire activity during the Late Pleistocene, with the first records of biomass burning being observed during the glacial-interglacial transition from 11,000 to 10,500 yrs BP (Escobar-Torrez et al., 2024).

Still, changes in the climate could provide an alternative explanation to the observed shifts in vegetation composition. Indeed, a wetter period took place in South America at the end of the Pleistocene (during the Younger Dryas, 12,900 to 11,700 yrs BP) (Escobar-Torrez et al., 2024). However, while this episode possibly contributed to vegetation changes towards more forested types, several authors insist that paleoclimate alone is unlikely to explain the replacement of most of these savannas by forests (Arruda et al., 2018; Dantas et al., 2020), and that megafauna extinction played a relevant role.

Throughout the Holocene, there were several episodes of rapid climate change (Araujo, Correa, et al., 2025). As a general trend, palynological studies support the hypothesis that there was a peak in moisture around 8,000 yrs BP, followed by dryness in the mid-Holocene until about 6,000-5,000 yrs BP, and a return of moisture in the Late Holocene (Araujo, Pilo, et al., 2006). However, these patterns of climate change seem to have varied across different regions in central Cerrado showing, in general, numerous fluctuations between wet and dry episodes (Araujo, Correa, et al., 2025). Overall, vegetation seems to have responded to the changes in rainfall and seasonality (Behling, 2003; Cassino, Ledru, et al., 2020; Salgado-Labouriau et al., 1997; Cassino, Sabino, et al., 2023), with Cerrado vegetation undergoing several episodes of expansion and retreat. Across different sites, vegetation became more arboreal in periods when rainfall increased, showing decreased or absent fire activity; while vegetation returned to more open grasslands during drier episodes, with increased fire activity as recorded by charcoal influx in the paleological records (Cassino, Sabino, et al., 2023; Escobar-Torrez et al., 2024; Cassino, Ledru, et al., 2020).

Overall, in the early Holocene until about 8,500 yrs BP, the landscape seems to have

been dominated by savannas and shrub woodlands (Behling, 2003). Over time, and following the aforementioned climatic fluctuations, grasslands and savannas gave way to tropical rainforest in the Amazonia and southeastern Atlantic region, as they became wetter (Behling, 2003); while they evolved into tropical dry forests in the transition area with present-day Caatinga in the east and northeast (Mota et al., 2019).

Between 8,000 and 2,000 yrs BP, a period sometimes referred to as the "Archaic Gap", human population density was generally low and unstable, appearing and disappearing from different areas (Araujo, Pilo, et al., 2006). Some authors argue that these fluctuations in human population were related to the rapid changes in the climate, rather than to the dry episodes *per se* (Araujo, Correa, et al., 2025). During this period, fire activity possibly had a natural cause and varied with the climate (Behling, 2003).

Human population started to increase steadily about 2,300 yrs BP, showing a major peak between 1,400 and 1,200 yrs BP (Araujo, Correa, et al., 2025), when it started conforming the modern indigenous population - like the Xavante and Xerente societies that occupied extensive areas of Cerrado (Klink and Moreira, 2002). Anthropological studies on indigenous groups show an active use of fire throughout the dry season for different purposes (see Section 2.1.5 for a more detailed explanation). Interestingly, studies in present-day Minas Gerais report a high fire activity period around 1,600 yrs BP burning arboreal vegetation (Cassino, Sabino, et al., 2023) that was not coincident with a dry event, while it did coincide with the arrival of ceramists-horticulturalists (Araujo, Correa, et al., 2025). Therefore, these late peaks in fire activity were most likely related to humans.

Indigenous population subsequently plummeted with the arrival of European colonisers (Araujo, Correa, et al., 2025). Furthermore, colonisers established bans to the use of fire to, among other reasons, ensure wood supply for shipbuilding (Pivello et al., 2021). More recently, the modern occupation of the Cerrado started from the south, in the area of São Paulo (Klink and Moreira, 2002).

Thus, present-day Cerrado and surrounding areas have dynamically changed over the Holocene, evolving in response to climate, megafauna extinction and, more recently, to

human expansion across the Cerrado. In particular, authors argue that megafauna extinction probably has had long-lasting legacy effects, and that Cerrado may still be experiencing changes in relation to it (Dantas et al., 2020; Doughty et al., 2016). As such, current Cerrado is the result of processes of change whose consequences are probably still ongoing.

Cerrado vegetation has responded to these changes or disturbances by adapting to new climatic conditions and to changes in herbivory consumption and in fire regimes (Araujo, Correa, et al., 2025). Furthermore, on the long run, such dynamism has probably contributed to the high levels of biodiversity and endemism of the Cerrado, and to its extraordinary heterogeneity. Still, overall, these perturbations and the consequent vegetation responses took place on scales of hundred to thousands of years. Furthermore, however drastic, none of this changes caused the immediate conversion of large tracts of Cerrado vegetation - as is the case of the recent anthropic expansion over the Cerrado that we will discuss in the next section.

2.1.2 Recent patterns of land use expansion

One of the striking characteristics of the current Cerrado is the large-scale level of land use conversion taken place over the past six decades (Sano, Rosa, et al., 2010; Alencar, Z. Shimbo, et al., 2020; Jepson et al., 2010; Grecchi et al., 2013; Espírito-Santo et al., 2016). Moreover, the rates of Cerrado conversion have often been faster than those of deforestation in the Amazon rainforest (Machado, 2016; Soterroni et al., 2019; Machado et al., 2024). However, despite its ecological importance, Cerrado conversion has attracted much less attention in the media and this region is less protected than the Amazon rainforest (Soterroni et al., 2019). As a consequence, the patterns of human land uses are an important aspect of the Cerrado, profoundly affecting its ecology, hydrology, and fire regimes (Silva Arruda et al., 2024; Silva, Nogueira, et al., 2021).

In the 1960s, the capital city of Brazil was established in Brasília, a newly-constructed city in the interior of the Cerrado (Soares-Filho et al., 2014). This event, accompanied by economic development policies from the Brazilian government, triggered the expansion

of agricultural lands and human settlements in the Cerrado (Soares-Filho et al., 2014). Given its proximity to the two major urban centres of Brazil, São Paulo and Rio de Janeiro, this conversion to agriculture started in the south, rapidly advancing towards the centre and, later, the northern areas of the Cerrado (Gottsberger et al., 2006). At first, Cerrado vegetation was primarily converted to pastures for cattle ranching. In the 1990s and 2000s, however, Cerrado was increasingly converted to commercial croplands, primarily soybean, sugarcane, corn and cotton (Rekow, 2019). In addition, since the 2000s, most of the Cerrado conversion took place in the Matopiba region, an area in the north of the Cerrado comprising parts of the Brazilian states of Maranhão, Tocantins, Piauí and Bahía (Machado et al., 2024). The Matopiba is where Cerrado conversion is currently most active (Machado et al., 2024), in part because most of the southern areas of the Cerrado have already been converted, especially the regions that are not formally protected.

Apart from the development policies, the low protection levels of the Cerrado also facilitated this rapid large-scale agricultural expansion. For example, Brazil's Forest Code requires only 20% of the native vegetation in a private land in the Cerrado to be preserved, while in the Amazon this requirement is of the 80% (Klink and Machado, 2005). Further, in 2006 a Soy Moratorium - an agreement prohibiting the commercialisation of soy grown in recently deforested land (Soterroni et al., 2019) - was approved for the Amazon, but it has not yet been extended to the Cerrado (Soterroni et al., 2019). Currently, only about 3% of the Cerrado is under strict protection, with a further 4% of its area classified as indigenous lands and 5% classified as areas for sustainable use (Carranza et al., 2014).

This rapid large-scale conversion has flagged the Cerrado as an urgent area for conservation, as it threatens its high levels of biodiversity and endemism (Myers et al., 2000). Further, studies warn about the wider effects of large-scale conversion on the hydrological cycles of the Cerrado (Spera et al., 2016), as well as on its large quantities of carbon stored in above- and below-ground biomass and in the soil (Bustamante et al., 2012).

Crucially, the speed and large scale of these land use transformations, together with the speed of current anthropic climate change, are in striking contrast with the previous disturbances that affected the Cerrado during the Holocene.

2.1.3 Current climate

The Cerrado has a tropical climate classified as Aw by the Köppen climate classification (Nascimento et al., 2020). The most relevant climatic characteristic is its strong seasonality, with a wet season from October to April (austral summer), and a dry season from May to September (austral winter). This seasonality is influenced by a confluence of air masses, primarily an Equatorial air mass coming from the Amazon region, generated by the rainforest evapotranspiration and water bodies (Nascimento et al., 2020), that causes the summer's rains; and a tropical air mass from the Atlantic that brings hot and dry air after traversing various topographical barriers, associated with the winter's dry season. As a consequence, the Cerrado presents a longitudinal gradient of precipitation increasing from east to west, varying between 800 mm and over 1,800 mm on average per year (Nascimento et al., 2020; Silva Arruda et al., 2024). The annual average temperatures of the Cerrado vary between 18°C and 28°C. Even though there is no strong temperature variation between the wet and dry seasons, the latter presents higher maximum temperatures on average in relation to the lower cloud formation and higher insolation during this period. In addition, Cerrado temperatures also show a latitudinal gradient increasing from the south towards the Equator in relation to the angle of solar radiation (Nascimento et al., 2020).

Over the past few decades, the temperatures of the Cerrado have been increasing in relation to anthropic climate change (Hofmann, Cardoso, et al., 2021), causing decreases in relative humidity and increases in vapour pressure deficit (VPD) (Hofmann, Cardoso, et al., 2021) - a measure of the drying capacity of the air -, along with generalised increases in evapotranspiration (Oliveira, Nearing, et al., 2014). Using data from climate re-analysis models, some studies report decreases in the dry season rainfall since the 1960s, particularly at the beginning of the dry season, in relation to changes in atmospheric circulation (Hofmann, Silva, et al., 2023). Therefore, the evidence indicates that the climate of the Cerrado is getting warmer and drier with climate change (Hofmann, Cardoso, et al., 2021), which expected to increase, in turn, the risk of fire occurrence under all Representative Concentration Pathways (RCP) of the International Panel for Climate Change

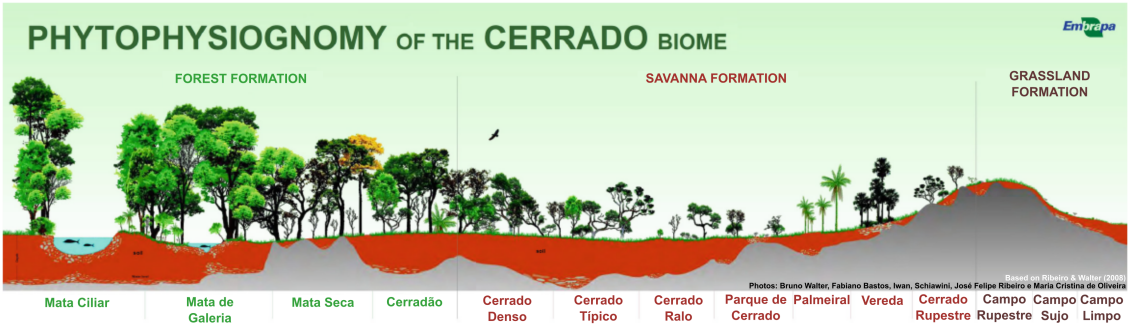

Figure 2.2: The different vegetation physiognomies of the Cerrado. Adapted from Ferreira et al. (2023), in turn adapted from Ribeiro and Walter (2008).

(IPCC) (Silva, Bastos, et al., 2019).

2.1.4 Current vegetation

The varied vegetation of the Cerrado comprises grasslands, savannas and forest formations (Ribeiro and Walter, 2008). Within each of these groups, there are in turn different types of vegetation physiognomies (Figure 2.2) presenting different structure, vegetation growth-forms, species composition, and other environmental factors like the soil composition, availability of water and nutrients, the occurrence of fires, or climatic characteristics (Ribeiro and Walter, 2008; Oliveira-Filho et al., 2002; Henriques et al., 2002). Even though the dominating vegetation form is that of a savanna with a grass layer and a varied but generally scarce tree cover (savanna *censu lato*) (Oliveira-Filho et al., 2002), Cerrado vegetation usually varies continuously in the scale of meters to kilometers between the different physiognomies. As a consequence, a typical Cerrado landscape is a matrix or mosaic of different vegetation types (L. Dantas et al., 2013).

Despite the predominance of savanna ecosystems across the Cerrado, we can distinguish certain areas with distinct dominant vegetation formations (Sano, Rosa, et al., 2010) (see Figure 2.1). The northern parts of the Cerrado, which in the past have sometimes been excluded from its official geographical limits (Vieira et al., 2022), are mostly dominated by forest formations, comprising both rainforest and dry forests (Sano, Rosa, et al., 2010). In the centre-west of the Cerrado, there is a seasonally-flooded region of savanna ecosys-

tems (Marimon et al., 2012), and there are patches dominated by grasslands in the eastern areas of the state of Tocantins (Alencar, Z. Shimbo, et al., 2020). Finally, along the border with the Amazon there is generally an ecotonal gradient of vegetation, especially in the western-most part of the Cerrado (Morandi et al., 2020; Marques et al., 2020).

This characteristic mosaic of generally open ecosystems is the result of a confluence of factors, including the seasonal climate, soil fertility, fire regime and the climatic and natural history of the Cerrado (Oliveira-Filho et al., 2002). Even though, the Cerrado's climate is considered to be moist enough to sustain forest formations despite the seasonal precipitation and generally low soil fertility (Franco, 2002), the periodic occurrence of fire has been signaled as a determining factor contributing to creating and maintaining the mosaic (L. Dantas et al., 2013). As we have seen, fire acted as an evolutionary force for Cerrado vegetation prompting species from nearby biodiverse fire-free ecosystems to develop varied adaptation strategies to this disturbance agent (Simon and Pennington, 2012) - including thick barks, underground organs and deep roots, fast resprouting capacity, or fire-stimulated flowering and germination (Miranda, Bustamante, et al., 2002). This process facilitated the expansion of the Cerrado and is also argued to explain its rich biodiversity (Simon and Pennington, 2012), as well as the small patches of fire-sensitive species that remain scattered across this region.

Vegetation adaptations to fire

In the Cerrado, different types of vegetation present different adaptations to fire that protect them from this disturbance or allow them to take advantage of this phenomenon (Pivello et al., 2021). The soil generally acts as an insulation layer against the temperature increase caused by the passage of fire (Coutinho, 1990; Pivello et al., 2021), and vegetation has developed fire adaptation strategies that take advantage of this fact. Soil heating caused by fires depends on the intensity of the fire, as well as on the soil's own moisture content (Mistry, 1998). In general, the greater the fuel load, the higher the temperatures that can be attained by the fire and the longer the residence time of the fire, as well as the larger the amount of ashes deposited on the surface, which can cause larger rises in soil

temperature (Coutinho, 1990). However, since savanna and grassland fires are usually fast and low intensity, the increase in soil temperature generally affects the most superficial layers (Mistry, 1998).

The species most resistant to fire are found among the herbaceous and undershrub flora (Coutinho, 1990), which present a wide variety of adaptations to this disturbance agent. For example, some species with annual life cycles avoid fire because they are in the form of seeds during the dry season and grow during the wet season (Coutinho, 1990). On the other hand, many perennial species present different underground structures - where they are protected from fire - such as bulbs, underground shoots, rhizomes and xylopodia that allow plants to survive fire (Coutinho, 1982). In particular, xylopodia are thick woody organs that store nutrients and can present dormant buds close to the soil surface from which plants can resprout (Coutinho, 1982) - which they can do just a few hours to days after a fire. Other woody species in the herbaceous layer protect themselves against fire by developing dense underground systems of trunks and branches, while presenting only a few branches and sprouts aboveground (Mistry, 1998).

Fire triggers flowering in many herbaceous and undershrub flora species, which can take place only a few days to weeks after the burn (Oliveira, Batista, et al., 1996). This strategy allows flowers, fruits, seeds and seedlings to escape fires and facilitates cross-pollination as a result of plants flowering at the same time (Coutinho, 1990). Finally, fire can also promote the germination of certain species for which the high temperatures crack the seeds' coats, allowing the later penetration of water into the seed (Coutinho, 1990).

Regarding Cerrado woody plants, fire rarely kills established individuals (Mistry, 1998). Most adult individuals of Cerrado tree species present thick barks in the trunk and branches that isolate the internal tissues protecting them from the fires' high temperatures (Medeiros and Miranda, 2008). Furthermore, these thick barks also protect buds, which allow the plant to resprout from branches (Medeiros and Miranda, 2008; Mistry, 1998). This process results in a symposial growth of the branches that gives rise to the characteristic tortuosity of Cerrado trees (Mistry, 1998).

2.1.5 Fire

In the savanna-like ecosystems of the Cerrado, fires are usually low intensity and fast spreading. Such fires generally consume the surface layer of the vegetation (Miranda, Bustamante, et al., 2002), formed of grasses and the non-woody part of shrubs, and do not necessarily affect the tree canopy (Mistry, 1998). Still, fire behaviour and vegetation consumption depend on the type of vegetation physiognomy (Miranda, Bustamante, et al., 2002) and weather conditions (Mistry, 1998).

Crucially, vegetation physiognomy affects fire behaviour because the structure of the vegetation and its composition determine the abundance and distribution of the fuel, and influence its moisture content (Kauffman et al., 1994). Often, denser forms of Cerrado savannas where grasses and shrubs connect with the tree canopy can experience intense fires because the different vertical layers of fuel are connected. On the other hand, patches of closed tree canopy seldom experience fire due to the absence of fuel on the surface layer and a generally moister understorey (Miranda, Bustamante, et al., 2002). Further, especially in the more open physiognomies, time since last burn also influences fire behaviour due to fuel accumulation during fire free periods (Fidelis et al., 2018). Generally, fires will burn with more intensity after long periods without fire than when they occur regularly (Miranda and Miranda, 1993).

Regarding weather conditions, the timing of fires during the dry season also affects fire behaviour. At the beginning of the dry season, vegetation still has high moisture contents, so fires tend to be patchy and have low intensity (Miranda and Miranda, 1993). As the dry season progresses and the fuel dries out, fires have higher intensity and are more homogeneous, peaking in the late dry season (Coutinho, 1990).

Ecological effects of fire regimes

The ecological effects of fires on Cerrado vegetation depend on fire behaviour (Henriques et al., 2002), the timing of fires during the growing cycle (Henriques et al., 2002) and, particularly, vegetation adaptations to fire (Hoffmann and Moreira, 2002). Other factors

such as subsequent rainfall (Henriques et al., 2002; Konduri et al., 2023) and herbivory pressure (Henriques et al., 2002) also influence the fires' ecological effects.

Fire plays an important role on nutrient cycling in the Cerrado (Coutinho, 1990; Oliveras et al., 2013), where soils are generally poor and acidic (Mistry, 1998). Through ash deposition, fires result in a temporary increase in nutrients on the soil surface layers that accelerates nutrient cycling by causing a shift of nutrient allocation from trees and shrubs to the herbaceous vegetation (Coutinho, 1990; Oliveras et al., 2013). However, studies have also shown that a large amount of nutrients are lost in the form of smoke during fires (Coutinho, 1990).

Several studies experimenting with fire exclusion or with increased fire frequencies have demonstrated that the behaviour and frequency of fire can shape vegetation structure and composition favouring certain types of vegetation (Pivello et al., 2021; Pinheiro et al., 2009; Klink and Moreira, 2002). On the one hand, periodic fires favour the establishment of grasses and herbs against trees (Medeiros and Miranda, 2008). While adult tree individuals are more prepared to survive fire, seedlings, saplings and younger individuals are vulnerable to fires (Medeiros and Miranda, 2008; Hoffmann, 1996). Thus, fire can prevent tree establishment (Medeiros and Miranda, 2008) or hamper tree growth preventing saplings from developing completely, which has been referred to as the "fire trap" (Stevens et al., 2017). However, high fire frequencies can eventually affect the adult specimens too as nutrients can become insufficient after their repeated requirement for tree recovery, resulting in less new sprouts and tree death (Medeiros and Miranda, 2008). In this sense, it has been demonstrated that frequent fires diminish the diversity of Cerrado woody species (Mistry, 1998).

On the other hand, suppression of fires for long periods (e.g. a few decades) favours the establishment of trees leading to forested ecosystems (Pivello et al., 2021) - a process termed as woody encroachment (Rosan, Aragão, et al., 2019). As trees grow and the canopy becomes more closed, light-demanding grasses and herbs start to disappear (Pivello et al., 2021). As these vegetation types are the most abundant in Cerrado ecosystems, their disappearance leads to acute losses in biodiversity, even if there are increases in di-

versity among tree species (Abreu et al., 2017). Furthermore, studies found that these fire-free periods can also have negative effects on Cerrado tree specialists: even if established individuals may survive, their seedlings have been found to be almost absent in these encroached forests, which will eventually lead to their disappearance from these sites (Abreu et al., 2017). Furthermore, in the process of encroachment, fuel buildup can lead to larger and more intense fires when these disturbances occur (Fidelis et al., 2018). These more severe fires can have negative consequences on fire-adapted species if their protective adaptations (e.g. thick bark, protected buds) become insufficient.

Therefore, both very frequent fires and the complete absence of fires bring about profound changes to Cerrado ecosystems and imply biodiversity losses. Currently, such extreme fire frequencies, both low and high, are widely observed across the Cerrado (Pivello, 2011; Pivello et al., 2021) in association with modern human activities and fire management policies (Pivello, 2011), as we will see in more detail in the next section. As these fire frequencies are associated with modern human activities and Cerrado species do not seem to be well adapted to them, such patterns of fire are considered to be alterations with respect to those fire regimes to which Cerrado vegetation would be typically adapted (Pivello et al., 2021). Furthermore, if these changes happen at large scales, they may lead to the loss of the vegetation mosaic that characterises the Cerrado and that enhances its biodiversity (Pivello et al., 2021).

It is for these reasons that Cerrado ecologists and conservationists insist on the importance of regulating with policies the use of fire in the Cerrado, as well as on the need to implement conservation plans that do not simply suppress all fires (Mistry, Bilbao, et al., 2016; Mistry, Schmidt, et al., 2019; Durigan, 2020). Overall, Cerrado ecologists recognise that fire management is a complex task that still has many unresolved questions (Pivello et al., 2021). Further, fire management decisions and action plans will inevitably target certain goals (be it enhancing biodiversity or certain ecosystem services) and, consequently, may have trade-off effects (Pivello et al., 2021). In any case, currently, there is agreement that fire prevention is definitely not a conservation goal in fire-adapted ecosystems (Mistry, Bilbao, et al., 2016; Mistry, Schmidt, et al., 2019; Durigan, 2020; Klink and Machado,

2005; Pivello et al., 2021). Rather, as some Cerrado ecologists put it, the question now is, with Cerrado conservation in mind, whether fires should be allowed to occur only if caused by lightning, or if a certain degree of prescribed fires should be used (Pivello et al., 2021).

Anthropic uses of fire

Even though lightning is a common cause of fire in savanna-like ecosystems of Brazil (Menezes et al., 2022; Schumacher, 2022), most fires in the Cerrado occur in relation to humans (Pivello et al., 2021). The range of different human communities and their diverse uses of fire deserves a brief introduction that will support the interpretation of the patterns of fire observed across the Cerrado.

Indigenous peoples in the Cerrado use fire for a variety of purposes including hunting, stimulating vegetation regeneration and fruit production, clearing areas for planting or as a protection against more intense fires (Mistry, Berardi, et al., 2005). In these practices, fires are set throughout the dry season (Melo et al., 2011), depending on the purpose (Mistry, Bilbao, et al., 2016). These uses of fires are planned by the community and based on in-depth knowledge about the fire ecology of the ecosystems where these communities live (Mistry, Berardi, et al., 2005; Mistry, Schmidt, et al., 2019), transmitted orally through generations (Mistry, Berardi, et al., 2005; Melo et al., 2011; Pivello, 2011). Similarly, although less well studied, fire is also used by non-indigenous traditional communities for pastoral management (Eloy et al., 2019). Among these, the *quilombola* communities stand out, formed by descendants of the African diaspora (Eloy et al., 2019). These communities also use fire at different times during the dry season, primarily for vegetation regrowth in pastures. Therefore, both traditional uses of fire by indigenous people and by traditional pastoral communities create a mosaic of patches with different fire histories (Mistry, Bilbao, et al., 2016; Eloy et al., 2019) argued to help maintain the heterogeneous vegetation of the Cerrado (Welch et al., 2013).

On the other hand, nowadays, most fires are assumed to be started in relation to modern industrial agricultural activities, either for cattle-ranching to renew pastures, in shifting

cultivation or to burn residues (Pivello, 2011). Often these activities cause large numbers of ignitions and generate high fire frequencies (Pivello, 2011). In addition, most of these fires are ignited in the late dry season (Pivello et al., 2021; Mataveli et al., 2018). However, modern agricultural activities can also decrease fire frequency by actively extinguishing fires or introducing fuel discontinuities in highly fragmented landscapes (Archibald, 2016). Finally, even though fire is often used in the conversion of native rainforests across Brazil (Brando et al., 2020), and it has often been assumed to be used in the conversion of Cerrado native vegetation (Pivello, 2011), recent studies show a rather limited use of fire in Cerrado vegetation conversion (Ribeiro, Santos, et al., 2024). The use of fire seems to be particularly limited in the conversion of savanna and grasslands, either to croplands and pastures, while its use seems more common in the conversion of forest vegetation growth-forms within the Cerrado (Ribeiro, Santos, et al., 2024).

Until very recently, the policies governing the use of fire across Brazil were those of "zero fire" (Durigan, 2020; Pivello et al., 2021), irrespective of the type of ecosystem. These policies have been common since colonial times (Pivello et al., 2021), further reinforced by the use of fire in rainforest deforestation and misconceptions about the role of this disturbance agent in savannas and grasslands (Durigan, 2020). However, as the study of Cerrado ecology and tropical savannas advanced throughout the second half of the nineteenth century, the ecological importance of fire began to be understood (Durigan and Ratter, 2016). In particular, experiments that completely restricted fire occurrence showed negative impacts on Cerrado vegetation, such as losses in biodiversity and the heterogeneous mosaic of the Cerrado (Durigan and Ratter, 2016). In addition, these changes in the structure of the vegetation led to fuel accumulation and increased risk of larger and more intense fires (Fidelis et al., 2018). Simultaneously, other studies started to explore the impacts of prescribed fire regimes, observing positive effects on these ecosystems (Miranda, 2010). Over the past couple of decades, there has been an increasing number of projects raising awareness about the ecological role of fire, practicing prescribed burns that build on traditional knowledge, and preventing irregular burning (Schmidt, Moura, et al., 2018; Mistry, Bilbao, et al., 2016; Mistry, Schmidt, et al., 2019; Eloy et al., 2019). In light of

these initiatives and the increasing recognition of traditional uses of fire (Mistry, Schmidt, et al., 2019), since the 2000s there has been a push to (re)introduce the use of fire to manage Cerrado protected areas for conservation. These practices are usually grouped under the term Integrated Fire Management (IFM), which was eventually included in the 2012 Brazilian New Forest Code (Pivello et al., 2021). Finally, very recently, a new Brazilian National Policy on IFM (Lei 14,944, 31st July 2024) has been adopted that considers the use of fires by local communities, promotes the use of prescribed burns for conservation and regulates the use of fire for agricultural practices (Schmidt and Eloy, 2020).

2.2 On humans and the climate as main drivers of the burned area of tropical savannas

The growing availability of remote sensing data products with increasingly longer times series, especially from the 2000s, has allowed the characterisation of global patterns of burned area and their changes in time (Werf, Randerson, Giglio, Gobron, et al., 2008). Since then, many studies have noted that most of the world's burned area is concentrated in regions with intermediate levels of precipitation and productivity, and with a long enough dry season (Werf, Randerson, Giglio, Gobron, et al., 2008; Archibald, Roy, et al., 2009; Aldersley et al., 2011), particularly in tropical and subtropical savanna ecosystems (Werf, Randerson, Giglio, Gobron, et al., 2008; Archibald, Roy, et al., 2009; Andela, Morton, Giglio, Chen, et al., 2017). However, studies also noted that global burned area decreased in the past few decades despite climate change, driven precisely by declines in tropical and subtropical savannas' burned area (Figure 2.3) (Andela, Morton, Giglio, Chen, et al., 2017; Wu et al., 2022; Jones et al., 2022).

Because the climate is a major driver of fire, these apparently contradicting processes have been an area of active research. Studies exploring climatic effects found that relations between rainfall or seasonality and burned area were often poor in tropical and subtropical savannas, pointing at the relevance of human factors acting as fire controls (Werf, Randerson, Giglio, Gobron, et al., 2008; Archibald, Roy, et al., 2009). Among

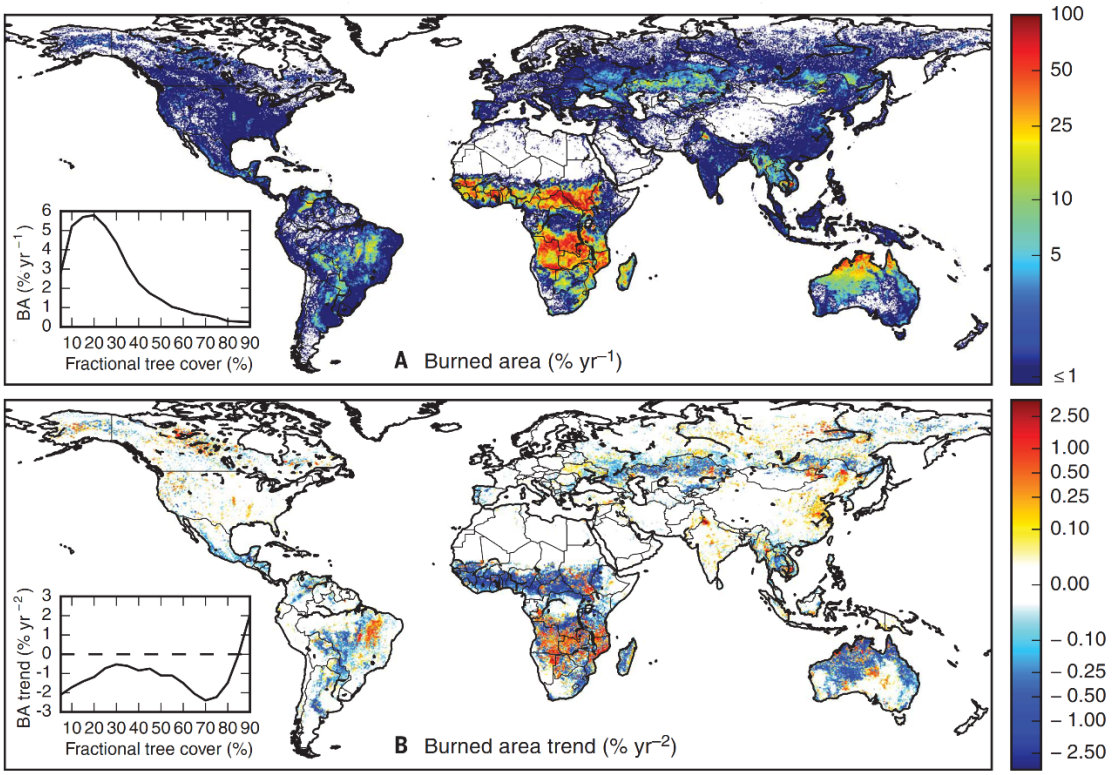

Figure 2.3: **a** Average annual burned area and, **b** trends in burned area between 1998 and 2015. Maps showing the highest levels of burned area in tropical savannas and grasslands, as well as decreases in burned area in some of these savannas (e.g. in the African northern hemisphere). Maps derived using data from the Global Fire Emissions Database version 4 (Werf, Randerson, Giglio, Leeuwen, et al., 2017). Source: Andela, Morton, Giglio, Chen, et al. (2017).

these factors, landscape fragmentation as a consequence of land use expansion was identified as a major driver of declines in savanna burned areas (Archibald, Scholes, et al., 2010; Archibald, Nickless, et al., 2010; Aldersley et al., 2011; Andela and Werf, 2014; Archibald, 2016; Andela, Morton, Giglio, Chen, et al., 2017; Haas et al., 2022), primarily in relation to the introduction of fuel discontinuities, along with other factors such as active fire suppression (Archibald, Roy, et al., 2009).

Disentangling the effects of landscape fragmentation and the climate is complex, especially since their interaction seems to vary regionally (Andela and Werf, 2014). For example, in savannas of the African northern hemisphere, declines in burned area are associated with combined effects of land use expansion and changes in rainfall patterns

(Andela and Werf, 2014); while in the southern hemisphere, upward trends in burned area are related to rainfall changes (Andela and Werf, 2014), although these climatic effects seem to be constrained by the level of human impact (Archibald, Nickless, et al., 2010; Andela and Werf, 2014).

In the Brazilian Cerrado, similar dynamics have been observed, where the expansion of landscape fragmentation is concomitant to declines in burned area (Rosan, Sitch, et al., 2022; Silva Arruda et al., 2024), while burned area increases are concentrated in regions with the largest remnants of native vegetation (Mataveli et al., 2017; Silva, Rodrigues, et al., 2020; Silva, Nogueira, et al., 2021; Silva Arruda et al., 2024) and correlated with temporal increases in fire weather (Silva, Rodrigues, et al., 2020). However, there seems to be an unresolved question regarding the fact that agricultural expansion, which is prevalent across the Cerrado, is correlated with decreases in burned area in some regions, but correlated with burned area increases in others (Silva, Rodrigues, et al., 2020; Silva, Nogueira, et al., 2021; Silva Arruda et al., 2024). Often, the simultaneous positive trends in burned area and in land use area have been related to the use of fire in Cerrado's native vegetation conversion (Silva, Rodrigues, et al., 2020). However, recent studies point at limited changes in fire activity during conversion of Cerrado's savannas and grasslands to pastures or croplands, except in the case of forest conversion (Ribeiro, Santos, et al., 2024). Finally, studies on Cerrado's burned area have usually characterised climatic and land use effects separately (Mataveli et al., 2017; Mataveli et al., 2018; Silva, Rodrigues, et al., 2020; Silva, Nogueira, et al., 2021; Silva Arruda et al., 2024), and few studies have considered their combined effects (Conciani et al., 2021). Interestingly, Conciani et al. (2021) found no strong relation between rainfall and the burned area of some protected areas, while the explanatory power of their model increased when including human factors. They suggested that human influence buffered the relation between climate and fire (Conciani et al., 2021).

Therefore, evidence points at a non-trivial relation between the effects of the climate and land uses on burned area in the Cerrado and other tropical savannas, suggesting human controls may hinder climatic effects (Conciani et al., 2021; Andela and Werf, 2014;

Archibald, Nickless, et al., 2010). However, further research is required to understand to what extent, and how, landscape fragmentation limits burned area responsiveness to climate in the Cerrado, and whether such controls act similarly for different climatic variables.

2.3 On the quantification of fire regimes and their changes through time

The occurrence of fire and its behaviour depends on the climate and type of vegetation (Archibald, Lehmann, Belcher, et al., 2018), as well as edaphic factors, topographic characteristics and the presence of human activities (Keeley and Syphard, 2019). As such, the frequency and characteristics of fires vary across the globe (Archibald, Lehmann, Gómez-Dans, et al., 2013; Chuvieco, Giglio, et al., 2008; Pais et al., 2023), and have also varied through time (Bowman et al., 2009; Keeley and Pausas, 2022). The patterns of fire that typically occur in a certain area over a period of time are known as fire regimes (Krawchuk et al., 2009; Archibald, Lehmann, Gómez-Dans, et al., 2013), and are usually quantified in terms of burned area, frequency, seasonality, fire size and intensity, or the shape of the fires (Martin et al., 1992). From an ecological perspective, analyses of fire regimes are very valuable because both the behaviour of a single fire and its impacts on the vegetation can only be fully understood or accounted for taking into consideration the current and historical patterns of fire of the ecosystem (Pivello et al., 2021).

Burned area is extensively used in the literature because it is a direct indication of the extent of fire occurrence, and it is readily obtained from many remote sensing products (Giglio, Boschetti, et al., 2018; Chuvieco, Englefield, et al., 2008). However, the development and refinement of geospatial data techniques to extract information at individual fire level (Archibald and Roy, 2009; Andela, Morton, Giglio, Paugam, et al., 2019; Laurent et al., 2018; Finco, 2012) has opened the avenue to characterise fire regimes altogether (Chuvieco, Englefield, et al., 2008; Archibald, Lehmann, Gómez-Dans, et al., 2013). Indeed, there is an increasing number of studies characterising fire regimes at regional

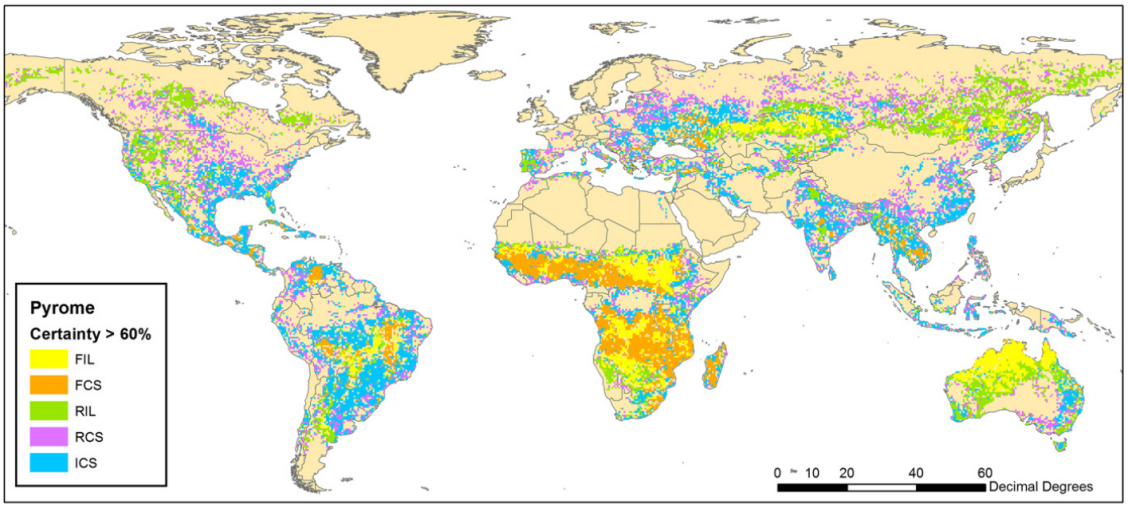

Figure 2.4: Distribution of different fire regimes at a global scale by a pioneering study mapping fire regimes using a clustering algorithm (Archibald, Lehmann, Gómez-Dans, et al., 2013). The map highlights five different fire regimes depending on the characteristics of the fires in each 0.5° grid cell in the period 1997 to 2010. Classification used data from the Global Fire Emissions Database version 3.1 (Werf, Randerson, Giglio, Leeuwen, et al., 2017), and the Moderate-resolution Imaging Spectroradiometer (MODIS) MCD45A1 (Araújo et al., 2015). The names of the fire regimes indicate their main characteristics: FIL, frequent-intense-large fires; FCS, frequent-cool-small fires; RIL, rare-intense-large fires; RCS, rare-cool-small fires; ICS, intermediate-cool-small fires. Source: Archibald, Lehmann, Gómez-Dans, et al. (2013).

(Cattau et al., 2022; Boulanger, Gauthier, Gray, et al., 2013; Elia et al., 2022), continental (Archibald, Scholes, et al., 2010; Galizia, Barbero, et al., 2023) and global scales (Archibald, Lehmann, Gómez-Dans, et al., 2013; Pais et al., 2023; García et al., 2022; Chuvieco, Englefield, et al., 2008), covering different periods of time (see for example Figure 2.4). These studies are allowing to understand the complexity of fire dynamics, the trade-offs between fire characteristics, and how these different characteristics are shaped by the climate, vegetation and human activities (Archibald, Lehmann, Gómez-Dans, et al., 2013). At a global scale, there are some general patterns, with regimes of frequent fires overlapping with tropical savannas and grasslands (Figure 2.4), while fires are generally infrequent across the arctic boreal regions (Archibald, Lehmann, Gómez-Dans, et al., 2013; Pais et al., 2023). However, these same studies also find that fire regimes imperfectly correspond to unique climates and vegetation types (Archibald, Lehmann, Gómez-Dans, et al., 2013; Pais et al., 2023), pointing at the role of other factors shaping

fire occurrence. The importance of these factors is further supported by regional studies, which provide more nuanced accounts of differences in fire regimes, especially uncovering contrasting dynamics at small scales (Cattau et al., 2022; Boulanger, Gauthier, and Burton, 2014; Elia et al., 2022; Galizia, Curt, et al., 2021; Silva, Nogueira, et al., 2021).

Ecosystems adapted to fire, like most of the ecological communities in the Cerrado, are actually adapted to certain patterns of fire frequency, intensity, severity, size distribution or seasonality, apart from burned area (Keeley and Pausas, 2022). That is, these ecosystems are adapted to a certain fire regime and it is the overall deviation from these patterns that can generate changes to the vegetation composition and structure (Pivello et al., 2021). Even though the characteristics of the natural fire regimes of the Cerrado remains an open question, the study of the current patterns of fire and how they are related to, and are changing with, climatic and human factors can allow a better understanding of the processes undergoing these savannas.

Until now, studies on the fire regimes of the Brazilian savannas have used the Cerrado's ecoregions (Sano, Rosa, et al., 2010) to study the spatial patterns of fire regimes (Silva, Nogueira, et al., 2021; Silva Arruda et al., 2024). Across the Cerrado, these studies have found that the different ecoregions present remarkable differences when considering different characteristics of fire individually (Silva Arruda et al., 2024), and when considering fire regimes as a whole (Silva, Nogueira, et al., 2021). These studies show an overall tendency of some ecoregions to concentrate large, frequent and intense fires, while other ecoregions present small, infrequent and cool fires (Silva, Nogueira, et al., 2021). In addition, the ecoregions with the latter patterns of fire are concentrated in the south of the Cerrado, where both the presence of humans and the landscape fragmentation are very high. In this sense, the fire regimes of the Cerrado seem to vary across a gradient of human land use intensity (Silva, Nogueira, et al., 2021; Rosan, Sitch, et al., 2022; Mataveli et al., 2018; Konduri et al., 2023), similarly to the patterns of fire observed in the southern African savannas (Archibald, Scholes, et al., 2010).

The ecoregions in which the Cerrado has been divided were identified based on rainfall patterns, topographic features, soil characteristics, land use and land cover, and conser-

vation units and indigenous lands (Sano, Rodrigues, et al., 2019). All of these variables are factors that affect the occurrence and behaviour of fire, so the characterisation of their fire regimes contributes to understanding the spatial patterns of fire across the Cerrado. However, the regions of the Cerrado with different fire regimes - henceforth fire regime regions - may not necessarily correspond geographically to these ecoregions. This may be because of the inherent heterogeneity of environmental characteristics within the ecoregions, or because of the similarity in patterns of fire between areas belonging to different ecoregions (Silva, Nogueira, et al., 2021). Furthermore, the climate and land use area of the Cerrado have experienced profound changes over the past five decades (Alencar, Z. Shimbo, et al., 2020; Hofmann, Cardoso, et al., 2021; Hofmann, Silva, et al., 2023). As a consequence, both the characteristics of the fire regimes (i.e. fire size, frequency, intensity, seasonality, etc.) and their geographical limits may have also changed over time. However, no studies so far have characterised the fire regime regions of the Cerrado without assuming spatial boundaries *a priori* nor studied how these may have changed. This constitutes a clear gap in the literature on the fire regimes of the Cerrado. Further, first delineating the fire regime regions, and only later studying their environmental characteristics, can help identify the main factors that explain the differences and similarities between the fire regime regions (Archibald, Lehmann, Gómez-Dans, et al., 2013).

2.4 On the causes of fire ignitions and their associated fire regimes

Lightning has been the main cause of fires for millions of years before the appearance of humans (Scott, 2018). As such, lightning played a crucial role on the evolution and expansion of fire-adapted ecosystems (Bowman et al., 2009), ultimately contributing to shaping the geographical patterns of vegetation (Bond, Woodward, et al., 2005). Nowadays, however, humans are the main cause of fire in most regions of the world (Janssen et al., 2023). In particular, humans ignite the majority of fires in the tropics (Archibald, Roy, et al., 2009), despite these being the regions where lightning densities are highest

(Christian et al., 2003). However, the attribution of ignition causes in tropical areas bears a high level of uncertainty (Janssen et al., 2023), indicating that more detailed regional studies are required to ascertain the relevance of lightning in these regions.

For a fire event to be successful - that is, to start and spread -, it requires an ignition source, a fuel bed with enough continuity, and adequate weather conditions spurring the flammability of the fuel (Archibald, Roy, et al., 2009; Pausas et al., 2009). Even though lightning densities are highest in the tropics, most lightning strikes take place during the wet season (Schumacher, 2022), which limits their ignition probability (Veraverbeke et al., 2017). In contrast, humans are less restricted than lightning in the timing of ignition throughout the year and the geographical location of their ignition (Balch et al., 2017), as long as the fuel bed is flammable and continuous enough. In particular, humans tend to generate excess number of ignitions in comparison to lightning, as well as igniting fires in different weather conditions (Balch et al., 2017), often giving rise to more extreme fires as a consequence (Hantson, Andela, et al., 2022). In addition, the use of fires in certain anthropic activities like agriculture can increase the recurrence of fire events in specific areas (Gottsberger et al., 2006; Pivello et al., 2021).

The extent to which fire regimes caused by humans differ from those created by lightning has implications on the design of fire management strategies for conservation (Van Wilgen et al., 2000), to better understand the pressures posed by human-caused fires on ecosystems - both fire-adapted and fire-sensitive -, but it can also inform questions regarding the natural history of ecosystems. For example, a study in the Kruger National Park in South Africa, formed by savanna ecosystems, found that the fire return interval of lightning-ignited fires was much longer than that of a fire regime of prescribed burns (Van Wilgen et al., 2000). This finding indicated that the frequency of prescribed fires may have been too high, with potentially degrading effects on these ecosystems. However, the lightning-ignited return intervals observed were so long, that it also posed the question on whether, after millions of years of human uses of fire, a regime solely ignited by lightning could also lead to losses in biodiversity and changes in ecosystem structure (Van Wilgen et al., 2000).

In the Cerrado, there is a limited number of studies exploring lightning-caused fires. In particular, the proportion of lightning to human-caused fires in the Cerrado has not yet been quantified, relying on estimates for the Pantanal (Menezes et al., 2022) - a savanna-like wetland south of the Cerrado. Therefore, the fact that humans are currently the main source of ignitions in the Cerrado is a commonly held perception stemming from experts knowledge on modern uses of fire (Pivello, 2011), and from observations on the mismatch between the lightning season - mostly coinciding with the wet season, October to April (Schumacher, 2022) - and the fire season - during the dry season, May to September (Mataveli et al., 2018; Silva, Nogueira, et al., 2021; Silva Arruda et al., 2024). A study focused on the south-western most part of the Cerrado carried out an identification of lightning-caused fires and found that these were mostly concentrated in the transition period from the dry to the wet season (Schumacher, 2022), but it also identified lightning-caused fires during the wet season. Further, different studies in the early 2000s focusing on the Emas National Park (Ramos-Neto et al., 2000; Pereira and França, 2005), the Serra da Canastra National Park (Medeiros and Fiedler, 2004) or the Chapada dos Veadeiros National Park (Fiedler et al., 2006), also reported the occurrence of lightning-caused fires during the wet and transition periods, indicating that lightning fires may be more frequent in the Cerrado than has been usually assumed (Ramos-Neto et al., 2000; Medeiros and Fiedler, 2004; Pereira and França, 2005; Fiedler et al., 2006). Moreover, they found that, while lightning fires were generally small, had a patchy shape, and extinguished naturally with rainfall, dry-season fires caused by humans were larger, fast spreading and required active extinction (Ramos-Neto et al., 2000; Medeiros and Fiedler, 2004; Pereira and França, 2005; Fiedler et al., 2006).

Therefore, the quantification of lightning fires against human-caused fires in the Cerrado, and the comparison of the fire regimes that each type of ignition cause creates is a major research gap. Addressing these questions can shed light on how and to what extent the current fire regimes of the Cerrado may differ from what would naturally occur, with important implications for Cerrado conservation.

2.5 Satellite remote sensing and ancillary data products to study large-scale dynamics of fire

Remote sensing encompasses a range of techniques for data collection where the sensor gathers data without physical contact with the study object, from a certain distance (Chuvieco, 2020). The advent of remote sensing has allowed the study of processes and phenomena taking place on the Earth's surface at a large-scale. Nowadays, remote sensors can be placed on different types of platforms, including, but not limited to, unmanned aerial vehicles (UAVs), airplanes, and satellites (Chuvieco, 2020). In this thesis, the major sources of data are based on spaceborne remote sensing products detecting fire occurrence, which is the main focus of this section. Remote sensing observations may be based on active or passive sensors depending on their technology.

Passive sensors detect the electromagnetic signal (EM) - the light - emitted by an object either due to its own temperature or the light reflected on the object from a light-emitting source such as the Sun. Both types of signals are extensively used to detect fire occurrence. In the first case, as fires are exothermic combustion reactions that emit light and heat, they produce strong signals in the infrared that are recorded on passive sensor images (Chuvieco, 2020). Fires can therefore be identified from these images using contextual algorithms that detect thermal anomalies - pixels with hotter temperature than their surroundings - and determine whether these anomalies are likely to have been produced by active fires (Giglio, Boschetti, et al., 2018; Schroeder et al., 2014). In the case of the reflected light, the identification of pixels corresponding to burned areas is based on the analysis of changes in the EM signature of pixels between consecutive satellite overpasses, and can use different parts or combinations of the EM spectrum (i.e. not only in the visible) (Chuvieco, 2020). Fire data products obtained in this way are usually referred to as burned area products.

Active sensors are so-called because they emit energy, be it radio waves (RADAR techonology) or laser pulses (LiDAR techonologies), and record the reflected signal to characterise

the study object. These technologies have applications on topographic mapping, detection and tracking of climatic phenomena, and have also been used in fire scar detection (Chuvieco, 2020).

The study of fire dynamics at a large-scale has benefited from the increasing wealth of satellites and sensors, covering increasingly longer periods of time and improvements in their quality, and spatial and temporal resolutions (Chuvieco, 2020). In addition, the advances in spaceborne fire data have been complemented with the creation of data products measuring various other environmental factors. Because of their relevance to this thesis, we can highlight the creation of land use and land cover maps, based on the classification of pixels from optical sensors; or climatic datasets, either from climate re-analysis models (like ERA5-Land product from the European Centre for Medium-Range Weather Forecasts, ECMWF, (Muñoz-Sabater et al., 2021)), from the combination of weather stations' data and satellite remote sensing data (like the Climate Hazards Group InfraRed Precipitation with Station, CHIRPS, (Funk et al., 2015)), or from the interpolation of various climate data sources (like TerraClimate (Abatzoglou et al., 2018)). Finally, the development of lightning strike datasets should also be highlighted, whether based on satellite detection or from ground sensor networks, as is the case in this thesis (see **Chapter 5 (Research Paper 3)** for a detailed description).

2.5.1 Burned area products

Burned area products are widely used in the study of the spatiotemporal dynamics of fire. Burned area is a direct measure of the extent of fire occurrence in an area, and is related to the number of fires and their size. In addition, the inter-annual variability of burned area responds to climatic variability (Jones et al., 2022), and the spatial patterns are related to vegetation, topographic and land use patterns (Archibald, Nickless, et al., 2010; Archibald, Roy, et al., 2009). Increasingly, when supported by ground-truth data, the change in the EM signature of the burned pixels is also being used as an indicator of the combustion completeness of the fire (Keeley, 2009).

Despite the advances on fire science enabled by spaceborne burned area products, these

data bear some limitations that must be taken into consideration. First, most products available until now suffer from a trade-off between the spatial and temporal resolutions related to the satellite's orbit, the sensor's characteristics and the swath width - the horizontal surface on Earth covered by the sensor (Chuvieco, 2020). Generally, sensors with a smaller field of view - covering small areas - have high spatial resolution but take long to revisit the same area of the Earth's surface. Analogously, sensors with larger fields of view can have short revisit cycles as they cover larger areas at a time, but have low spatial resolutions as a consequence. Recently, these trade-offs have been addressed by using constellations of satellites with high resolutions, reducing the time span between observations of the same points on Earth.

The presence of clouds at the time of satellite overpass can also obstruct fire identification (Libonati et al., 2015; Pereira, Pereira, et al., 2017), especially in the case of longer revisit cycles and in ecosystems and times of the year when vegetation recovers swiftly. On the other hand, the spatial resolution of the sensor limits the ability to detect small fires (Campagnolo et al., 2021). This limitation is accentuated in the case of highly fragmented landscapes, where the burned signal may be confused with that of agricultural areas (Rodrigues et al., 2019).

MapBiomas Fogo dataset

In **Chapters 3 (Research Paper 1) and 4 (Research Paper 2)**, the burned area dataset used was the one created by the MapBiomas project (MapBiomas Fogo Collection 1.0 in **Chapter 3 (Research Paper 1)** and Collection 2.0 in **Chapter 4 (Research Paper 2)**, (Alencar, Arruda, et al., 2022)). This dataset is based on Landsat and provides data for the period 1985-2023 (in the most recent version of the product), even though this thesis focused on the period 1985-2020.

The Landsat programme consists of a series of missions launching satellites for Earth Observation, and has provided satellite images continuously since the 1970s (Irons et al., 2012). Landsat sensors have a spatial resolution of 30 m and a revisit cycle between 15-16 days or 7-8 days, depending on the period. The MapBiomas project bases its data

products on the Landsat sensors Thematic Mapper (TM), Enhanced Thematic Mapper Plus (ETM+), and the Operational Land Imager and Thermal Infrared Sensor (OLI-TIRS), onboard of Landsat 5, Landsat 7, Landsat 8, and Landsat 9, respectively (Alencar, Arruda, et al., 2022).

This dataset was chosen for various reasons. First, MapBiomas Fogo provides the longest time series of annual burned area data for the whole of Brazil. This was one of the main advantages for this thesis, as it allowed to explore changes in Cerrado fire dynamics before the 2000s, which has seldom been explored in the literature. In addition, the MapBiomas project offers a suite of geospatial products based on Landsat, highlighting the MapBiomas land-cover and land use data product (Souza et al., 2020). As such, these two datasets offered the opportunity of studying the relation between burned area and land use area not only with the same spatial resolution, but also developed by the same team of experts, granting a degree of coordination in their production. Finally, MapBiomas data are publicly available and easy to access for quick visual inspection on their website, and easily downloadable through Google Earth Engine (Gorelick et al., 2017). Further details on the algorithms used by the MapBiomas project are provided in the Methods section of **Chapter 3 (Research Paper 1)** and **Chapter 4 (Research Paper 2)**.

The main limitation of this dataset resides on its omission errors, particularly the detection of small fires and the mapping of burned areas in highly fragmented landscapes (Nogueira et al., 2016; Alencar, Arruda, et al., 2022), possibly leading to an underestimation of burned area particularly in the southern regions of the Cerrado. Another main limitation is the high uncertainty on the estimation of the timing of burn occurrence. This limitation stems from the long revisit cycle of the Landsat mission, but is also related to the methodology used by MapBiomas to generate their burned area product, which creates annual maps of burned area without aiming to maximise the precision of the burn date. However, despite the uncertainty of burn date at pixel level, the seasonal patterns of fire detected across the Cerrado with MapBiomas Fogo data (Alencar, Arruda, et al., 2022; Silva Arruda et al., 2024) agree with the patterns previously detected using other satellite-based burned area products (Mataveli et al., 2017; Mataveli et al., 2018; Silva,

Rodrigues, et al., 2020; Silva, Nogueira, et al., 2021).

2.5.2 Mapping individual fire events

While spaceborne burned area products are readily available for studying patterns of fire, the characterisation of fire regimes requires going a few steps further. In particular, information is required at the individual fire level so that characteristics like fire size or the number of fires can be estimated (Nogueira et al., 2016). However, burned area products only provide information on whether a pixel burned, and an estimation of when it burned. Therefore, information at the individual fire level requires further processing of the burned area data designing algorithms to group pixels into fire events (Archibald and Roy, 2009).

Different studies have used different approaches to mapping individual fire events. To group pixels from coarse-resolution burned area products with a daily revisit cycle, some studies used a *flood-fill* algorithm in which contiguous pixels are mapped together if the difference between their burn dates is smaller than a certain threshold (Archibald and Roy, 2009; Laurent et al., 2018). Other approaches have been developed to map fire events based on Landsat data (Finco, 2012; Goodwin et al., 2014; Bastarrika et al., 2011). In particular, a *region growing* algorithm identified seed Landsat pixels using active fire data, and then incorporated neighbouring pixels based on spatial and spectral properties (Bastarrika et al., 2011).

A more elaborate approach to map individual fire events was implemented in the Global Fire Atlas dataset (GFA) (Andela, Morton, Giglio, Paugam, et al., 2019), based on the Moderate-Resolution Imaging Spectroradiometer (MODIS) MCD64A1 Collection 6.1 burned area data (Giglio, Schroeder, et al., 2016), which has a spatial resolution of 500 m and a daily revisit cycle. Apart from mapping individual fires, GFA also provides an estimation of the day and location of the fire ignition, along with information on the daily expansion of the fire, fire line length, speed and direction of spread, as well as the size of the fire and its duration (Andela, Morton, Giglio, Paugam, et al., 2019; Andela and Jones, 2024). The GFA algorithm first identifies clusters of contiguous pixels based on the spa-

tial patterns of the burn dates, and then ignition point candidates are identified using a multi-step procedure searching for local minima out of each cluster's burn dates (Andela, Morton, Giglio, Paugam, et al., 2019). This algorithm was later applied to re-scaled active fire data from the Visible Infrared Imaging Radiometer Suite (VIIRS) (Schroeder et al., 2014) to produce the Amazon Dashboard dataset (Andela, Morton, Schroeder, et al., 2022). VIIRS has a daily overpass and 375 m spatial resolution, and detects active fires based on thermal anomalies (Schroeder et al., 2014). The GFA dataset was used in **Chapter 5 (Research Paper 3)** of this thesis.

A custom algorithm to map individual fire events for MapBiomas Fogo data

To enable the characterisation of the fire regimes of the Cerrado in **Chapter 4 (Research Paper 2)**, a custom algorithm was designed to group together pixels that were likely to be part of the same fire event. This algorithm was based on the same principles of the algorithms described above: grouping spatially contiguous pixels with consecutive burn dates - months in the case of MapBiomas Fogo data. In this case, however, the 1) uncertainty on the burn date, 2) the observation of highly fragmented fire events, and 3) an excessive number of very small fire polygons meant that some further adjustments had to be implemented. As such, we grouped together as part of the same fire event those polygons belonging to the same month that were up to 150 m apart from each other, and we only considered those polygons larger than 3 ha. The algorithm steps are described in the Methods section of **Chapter 4 (Research Paper 2)**.

2.5.3 Other ancillary data products

Fire is a complex phenomenon that depends on - and in turn affects - the climate, the type of vegetation and human presence among others. As such, besides data on fire occurrence and behaviour, the study of fire dynamics is usually complemented with ancillary data products providing information on these other factors. The main aim of this thesis is to understand how the patterns of fire of the Cerrado are related to the climate and patterns of land use expansion. Further, in **Chapter 5 (Research Paper 3)**, the aim is to identify the

most likely cause of fire ignition, whether lightning or humans. Therefore, there are a few datasets on climate variables, land use and land cover class, and on lightning occurrence that have played a major role in this thesis. Here, we provide some context on the datasets used and comment on their advantages and limitations.

Land use area data

Every research chapter of this thesis has used data on land use area for the whole Cerrado from the same product, the MapBiomas land use and land cover dataset (Souza et al., 2020). MapBiomas is a project co-created and led by a network of Brazilian institutions including universities, non-governmental organisations, and technology companies that was launched in the year 2015. Initially, their main objective was to create annual maps of land use and land cover for all of Brazil using remote sensing data in a cheaper and faster manner than other existing methods and projects, as well as providing a longer time series of data into the past. Besides, they intended that this project would be completely open, from the processing scripts to the data, so that it could be easily replicated in other areas of the world (Souza et al., 2020).

With this objective, MapBiomas decided to use Landsat imagery, as it would allow them to produce annual maps as far back as 1985 with medium resolution (Souza et al., 2020). In addition, the project network decided to use Google Earth Engine (Gorelick et al., 2017) as their processing platform, from which users can also access the processing scripts and data for downloading, which also reduced the costs of producing such dataset. With time, the project has diversified the number and type of data products that they provide, including the burned area product MapBiomas Fogo dataset used in **Chapter 3 (Research Paper 1)** and **Chapter 4 (Research Paper 2)** of this thesis.

MapBiomas released the first version of their land use and land cover map in 2016 providing data for the period 2008 to 2015 using a simplified legend with only 7 land use and land cover categories. Subsequently, every year they have released an updated version of their product covering increasingly longer periods, expanding and refining the legend, and improving their algorithms and methodologies. In 2018 they released the first version

covering the full period 1985 to 2017, MapBiomas Collection 3 (Souza et al., 2020). Currently, the last release was in 2024, MapBiomas Collection 9, covering the period 1985 to 2023. In this thesis, MapBiomas Collection 6.0 was used in **Chapter 3 (Research Paper 1)**, Collection 8.0 was used in **Chapter 4 (Research Paper 2)** and in **Chapter 5 (Research Paper 3)**.

MapBiomas produces their annual land use and land cover maps for each year independently. First, annual mosaics of Landsat images are created filtering out pixels containing clouds or smoke (Souza et al., 2020). These mosaics contain summaries of the information of the different Landsat bands throughout the year (average, maximum, standard deviation or minimum value), as well as vegetation indices calculated combining bands (Souza et al., 2020). These different summary values and indices are later used by machine learning algorithms to classify pixels. Then, different teams within MapBiomas are in charge of carrying out the pixel classification for different regions (i.e. Amazon, Cerrado, Caatinga, Pantanal, Mata Atlântica, and Pampa), and for different "cross-cutting themes" (i.e. forest, grassland, agriculture, pasture, urban area, water, etc.) (Souza et al., 2020). In this manner, each team can adapt the algorithm to improve their pixel classification by, for example, using pixel data from the period of the year that may be most optimal to identifying certain types of land use and cover classes in a specific type of vegetation. Furthermore, each team produces their own training dataset by visually identifying the land use and land cover class of a number of pixels - which varies depending on the region and class. Then, the teams classify the pixels using the Random Forests algorithm implementation of Google Earth Engine (Gorelick et al., 2017). In this manner, they obtain a classified map for each land use and land cover class and region (Souza et al., 2020). Then, each team applies spatial and temporal filters to these maps to increase the consistency of the classification based on a set of rules (Souza et al., 2020).

Next, they integrate the maps for the different land use and land cover classes into a single map for each region using a set of rules to decide which classification decision to keep when there are inconsistencies. This step is still done by region so that different criteria can be applied for each different context (Souza et al., 2020). Finally, they integrate

together the maps for the different regions applying a few last spatial filters to diminish inconsistencies (Souza et al., 2020), as well as transition filters that will detect and address class transitions that are not reasonable or impossible between consecutive years (Souza et al., 2020).

MapBiomas land use and land cover maps in Collections 6.0 and 8.0 have an accuracy around 75%. One of the main advantages of this product for the aims of this thesis - apart from the long time series and the fact that it is easily matched with MapBiomas Fogo data - is the fact that MapBiomas land use and land cover data product distinguishes pastures from grasslands and savannas. This turned out to be a key factor for the aims of this thesis as it allowed to disentangle drivers of fire in this region - which has not been possible by other studies using land use and land cover data that did not fully distinguish these two classes in the Cerrado (Mataveli et al., 2018; Haas et al., 2022).

Climate data

Currently, global and quasi-global gridded climate data products are widely used by the scientific community in a large variety of applications. Over the past few decades, there has been an increase in the number of such data products with increasing accuracy, offering data for longer time periods increasing temporal and spatial resolutions, and offering wider variety of climate variables (Abatzoglou et al., 2018). Their usage in different biogeoscience disciplines has been stimulated by the parallel development of other gridded data products - typically based on remote sensing products - describing other Earth system variables, such as the aforementioned fire data products.

Indeed, because the climate is one of the main drivers of fire (Jones et al., 2022), such climate datasets are commonly used in the study of fire dynamics. The combination of these two types of gridded datasets - along with ancillary data products like land use data - has allowed a better understanding of how spatial and temporal patterns of fire are affected by different climate variables (Jones et al., 2022), as well as contributed to improved fire modelling efforts (Haas et al., 2022; Hantson, Arneth, et al., 2016).

Climate data products may be produced based on meteorological observations from weather

stations, satellite remote sensing products, climate reanalysis models and combinations of these (Abatzoglou et al., 2018). In this thesis, climate data from three different products have been used to describe different climate variables. In this section, we first describe the climate data products used, and then we discuss the rationale for combining data from these three data products.

- **Temperature-related variables**

In this thesis, we used temperature-related variables from ERA5-Land (Muñoz-Sabater et al., 2021), a climate reanalysis product that was developed as an enhancement of the land component of the fifth generation European ReAnalysis (ERA5) data product- which in turn is an improvement of the earlier ERA-Interim product (Hersbach et al., 2020). Climate reanalysis products are a type of gridded climate data product generated by combining past observations from weather stations, in situ meteorological measurements and remote sensing data with physical models of the climate to generate time series of multiple climate variables (Hersbach et al., 2020). Both ERA5 and ERA5-Land were created and are maintained by the European Centre for Medium-Range Weather Forecasts (ECMWF), and both are part of the Copernicus Climate Change Service of the European Commission (Hersbach et al., 2020; Muñoz-Sabater et al., 2021).

ERA5 provides data on different climate variables describing the global atmosphere, land surface, as well as on ocean waves from 1940 onward with 31 km spatial resolution, and both monthly and hourly time steps (Hersbach et al., 2020). ERA5-Land provides climate data over the Earth's land surface with a higher spatial resolution than ERA5 - 9 km -, and was produced with higher resolution in the numerical calculations of the ECMWF land surface model and including topographic elevation corrections (Muñoz-Sabater et al., 2021). An evaluation against in situ data showed that ERA5-Land provides a better description of the hydrological cycle than ERA5 (Muñoz-Sabater et al., 2021). Furthermore, even though ERA5 and ERA5-Land provide very similar estimations of land surface temperature, ERA5-Land shows better correlation with MODIS data in the tropics than ERA5 (Muñoz-Sabater et al., 2021).

In each of the three results chapters, we used monthly averaged ERA5-Land data on air temperature at 2 m above the surface of land (ERA5-Land variable "2 meter temperature"), and the dewpoint temperature at 2 m (ERA5-Land variable "2 meter dewpoint temperature"). Dewpoint temperature is the temperature to which the air would have to be cooled at constant pressure to produce air saturation (Muñoz-Sabater et al., 2021). We used the combination of these two variables to calculate Vapour Pressure Deficit (VPD), a direct measure of the atmospheric demand for water, which we calculated following the procedure detailed in Allen et al. (1998).

- **Precipitation**

To represent precipitation in each of the three results chapters, we used data from the Climate Hazards Group InfraRed Precipitation with Station data (CHIRPS) V2.0 (Funk et al., 2015), created by the United States Geological Survey and the Climate Hazards Group at the University of California, Irvine. CHIRPS is a quasi-global gridded data product providing rainfall data at a 0.05^{o} for the period 1981 to present (Funk et al., 2015). This rainfall dataset is produced by blending advanced interpolation techniques of precipitation data from gauge station with satellite remote sensing data to represent locations where gauge stations are sparse (Funk et al., 2015). CHIRPS dataset was created to allow scientists to assess recent extreme rainfall and drought events in a historical context by providing long records of precipitation data with high temporal and spatial resolution (Funk et al., 2015).

- **Potential Evapotranspiration**

Finally, in **Chapter 3 (Research Paper 1)** and **Chapter 4 (Research Paper 2)**, we used data on Potential Evapotranspiration (PET) from the TerraClimate dataset (Abatzoglou et al., 2018). This dataset provides climate data on different primary climate variables (like maximum and minimum temperature, precipitation accumulation or wind-speed) along with derived variables (like PET, runoff, or soil moisture). These variables are obtained with an interpolation algorithm of climate data from various sources: high spatial resolution climatological normals from the WorldClim dataset, and coarser resolution monthly

data from the Climate Research Unit and the Japanese 55-year reanalysis (Abatzoglou et al., 2018).

TerraClimate estimates monthly PET using the Penman Monteith approach, that is, based on an energy balance instead of obtaining PET purely from temperature-based metrics and incorporating some modifications to improve PET estimations over snow (Abatzoglou et al., 2018). Overall, TerraClimate shows good performance when validated against station-based observations (Abatzoglou et al., 2018). In particular, annual PET estimations show agreement with station-based PET data from FLUXNET stations (Abatzoglou et al., 2018).

- **Rationale for choosing climate data products**

Even though gridded climate data products are widely used in studies of different scales across the world, these products often perform poorly over regions with sparse in situ meteorological observations (Burton et al., 2018). In this sense, tropical areas present the greatest challenge because they are regions where meteorological stations are sparse and because, particularly over tropical forests, land-atmosphere feedbacks are complex and vary within small spatial scales (Burton et al., 2018).

Regarding the Brazilian Cerrado, findings on trends in different climate variables across the Cerrado seem to strongly depend on the source of data - whether on-ground weather station data (Hofmann, Cardoso, et al., 2021), remote sensing data (Oliveira, Nearing, et al., 2014), or climate reanalysis data from ERA5 (Hofmann, Silva, et al., 2023). First, a study on climate trends based on weather station data from the Brazilian National Meteorology Institute (Instituto Nacional de Meteorologia) found that temperature and VPD had increased across the Cerrado over the period 1961-2019 (Hofmann, Cardoso, et al., 2021). While this study concluded that the Cerrado is becoming hotter and drier, such drying trends were derived from decreases in relative humidity (that is, derived from temperature-related variables), while the study did not mention changes in rainfall. Similarly, using rainfall data from the Tropical Rainfall and Monitoring Mission (TRMM) - a research satellite providing information on rainfall over tropical and subtropical regions

from 1997 to 2015 (Liu et al., 2012) -, another study over the Brazilian Cerrado found increases in average annual evapotranspiration, but it did not report any trends on rainfall (Oliveira, Nearing, et al., 2014). In contrast, a study based on ERA5 climate data found rainfall reductions of up to 50% in the period 1960 to 2021 (Hofmann, Silva, et al., 2023). Therefore, there seem to be disagreements about Cerrado's climate trends in recent decades, particularly when comparing satellite data against climate reanalysis products.

Burton et al. (2018) carried out an assessment aiming to show which gridded climate data products performed better over tropical areas. Thus, they compared on-ground data from meteorological stations against the climate estimates from various global and quasi-global products (Burton et al., 2018). Their results indicate that ERA-Interim (the precursor to ERA5 and ERA5-Land) was one of the most reliable datasets regarding temperature-related variables over the tropics. However, they found that ERA-Interim significantly overestimated tropical rainfall (Burton et al., 2018). In this sense, Burton et al. (2018) found that CHIRPS and TRMM were the best-performing rainfall dataset in the tropics, as their precipitation data were in close agreement with rainfall gauge data from meteorological stations. Still, their results also showed a generalised tendency to considerably underestimate precipitation in high rainfall months, and to slightly overestimate precipitation in low rainfall months (Burton et al., 2018).

Therefore, based on the recommendations derived from the inter-comparison of climate data products over the tropics (Burton et al., 2018), on the findings of no clear trends in rainfall when using TRMM data (Oliveira, Nearing, et al., 2014) nor when using CHIRPS (see **Chapter 3 (Research Paper 1)**)), which are in contrast to findings of decreasing precipitation when using ERA5 data (Hofmann, Cardoso, et al., 2021); we decided to use CHIRPS data to inform precipitation, and ERA5-Land to inform temperature-related variables. Finally, because we needed to compare precipitation against PET to identify the dry season months but CHIRPS only provides rainfall data, we decided to use PET from TerraClimate (see **Chapter 3 (Research Paper 1)** and **Chapter 4 (Research Paper 2)**).

Lightning data

Lightning strikes are the main natural cause of fire ignitions. Therefore, the identification of fires caused by lightning is an active research field within fire science community (Veraverbeke et al., 2017; Moris et al., 2023), from the ecological role of lightning as a cause of disturbance (Veraverbeke et al., 2017; Janssen et al., 2023) to assessing the risks posed by this natural phenomenon to human lives and infrastructure. As with other aspects related with fire, the study of lightning as a fire ignition cause has benefited from the development of lightning detection technologies over the past few decades and the increasing availability of data (Said, 2017).

Lightning strikes are electrical discharges that can occur in the atmosphere as a consequence of charge separation buildup in clouds produced by particle movement within the cloud, which can in turn cause charge buildup on the Earth's surface underneath the cloud (Dwyer et al., 2014). These electrical discharges can partially neutralise the charge separation within the cloud (cloud flashes), or lower charge to the ground (cloud-to-ground, CG, strikes) (Said, 2017; Pohjola et al., 2013). CG strikes can last just a few microseconds and can measure on the order of 10,000 A to 100,000 A (Said, 2017). These current channels produce very high temperatures (Dwyer et al., 2014), which can in turn spark a fire once they hit the ground if there is enough flammable fuel (Rego et al., 2021).

These current discharges radiate energy in a wide range of the EM spectrum: from radio emissions, through the optical range, and even up to gamma rays (very high frequency EM emissions) (Said, 2017; Pohjola et al., 2013). These emissions can be detected and located by Lightning Location Systems (LLS) which, depending on their characteristics, will capture specific aspects of lightning discharges (Said, 2017). For example, sensors of the optical and near infrared range of the EM spectrum onboard satellites can detect lightning discharges (Said, 2017). Such sensors are of course limited by their spatial resolution but, crucially, by their overpass cycles - even though lightning detectors are increasingly being placed on geostationary satellites (Said, 2017).

Lightning strikes are commonly detected by dense networks of ground sensors. The tech-

nologies of these sensors focus either on Very High Frequencies (VHF), or Medium, Low and Very Low Frequencies (MF, LF, and VLF) (Pohjola et al., 2013). VHF signals (30-300 MHz) travel directly through the atmosphere, so they can easily be detected by sensors, but do not reach distances larger than 100-200 km (Pohjola et al., 2013). Therefore, a high-accuracy coverage of lightning strikes by VHF sensors requires a large number of sensors (Said, 2017). Finally, CG strokes generate a distinctive signal on the MF to VLF range (3 kHz - 3 MHz) (Pohjola et al., 2013; Said, 2017). This signal can travel as a ground wave - which can be detected several hundreds of kilometers away -, as well as through the atmosphere bouncing between the ground and the ionosphere - which can be detected thousands of kilometers away (Pohjola et al., 2013).

In **Chapter 5 (Research Paper 3)** of this thesis, the aim was to quantify the proportion of fire ignited by lightning and by humans, and compare aspects of the fire regimes created by each type of ignition. Lightning data for this chapter was provided by co-authors, which in turn was produced by the Vaisala Global Lightning Detection Network GLD360, a network of ground VLF sensors with a global-scale coverage owned by Vaisala Inc. and launched in 2009 (Said, 2017). This company's lightning strikes dataset provides the geolocation of the different strokes, an uncertainty measure of their location, as well as data on the polarity and the peak current of the lightning strike (Said, 2017). However, this company does not disclose the location of their LLS sensors, which hampers the assessment of the overall quality of their network (Pohjola et al., 2013).

2.6 References

Abatzoglou, John T. et al. (2018). "TerraClimate, a high-resolution global dataset of monthly climate and climatic water balance from 1958–2015". In: *Scientific Data* 5.1, p. 170191.

Abreu, Rodolfo C. R. et al. (2017). "The biodiversity cost of carbon sequestration in tropical savanna". In: *Science Advances* 3.8, e1701284.

Aldersley, Andrew, Steven J. Murray, and Sarah E. Cornell (2011). "Global and regional analysis of climate and human drivers of wildfire". In: *Science of The Total Environment* 409.18, pp. 3472–3481.

Alencar, Ane, Julia Z. Shimbo, et al. (2020). “Mapping Three Decades of Changes in the Brazilian Savanna Native Vegetation Using Landsat Data Processed in the Google Earth Engine Platform”. In: *Remote Sensing* 12.6, p. 924.

Alencar, Ane A. C., Vera L. S. Arruda, et al. (2022). “Long-Term Landsat-Based Monthly Burned Area Dataset for the Brazilian Biomes Using Deep Learning”. In: *Remote Sensing* 14.11, p. 2510.

Allen, Richard G. et al. (1998). *Crop evapotranspiration - Guidelines for computing crop water requirements*. FAO - Food and Agriculture Organization of the United Nations.

Andela, N., D. C. Morton, L. Giglio, Y. Chen, et al. (2017). “A human-driven decline in global burned area”. In: *Science* 356.6345, pp. 1356–1362.

Andela, Niels and Matthew William Jones (2024). *Update of: The Global Fire Atlas of individual fire size, duration, speed and direction*. Version v20240409. Zenodo.

Andela, Niels, Douglas C Morton, Louis Giglio, Ronan Paugam, et al. (2019). “The Global Fire Atlas of individual fire size, duration, speed and direction”. In.

Andela, Niels, Douglas C Morton, Wilfrid Schroeder, et al. (2022). “Tracking and classifying Amazon fire events in near real time”. In: *Science advances* 8.30. Publisher: American Association for the Advancement of Science, eabd2713.

Andela, Niels and Guido R. van der Werf (2014). “Recent trends in African fires driven by cropland expansion and El Niño to La Niña transition”. In: *Nature Climate Change* 4.9, pp. 791–795.

Araujo, Astolfo G de M, Luís B Pilo, et al. (2006). “Human occupation and paleoenvironments in South America: expanding the notion of an “Archaic Gap””. In: *Revista do Museu de Arqueologia e Etnologia* 15-16, pp. 3–35.

Araujo, Astolfo GM, Letícia Cristina Correa, et al. (2025). “Human-environment interaction during the Holocene in Eastern South America: Rapid climate changes and population dynamics”. In: *PloS one* 20.2, e0315747.

Araújo, Fernando Moreira De and Laerte G. Ferreira (2015). “Satellite-based automated burned area detection: A performance assessment of the MODIS MCD45A1 in the Brazilian savanna”. In: *International Journal of Applied Earth Observation and Geoinformation* 36, pp. 94–102.

Archibald, S, C E R Lehmann, C M Belcher, et al. (2018). “Biological and geophysical feedbacks with fire in the Earth system”. In: *Environmental Research Letters* 13.3, p. 033003.

Archibald, S., A. Nickless, et al. (2010). “Climate and the inter-annual variability of fire in southern Africa: a meta-analysis using long-term field data and satellite-derived burnt area data: Fire-climate interactions”. In: *Global Ecology and Biogeography* 19.6, pp. 794–809.

Archibald, S. and D. P. Roy (2009). “Identifying individual fires from satellite-derived burned area data”. In: *2009 IEEE International Geoscience and Remote Sensing Symposium*. 2009 IEEE International Geoscience and Remote Sensing Symposium. Cape Town, South Africa: IEEE, pp. III–160–III–163.

Archibald, S., R. J. Scholes, et al. (2010). “Southern African fire regimes as revealed by remote sensing”. In: *International Journal of Wildland Fire* 19.7, p. 861.

Archibald, Sally (2016). “Managing the human component of fire regimes: lessons from Africa”. In: *Philosophical Transactions of the Royal Society B: Biological Sciences* 371.1696, p. 20150346.

Archibald, Sally, Caroline E. R. Lehmann, Jose L. Gómez-Dans, et al. (2013). “Defining pyromes and global syndromes of fire regimes”. In: *Proceedings of the National Academy of Sciences* 110.16, pp. 6442–6447.

Archibald, Sally, David P. Roy, et al. (2009). “What limits fire? An examination of drivers of burnt area in Southern Africa”. In: *Global Change Biology* 15.3, pp. 613–630.

Arruda, Daniel M et al. (2018). “Vegetation cover of Brazil in the last 21 ka: New insights into the Amazonian refugia and Pleistocenic arc hypotheses”. In: *Global Ecology and Biogeography* 27.1, pp. 47–56.

Balch, Jennifer K. et al. (2017). “Human-started wildfires expand the fire niche across the United States”. In: *Proceedings of the National Academy of Sciences* 114.11, pp. 2946–2951.

Bastarrika, Aitor, Emilio Chuvieco, and M. Pilar Martín (2011). “Mapping burned areas from Landsat TM/ETM+ data with a two-phase algorithm: Balancing omission and commission errors”. In: *Remote Sensing of Environment* 115.4, pp. 1003–1012.

Behling, Hermann (2003). “Late glacial and Holocene vegetation, climate and fire history inferred from Lagoa Nova in the southeastern Brazilian lowland”. In: *Vegetation History and Archaeobotany* 12, pp. 263–270.

Biomas, IBGE (2019). “Sistema Costeiro-Marinho do Brasil: compatível com a escala 1: 250.000”. In: *Série Relatórios Metodológicos* 45.

Bond, W and J Keeley (2005). “Fire as a global ‘herbivore’: the ecology and evolution of flammable ecosystems”. In: *Trends in Ecology & Evolution* 20.7, pp. 387–394.

Bond, W. J., F. I. Woodward, and G. F. Midgley (2005). “The global distribution of ecosystems in a world without fire”. In: *New Phytologist* 165.2, pp. 525–538.

Boulanger, Yan, Sylvie Gauthier, and Philip J. Burton (2014). “A refinement of models projecting future Canadian fire regimes using homogeneous fire regime zones”. In: *Canadian Journal of Forest Research* 44.4, pp. 365–376.

Boulanger, Yan, Sylvie Gauthier, David R. Gray, et al. (2013). “Fire regime zonation under current and future climate over eastern Canada”. In: *Ecological Applications* 23.4, pp. 904–923.

Bowman, David M. J. S. et al. (2009). “Fire in the Earth System”. In: *Science* 324.5926, pp. 481–484.

Brando, P. M. et al. (2020). “The gathering firestorm in southern Amazonia”. In: *Science Advances* 6.2, eaay1632.

Burton, C., S. Rifai, and Y. Malhi (2018). “Inter-comparison and assessment of gridded climate products over tropical forests during the 2015/2016 El Niño”. In: *Philosophical Transactions of the Royal Society B: Biological Sciences* 373.1760, p. 20170406.

Bustamante, Mercedes M. C. et al. (2012). “Estimating greenhouse gas emissions from cattle raising in Brazil”. In: *Climatic Change* 115.3, pp. 559–577.

Campagnolo, M.L. et al. (2021). “A comprehensive characterization of MODIS daily burned area mapping accuracy across fire sizes in tropical savannas”. In: *Remote Sensing of Environment* 252, p. 112115.

Carranza, Tharsila et al. (2014). “Protected Area Effectiveness in Reducing Conversion in a Rapidly Vanishing Ecosystem: The Brazilian Cerrado: Protected area effectiveness in Cerrado”. In: *Conservation Letters* 7.3, pp. 216–223.

Cassino, Raquel Franco, Marie-Pierre Ledru, et al. (2020). “Vegetation and fire variability in the central Cerrados (Brazil) during the Pleistocene-Holocene transition was influenced by oscillations in the SASM boundary belt”. In: *Quaternary Science Reviews* 232, p. 106209.

Cassino, Raquel Franco, Shirley Maria Lima Sabino, et al. (2023). “Millennial-scale variability of water supply, vegetation and fire activity on a tropical wetland in central Brazil”. In: *Palaeogeography, Palaeoclimatology, Palaeoecology* 619, p. 111545.

Cattau, Megan et al. (2022). “Modern Pyromes: Biogeographical Patterns of Fire Characteristics across the Contiguous United States”. In: *Fire* 5.4, p. 95.

Christian, Hugh J. et al. (2003). “Global frequency and distribution of lightning as observed from space by the Optical Transient Detector”. In: *Journal of Geophysical Research: Atmospheres* 108 (D1).

Chuvieco, Emilio (2020). *Fundamentals of satellite remote sensing: An environmental approach*. CRC press.

Chuvieco, Emilio, Peter Englefield, et al. (2008). “Generation of long time series of burn area maps of the boreal forest from NOAA–AVHRR composite data”. In: *Remote Sensing of Environment* 112.5, pp. 2381–2396.

Chuvieco, Emilio, Louis Giglio, and Chris Justice (2008). “Global characterization of fire activity: toward defining fire regimes from Earth observation data”. In: *Global Change Biology* 14.7, pp. 1488–1502.

Conciani, Dhemerson E. et al. (2021). “Human-climate interactions shape fire regimes in the Cerrado of São Paulo state, Brazil”. In: *Journal for Nature Conservation* 61, p. 126006.

Coutinho, L. M. (1982). “Ecological Effects of Fire in Brazilian Cerrado”. In: *Ecology of Tropical Savannas*. Ed. by Brian J. Huntley and Brian H. Walker. Red. by W. D. Billings et al. Vol. 42. Series Title: Ecological Studies. Berlin, Heidelberg: Springer Berlin Heidelberg, pp. 273–291.

– (1990). “Fire in the Ecology of the Brazilian Cerrado”. In: *Fire in the Tropical Biota*. Ed. by Johann Georg Goldammer. Red. by W. D. Billings et al. Vol. 84. Series Title: Ecological Studies. Berlin, Heidelberg: Springer Berlin Heidelberg, pp. 82–105.

Dantas, Vinicius L and Juli G Pausas (2020). “Megafauna biogeography explains plant functional trait variability in the tropics”. In: *Global Ecology and Biogeography* 29.8, pp. 1288–1298.

Doughty, Christopher E, Søren Faurby, and Jens-Christian Svenning (2016). “The impact of the megafauna extinctions on savanna woody cover in South America”. In: *Ecography* 39.2, pp. 213–222.

Durigan, Giselda (2020). “Zero-fire: Not possible nor desirable in the Cerrado of Brazil”. In: *Flora* 268, p. 151612.

Durigan, Giselda and James A. Ratter (2016). “The need for a consistent fire policy for Cerrado conservation”. In: *Journal of Applied Ecology* 53.1. Ed. by Jeremy James, pp. 11–15.

Dwyer, Joseph R and Martin A Uman (2014). “The physics of lightning”. In: *Physics Reports* 534.4, pp. 147–241.

Elia, Mario et al. (2022). “Uncovering current pyroregions in Italy using wildfire metrics”. In: *Ecological Processes* 11.1, p. 15.

Eloy, Ludivine et al. (2019). “Seasonal fire management by traditional cattle ranchers prevents the spread of wildfire in the Brazilian Cerrado”. In: *Ambio* 48.8, pp. 890–899.

Escobar-Torrez, Katerine et al. (2024). “Long-and short-term vegetation change and inferred climate dynamics and anthropogenic activity in the central Cerrado during the Holocene”. In: *Journal of Quaternary Science* 39.1, pp. 130–144.

Espírito-Santo, Mário M. et al. (2016). “Understanding patterns of land-cover change in the Brazilian Cerrado from 2000 to 2015”. In: *Philosophical Transactions of the Royal Society B: Biological Sciences* 371.1703, p. 20150435.

Ferreira, Heitor F et al. (2023). “Stochastic Model for Wildfire Simulation Based on the Characteristics of the Brazilian Cerrado”. In: *International Conference on Artificial Intelligence and Soft Computing*. Springer, pp. 487–496.

Fidelis, Alessandra et al. (2018). “The Year 2017: Megafires and Management in the Cerrado”. In: *Fire* 1.3, p. 49.

Fiedler, Nilton César, Daniela Araújo Merlo, and Marcelo Brilhante de Medeiros (2006). “Ocorrência de incêndios florestais no Parque Nacional da Chapada dos Veadeiros, Goiás.” In: *Ciência Florestal* 16.2, pp. 153–161.

Finco, Mark (2012). “Monitoring Trends and Burn Severity (MTBS): Monitoring wildfire activity for the past quarter century using landsat data”. In.

Franco, Augusto C. (2002). “10. Ecophysiology of Woody Plants”. In: *Ecology and Natural History of a Neotropical Savanna*. Ed. by Paulo S. Oliveira and Robert J. Marquis. New York Chichester, West Sussex: Columbia University Press, pp. 178–198.

Funk, Chris et al. (2015). “The climate hazards infrared precipitation with stations—a new environmental record for monitoring extremes”. In: *Scientific Data* 2.1, p. 150066.

Galizia, Luiz Felipe, Renaud Barbero, et al. (2023). “Global Warming Reshapes European Pyroregions”. In: *Earth’s Future* 11.5, e2022EF003182.

Galizia, Luiz Felipe, Thomas Curt, et al. (2021). “Understanding fire regimes in Europe”. In: *International Journal of Wildland Fire* 31.1, pp. 56–66.

García, Mariano et al. (2022). “Characterizing Global Fire Regimes from Satellite-Derived Products”. In: *Forests* 13.5, p. 699.

Giglio, Louis, Luigi Boschetti, et al. (2018). “The Collection 6 MODIS burned area mapping algorithm and product”. In: *Remote Sensing of Environment* 217, pp. 72–85.

Giglio, Louis, Wilfrid Schroeder, and Christopher O. Justice (2016). “The collection 6 MODIS active fire detection algorithm and fire products”. In: *Remote Sensing of Environment* 178, pp. 31–41.

Goodwin, Nicholas R. and Lisa J. Collett (2014). “Development of an automated method for mapping fire history captured in Landsat TM and ETM + time series across Queensland, Australia”. In: *Remote Sensing of Environment* 148, pp. 206–221.

Gorelick, Noel et al. (2017). “Google Earth Engine: Planetary-scale geospatial analysis for everyone”. In: *Remote sensing of Environment* 202. Publisher: Elsevier, pp. 18–27.

Gottsberger, Gerhard and Ilse Silberbauer-Gottsberger (2006). “Life in the Cerrado”. In: *Vol. I. Origin, Structure, Dynamics and Plant Use. Reta, Ulm*.

Grecchi, Rosana Cristina et al. (2013). “Assessing the spatio-temporal rates and patterns of land-use and land-cover changes in the Cerrados of southeastern Mato Grosso, Brazil”. In: *International Journal of Remote Sensing* 34.15, pp. 5369–5392.

Haas, Olivia, Iain Colin Prentice, and Sandy P Harrison (2022). “Global environmental controls on wildfire burnt area, size, and intensity”. In: *Environmental Research Letters* 17.6, p. 065004.

Hantson, Stijn, Niels Andela, et al. (2022). “Human-ignited fires result in more extreme fire behavior and ecosystem impacts”. In: *Nature Communications* 13.1, p. 2717.

Hantson, Stijn, Almut Arneth, et al. (2016). “The status and challenge of global fire modelling”. In: *Biogeosciences* 13.11, pp. 3359–3375.

Henriques, Raimundo PB and John D Hay (2002). “Patterns and dynamics of plant populations”. In: *The cerrados of Brazil: ecology and natural history of a neotropical savanna*. Columbia University Press, pp. 140–158.

Hersbach, Hans et al. (2020). “The ERA5 global reanalysis”. In: *Quarterly journal of the royal meteorological society* 146.730, pp. 1999–2049.

Hoffmann, William A (1996). “The effects of fire and cover on seedling establishment in a neotropical savanna”. In: *Journal of ecology*, pp. 383–393.

Hoffmann, William A and Adriana G Moreira (2002). “The role of fire in population dynamics of woody plants”. In: *The Cerrados of Brazil: ecology and natural history of a neotropical savanna*. Columbia University Press, pp. 159–177.

Hofmann, G. S., R. C. Silva, et al. (2023). “Changes in atmospheric circulation and evapotranspiration are reducing rainfall in the Brazilian Cerrado”. In: *Scientific Reports* 13.1, p. 11236.

Hofmann, Gabriel S., Manoel F. Cardoso, et al. (2021). “The Brazilian Cerrado is becoming hotter and drier”. In: *Global Change Biology* 27.17, pp. 4060–4073.

Irons, James R, John L Dwyer, and Julia A Barsi (2012). “The next Landsat satellite: The Landsat data continuity mission”. In: *Remote sensing of environment* 122. Publisher: Elsevier, pp. 11–21.

Janssen, Thomas A. J. et al. (2023). “Extratropical forests increasingly at risk due to lightning fires”. In: *Nature Geoscience*.

Jepson, Wendy, Christian Brannstrom, and Anthony Filippi (2010). "Access Regimes and Regional Land Change in the Brazilian Cerrado, 1972–2002". In: *Annals of the Association of American Geographers* 100.1, pp. 87–111.

Johnson, Christopher N (2009). "Ecological consequences of Late Quaternary extinctions of megafauna". In: *Proceedings of the Royal Society B: Biological Sciences* 276.1667, pp. 2509–2519.

Jones, Matthew W. et al. (2022). "Global and Regional Trends and Drivers of Fire Under Climate Change". In: *Reviews of Geophysics* 60.3, e2020RG000726.

Kauffman, J Boone, DL Cummings, and DE Ward (1994). "Relationships of fire, biomass and nutrient dynamics along a vegetation gradient in the Brazilian cerrado". In: *Journal of ecology*, pp. 519–531.

Keeley, Jon E. (2009). "Fire intensity, fire severity and burn severity: a brief review and suggested usage". In: *International Journal of Wildland Fire* 18.1, p. 116.

Keeley, Jon E. and Juli G. Pausas (2022). "Evolutionary Ecology of Fire". In: *Annual Review of Ecology, Evolution, and Systematics* 53.1, pp. 203–225.

Keeley, Jon E. and Alexandra D. Syphard (2019). "Twenty-first century California, USA, wildfires: fuel-dominated vs. wind-dominated fires". In: *Fire Ecology* 15.1, 24, s42408–019–0041–.

Klink, Carlos A and Adriana G Moreira (2002). "Past and current human occupation, and land use". In: *The cerrados of Brazil: ecology and natural history of a neotropical savanna*. Columbia University Press, pp. 69–88.

Klink, Carlos A. and Ricardo B. Machado (2005). "Conservation of the Brazilian Cerrado". In: *Conservation Biology* 19.3, pp. 707–713.

Konduri, Venkata Shashank, Douglas C Morton, and Niels Andela (2023). "Tracking changes in vegetation structure following fire in the Cerrado biome using ICESat-2". In: *Journal of Geophysical Research: Biogeosciences* 128.5. Publisher: Wiley Online Library, e2022JG007046.

Krawchuk, Meg A. et al. (2009). "Global Pyrogeography: the Current and Future Distribution of Wildfire". In: *PLoS ONE* 4.4. Ed. by Jerome Chave, e5102.

L. Dantas, Vinícius de, Marco A Batalha, and Juli G Pausas (2013). "Fire drives functional thresholds on the savanna–forest transition". In: *Ecology* 94.11. Publisher: Wiley Online Library, pp. 2454–2463.

Laurent, Pierre et al. (2018). "FRY, a global database of fire patch functional traits derived from space-borne burned area products". In: *Scientific Data* 5.1, p. 180132.

Libonati, Renata et al. (2015). "An Algorithm for Burned Area Detection in the Brazilian Cerrado Using 4 μm MODIS Imagery". In: *Remote Sensing* 7.11, pp. 15782–15803.

Liu, Zhong et al. (2012). "Tropical Rainfall Measuring Mission (TRMM) precipitation data and services for research and applications". In: *Bulletin of the American Meteorological Society* 93.9, pp. 1317–1325.

Machado, Ricardo B (2016). "Estimativa de perda da área do Cerrado brasileiro". In: *Relatório Técnico Não Publicado, Conservation International do Brasil, Brasília*.

Machado, Ricardo B, Ludmilla MS Aguiar, and Mercedes MC Bustamante (2024). “Why is it so easy to undergo devegetation in the Brazilian Cerrado?” In: *Perspectives in Ecology and Conservation*. Publisher: Elsevier.

Marimon, Beatriz Schwantes et al. (2012). “Florística dos campos de murundus do Pantanal do Araguaia, Mato Grosso, Brasil”. In: *Acta Botanica Brasilica* 26.1, pp. 181–196.

Marques, Eduardo Q. et al. (2020). “Redefining the Cerrado–Amazonia transition: implications for conservation”. In: *Biodiversity and Conservation* 29.5, pp. 1501–1517.

Martin, Robert E and David B Sapsis (1992). “Fires as agents of biodiversity: pyrodiversity promotes biodiversity”. In: *Proceedings of the conference on biodiversity of northwest California ecosystems. Cooperative Extension, University of California, Berkeley*, pp. 150–157.

Mataveli, Guilherme Augusto Verola et al. (2017). *Analysis of fire dynamics in the Brazilian savannas*. preprint. Other Hazards (e.g., Glacial, Snow Hazards, Karst, Wildfires Hazards, and Medical Geo-Hazards).

– (2018). “Satellite observations for describing fire patterns and climate-related fire drivers in the Brazilian savannas”. In: *Natural Hazards and Earth System Sciences* 18.1, pp. 125–144.

Medeiros, Marcelo Brilhante de and Nilton Cezar Fiedler (2004). “Incêndios florestais no parque nacional da Serra da Canastra: desafios para a conservação da biodiversidade.” In: *Ciência Florestal* 14.2, pp. 157–168.

Medeiros, MB and HS Miranda (2008). “Post-fire resprouting and mortality in cerrado woody plant species over a three-year period”. In: *Edinburgh Journal of Botany* 65.1, pp. 53–68.

Melo, Mônica Martins and Carlos Hiroo Saito (2011). “Regime de queima das caçadas com uso do fogo realizadas pelos Xavante no Cerrado”. In: *Biodiversidade Brasileira* 1.2, pp. 97–109.

Menezes, Lucas S et al. (2022). “Lightning patterns in the Pantanal: Untangling natural and anthropogenic-induced wildfires”. In: *Science of the Total Environment*.

Miranda, AC and HS Miranda (1993). “Efeitos de diferentes regimes de queima na estrutura e dinâmica de comunidades de cerrado”. In: *RelatoÂrio final. Brasilia, DF: Departmento de Ecologia, Universidade de Brasilia*.

Miranda, Heloisa S, Mercedes MC Bustamante, and Antonio C Miranda (2002). “The fire factor”. In: *The cerrados of Brazil: ecology and natural history of a neotropical savanna*. Columbia University Press, pp. 51–68.

Miranda, Heloisa Sinátora, ed. (2010). *Efeitos do regime de fogo sobre a estrutura de comunidades de Cerrado: Projeto Fogo*. Brasília: Ibama MMA. 144 pp.

Mistry, Jayalaxshmi (1998). “Fire in the cerrado (savannas) of Brazil: an ecological review”. In: *Progress in Physical Geography* 22.4, pp. 425–448.

Mistry, Jayalaxshmi, Andrea Berardi, et al. (2005). “Indigenous Fire Management in the cerrado of Brazil: The Case of the Krahô of Tocantíns”. In: *Human Ecology* 33.3, pp. 365–386.

Mistry, Jayalaxshmi, Bibiana A. Bilbao, and Andrea Berardi (2016). “Community owned solutions for fire management in tropical ecosystems: case studies from Indigenous communities of South

America". In: *Philosophical Transactions of the Royal Society B: Biological Sciences* 371.1696, p. 20150174.

Mistry, Jayalaxshmi, Isabel Belloni Schmidt, et al. (2019). "New perspectives in fire management in South American savannas: The importance of intercultural governance". In: *Ambio* 48.2, pp. 172–179.

Morandi, Paulo S. et al. (2020). "Tree diversity and above-ground biomass in the South America Cerrado biome and their conservation implications". In: *Biodiversity and Conservation* 29.5, pp. 1519–1536.

Moris, Jose V. et al. (2023). "A global database on holdover time of lightning-ignited wildfires". In: *Earth System Science Data* 15.3, pp. 1151–1163.

Mota, Leidiana and Rita Scheel-Ybert (2019). "Landscape and firewood use in Toca do Boqueirão da Pedra Furada (Piauí, Brazil) during early and Mid-Holocene". In: *Journal of Archaeological Science: Reports* 23, pp. 281–290.

Muñoz-Sabater, Joaquín et al. (2021). "ERA5-Land: a state-of-the-art global reanalysis dataset for land applications". In: *Earth System Science Data* 13.9, pp. 4349–4383.

Myers, Norman et al. (2000). "Biodiversity hotspots for conservation priorities". In: *Nature* 403.6772, pp. 853–858.

Nascimento, Diego Tarley Ferreira and Giuliano Tostes Novais (2020). "Clima do Cerrado: dinâmica atmosférica e características, variabilidades e tipologias climáticas". In.

Nogueira, Joana et al. (2016). "Can We Go Beyond Burned Area in the Assessment of Global Remote Sensing Products with Fire Patch Metrics?" In: *Remote Sensing* 9.1, p. 7.

Oliveira, Paulo Tarso S., Mark A. Nearing, et al. (2014). "Trends in water balance components across the Brazilian Cerrado". In: *Water Resources Research* 50.9, pp. 7100–7114.

Oliveira, RS, JAN Batista, et al. (1996). "Influência do fogo na floração de espécies de Orchidaceae em cerrado". In: *Impactos de queimadas em áreas de cerrado e restinga*, pp. 61–67.

Oliveira-Filho, Ary T and James A Ratter (2002). "Vegetation physiognomies and woody flora of the cerrado biome". In: *The cerrados of Brazil: ecology and natural history of a neotropical savanna*. Columbia University Press, pp. 91–120.

Oliveras, Immaculada et al. (2013). "Effects of fire regimes on herbaceous biomass and nutrient dynamics in the Brazilian savanna". In: *International Journal of Wildland Fire* 22.3, p. 368.

Pais, Cristobal et al. (2023). "Global scale coupling of pyromes and fire regimes". In: *Communications Earth & Environment* 4.1, p. 267.

Pausas, Juli G. and Jon E. Keeley (2009). "A Burning Story: The Role of Fire in the History of Life". In: *BioScience* 59.7, pp. 593–601.

Pereira, Alfredo and Helena França (2005). "Identificação de queimadas naturais ocorridas no período chuvoso de 2003-2004 no Parque Nacional das Emas, Brasil, por meio de imagens dos sensores do satélite CBERS-2". In: *Anais XII Simpósio Brasileiro de Sensoriamento Remoto, Goiânia, Brasil, INPE*, pp. 3245–3252.

Pereira, Allan, José Pereira, et al. (2017). “Burned Area Mapping in the Brazilian Savanna Using a One-Class Support Vector Machine Trained by Active Fires”. In: *Remote Sensing* 9.11, p. 1161.

Pinheiro, Eduardo Da Silva and Giselda Durigan (2009). “Dinâmica espaço-temporal (1962-2006) das fitofisionomias em unidade de conservação do Cerrado no sudeste do Brasil”. In: *Brazilian Journal of Botany* 32, pp. 441–454.

Pivello, Vânia R. (2011). “The Use of Fire in the Cerrado and Amazonian Rainforests of Brazil: Past and Present”. In: *Fire Ecology* 7.1, pp. 24–39.

Pivello, Vânia R. et al. (2021). “Understanding Brazil’s catastrophic fires: Causes, consequences and policy needed to prevent future tragedies”. In: *Perspectives in Ecology and Conservation* 19.3, pp. 233–255.

Pohjola, Heikki and Antti Mäkelä (2013). “The comparison of GLD360 and EUCLID lightning location systems in Europe”. In: *Atmospheric research* 123, pp. 117–128.

Prates, Luciano and S Ivan Perez (2021). “Late Pleistocene South American megafaunal extinctions associated with rise of Fishtail points and human population”. In: *Nature communications* 12.1, p. 2175.

Ramos-Neto, Mário Barroso and Vânia Regina Pivello (2000). “Lightning Fires in a Brazilian Savanna National Park: Rethinking Management Strategies”. In: *Environmental Management* 26.6, pp. 675–684.

Rego, Francisco Castro et al. (2021). *Fire Science: From Chemistry to Landscape Management*. Springer Textbooks in Earth Sciences, Geography and Environment. Cham: Springer International Publishing.

Rekow, Lea (2019). “Socio-Ecological Implications of Soy in the Brazilian Cerrado”. In: *Challenges in Sustainability* 7.1, pp. 7–29.

Ribeiro, Andreia F. S., Lucas Santos, et al. (2024). “The time since land-use transition drives changes in fire activity in the Amazon-Cerrado region”. In: *Communications Earth & Environment* 5.1, p. 96.

Ribeiro, J.F. and B.M.T. Walter (2008). “Cerrado Ecologia e Flora”. In: *As principais fitofisionomias do Bioma Cerrado.* Embrapa, pp. 152–212.

Rodrigues, Julia A. et al. (2019). “How well do global burned area products represent fire patterns in the Brazilian Savannas biome? An accuracy assessment of the MCD64 collections”. In: *International Journal of Applied Earth Observation and Geoinformation* 78, pp. 318–331.

Rosan, Thais M., Luiz E.O.C. Aragão, et al. (2019). “Extensive 21st-Century Woody Encroachment in South America’s Savanna”. In: *Geophysical Research Letters* 46.12, pp. 6594–6603.

Rosan, Thais M., Stephen Sitch, et al. (2022). “Fragmentation-Driven Divergent Trends in Burned Area in Amazonia and Cerrado”. In: *Frontiers in Forests and Global Change* 5, p. 801408.

Said, Ryan (2017). “Towards a global lightning locating system.” In: *Weather (00431656)* 72.2.

Salgado-Labouriau, Maria Léa et al. (1997). “Late Quaternary vegetational and climatic changes in cerrado and palm swamp from Central Brazil”. In: *Palaeogeography, Palaeoclimatology, Palaeoecology* 128.1-4, pp. 215–226.

Sano, Edson E., Ariane A. Rodrigues, et al. (2019). “Cerrado ecoregions: A spatial framework to assess and prioritize Brazilian savanna environmental diversity for conservation”. In: *Journal of Environmental Management* 232, pp. 818–828.

Sano, Edson E., Roberto Rosa, et al. (2010). “Land cover mapping of the tropical savanna region in Brazil”. In: *Environmental Monitoring and Assessment* 166.1, pp. 113–124.

Schmidt, Isabel B., Lívia C. Moura, et al. (2018). “Fire management in the Brazilian savanna: First steps and the way forward”. In: *Journal of Applied Ecology* 55.5. Ed. by Rafael Zenni, pp. 2094–2101.

Schmidt, Isabel Belloni and Ludivine Eloy (2020). “Fire regime in the Brazilian Savanna: Recent changes, policy and management”. In: *Flora* 268, p. 151613.

Schroeder, Wilfrid et al. (2014). “The New VIIRS 375 m active fire detection data product: Algorithm description and initial assessment”. In: *Remote Sensing of Environment* 143. Publisher: Elsevier, pp. 85–96.

Schumacher, Vanúcia (2022). “Characteristics of lightning-caused wildfires in central Brazil in relation to cloud-ground and dry lightning”. In: *Agricultural and Forest Meteorology*.

Scott, Andrew C. (2018). *Burning planet: the story of fire through time*. First edition. Oxford: Oxford University Press. 231 pp.

Silva, P S, J A Rodrigues, et al. (2020). “Drivers of burned area patterns in Cerrado: the case of MATOPIBA region”. In: *2020 IEEE Latin American GRSS & ISPRS Remote Sensing Conference (LAGIRS)*.

Silva, Patrícia S., Ana Bastos, et al. (2019). “Impacts of the 1.5 °C global warming target on future burned area in the Brazilian Cerrado”. In: *Forest Ecology and Management* 446, pp. 193–203.

Silva, Patrícia S., Joana Nogueira, et al. (2021). “Putting fire on the map of Brazilian savanna ecoregions”. In: *Journal of Environmental Management* 296, p. 113098.

Silva Arruda, Vera Laísa da et al. (2024). “Assessing four decades of fire behavior dynamics in the Cerrado biome (1985 to 2022)”. In: *Fire Ecology* 20.1, p. 64.

Simon, Marcelo F., Rosaura Grether, et al. (2009). “Recent assembly of the Cerrado, a neotropical plant diversity hotspot, by in situ evolution of adaptations to fire”. In: *Proceedings of the National Academy of Sciences* 106.48, pp. 20359–20364.

Simon, Marcelo F. and Toby Pennington (2012). “Evidence for Adaptation to Fire Regimes in the Tropical Savannas of the Brazilian Cerrado”. In: *International Journal of Plant Sciences* 173.6, pp. 711–723.

Soares-Filho, Britaldo et al. (2014). “Cracking Brazil’s forest code”. In: *Science* 344.6182. Publisher: American Association for the Advancement of Science, pp. 363–364.

Soterroni, Aline C et al. (2019). “Expanding the soy moratorium to Brazil’s Cerrado”. In: *Science advances* 5.7. Publisher: American Association for the Advancement of Science, eaav7336.

Souza, Carlos M. et al. (2020). “Reconstructing Three Decades of Land Use and Land Cover Changes in Brazilian Biomes with Landsat Archive and Earth Engine”. In: *Remote Sensing* 12.17, p. 2735.

Spera, Stephanie A. et al. (2016). “Land-use change affects water recycling in Brazil’s last agricultural frontier”. In: *Global Change Biology* 22.10, pp. 3405–3413.

Stevens, Nicola et al. (2017). “Savanna woody encroachment is widespread across three continents”. In: *Global Change Biology* 23.1, pp. 235–244.

Van Wilgen, BW et al. (2000). “A fire history of the savanna ecosystems in the Kruger National Park, South Africa, between 1941 and 1996”. In: *South African Journal of Science* 96.4. Publisher: Academy of Science for South Africa (ASSAf), pp. 167–178.

Veraverbeke, Sander et al. (2017). “Lightning as a major driver of recent large fire years in North American boreal forests”. In: *Nature Climate Change* 7.7, pp. 529–534.

Vialou, Denis et al. (2017). “Peopling South America’s centre: the late Pleistocene site of Santa Elina”. In: *antiquity* 91.358, pp. 865–884.

Vieira, Leandro T.A. et al. (2022). “Reviewing the Cerrado’s limits, flora distribution patterns, and conservation status for policy decisions”. In: *Land Use Policy* 115, p. 106038.

Welch, James R. et al. (2013). “Indigenous Burning as Conservation Practice: Neotropical Savanna Recovery amid Agribusiness Deforestation in Central Brazil”. In: *PLoS ONE* 8.12. Ed. by Brock Fenton, e81226.

Werf, G. R. van der, J. T. Randerson, L. Giglio, T. T. van Leeuwen, et al. (2017). “Global fire emissions estimates during 1997–2016”. In: *Earth System Science Data* 9.2, pp. 697–720.

Werf, Guido R. van der, James T. Randerson, Louis Giglio, Nadine Gobron, et al. (2008). “Climate controls on the variability of fires in the tropics and subtropics”. In: *Global Biogeochemical Cycles* 22.3, 2007GB003122.

Wu, Chao et al. (2022). “Reduced global fire activity due to human demography slows global warming by enhanced land carbon uptake”. In: *Proceedings of the National Academy of Sciences* 119.20, e2101186119.

3 | Human land occupation regulates the effect of the climate on the burned area of the Brazilian Cerrado (Research Paper 1)

By: Carlota Segura-Garcia, David Bauman, Vera L. S. Arruda, Ane A. C. Alencar, Imma Oliveras Menor

Linking statement: This first chapter was motivated by the need to understand whether and how the opposing trends in burned area observed across the Brazilian Cerrado were explained by the generalised increases in temperature and in land use area in this region over the past four decades. Some studies in the Cerrado had suggested that decreases in burned area could be related to increases in land use area, while climate change was related to increases in burned area. However, no studies thus far had provided a clear explanation for how these two drivers of fire, land use area and the climate, combined to affect the burned area of the Cerrado. Therefore, as a first step to understanding how the dynamics of fire of the Cerrado have been changing over the past few decades, this chapter focused on characterising the interaction between land use area and the climate as drivers of burned area.

This chapter was published on 6th July, 2024 in *Communications Earth & Environment* (https://doi.org/10.1038/s43247-024-01521-5). It has been included in this thesis in the same structure in which it was published, with the Methods section after the Discussion.

Results were presented as an oral presentation at the 59th Annual Meeting of the Association for Tropical Biology and Conservation in Coimbatore, India, and at the General Assembly of the European Geosciences Union in Vienna, Austria.

Contribution Statement: I, Carlota Segura-Garcia, conducted the conceptualization, methodology development, data processing and data analysis, investigation, visualization of the results, and writing of the manuscript. In addition, I responded to all review comments during the peer review process. Dr David Bauman helped in the methodology,

analysis and reviewing of the manuscript and of the responses to the reviewer's comments. Vera L. S. Arruda and Dr Ane Alencar helped in the conceptualization, investigation and reviewing of the manuscript. Finally, Dr Imma Oliveras Menor supervised and was involved in all steps of this work.

3.1 Abstract

Human activities and climate change are transforming fire regimes globally. The interaction between these two drivers is poorly understood, yet critical if we aim at predicting how biomes will respond to novel fire regimes. In the Brazilian Cerrado, altered fire regimes are threatening its unique biodiversity and ecosystem functioning. Here, using geospatial data for the period 1985-2020 and a causal inference framework to design Bayesian statistical models, we demonstrate that a larger human presence in the landscape ($\geq$40% land use area) reduces the Cerrado's burned area and hinders its responsiveness to climate; while climatic effects only become apparent in landscapes with little human presence, where hotter and drier conditions increase burned area. Finally, we find spatially heterogeneous burned area trends over time, with increases associated with climate change in landscapes that have remained mostly intact, and decreases caused by anthropic expansion. Both diverging trends have important implications for the conservation of the Cerrado as land use expansion and climate change continue to unfold.

Keywords **-** fire, climate change, climate-human interactions, neotropical savannas

3.2 Introduction

Fire is a complex process that involves the interplay between anthropic activities, the climate, and vegetation structure that both shape and are in turn affected by this phenomenon (Archibald, Lehmann, et al., 2018). Understanding the drivers of fire and how they interact is essential to tackling the many challenges which fire poses globally, from human health and the economy (Mendonça et al., 2004; Xu et al., 2020) to its influences on the Earth's biogeochemical cycles (Archibald, Lehmann, et al., 2018; Wu, Sitch, et al., 2022), and the conservation of both fire-adapted and fire-sensitive ecosystems (Pivello, 2011). Indeed, fire is a natural disturbance process playing a crucial role in shaping ecosystems (Bond et al., 2005), but human activities are altering the Earth's fire regimes (Kelly et al., 2020; Archibald, 2016). Over the last two decades, global burned area has declined in

association with agricultural expansion and intensification, with greater declines concentrated in savannas (Andela et al., 2017). In other regions, modern human activities have escalated the occurrence of fire (Barlow et al., 2020) indicating that anthropic effects vary depending on the context (Andela et al., 2017). Simultaneously, climate change is intensifying the risk of fire weather conditions (Jolly et al., 2015; Abatzoglou, Williams, et al., 2019) and the frequency of extreme weather events (Stott, 2016), exacerbating fire activity and burned area. Therefore, globally, the two main drivers of fire, humans and the climate, could be pushing burned area in opposite directions, but there is still considerable uncertainty in how they interact (Archibald, Roy, et al., 2009; Aldersley et al., 2011). Quantifying such interactions is fundamental to improve our understanding of feedbacks between the climate, fires and vegetation (Wu, Venevsky, et al., 2021; Wu, Sitch, et al., 2022).

Savanna ecosystems stand out as a paradigmatic case of these apparently contrasting processes (Archibald, Scholes, et al., 2010). Savannas are a predominant biome covering around 20% of the terrestrial surface with extensive presence of humans. These ecosystems play a relevant role on the Earth's carbon cycle contributing to around 25% of the total gross primary productivity (Beer et al., 2010) and have an - often neglected - high biodiversity and ecological value (Parr et al., 2014; Veldman, Overbeck, et al., 2015; Veldman, Buisson, et al., 2015). Savannas are composed of fire-adapted vegetation that depends on this natural disturbance for their continuity and the preservation of their biodiversity (He et al., 2019). Therefore, departures from the historical fire regimes in either direction can have important ecological consequences potentially resulting in ecosystem shifts to other forms (Staver et al., 2011; Oliveras et al., 2016), as well as effects on the Earth's carbon cycle that can feed back to the climate (Wu, Sitch, et al., 2022). In these regions, the observed declines in burned area (Archibald, Scholes, et al., 2010; Silva, Rodrigues, et al., 2020) are often linked to landscape fragmentation (Archibald, Scholes, et al., 2010; Rosan, Sitch, et al., 2022), population density, certain agricultural practices or increasing grazing pressure that disrupt fuel continuity impairing fire spread. Active fire suppression is also a relevant cause of burned area reduction, known to lead to woody en-

croachment causing biodiversity losses (Stevens et al., 2017; Rosan, Aragão, et al., 2019) and increasing the risk of more severe wildfire events (Fidelis et al., 2018). Regarding the climate, some studies forecast increases in savannas' burned area associated with warming and the lengthening of the dry season (Wu, Venevsky, et al., 2021). However, it has also been suggested that human controls on savannas' burned area may limit its responsiveness to climatic conditions (Archibald, Nickless, et al., 2010; Conciani et al., 2021), but it is still unclear how much human activities regulate the climate effects on fire.

Here, we focus on the Cerrado, a Brazilian ecoregion comprising several savanna ecosystems and considered to be a biodiversity hotspot (Myers et al., 2000). The Cerrado occupies over 2 million km^2, with around 50% of its area already converted to anthropic land uses (Souza et al., 2020), and undergoing a warming and drying process (Hofmann et al., 2021) associated with climate change (Li et al., 2021). These savannas present spatially heterogeneous patterns of burned area (Silva, Nogueira, et al., 2021) in accordance with its mosaic vegetation and widespread agricultural areas, with both increasing and decreasing burned area trends (Silva, Rodrigues, et al., 2020; Rosan, Sitch, et al., 2022; Mataveli et al., 2018). Much research has been devoted to studying climate effects on the intra-annual (Libonati et al., 2015; Moreira de Araújo et al., 2012; Nogueira et al., 2017) and inter-annual (Libonati et al., 2015; Li et al., 2021) variability of burned area, identifying increasing burned area trends in relation to climate change (Silva, Rodrigues, et al., 2020; Silva, Bastos, et al., 2019). Regarding anthropic area and landscape fragmentation, these seem to have a more complex association with fire activity (Silva, Rodrigues, et al., 2020; Rosan, Sitch, et al., 2022; Conciani et al., 2021), while burned area is concentrated in regions with larger natural remnants (Moreira de Araújo et al., 2012; Silva, Nogueira, et al., 2021). Disentangling the effects of climate change and human presence is essential to devise effective fire management policies and conservation plans that are targeted to the characteristics of the landscape and to its vegetation composition.

Using a causal inference framework and a Bayesian approach, we aim to study whether and how the level of human presence in the landscape regulates the effects of the climate on the burned area of the Cerrado. We use the percentage of anthropic area - comprising

agricultural, urban and mining land uses - as a proxy for the level of human presence in the landscape to, first, determine its effects on burned natural area - measured as the percentage area of Cerrado native vegetation that burned. Then, we quantify the interaction between the climate and human presence by modelling the effects of the climate on burned area in landscapes with different levels of human presence using Bayesian multilevel regression models. Finally, we explore the spatial distribution of the temporal trends in burned area, climate and anthropic expansion and build a model to determine the causal effects of the last two as predictors of the former.

3.3 Results

3.3.1 Limited burned natural area in human-dominated landscapes

First, we modelled the causal effect of anthropic area percentage on the burned natural area percentage of the Cerrado. With this aim, we combined annual land use and burned area data on a 0.2^{o} grid over the Cerrado for the period 1985 to 2020 (see Methods). As we were interested in studying the causal effect of the predictor - anthropic area - , we used a structural causal modelling framework (Arif et al., 2023) which, based on assumptions and *a priori* knowledge about our study system, provides a set of rules - known as the backdoor criterion (Pearl et al., 2016; Arif et al., 2023) - to design models with the sufficient statistical adjustments to limit bias and confounding, thus enabling causal inference.

Therefore, we first designed a Directed Acyclic Graph (DAG), DAG1 (Supplementary Fig. S3.1), a form of heuristic causal model used to visually represent the causal relations between the different variables of our system and inform covariate selection (see Methods and Supplementary Methods). This DAG was designed based on author's expert knowledge about savanna fire and its drivers, the literature and exploratory data analysis, and reflects our assumptions about how the different variables affect each other (see Methods and Supplementary Methods). Hence, based on DAG1, we built model M1 (Equation 3.3). This model included anthropic area percentage as the explanatory variable of interest for

which we wanted to determine its total causal effects on burned natural area, along with protected area and latitude as control variables. These last two covariates were needed according to the backdoor criterion to enable the causal interpretation of anthropic area effects, but it is important to stress that their own modelled effects cannot be interpreted causally (see Methods).

With model M1, we found that the higher the presence of humans in the landscape in terms of area occupied, the smaller the fraction of burned natural area (Supplementary Fig. S3.2, slope coefficient: -0.130, [-0.135, -0.126], 95% Highest Posterior Density Interval, HPDI, % burned natural area % anthropic area^{-1}), implying that human dominance of a landscape acts to limit the fraction of burned area in Cerrado's native vegetation as hypothesised.

Finally, we calculated the R-squared coefficient adjusted for Bayesian inference (Gelman et al., 2019) of model M1 (0.544 [0.542, 0.547] 95% confidence interval, Supplementary Table S3.1). However, it is important to bear in mind that the aim of this study was to determine total causal effects, not to maximise model predictability. Therefore, in this and subsequent models, the R-squared coefficient was calculated just as an indication of the proportion of variance explained by the model, but it should not be interpreted as a measure of the causal relation between the predictors and the response variable.

3.3.2 Climate effects on burned natural area are conditional on human landscape dominance

Then, we assessed the causal effects of climatic controls on the burned natural area of the Cerrado, and the extent to which these controls depend on anthropic factors such as anthropic area. Thus, we quantified the causal effects of temperature, vapour pressure deficit (VPD), same and previous year total precipitation and dry season precipitation (Supplementary Fig. S3.3) on the observed percentage of burned natural area (Supplementary Fig. S3.4) using climate data from different sources (see Methods).

Using the same DAG1 as before, we built two Bayesian multilevel models (M2 and M3,

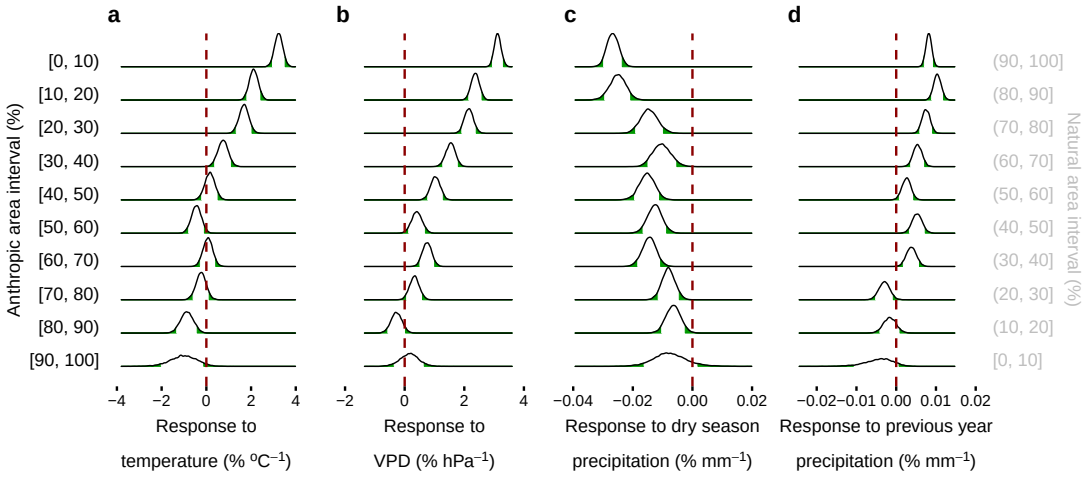

Figure 3.1: **Posterior distributions of the covariate slopes from multilevel regression models M2 and M3.** These models use a focal climatic variable of interest as predictor to explain percentage of burned natural area, while allowing the climate effect (x-axis) to vary by decile of anthropic area percentage (y-axis). Predictor variables: **a** temperature, **b** vapour pressure deficit (VPD), **c** same year dry season precipitation, and **d** previous-year total precipitation. As calculated, natural area percentage and anthropic area percentage add to 100%. Green shaded areas indicate the regions of the posterior distributions falling outside the 90% HPDI, which we use as credibility interval. Red dashed lines are drawn as a reference to indicate whether 0 (i.e. no clear effect) is a likely outcome of the posterior distributions.

Equations 3.4 and 3.5, see Methods) where we allowed the climate effect coefficients to vary by decile of anthropic area percentage (Supplementary Fig. S3.5) to determine the interaction of the climate covariates with the level of human occupation (Fig. 3.1, see R-squared coefficients in Supplementary Table S3.2). Using the backdoor criterion, we included latitude as a control variable to avoid confounding in model M2 for temperature and VPD (see Methods), while no covariates were needed in model M3 for the different precipitation variables.

We found that the slope coefficients for all climate predictors showed a non-linear change in behaviour with the level of human presence in the landscape (Fig. 3.1). In cells with a large area of natural vegetation - around 40% or less of anthropic area -, we observed the expected effect of the climate on burned natural area: increases in temperature and VPD cause increases in burned natural area; the lower the dry season precipitation, the

larger the burned area; and higher precipitation in the previous year brought about larger burned area in the following year. We found no strong causal effect of same year total precipitation (Supplementary Fig. S3.6a). In contrast, where anthropic land uses dominate the landscape - around 40 % or more of the cell's area -, we observed no effect of these climatic variables on the percentage of burned natural area, suggesting strong controls of land use activities.

Those observations in the [90-100]% decile of anthropic area showed negligible effects of any climatic variables on burned natural area (Fig. 3.1). We used these results as a reference to test the presence of thresholds from which the effect of the climate in following deciles was different compared to this extreme case. With this aim, for each climate covariate, we generated pairwise contrasts by subtracting the posterior distribution of the slope coefficient obtained for the [90, 100] % decile from the corresponding posterior of every other decile (Supplementary Fig. S3.7). We considered that if the 90% HPDI of the pairwise contrast (the difference between the posteriors) did not encompass 0, then there was an effect of the climate on the burned natural area in that decile compared to the no-effect [90, 100] % reference. Indeed, we found that below some anthropic area percentage, temperature (50% anthropic area), VPD (40%), previous year precipitation (40%), and dry season precipitation (20%) had an effect on burned natural area. Hence, for each climatic variable there was a certain threshold value of anthropic area percentage at which burned natural area transitioned from being not responsive to becoming increasingly affected by climate. This transition was sudden, that is, non-linear.

Among these climatic variables, VPD and temperature seemed to have a more marked effect on burned area than dry season and previous year precipitation (Fig. 3.1), suggesting the former two may emerge as stronger climatic controls of burned natural area. We explored this further by comparing the predicted effect on burned natural area of each climate variable at their average value to their predicted effect at their average value plus (minus in the case of dry season precipitation) 2 standard deviations in each anthropic area decile (Supplementary Fig. S3.8). We observed that, in the less anthropic landscapes (particularly the [0, 10)% decile, see Supplementary Fig. S3.9), when increasing

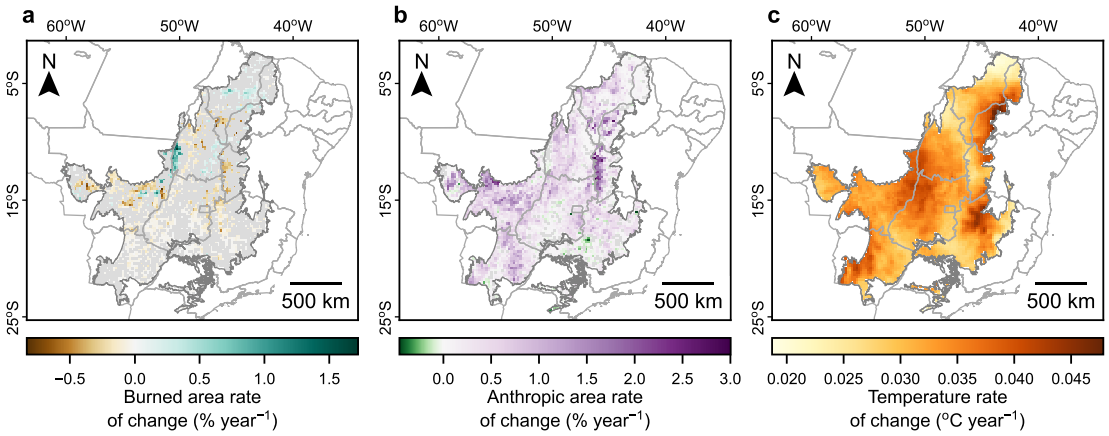

Figure 3.2: **Spatial distribution of the trends in time (slope coefficients) obtained from model M4 for each cell in a 0.2º grid over the Cerrado using the year as the predictor over the period 1985-2020.** Trends for **a** burned natural area percentage, **b** anthropic area percentage, and **c** temperature. Grey indicates cells with no evidence of clear trends - the 95% HPDI encompasses 0.

(decreasing) each climatic variable's value by 2 standard deviations, VPD was the variable with the largest increase in burned natural area, followed by temperature; while the change in effect of dry season and previous year precipitation was more limited.

3.3.3 Trends in burned natural area, climate change and anthropic expansion

We explored the spatial distribution of the temporal trends in burned natural area, the climate and anthropic area (Fig. 3.2) using a Bayesian linear regression model with year as the independent variable (model M4, Equation 3.6). We observed a heterogeneous spatial structure of increases and decreases in burned natural area percentage over the period 1985-2020 (Fig. 3.2a). We also detected a widespread expansion of human land uses (Fig. 3.2b) particularly acute in some regions that were mostly natural at the beginning of the study period (Supplementary Fig. S3.5a). Regarding the climate, there was a generalised increase in temperature in the Cerrado (Fig. 3.2c), but we found no evidence of clear trends in precipitation, in agreement with previous studies (Hofmann et al., 2021).

Then, we studied whether these trends in temperature (tT) and in anthropic area (tA) had

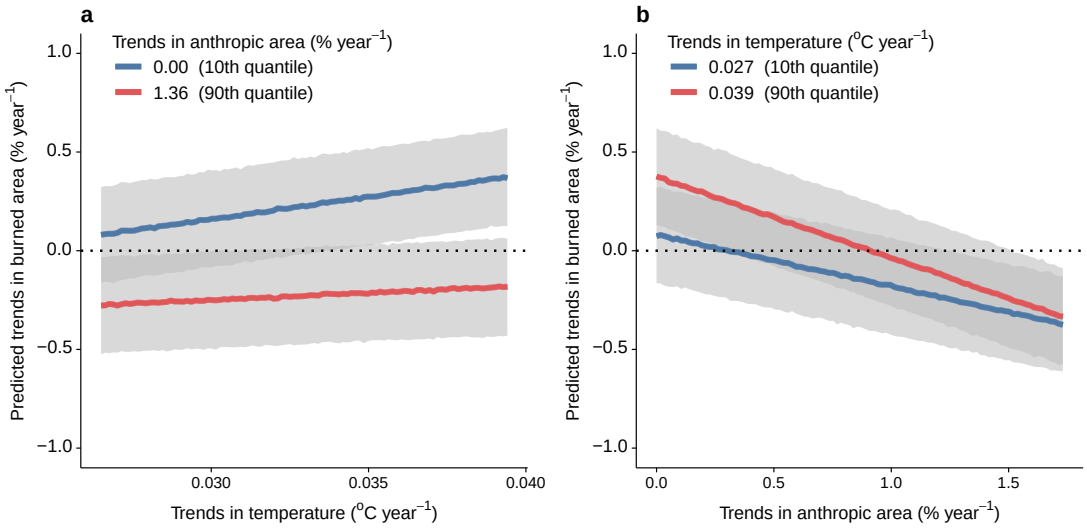

Figure 3.3: **Predicted temporal trends in burned natural area (tBA) from model M5 for those cells that were mostly intact in 1985, with 0 - 20% of anthropic area (80 - 100% of natural area).** These predictions are generated by fixing one predictor and exploring the effects of varying the other. **a** The effects of trends in temperature (tT) on tBA for two fixed values of trends in anthropic area (tA) corresponding to the 10th percentile (0.00 % year^{-1}) and 90th percentile (1.36 % year^{-1}, or 48.96 % in the period) of the range of tA values observed in this group of cells. **b** The effects of tA after fixing tT at the 10th (0.027 ^{o}C year $^{-1}$, or 0.97 ^{o}C in the period) and 90th (0.039 ^{o}C year $^{-1}$, or 1.40 ^{o}C in the period) percentiles of its observed data values for this group of cells. Grey shaded areas correspond to the 80% HPDI.

a causal effect on the temporal changes in burned natural area (tBA), and whether these variables mediated each other's effects. With this aim, we built a second DAG (DAG2, Supplementary Fig. S3.10) representing the relations between these different trends in time. Since the extent of anthropic area expansion was contingent on the level of human occupation at the beginning of the study period, we grouped the cells in five intervals of 20% anthropic area in 1985. Hence, we modelled the causal effects of tT and tA allowing the slope coefficients to vary by interval using a Bayesian multilevel model (model M5, Equation 3.7) based on DAG2. In addition, we included an interaction term between tT and tA to allow the effect of climate change severity to depend on the level of change in anthropic area. Finally, we explored the implications of model M5 looking at the implied posterior predictions of tT and tA on tBA in the study period (Fig. 3.3 and Supplementary Figs. S3.11 and S3.12). That is, we explored the values of tBA predicted by model M5

for different combinations of tA and tT.

We found that, indeed, the effects on tBA exerted by tT and tA varied depending on the pre-existing levels of anthropic area in 1985 (Supplementary Figs. S3.11 and S3.12, see R-squared coefficients in Supplementary Table S3.3). For those cells that were mostly anthropic in 1985 (more than 40% of anthropic area), we found that both predictors had limited to no effects on tBA. However, for those cells that were mostly natural at the beginning of the period (less than 40% of anthropic area), model M5 predicted a different effect for each predictor. These differing effects were even more evident in cells with $<$20% of anthropic area in 1985 (Fig. 3.3).

In these cells, the effects of the rate of temperature increase seemed to be mediated by the extent of anthropic expansion (Fig. 3.3a). Where human presence in the form of land uses markedly expanded (tA value of 1.36% per year, or 48.96% in the period, red line in Fig. 3.3a), burned natural area decreased over time (negative tBA) regardless of tT. In contrast, where anthropic area remained low and roughly at the same level (tA of 0%, blue line in Fig. 3.3a), we found that warming caused increases in burned natural area over time (positive tBA), and the more acute the temperature increase, the greater the increase in burned natural area over time.

This behaviour became even clearer when we fixed tT at a large (0.039 ^{o}C year^{-1}, or 1.40 ^{o}C in 36 years, red line in Fig. 3.3b) and small (0.027 ^{o}C year^{-1}, or 0.97 ^{o}C in 36 years, blue line in Fig. 3.3b) value and looked at the effect on tBA of varying tA (Fig. 3.3b). In both cases, when tA is small (limited anthropic expansion), burned natural area increases over time (positive tBA), and the larger the increase in temperature (tT), the larger the tBA (larger tBA value in the red line than in the blue line in Fig. 3.3b). However, when tA is large (large anthropic expansion) tBA becomes negative (burned area decreases over time) independently of tT value (similar tBA values in the red and blue predicted values).

3.4 Discussion

This study demonstrates that anthropic land use activities limit the responsiveness of burned natural area to climatic conditions in areas of the Brazilian savannas where humans have a substantial presence (Fig. 3.1). Moreover, we find that the interaction between these two drivers is non-linear: humans completely limit burned natural area responses to climate up to a certain level of anthropic area percentage beneath which the expected relation between the climate and burned natural area is recovered. These mitigating effects extend to areas where anthropic land uses are not the major land cover (up to 30-40% of the area, Supplementary Fig. S3.7), indicating that human controls on fire stretch to landscapes where considerable natural vegetation remains. In addition, we find that a larger anthropic area is associated with an overall reduced percentage of burned area in natural land cover areas (Supplementary Fig. S3.2).

We use anthropic area percentage as an indicator of the presence of human activities and their influence in the landscape, as it encompasses a series of direct anthropic effects on burned natural area. Most anthropic area in the Cerrado consists of agricultural land (Souza et al., 2020) conforming fragmented landscapes (Rosan, Sitch, et al., 2022), which limits fire spread through fuel discontinuities (Archibald, Roy, et al., 2009). Another cause of burned area limitation is active fire suppression, a common practice in the Cerrado enforced by policies (Durigan and Ratter, 2016), although there have been substantial efforts to change these approaches (Durigan and Ratter, 2016; Durigan, 2020; Schmidt et al., 2020). Among other consequences, this reduction in burned natural area contributes to woody encroachment (Rosan, Aragão, et al., 2019; Stevens et al., 2017), in turn leading to the loss of biodiversity (Abreu et al., 2017) and potential ecosystem shifts (Oliveras et al., 2016).

On the other hand, where anthropic area is much smaller, landscape fragmentation is reduced and, consequently, fuel bed continuity may no longer be a limiting factor to fire spread (Archibald, Roy, et al., 2009). Furthermore, access to these areas may be more challenging, reducing fire suppression opportunities. Accordingly, in mostly natural land

cover areas fuel load and its flammability may become more relevant determinants of burned area (Rego et al., 2021), both of which are influenced by climate. Indeed, our results demonstrate that in these landscapes climate is a driver of burned natural area (Fig. 3.1). We find that a higher temperature and VPD causes an increase in burned natural area, as expected, since temperature increases the moisture holding capacity of the air, drying the fuel and making it more flammable (Westerling et al., 2006). In agreement with earlier studies, we observe that lower precipitation in the dry season contributes to larger burned areas as it also influences fuel flammability (Flannigan et al., 2013; Conciani et al., 2021), while higher precipitation in the previous year causes larger burned areas as it affects vegetation productivity and, hence, fuel load (Pausas et al., 2013). However, although these fires are occurring in mostly non-anthropic land cover areas, they are not necessarily naturally ignited (e.g. by lightning), as humans are still the main ignition source (Pivello, 2011). This fact does not conflict with the low presence of humans in these landscapes because most burned area is produced by few very large fires (Hantson et al., 2016), so a small number of ignitions can result in large burned areas (Archibald, Roy, et al., 2009), especially under hot and dry conditions.

Regarding the trends in time, we find a heterogeneous pattern of increases and decreases in burned area (Fig. 3.2), in line with previous studies (Mataveli et al., 2018; Silva, Rodrigues, et al., 2020; Silva, Nogueira, et al., 2021). When exploring the relation between trends in burned natural area, anthropic expansion and climate change, model predictions reinforce our results presented above. First, changes in burned natural area over time are conditional on the extent of anthropic area at the beginning of the period. Landscapes that were mostly anthropic in 1985 do not present strong trends because burned natural area was already limited and not responsive to climate (Supplementary Figs. S3.11 and S3.12). As such, significant trends in burned natural area are concentrated in cells that were mostly natural in 1985. We find that, in these areas, trends are firstly subject to the extent of anthropic area increases (Fig. 3.3), which brings about a reduction in burned natural area - adding to 31.1% of the cells -, probably in relation to increasing fragmentation and human controls on fire. In contrast, those cells that have remained more intact

are the ones where burned natural area increased over time, totalling 9.7% of the cells. Our model indicates that these increases are associated with the warming and drying of the Cerrado due to climate change.

Indeed, both VPD and temperature, which we identify as the strongest climatic drivers of burned natural area change out of those considered (Supplementary Figs. S3.8 and S3.9), have increased over the Cerrado in the past few decades and are expected to continue rising (Hofmann et al., 2021). Such increases have been particularly acute towards the end of the dry season (Hofmann et al., 2021) when climatic conditions are most favourable for fire spread and when most human-started fires occur (Silva, Nogueira, et al., 2021). Our findings indicate that as the warming and drying conditions continue lengthening and exacerbating under climate change, we can expect these increasing trends in the burned areas of the more intact regions of the Cerrado to continue. Therefore, we identify those areas with larger natural vegetation remnants as being more vulnerable to climate change. Among these, the region of the Parque Estadual do Araguaia in the centre-west of the Cerrado stands out for its considerable increase in burned natural area over the period. This area is formed by seasonally flooded savannas particularly vulnerable to droughts (Souza Neves et al., 2018), suggesting that the type of vegetation may be important in the evolution of fire activity. Although savannas are fire-adapted ecosystems, changes in fire regimes towards larger, more frequent, and intense events under climate change may have degradation effects on these ecosystems, which could hamper their recovery following disturbances in the future (Pivello et al., 2021). In this sense, practices such as integrated fire management are proving to be effective strategies to prevent large and severe fires while contributing to preserve the Cerrado's vegetation mosaic (Fidelis et al., 2018; Santos et al., 2021; Franke et al., 2024).

In conclusion, climate change and human land use activities in the Cerrado are altering the fire regimes of the region, both with important ecological consequences. Importantly, we show that human controls over the Cerrado's fire dynamics are substantial and act to limit burned area and to regulate the effect of climate and climate change, contributing to the growing recognition of the role of humans on shaping fire patterns (Andela et al.,

2017; Bowman et al., 2009; Archibald, Roy, et al., 2009; Conciani et al., 2021) and emphasising the need to improve their representation in projections of fire activity and in climate-vegetation models (Wu, Venevsky, et al., 2021; Wu, Sitch, et al., 2022). We find that the greatest changes in burned natural areas over time occurred in the most intact areas, which experienced increases in burned area due to climate change, and in areas with more severe agricultural expansion, which brought about decreases in the proportion of burned natural area. Both directions of burned area change can have important deleterious effects on Cerrado vegetation. Future research could build upon these results by exploring whether these responses to human activities and the climate differ between vegetation formations or land use type - mainly croplands or pastures (Rosan, Sitch, et al., 2022). The widespread changes of fire activity in either direction, in combination with other consequences of large-scale agricultural expansion and climate change, highlight the multiple pressures the Brazilian savannas are subject to. Considering the importance of the Cerrado in providing local livelihoods, its major role providing and distributing regional water resources (Oliveira et al., 2014), and its rich biodiversity and high levels of endemism (Myers et al., 2000), our findings stress the urgent need to extend conservation practices beyond protected areas and to deploy appropriate fire management policies (Durigan and Ratter, 2016; Durigan, 2020).

3.5 Methods

3.5.1 Study area

In this study we focus on the Cerrado, a region of over 2 million km^2 comprising the Brazilian savannas. These savannas are very biodiverse (Myers et al., 2000) and spatially heterogeneous, with vegetation ranging from grasslands to tracts of gallery forests and other woody forms (Ribeiro et al., 2008). The climate of the Cerrado is characterised by a strong seasonality, with a wet and a dry season, when most burned area occurs (Silva, Nogueira, et al., 2021). The average temperatures range between 18°C and 28°C increasing about a latitudinal gradient towards the Equator (Supplementary Fig. S3.3a).

Precipitation varies from about 800 mm to 2000 mm of total annual precipitation, roughly increasing from east to west towards the Amazon (Supplementary Fig. S3.3b).

Over the last four decades, the Cerrado has experienced a rapid agricultural expansion affecting around 45% of its area (Alencar, Z. Shimbo, et al., 2020). In this study, we focus on the 36 year period from 1985 to 2020. It is important to note that already in 1985 large areas in the south of the Cerrado had been converted to pastures and croplands (Supplementary Fig. S3.5a).

As we use data from different sources with various spatial resolutions, we divide the Cerrado into a 0.2^{o} grid (about 22.2 km^2) and summarise the different variables at the cell level (see details below). In the analysis, we only include cells with more than 90% of their area within the Cerrado.

3.5.2 Land use data

We use annual maps of land use and land cover from MapBiomas (Collection 6.0, (Souza et al., 2020)) for the period 1985 to 2020. This open data and open source project used a random forest algorithm to classify pixels from annual mosaics of Landsat images at 30 m spatial resolution into several categories. This dataset was developed using Google Earth Engine (Gorelick et al., 2017) and is available through the MapBiomas toolkit on the same platform.

In this study, we first simplify the MapBiomas categorisation to either natural land cover pixels (herein natural pixels), anthropic land use pixels (anthropic pixels), or other pixels based on the legend codes of Collection 6.0 (Souza et al., 2020). Under natural land cover, we group all subcategories under "Forest", those of "Non Forest Natural Formation", and "Beach, Dune and Sand Spot". As anthropic land uses, we group all subcategories under "Farming", along with "Urban Area" and "Mining". The remaining categories - "Other non Vegetated Area", "Water" and "Non Observed" - are grouped as "other".

For each cell and year, we calculate the percentage of anthropic area as

$$\% \text{ anthropic area} = 100 \cdot \frac{\text{N anthropic pixels}}{\text{N anthropic pixels} + \text{N natural pixels}}, \tag{3.1}$$

where N stands for number. Therefore, % anthropic area $= 100 -$ % natural area, as we are leaving out of the calculation the "other" categories because they are not susceptible to burning.

3.5.3 Burned area data

We obtain the burned area data from MapBiomas Fogo (Collection 1.0, (Alencar, Arruda, et al., 2022)) for the study period, 1985-2020. This dataset consists of maps where pixels are identified as either burned or not burned, along with the month in which the pixel was mapped as such. These maps were created from mosaics of Landsat images at 30 m spatial resolution with a 16-day interval.

For each cell and year, we use the number of natural pixels classified as burned to calculate our main variable of interest, the percentage of natural area that burned (herein burned natural area),

$$\% \text{ burned natural area} = 100 \cdot \frac{\text{N burned natural pixels}}{\text{N natural pixels}}. \tag{3.2}$$

3.5.4 Climate reanalysis data

We use various climatic variables from different data products because of their relation to burned area. We use the 2 metre temperature parameter from ERA5-Land Monthly Averaged climate reanalysis data at 9 km spatial resolution (Muñoz-Sabater et al., 2021). We use this variable along with the 2 metre dewpoint temperature from the same dataset to calculate vapour pressure deficit (VPD), a direct measure of the atmospheric demand for water. We calculate VPD as the difference between saturation pressure (e_s) and actual vapour pressure (e_a) following the procedure detailed in (Allen et al., 1998). Finally, we calculate the annual average temperature and VPD for each cell and year.

We use precipitation data from the Climate Hazards Group InfraRed Precipitation with Station data (CHIRPS, version 2.0), a quasi-global rainfall dataset with 0.05° spatial resolution covering more than 35 years (Funk et al., 2015). This data was acquired in the Pentad version (5-day precipitation accumulation in mm). To obtain the total precipitation per year and cell, we first calculate the monthly total precipitation per pixel, then we calculate the monthly precipitation per cell taking the spatial average, finally adding up the monthly averages to the annual precipitation.

For each calendar year, we calculate the total dry season precipitation as the sum of the monthly precipitation of the dry season months (usually around May to September). We identify the dry season months for each year as those in which precipitation is smaller than the potential evapotranspiration (PET). We obtain the PET from TerraClimate (Abatzoglou, Dobrowski, et al., 2018), a dataset of monthly climate data at the global scale and 0.5° resolution, and calculate the cell's spatial average PET.

All climate data from the different products were downloaded through Google Earth Engine (Gorelick et al., 2017).

3.5.5 Protected area data

In the first model, we include the percentage of protected area in a cell and year as a covariate. We obtained the data on the conservation units and indigenous lands of Brazil from the Ministério de Meio Ambiente do Brasil (MMA) (*Cadastro Nacional de Unidades de Conservação/Ministério de Meio Ambiente* 2019). We calculated the percentage area of each cell and year occupied by those protected area established on or before the year.

3.5.6 Data analysis

To tackle the different research questions, we use various Bayesian linear regression models and Bayesian multilevel models (M1 through to M5), whose structure and variable inclusions were guided to allow causal inference. With this aim, we first draw two Directed

Acyclic Graphs (DAGs) describing our system (DAG1 and DAG2, Supplementary Figs. S3.1 and S3.10). Based on these DAGs, and depending on the causal effects of interest, we applied the backdoor criterion - a test that allows to determine whether and how we can compute a causal effect - to inform our modelling strategy and the selection of covariates to explore causal implications (McElreath, 2018; Pearl et al., 2016; Arif et al., 2023; Addicott et al., 2022; Laubach et al., 2021).

Creation of a causal inference framework

Directed Acyclic Graphs (DAGs) are graphical representations of the causal relations between the different variables of interest, along with other variables that may bias or alter the causal association between a given explanatory variable of interest and the response variables (Pearl et al., 2016; Arif et al., 2023). We build DAG1 (Supplementary Fig. S3.1) to represent the relations between the variables that may affect the percentage of burned natural area, and DAG2 (Supplementary Fig. S3.10) to depict the relations between the different variables that may affect trends in burned natural area with time. The design of both DAGs is based on the authors' expertise, on supporting literature, and exploratory data analysis of the variables that may play a role in the system and their relations.

Fire, and burned area in specific, is a complex phenomenon that involves many different drivers and actors interacting in an intricate manner, and while fully describing complex multifactorial systems such as the one studied here can be challenging, we explicitly acknowledged and accounted for what we consider to be all the major nodes and causal links relevant to the questions of the present work (details in Supplementary Methods). These DAGs therefore provided a rational basis upon which we conditioned causal inference using statistical models, while making the ecological assumptions underlying our models and causal inferences transparent. DAGs entail testable implications of relations between variables, like conditional independencies (McElreath, 2018; Addicott et al., 2022), that we have checked based on the associations and conditional associations in the data to validate the DAG structure, wherever possible. See Supplementary Methods for an in-depth explanation of the DAGs designed.

The main interest of this study is to explore causal effects of different explanatory variables of interest to help understand the specific mechanisms by which human land occupation and the climate affect burned area, and how they interact. Thus, each model we build (see following sections) is aimed at quantifying the total causal effects of a variable of interest, notwithstanding the predictive power of the model. For each explanatory variable of interest (anthropic area percentage, climatic variables, or trends in these variables), the corresponding DAG shows the direct and indirect causal paths between this causal variable and the response variable (burned natural area percentage, or its trends), and helps identify the covariates that we need to control for to avoid confounding: that is, those variables that are necessary to close the non-causal paths between the explanatory and response variables that could introduce bias. These control variables (protected area and latitude in model M1, and latitude in model M2, see following sections) are identified using the backdoor criterion. Furthermore, this criterion also indicates those variables that must not be included to avoid opening non-causal paths. As the non-causal paths may be different for each variable of interest, the backdoor criterion may indicate different choices of covariates for each causal question and, thus, imply building different models. It is important to emphasise that, as a consequence of building our models in this manner, only the effects of the variables of interest can be interpreted causally, while the model outcomes for the control covariates have no causal interpretation as they could be confounded - and thus their specific quantification is not relevant to our research questions.

Finally, we would like to remark that, as a consequence of the explained above, our models include only those variables needed to address our research questions about causal relations. Therefore, there may be of course other variables that also affect burned area causally, or that are good predictors of this variable, but that we have not included in our models because they are neither the variables of interest to the research questions nor needed for control. In addition, because the models are not designed to maximise their predictability, their overall explanatory power may be limited. Instead, the results from this work should be assessed in the light of the uncertainty of the model parameters,

which, as we are using a Bayesian approach, stems from the posterior probability densities - which we summarise using the High Posterior Density Interval, the shortest interval in a posterior probability representing a certain confidence interval.

Effect of anthropic area on burned natural area

Model M1 is a Bayesian linear regression model with anthropic area percentage as the predictive variable of interest and the percentage of burned natural area as the response variable. We run this model for all data points, consisting of each grid cell per year. We construct the model based on DAG1 (Supplementary Fig. S3.1). In our system, the causal effect of anthropic area percentage on natural area burned may be confounded by the extent of protected area and by the latitude (see Supplementary Methods for further explanation), since both are common causes of the explanatory and the outcome variables (backdoor paths). Therefore, we include these two variables as controls to block the non-causal paths, so that the slope coefficient of the anthropic area covariate will be the total causal effect of this variable on burned natural area (conditional on our DAG) (McElreath, 2018; Laubach et al., 2021). We therefore model burned natural area as

$$\begin{aligned} \mathrm{BA}_i &\sim \mathrm{N}\left(\mu_i, \sigma\right) \\ \mu_i &= \alpha + \beta \mathrm{A}_i + \eta \mathrm{L}_i + \psi \mathrm{PA}_i + \gamma_{\text{cell}} + \theta_t, \end{aligned} \tag{3.3}$$

where BA represents percentage of burned natural area; α is the expected average BA when all covariates are zero (intercept); β, η, and ψ represent the burned natural area response to anthropic area percentage (A), latitude (L) and percentage of protected area (PA). It is worth stressing here that in this model only β is to be interpreted causally, while η, and ψ are only there to block non-causal paths (see above). We use parameters γ_{cell} and θ_t as varying intercepts to capture the residual variation in expected burned natural area among grid cells and years respectively. Full model specification is in Supplementary Methods.

Climate effects on burned natural area and mediation by anthropic area percentage

In models M2 and M3, we use data for the cell per year observations to test the effect of the climate on the percentage of burned natural area for different levels of anthropic area percentage. However, burned area is a stochastic process that usually follows a distribution within the family of heavy-tail distributions (Hantson et al., 2016): small burned areas are considerably more frequent than extreme events (larger burned areas), which occur only rarely. In our data, we observe this structure for each interval of each climatic variable (Supplementary Fig. S3.13). We notice that it is the likelihood of the larger burned areas - the tail of the power law - that changes with the climate (Supplementary Fig. S3.13). Therefore, we build these two models using a subset of the data comprising the larger events per climatic interval. That is, we divide the values of a certain climatic variable into regular intervals, and for each interval we subset those data points corresponding to the upper 95th percentile of burned natural area.

Additionally, we observe that the cell-year observations experiencing the highest temperatures in the study period (1985-2020) do not follow the same behaviour than the rest of the data points (Supplementary Fig. S3.14a): all the burned natural area events for these temperatures are far smaller than the events with temperature immediately lower. When mapping the number of years each cell has experienced an average temperature equal or larger than 28.5 ^{o}C, we find that these events occurred in a small number of cells, which are clustered together and located at the border with the Caatinga biome (Supplementary Fig. S3.14b). This difference in behaviour could hence be related to this area's vegetation being more similar to that of the Caatinga (xeric shrubland and thorn forest), with distinct fuel types and loads. We briefly explored the climate of these cells and found that they also present some of the more extreme maximum climatological water deficit (MCWD) values in the Cerrado (Supplementary Fig. S3.14c), but we do not investigate this matter further as it is beyond the scope of the study. Since these cells are clustered together and jointly present a markedly different behaviour, we excluded them from this part of the analysis.

Based on DAG1 (Supplementary Fig. S3.1), we use two different models to quantify the causal relations of the climate on the burned natural area. When studying the effect of temperature and VPD, our model must include latitude as a predictor (model M2). This is because latitude is a parent cause to temperature (and therefore to VPD) and to burned natural area, hence expected to confound the causal effect of temperature on burned natural area if not controlled for. To explore the causal effects of the different precipitation-related variables (same year total precipitation, same year dry season precipitation, and previous year total precipitation), there is no need to control for any other variable (model M3), as there are no alternative paths going through a common cause between the predictor and the response variable (Supplementary Fig. S3.1).

Models M2 and M3 have a two-level hierarchical structure where we use a linear regression to predict percentage of burned natural area (BA) as a function of a climatic variable (C) while allowing both the slope and intercept coefficients to vary by decile of the anthropic area percentage factor, with 10 levels. That is,

$$\begin{aligned} \mathrm{BA}_i &\sim \mathrm{N}\left(\mu_i, \sigma\right) \\ \mu_i &= \alpha_{[\mathrm{A}]} + \beta_{[\mathrm{A}]}\mathrm{C}_i + \gamma_{\text{cell}} + \theta_t + \eta \mathrm{L}_i, \end{aligned} \tag{3.4}$$

and

$$\begin{aligned} \mathrm{BA}_i &\sim \mathrm{N}\left(\mu_i, \sigma\right) \\ \mu_i &= \alpha_{[\mathrm{A}]} + \beta_{[\mathrm{A}]}\mathrm{C}_i + \gamma_{\text{cell}} + \theta_t. \end{aligned} \tag{3.5}$$

In the models, [A] indicates that the corresponding coefficient is allowed to vary by decile of anthropic area, $\alpha_{[\mathrm{A}]}$ are the expected average burned natural area for each decile (intercepts), and $\beta_{[\mathrm{A}]}$ correspond to the effect of each climatic variable on the percentage of burned natural area in each decile. Parameters γ_{cell} and θ_t are varying intercepts used to capture the residual variation in expected burned natural area among cells and years respectively. Lastly, η represents the relation between burned natural area and latitude (L). Again, only the $\beta_{[\mathrm{A}]}$ coefficients are to be interpreted causally. The full model specifica-

tions including group-level covariance matrices, prior and hyperprior specifications can be found in the Supplementary Methods. Model M2 was run separately for T and VPD, and model M3 was run separately for same year total precipitation, same year dry season precipitation, and previous year total precipitation.

Finally, we compare the effects of the different climatic variables to explore whether any of them may have a stronger effect on burned natural area than the others. With this aim, we explore the change in burned natural area when increasing (decreasing in the case of dry season precipitation) the value of each climatic variable by 2 standard deviations from their average observed value for each decile of anthropic area. That is, we use the joint posterior of the fitted models to generate burned natural area distributions under a "mean value" and under a "mean value + (or -) 2 standard deviations" of the climatic variables. This results in two predictive posteriors for each anthropic area decile group. We then calculate the "contrasts", that is, we subtract the two group-level posteriors for each variable and decile. In this manner, we can compare the change in burned natural area when varying all climatic variables by the same amount (within each variable's distribution).

Trends in burned natural area, climate change and anthropic expansion

For each cell in the 0.2º grid over the Cerrado, we estimated the annual rate of change (temporal trends) over the period 1985-2020 of burned natural area percentage, anthropic area percentage and various climatic variables. We calculated the trends using Bayesian linear regression,

$$\begin{aligned} \mathrm{V}_i &\sim \mathrm{N}\left(\mu_i, \sigma\right) \\ \mu_i &= \alpha + \beta \mathrm{t}, \end{aligned} \tag{3.6}$$

where V generically represents the response variables of interest for a cell i in a certain year, t represents time measured in years, α characterises the average value V of a cell in 1985, and β is the annual rate of change of V - the parameter of interest. We ran this model separately for burned natural area, anthropic area, temperature, VPD, and precipitation

using uninformative priors (see Supplementary Methods). We consider that a certain cell does not show clear trends in time if the its 95% HPDI of the posterior distribution for β encompasses 0. Finally, we map the temporal trends obtained for each variable (Fig. 3.2) over the Cerrado.

We then proceed with a model (M5) aiming to test whether and how the temporal trends in anthropic area (tA) expansion and in temperature (tT) are responsible for the spatial variation in the temporal change in burned natural area (tBA). These temporal trends are the β parameters obtained in model M4. In this case, we only use those cells that show clear trends in slopes for tA, tT and tBA (95% HPDI). We built model M5 based on DAG2 (Supplementary Fig. S3.10), which we designed using existing knowledge of similar systems and testing the associations and conditional associations implied by the DAG among the variables to validate its statistical plausibility. In the model, we include a linear interaction term between tT and tA to allow each predictor to regulate the effect of the other. However, the extent of anthropic expansion in the study period is contingent on the percentage of anthropic area in each cell in the year 1985: cells that were mostly intact at the beginning of the period could experience any degree of expansion in anthropic area, large or small, and they consequently show a wide range of tA values. By contrast, cells that were already largely converted in 1985 could only experience small tA values. Hence, we can expect different effects of the predictor variables depending on the anthropic area extent of the cells at the start of the period. Therefore, we classify cells in five intervals of 20% of anthropic area percentage in 1985, and allow the intercept and slope coefficients of tT and tA to vary by group by building M5 as a Bayesian multilevel model,

$$\begin{aligned} \mathrm{tBA}_i &\sim \mathrm{N}\left(\mu_i, \sigma\right) \\ \mu_i &= \alpha_{[\mathrm{A}_{85}]} + \beta_{1,[\mathrm{A}_{85}]}\mathrm{tA}_i + \beta_{2,[\mathrm{A}_{85}]}\mathrm{tT}_i + \beta_{3,[\mathrm{A}_{85}]}\mathrm{tA}_i\mathrm{tT}_i, \end{aligned} \tag{3.7}$$

where $\alpha_{[\mathrm{A}_{85}]}$ characterises the average tBA of cells with a certain level of anthropic area in 1985 [A_{85}], and $\beta_{1,[\mathrm{A}_{85}]}$, $\beta_{2,[\mathrm{A}_{85}]}$, and $\beta_{3,[\mathrm{A}_{85}]}$ characterise the response of tBA to tA, tT and their interaction, respectively, for each [A_{85}] group. The full model specification is in

the Supplementary Methods.

Finally, we explore the implications of model M5 generating predictive posterior draws for each A_{85} group by fixing one of the predictors (at its 90th and 10th percentile for each A_{85} group) and exploring the effects of the other predictor on tBA throughout its observed value range (Fig. 3.3 and Supplementary Figs. S3.11 and S3.12).

3.6 Data availability

The climate data used in this study are publicly available from ERA5-Land Monthly Averaged at https://www.ecmwf.int/en/forecasts/dataset/ecmwf-reanalysis-v5-land, Climate Hazards Group InfraRed Precipitation with Station data version 2.0 at https://data.chc.ucsb.edu/products/CHIRPS-2.0/, and TerraClimate at https://www.climatologylab.org/terraclimate.html. The land use data are publicly available from MapBiomas collection 6.0 at https://brasil.mapbiomas.org/en/colecoes-mapbiomas/. The burned area data are publicly available from MapBiomas Fogo Collection 1.0 at https://brasil.mapbiomas.org/en/colecoes-mapbiomas/. Finally, the shapefiles used for protected area data (conservation units and indigenous lands) are publicly available from the Ministério de Meio Ambiente do Brasil http://www.mma.gov.br/areas-protegidas/cadastro-nacional-de-ucs.

3.7 Code availability

All code used in the study for data processing, analysis and modelling is publicly available at: https://doi.org/10.5281/zenodo.10908497.

3.8 Acknowledgements

We thank the Ecosystems Lab Group at the Environmental Change Institute, School of Geography and the Environment, University of Oxford, and the Science Team at the Instituto de Pesquisa Ambiental da Amazônia (IPAM), Brazil, for helpful feedback during discussions. We thank Michael Collins for feedback on the manuscript, and Dr Fabian

Aguirre-Lopez and Dr Blas Kolic for their suggestions on early stages of the work. We would like to thank the reviewers for providing useful feedback to improve the readability and content of the manuscript. CSG was supported by the UK Natural Environment Research Council under grant number NE/S007474/1. DB was supported by the European Union's Horizon 2020 research and innovation programme under the Marie Skłodowska-Curie grant agreement no. 895799.

3.9 Author contributions

C. S. G. contributed to the conceptualization, data curation, methodology, formal analysis, investigation, visualization, writing original draft, and reviewing and editing. D. B. contributed to the methodology, formal analysis, investigation, visualization, and reviewing and editing; V. A. and A. A. contributed to the methodology, investigation, and reviewing and editing; I. O. M. contributed to the conceptualization, methodology, formal analysis, investigation, reviewing and editing, and the supervision.

3.10 References

Abatzoglou, John T., Solomon Z. Dobrowski, et al. (2018). "TerraClimate, a high-resolution global dataset of monthly climate and climatic water balance from 1958–2015". In: *Scientific Data* 5.1, p. 170191.

Abatzoglou, John T., A. Park Williams, and Renaud Barbero (2019). "Global Emergence of Anthropogenic Climate Change in Fire Weather Indices". In: *Geophysical Research Letters* 46.1, pp. 326–336.

Abreu, Rodolfo C. R. et al. (2017). "The biodiversity cost of carbon sequestration in tropical savanna". In: *Science Advances* 3.8, e1701284.

Addicott, Ethan T et al. (2022). "Toward an improved understanding of causation in the ecological sciences". In: *Frontiers in Ecology and the Environment* 20.8, pp. 474–480.

Aldersley, Andrew, Steven J. Murray, and Sarah E. Cornell (2011). "Global and regional analysis of climate and human drivers of wildfire". In: *Science of The Total Environment* 409.18, pp. 3472–3481.

Alencar, Ane, Julia Z. Shimbo, et al. (2020). "Mapping Three Decades of Changes in the Brazilian Savanna Native Vegetation Using Landsat Data Processed in the Google Earth Engine Platform". In: *Remote Sensing* 12.6, p. 924.

Alencar, Ane A. C., Vera L. S. Arruda, et al. (2022). “Long-Term Landsat-Based Monthly Burned Area Dataset for the Brazilian Biomes Using Deep Learning”. In: *Remote Sensing* 14.11, p. 2510.

Allen, Richard G. et al. (1998). *Crop evapotranspiration - Guidelines for computing crop water requirements*. FAO - Food and Agriculture Organization of the United Nations.

Andela, N. et al. (2017). “A human-driven decline in global burned area”. In: *Science* 356.6345, pp. 1356–1362.

Archibald, S, C E R Lehmann, et al. (2018). “Biological and geophysical feedbacks with fire in the Earth system”. In: *Environmental Research Letters* 13.3, p. 033003.

Archibald, S., A. Nickless, et al. (2010). “Climate and the inter-annual variability of fire in southern Africa: a meta-analysis using long-term field data and satellite-derived burnt area data: Fire-climate interactions”. In: *Global Ecology and Biogeography* 19.6, pp. 794–809.

Archibald, S., R. J. Scholes, et al. (2010). “Southern African fire regimes as revealed by remote sensing”. In: *International Journal of Wildland Fire* 19.7, p. 861.

Archibald, Sally (2016). “Managing the human component of fire regimes: lessons from Africa”. In: *Philosophical Transactions of the Royal Society B: Biological Sciences* 371.1696, p. 20150346.

Archibald, Sally, David P. Roy, et al. (2009). “What limits fire? An examination of drivers of burnt area in Southern Africa”. In: *Global Change Biology* 15.3, pp. 613–630.

Arif, Suchinta and M. Aaron MacNeil (2023). “Applying the structural causal model framework for observational causal inference in ecology”. In: *Ecological Monographs* 93.1.

Barlow, Jos et al. (2020). “Clarifying Amazonia’s burning crisis”. In: *Global Change Biology* 26.2, pp. 319–321.

Beer, Christian et al. (2010). “Terrestrial Gross Carbon Dioxide Uptake: Global Distribution and Covariation with Climate”. In: *Science* 329.5993, pp. 834–838.

Bond, W. J., F. I. Woodward, and G. F. Midgley (2005). “The global distribution of ecosystems in a world without fire”. In: *New Phytologist* 165.2, pp. 525–538.

Bowman, David M. J. S. et al. (2009). “Fire in the Earth System”. In: *Science* 324.5926, pp. 481–484.

Cadastro Nacional de Unidades de Conservação/Ministério de Meio Ambiente (2019). http://www.mma.gov.br/areas-protegidas/cadastro-nacional-de-ucs. Accessed: 2022-07-04.

Conciani, Dhemerson E. et al. (2021). “Human-climate interactions shape fire regimes in the Cerrado of São Paulo state, Brazil”. In: *Journal for Nature Conservation* 61, p. 126006.

Durigan, Giselda (2020). “Zero-fire: Not possible nor desirable in the Cerrado of Brazil”. In: *Flora* 268, p. 151612.

Durigan, Giselda and James A. Ratter (2016). “The need for a consistent fire policy for Cerrado conservation”. In: *Journal of Applied Ecology* 53.1. Ed. by Jeremy James, pp. 11–15.

Fidelis, Alessandra et al. (2018). “The Year 2017: Megafires and Management in the Cerrado”. In: *Fire* 1.3, p. 49.

Flannigan, Mike et al. (2013). “Global wildland fire season severity in the 21st century”. In: *Forest Ecology and Management* 294, pp. 54–61.

Franke, Jonas et al. (2024). “Prescribed burning and integrated fire management in the Brazilian Cerrado: demonstrated impacts and scale-up potential for emission abatement”. In: *Environmental Research Letters*.

Funk, Chris et al. (2015). “The climate hazards infrared precipitation with stations—a new environmental record for monitoring extremes”. In: *Scientific Data* 2.1, p. 150066.

Gelman, Andrew et al. (2019). “R-squared for Bayesian Regression Models”. In: *The American Statistician* 73.3, pp. 307–309.

Gorelick, Noel et al. (2017). “Google Earth Engine: Planetary-scale geospatial analysis for everyone”. In: *Remote sensing of Environment* 202. Publisher: Elsevier, pp. 18–27.

Hantson, Stijn et al. (2016). “The status and challenge of global fire modelling”. In: *Biogeosciences* 13.11, pp. 3359–3375.

He, Tianhua, Byron B. Lamont, and Juli G. Pausas (2019). “Fire as a key driver of Earth’s biodiversity”. In: *Biological Reviews* 94.6, pp. 1983–2010.

Hofmann, Gabriel S. et al. (2021). “The Brazilian Cerrado is becoming hotter and drier”. In: *Global Change Biology* 27.17, pp. 4060–4073.

Jolly, W. Matt et al. (2015). “Climate-induced variations in global wildfire danger from 1979 to 2013”. In: *Nature Communications* 6.1, p. 7537.

Kelly, Luke T. et al. (2020). “Fire and biodiversity in the Anthropocene”. In: *Science* 370.6519, eabb0355.

Laubach, Zachary M. et al. (2021). “A biologist’s guide to model selection and causal inference”. In: *Proceedings of the Royal Society B: Biological Sciences* 288.1943, p. 20202815.

Li, Sihan et al. (2021). “Anthropogenic climate change contribution to wildfire-prone weather conditions in the Cerrado and Arc of deforestation”. In: *Environmental Research Letters* 16.9, p. 094051.

Libonati, Renata et al. (2015). “Spatio-temporal variability of burned area over Brazil for the period 2005–2010 using MODIS data”. In: *Proceedings of the XVII Brazilian Symposium on Remote Sensing*, pp. 25–29.

Mataveli, Guilherme Augusto Verola et al. (2018). “Satellite observations for describing fire patterns and climate-related fire drivers in the Brazilian savannas”. In: *Natural Hazards and Earth System Sciences* 18.1, pp. 125–144.

McElreath, Richard (2018). *Statistical rethinking: A Bayesian course with examples in R and Stan*. Chapman and Hall/CRC.

Mendonça, Mário Jorge Cardoso de et al. (2004). “The economic cost of the use of fire in the Amazon”. In: *Ecological Economics* 49.1, pp. 89–105.

Moreira de Araújo, Fernando, Laerte Guimarães Ferreira, and Arielle Elias Arantes (2012). “Distribution Patterns of Burned Areas in the Brazilian Biomes: An Analysis Based on Satellite Data for the 2002–2010 Period”. In: *Remote Sensing* 4.7, pp. 1929–1946.

Muñoz-Sabater, Joaquín et al. (2021). “ERA5-Land: a state-of-the-art global reanalysis dataset for land applications”. In: *Earth System Science Data* 13.9, pp. 4349–4383.

Myers, Norman et al. (2000). “Biodiversity hotspots for conservation priorities”. In: *Nature* 403.6772, pp. 853–858.

Nogueira, Joana et al. (2017). “Spatial Pattern of the Seasonal Drought/Burned Area Relationship across Brazilian Biomes: Sensitivity to Drought Metrics and Global Remote-Sensing Fire Products”. In: *Climate* 5.2, p. 42.

Oliveira, Paulo Tarso S. et al. (2014). “Trends in water balance components across the Brazilian Cerrado”. In: *Water Resources Research* 50.9, pp. 7100–7114.

Oliveras, Immaculada and Yadvinder Malhi (2016). “Many shades of green: the dynamic tropical forest–savannah transition zones”. In: *Philosophical Transactions of the Royal Society B: Biological Sciences* 371.1703, p. 20150308.

Parr, Catherine L. et al. (2014). “Tropical grassy biomes: misunderstood, neglected, and under threat”. In: *Trends in Ecology & Evolution* 29.4, pp. 205–213.

Pausas, Juli G. and Eloi Ribeiro (2013). “The global fire-productivity relationship: Fire and productivity”. In: *Global Ecology and Biogeography* 22.6, pp. 728–736.

Pearl, Judea, Madelyn Glymour, and Nicholas P Jewell (2016). *Causal inference in statistics: A primer*. John Wiley & Sons.

Pivello, Vânia R. (2011). “The Use of Fire in the Cerrado and Amazonian Rainforests of Brazil: Past and Present”. In: *Fire Ecology* 7.1, pp. 24–39.

Pivello, Vânia R. et al. (2021). “Understanding Brazil’s catastrophic fires: Causes, consequences and policy needed to prevent future tragedies”. In: *Perspectives in Ecology and Conservation* 19.3, pp. 233–255.

Rego, Francisco Castro et al. (2021). *Fire Science: From Chemistry to Landscape Management*. Springer Textbooks in Earth Sciences, Geography and Environment. Cham: Springer International Publishing.

Ribeiro, J.F. and B.M.T. Walter (2008). “Cerrado Ecologia e Flora”. In: *As principais fitofisionomias do Bioma Cerrado*. Embrapa, pp. 152–212.

Rosan, Thais M., Luiz E.O.C. Aragão, et al. (2019). “Extensive 21st-Century Woody Encroachment in South America’s Savanna”. In: *Geophysical Research Letters* 46.12, pp. 6594–6603.

Rosan, Thais M., Stephen Sitch, et al. (2022). “Fragmentation-Driven Divergent Trends in Burned Area in Amazonia and Cerrado”. In: *Frontiers in Forests and Global Change* 5, p. 801408.

Santos, Filippe L.M. et al. (2021). “Prescribed Burning Reduces Large, High-Intensity Wildfires and Emissions in the Brazilian Savanna”. In: *Fire* 4.3, p. 56.

Schmidt, Isabel Belloni and Ludivine Eloy (2020). “Fire regime in the Brazilian Savanna: Recent changes, policy and management”. In: *Flora* 268, p. 151613.

Silva, P S, J A Rodrigues, et al. (2020). “Drivers of burned area patterns in Cerrado: the case of MATOPIBA region”. In: *2020 IEEE Latin American GRSS & ISPRS Remote Sensing Conference (LAGIRS)*.

Silva, Patrícia S., Ana Bastos, et al. (2019). “Impacts of the 1.5 °C global warming target on future burned area in the Brazilian Cerrado”. In: *Forest Ecology and Management* 446, pp. 193–203.

Silva, Patrícia S., Joana Nogueira, et al. (2021). “Putting fire on the map of Brazilian savanna ecoregions”. In: *Journal of Environmental Management* 296, p. 113098.

Souza, Carlos M. et al. (2020). “Reconstructing Three Decades of Land Use and Land Cover Changes in Brazilian Biomes with Landsat Archive and Earth Engine”. In: *Remote Sensing* 12.17, p. 2735.

Souza Neves, Laís Fernandes de et al. (2018). “Dinâmica do fogo no Parque Estadual do Araguaia, zona de transição Amazônia-Cerrado”. In: *Ra’e Ga* 44.

Staver, A. Carla, Sally Archibald, and Simon A. Levin (2011). “The Global Extent and Determinants of Savanna and Forest as Alternative Biome States”. In: *Science* 334.6053, pp. 230–232.

Stevens, Nicola et al. (2017). “Savanna woody encroachment is widespread across three continents”. In: *Global Change Biology* 23.1, pp. 235–244.

Stott, Peter (2016). “How climate change affects extreme weather events”. In: *Science* 352.6293, pp. 1517–1518.

Veldman, Joseph W, Elise Buisson, et al. (2015). “Toward an old-growth concept for grasslands, savannas, and woodlands”. In: *Frontiers in Ecology and the Environment* 13.3. Publisher: Wiley Online Library, pp. 154–162.

Veldman, Joseph W., Gerhard E. Overbeck, et al. (2015). “Where Tree Planting and Forest Expansion are Bad for Biodiversity and Ecosystem Services”. In: *BioScience* 65.10, pp. 1011–1018.

Westerling, A. L. et al. (2006). “Warming and Earlier Spring Increase Western U.S. Forest Wildfire Activity”. In: *Science* 313.5789, pp. 940–943.

Wu, Chao, Stephen Sitch, et al. (2022). “Reduced global fire activity due to human demography slows global warming by enhanced land carbon uptake”. In: *Proceedings of the National Academy of Sciences* 119.20, e2101186119.

Wu, Chao, Sergey Venevsky, et al. (2021). “Historical and future global burned area with changing climate and human demography”. In: *One Earth* 4.4, pp. 517–530.

Xu, Rongbin et al. (2020). “Wildfires, Global Climate Change, and Human Health”. In: *n engl j med*.

3.11 Supplementary Information

3.11.1 Supplementary Methods

Directed Acyclic Graphs

We used Directed Acyclic Graphs to inform the covariate selection in our models in order to perform causal inference. We used two different DAGs: DAG1 represented those variables that may affect the percentage of burned natural area, and we used it to design models M1, M2 and M3; DAG2 represented those variables that may affect the temporal trends of change in the percentage of natural burned area, and we used it to inform model M5.

In this section, we explain the reasoning behind each of the DAGs, discuss the implications of the main causal relations, as well as the relative importance of the presence and direction of some causal relations in designing the models and making causal inference.

DAG1

DAG1 (Supplementary Fig. S3.1) represents the various variables that are - or may be - involved in causal relations with burned natural area, either directly or indirectly. The main variables of interest for this study were the percentage of burned natural area as the outcome, and anthropic area percentage, temperature, VPD, dry season precipitation, and same and previous year precipitation as separate predictors.

The different climatic variables affect the effective availability of fuel and its continuity - its load and flammability - which directly affect burned area. Temperature, VPD and the amount of precipitation in the dry season - when most fires occur (Silva et al., 2021) - influence fuel flammability, as they directly affect how dry the fuel is (Westerling et al., 2006; Flannigan et al., 2013). In turn, the flammability state of the fuel influences the amount of combustible that will readily burn - the effective fuel load (Rego et al., 2021). As well, precipitation in the growing season affects vegetation productivity and, hence, fuel load. Both fuel load and flammability indirectly affect burned area through ignitions,

because they affect the success of the fire onset (Rego et al., 2021).

On the other hand, we are using anthropic area percentage as an indicator of the presence and extent of human land use activities in the landscape. These activities bring about landscape fragmentation (Rosan et al., 2022), ignition (Pivello, 2011), but also active fire suppression (Durigan et al., 2016; Schmidt et al., 2020), and influence road density. We calculated anthropic area as the corresponding percentage of the sum of natural and anthropic area (see Methods). However, the presence and extent of anthropic area in any cell could be argued to being conditional on the presence of areas demarcated as protected, so there would be a causal link between the extent of protected areas and those of human land uses, as supported by a statistical association in the data (not shown). But protected areas also shape the level of fragmentation and the road density, they would also have their own fire suppression or prevention policies (Durigan et al., 2016), and would also probably be associated with a particular ignition regime. The potential existence of these causal relations that involve protected area percentage as a cause of burned natural area both through anthropic area - the variable of interest - and through an alternative *backdoor causal path* (Pearl et al., 2016; Laubach et al., 2021), imply that protected area must be included when studying the effects of anthropic area in model M1, based on the backdoor criterion.

Another aspect to highlight of DAG1 is the inclusion of *latitude* and *history*, which has important implications for the models' design. In addition to the well known causal relation between latitude and temperature due to the angle of solar radiation, there is a path between latitude and anthropic area as a result of the fact that human expansion in the Cerrado primarily developed from the southern regions towards the northern areas (Jepson, 2005). This link is symbolised through the inclusion of *history* as an unobserved (or latent) variable, and implies that latitude is simultaneously a causal parent (i.e. a cause) of anthropic area and of temperature and VPD. For this reason, models M1 and M2, studying the effects of anthropic area and temperature or VPD respectively, must include latitude as a covariate to allow causal inference of the variables of interest, by blocking the non-causal path going to percentage of burned natural area through latitude

(see Supplementary Fig. S3.1).

Finally, it is worth mentioning that the conditional independencies implied by DAG1 and including unobserved variables (grey circles, Supplementary Fig. S3.1) could not be assessed from the raw data, given the unobserved nature of such variables. However, regarding the variables of interest and the overall causal structure of the DAG that concerns them, nor the presence/absence of most of the arrows related to unobserved variables nor their direction would change the models' design nor our ability to draw causal inference - conditional on the rest of the DAG being correct, of course. This is because the potential backdoor paths that these arrows create between these unobserved variables include causal structures called inverted forks or colliders, that is, non-causal paths that are already closed by default, and would only be opened by conditioning on the collider (see details in (McElreath, 2018; Elwert et al., 2014)).

DAG2

DAG2 (Supplementary Fig. S3.10) represented the relations between the temporal trends in burned natural area percentage (tBA) as the outcome, and temporal trends in anthropic area percentage (tA) and in temperature (tT) as predictors. We included the percentage of anthropic area in 1985 (A_{85}) because it constrains the extent of further land use expansion. In this case, we validated the DAG by using the data to test the conditional independencies implied by the DAG, i.e. the correlations and conditional correlations among the represented variables. This step also allowed us to discard alternative DAGs and additional arrows between the observed variables (McElreath, 2018; Laubach et al., 2021).

Models Specifications

Model M1

$$\mathrm{BA}_i \sim \mathrm{N}\left(\mu_i, \sigma\right) \qquad \text{[Likelihood]}$$

$$\mu_i = \alpha + \beta \mathrm{A}_i + \eta \mathrm{L}_i + \psi \mathrm{PA}_i + \gamma_{\text{cell}} + \theta_t, \qquad \text{[Linear model]}$$

$$\alpha, \beta, \eta, \psi \sim \mathrm{N}(0, \sigma_{\alpha,\beta,\eta,\psi}) \qquad \text{[Priors for intercept and slopes]}$$

$$\gamma_{\text{cell}} \sim \mathrm{N}\left(0, \sigma_\gamma\right) \qquad \text{[Adaptive priors for cells]}$$

$$\theta_t \sim \mathrm{N}\left(0, \sigma_t\right) \qquad \text{[Adaptive priors for the } t \text{ years]}$$

$$\sigma_\alpha, \sigma_\beta, \sigma_\gamma, \sigma_\psi, \sigma_t, \sigma_{\text{lat}}, \sigma \sim \mathrm{Exp}(1) \qquad \text{[Priors for standard deviation]}$$

Markov chain Monte Carlo settings: Model was run using R package brms (Bürkner, 2017) with 2000 total iterations per chain, 1000 warmup iterations, 8 Markov chains, a 0.98 threshold to accept a sampling step of the NUTS (no-U-turn sampler), a seed value of 9.

Model M2

$$\mathrm{BA}_i \sim \mathrm{N}\left(\mu_i, \sigma\right) \quad \text{[Likelihood]}$$

$$\mu_i = \alpha_{[\mathrm{A}]} + \beta_{[\mathrm{A}]}\mathrm{C}_i + \gamma_{\text{cell}} + \theta_t + \eta L_i \quad \text{[Linear Model]}$$

$$\begin{pmatrix} \alpha_{[\mathrm{A}]} \\ \beta_{[\mathrm{A}]} \end{pmatrix} \sim \mathrm{MVNormal}\left(\begin{pmatrix} \alpha \\ \beta \end{pmatrix}, \mathbf{S}\right) \quad \text{[Adaptive priors for each A]}$$

$$\mathbf{S} = \begin{pmatrix} \sigma_\alpha & 0 \\ 0 & \sigma_\beta \end{pmatrix} \mathbf{R} \begin{pmatrix} \sigma_\alpha & 0 \\ 0 & \sigma_\beta \end{pmatrix} \quad \text{[Covariance matrix]}$$

$$\mathbf{R} = \begin{pmatrix} 1 & \rho_{\alpha,\beta} \\ \rho_{\beta,\alpha} & 1 \end{pmatrix} \quad \text{[Correlation matrix for A]}$$

$$\mathbf{R} \sim \mathrm{LKJcorr}(2) \quad \text{[Prior for correlation matrix]}$$

$$\alpha, \beta \sim \mathrm{N}(0, 10) \quad \text{[Priors for intercept and slope]}$$

$$\gamma_{\text{cell}} \sim \mathrm{N}\left(0, \sigma_\gamma\right) \quad \text{[Adaptive priors for cells]}$$

$$\theta_t \sim \mathrm{N}\left(0, \sigma_t\right) \quad \text{[Adaptive priors for the } t \text{ years]}$$

$$\eta \sim \mathrm{N}\left(0, \sigma_{\text{lat}}\right) \quad \text{[Adaptive priors for } lat \text{ latitude]}$$

$$\sigma_\alpha, \sigma_\beta, \sigma_\gamma, \sigma_t, \sigma_{\text{lat}}, \sigma \sim \mathrm{Exp}(1) \quad \text{[Priors for standard deviation]}$$

Markov chain Monte Carlo settings: Model was run using R package brms (Bürkner, 2017) with 2000 total iterations per chain, 1000 warmup iterations, 8 Markov chains, a 0.98 threshold to accept a sampling step of the NUTS (no-U-turn sampler), a seed value of 9.

Model M3

$$\mathrm{BA}_i \sim \mathrm{N}\left(\mu_i, \sigma\right) \quad \text{[Likelihood]}$$

$$\mu_i = \alpha_{[\mathrm{A}]} + \beta_{[\mathrm{A}]}\mathrm{C}_i + \gamma_{\text{cell}} + \theta_t \quad \text{[Linear Model]}$$

$$\begin{pmatrix} \alpha_{[\mathrm{A}]} \\ \beta_{[\mathrm{A}]} \end{pmatrix} \sim \text{MVNormal}\left(\begin{pmatrix} \alpha \\ \beta \end{pmatrix}, \mathbf{S}\right) \quad \text{[Adaptive priors for each A]}$$

$$\mathbf{S} = \begin{pmatrix} \sigma_\alpha & 0 \\ 0 & \sigma_\beta \end{pmatrix} \mathbf{R} \begin{pmatrix} \sigma_\alpha & 0 \\ 0 & \sigma_\beta \end{pmatrix} \quad \text{[Covariance matrix]}$$

$$\mathbf{R} = \begin{pmatrix} 1 & \rho_{\alpha,\beta} \\ \rho_{\beta,\alpha} & 1 \end{pmatrix} \quad \text{[Correlation matrix for A]}$$

$$\mathbf{R} \sim \text{LKJcorr}(2) \quad \text{[Prior for correlation matrix]}$$

$$\alpha, \beta \sim \mathrm{N}(0, 10) \quad \text{[Priors for intercept and slope]}$$

$$\gamma_{\text{cell}} \sim \mathrm{N}\left(0, \sigma_\gamma\right) \quad \text{[Adaptive priors for cells]}$$

$$\theta_t \sim \mathrm{N}\left(0, \sigma_t\right) \quad \text{[Adaptive priors for the } t \text{ years]}$$

$$\sigma_\alpha, \sigma_\beta, \sigma_\gamma, \sigma_t, \sigma \sim \text{Exp}(1) \quad \text{[Priors for standard deviation]}$$

Markov chain Monte Carlo settings: Model was run using R package brms (Bürkner, 2017) with 2000 total iterations per chain, 1000 warmup iterations, 8 Markov chains, a 0.98 threshold to accept a sampling step of the NUTS (no-U-turn sampler), a seed value of 9.

Model M4

$$
\begin{aligned}
\mathrm{V}_i &\sim \mathrm{N}\left(\mu_i, \sigma\right) && \text{[Likelihood]} \\
\mu_i &= \alpha + \beta \mathrm{t} && \text{[Linear Model]} \\
\alpha, \beta &\sim \mathrm{N}(0, 10) && \text{[Priors for coefficients]} \\
\sigma &\sim \mathrm{Exp}(1) && \text{[Prior for st. deviation]}
\end{aligned}
$$

Markov chain Monte Carlo settings: Model was run using R package brms (Bürkner, 2017) with 2000 total iterations per chain, 1000 warmup iterations, 2 Markov chains, a 0.98 threshold to accept a sampling step of the NUTS (no-U-turn sampler), a seed value of 9.

Model M5

$$\text{tBA}_i \sim \text{N}\left(\mu_i, \sigma\right) \qquad \text{[Likelihood]}$$

$$\mu_i = \alpha_{[\text{A}_{85}]} + \beta_{1,[\text{A}_{85}]}\text{tA}_i + \beta_{2,[\text{A}_{85}]}\text{tT}_i + \beta_{3,[\text{A}_{85}]}\text{tA}_i\text{tT}_i \qquad \text{[Linear Model]}$$

$$\begin{pmatrix} \alpha_{[\text{A}_{85}]} \\ \beta_{1,[\text{A}_{85}]} \\ \beta_{2,[\text{A}_{85}]} \\ \beta_{3,[\text{A}_{85}]} \end{pmatrix} \sim \text{MVNormal}\left(\begin{pmatrix} \alpha \\ \beta_1 \\ \beta_2 \\ \beta_3 \end{pmatrix}, \mathbf{S}\right) \qquad [\text{Adaptive priors for } \text{A}_{85}]$$

$$\mathbf{S} = \begin{pmatrix} \sigma_\alpha & 0 & 0 & 0 \\ 0 & \sigma_{\beta_1} & 0 & 0 \\ 0 & 0 & \sigma_{\beta_2} & 0 \\ 0 & 0 & 0 & \sigma_{\beta_3} \end{pmatrix} \mathbf{R} \begin{pmatrix} \sigma_\alpha & 0 & 0 & 0 \\ 0 & \sigma_{\beta_1} & 0 & 0 \\ 0 & 0 & \sigma_{\beta_2} & 0 \\ 0 & 0 & 0 & \sigma_{\beta_3} \end{pmatrix} \qquad \text{[Covariance matrix]}$$

$$\mathbf{R} = \begin{pmatrix} 1 & \rho_{\alpha,\beta_1} & \rho_{\alpha,\beta_2} & \rho_{\alpha,\beta_3} \\ \rho_{\beta_1,\alpha} & 1 & \rho_{\beta_1,\beta_2} & \rho_{\beta_1,\beta_3} \\ \rho_{\beta_2,\alpha} & \rho_{\beta_2,\beta_1} & 1 & \rho_{\beta_2,\beta_3} \\ \rho_{\beta_3,\alpha} & \rho_{\beta_3,\beta_1} & \rho_{\beta_3,\beta_2} & 1 \end{pmatrix} \qquad \text{[Correlation matrix]}$$

$$\mathbf{R} \sim \text{LKJcorr}(2) \qquad \text{[Prior for corr. matrix]}$$

$$\alpha, \beta_1, \beta_2, \beta_3 \sim \text{N}(0, 10) \qquad \text{[Priors for coefficients]}$$

$$\gamma_{\text{cell}} \sim \text{N}\left(0, \sigma_\gamma\right) \qquad \text{[Adaptive priors for cells]}$$

$$\theta_t \sim \text{N}\left(0, \sigma_t\right) \qquad \text{[Adaptive prior for } t\text{]}$$

$$\eta \sim \text{N}\left(0, \sigma_{\text{lat}}\right) \qquad \text{[Adaptive priors for } lat\text{]}$$

$$\sigma_\alpha, \sigma_{\beta_1}, \sigma_{\beta_2}, \sigma_{\beta_3}, \sigma_\gamma, \sigma_t, \sigma_{\text{lat}}, \sigma \sim \text{Exp}(1) \qquad \text{[Priors for st. deviation]}$$

Markov chain Monte Carlo settings: Model was run using R package brms (Bürkner, 2017) with 2000 total iterations per chain, 1000 warmup iterations, 8 Markov chains, a 0.98 threshold to accept a sampling step of the NUTS (no-U-turn sampler), a seed value of 9.

3.11.2 Supplementary Figures

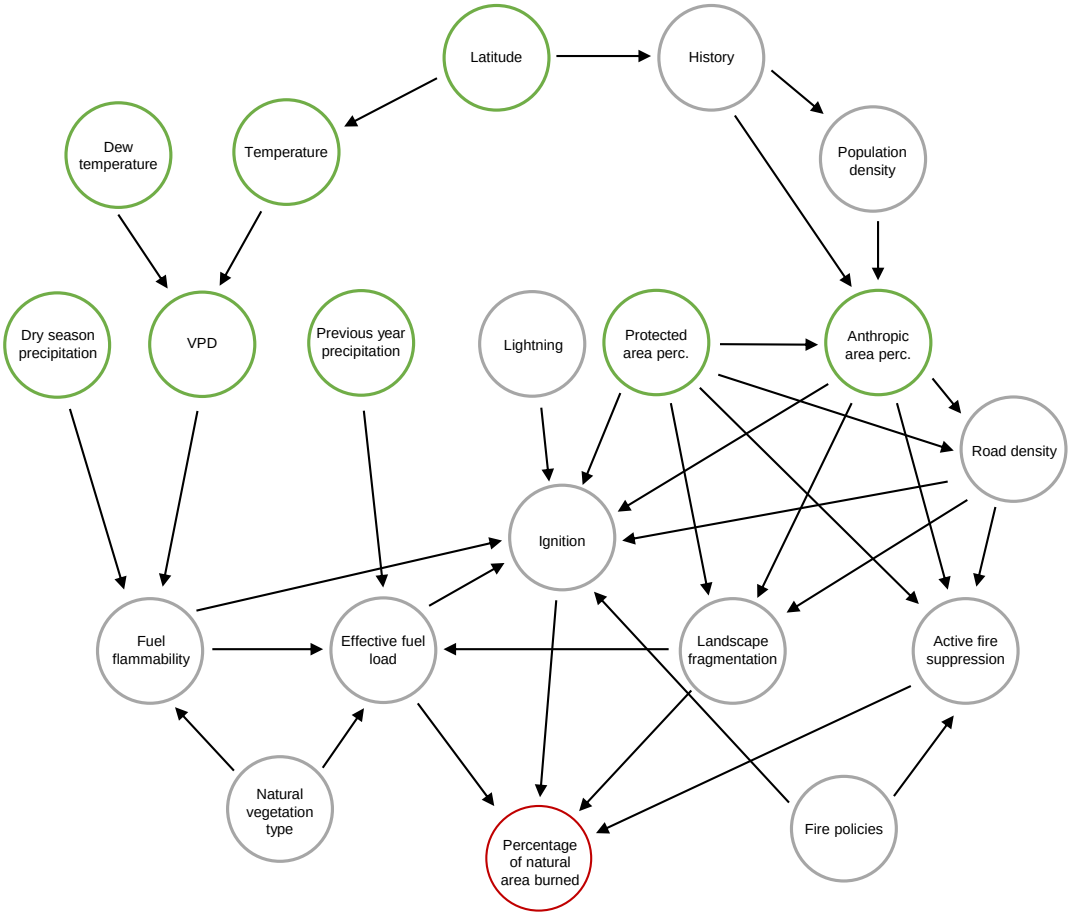

Figure S3.1: **Directed Acyclic Graph, DAG1, describing the set of variables that influence directly or indirectly the burned natural area percentage and the causal relations between them.** We used this DAG in combination with the backdoor criterion (see *Materials and Methods*) to inform the design of models M1, M2 and M3. Green circles indicate those variables that we have included in the study either directly as covariates or in the calculation of other covariates (like in the case of dew temperature, used to calculate VPD), the red circle indicates the outcome variable, and grey circles indicate unobserved variables. Unobserved variables comprise variables that could be measured but were not included in the study, and variables that could not be directly measured. The variable "history" serves to indicate the link between latitude and anthropic area expansion in the Cerrado, as land use conversion mostly started developing in the southern regions towards the northern areas (see Supplementary Fig. S3.5).

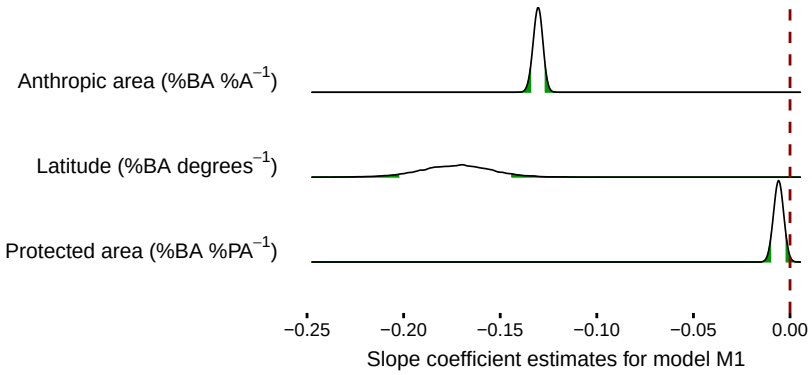

Figure S3.2: **Posterior distribution of the slope coefficients obtained for the different covariates in model M1**. Effect of anthropic area percentage (top), the explanatory variable of interest and the only covariate whose effects can be interpreted causally. Slope coefficients of control variables latitude (middle) and protected area percentage (bottom), which were included in the model to avoid confounding, and whose effects cannot be interpreted causally (see Methods). Green coloured areas indicate the region of the posterior distributions falling outside the 90% HPDI, which we use as credibility interval. The red dashed line is drawn as a reference to indicate whether 0 is a likely outcome of the posterior distributions.

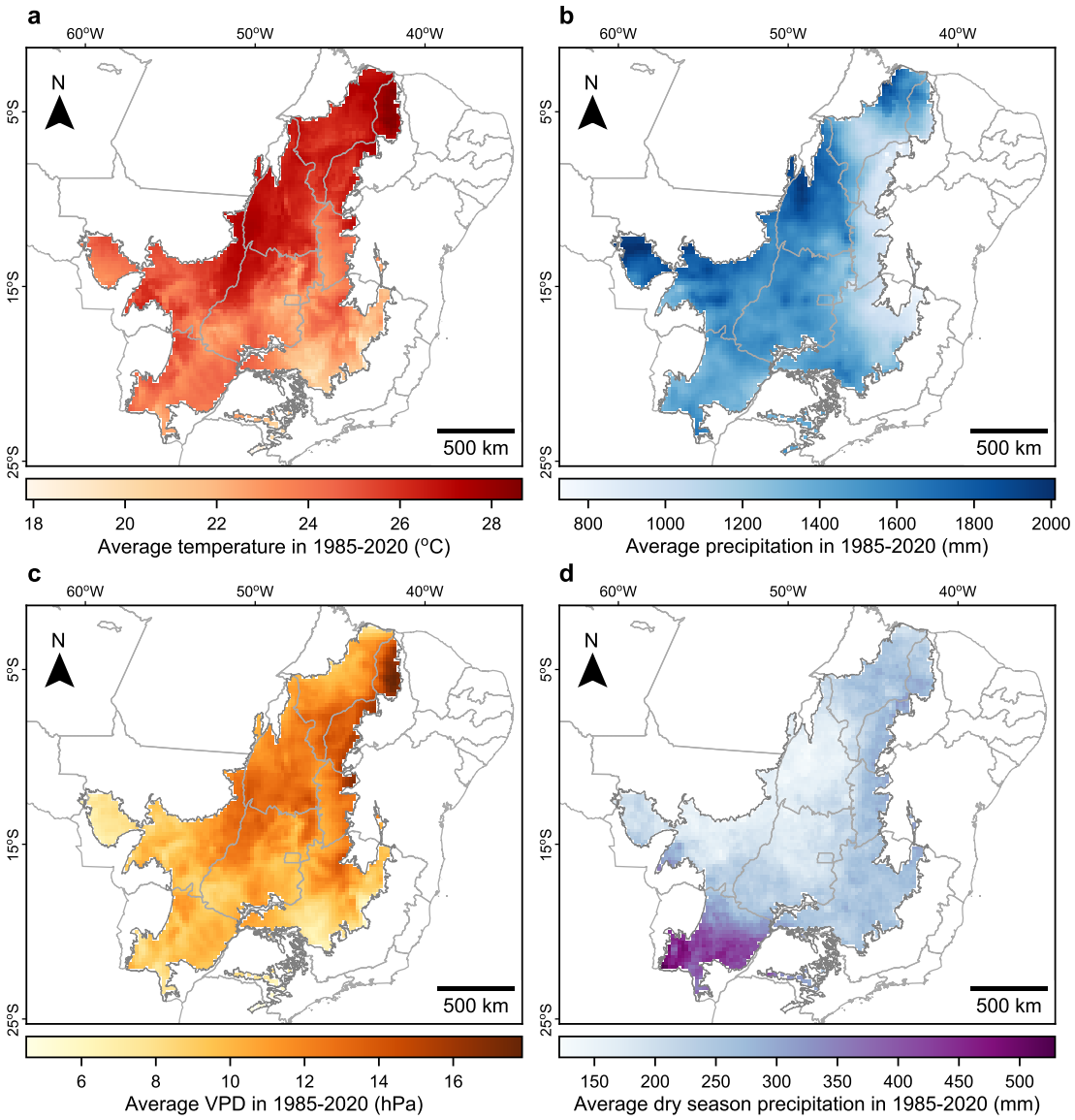

Figure S3.3: **Maps showing the average values of the different climatic variables in the period 1985-2020**. **a** Annual temperature, **b** average total annual precipitation, **c** average VPD, and **d** average dry season precipitation. We can see a latitudinal gradient of increasing average temperature, and an east-west gradient of increase in precipitation.

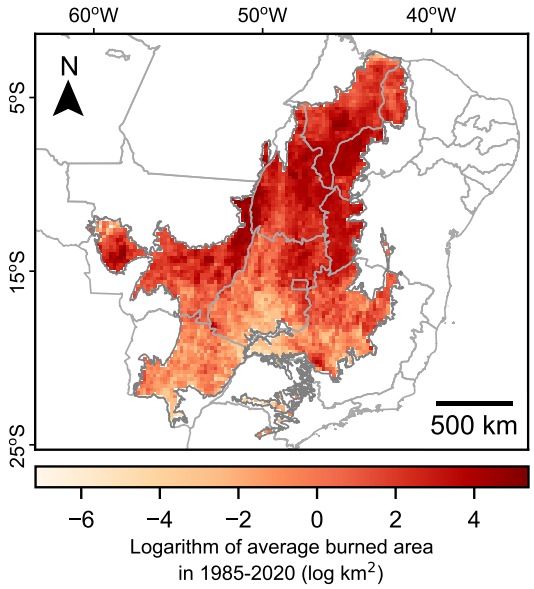

Figure S3.4: **Map of the logarithm average burned area in the period 1985-2020.**

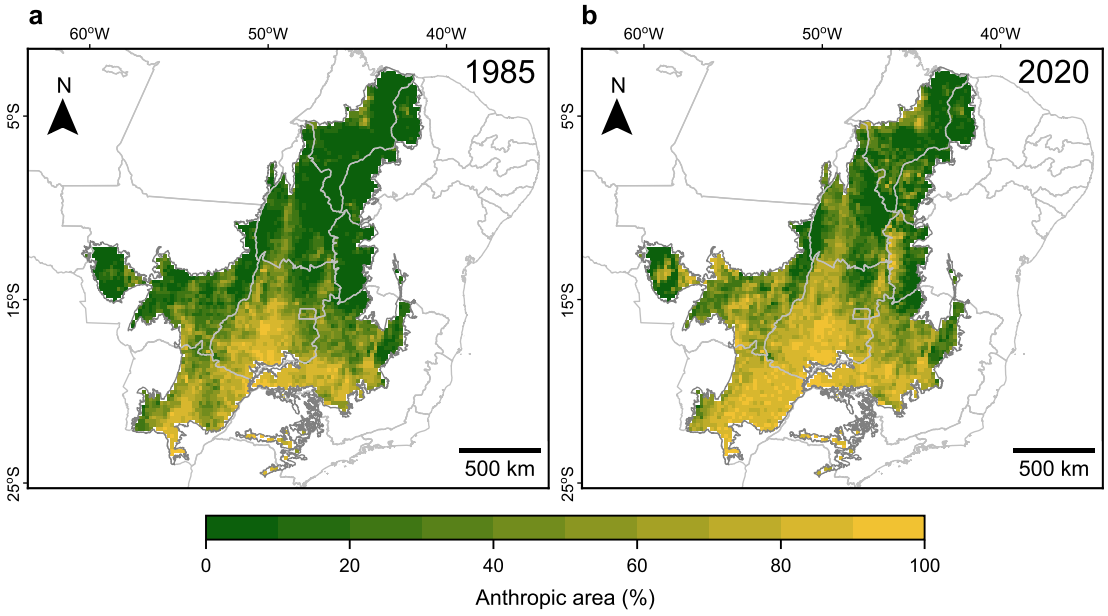

Figure S3.5: **Maps of anthropic area percentage at the beginning and end of the study period**. Anthropic area in **a** 1985 and in **b** 2020, ranging from 0% (green) to 100% (orange).

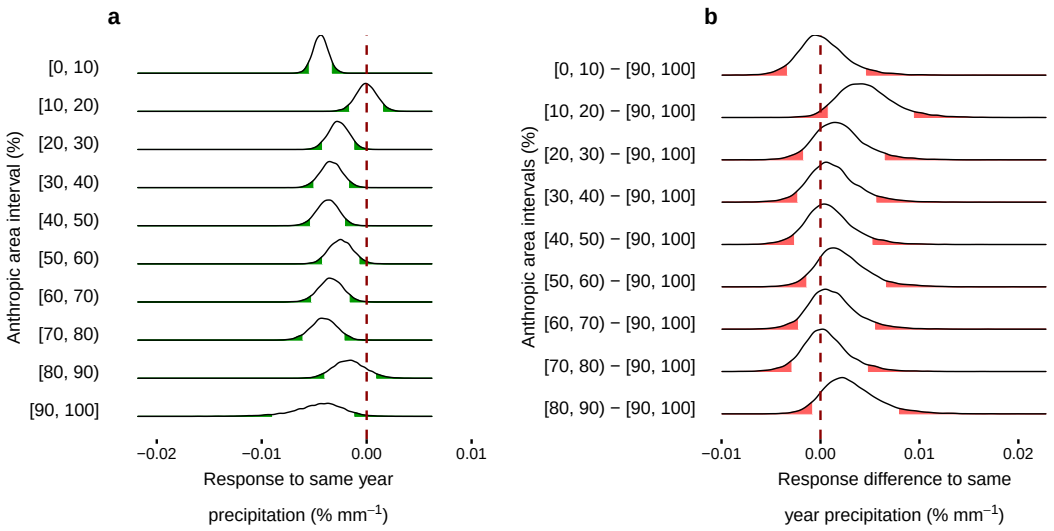

Figure S3.6: **Posterior distributions of same year precipitation effects on burned natural area. a** Posterior distribution of the covariate slopes from multilevel model M3 using same year precipitation as the variable of interest to explain percentage of burned natural area. We use a multilevel model to allow the climate effect (x-axis) to vary by decile of anthropic area percentage (y-axis). **b** Pairwise posterior distribution contrasts showing the difference in the effect of same year precipitation between each decile of anthropic area and the case where human land uses occupy most of the landscape (90-100% of the cell's area) - see Supplementary Fig. S3.8 for a more detailed explanation. Green and red coloured areas indicate the region of the posterior distributions falling outside the 90% HPDI, which we use as credibility interval. Red dashed lines are drawn as a reference to indicate whether 0 is a likely outcome of the posterior distributions.

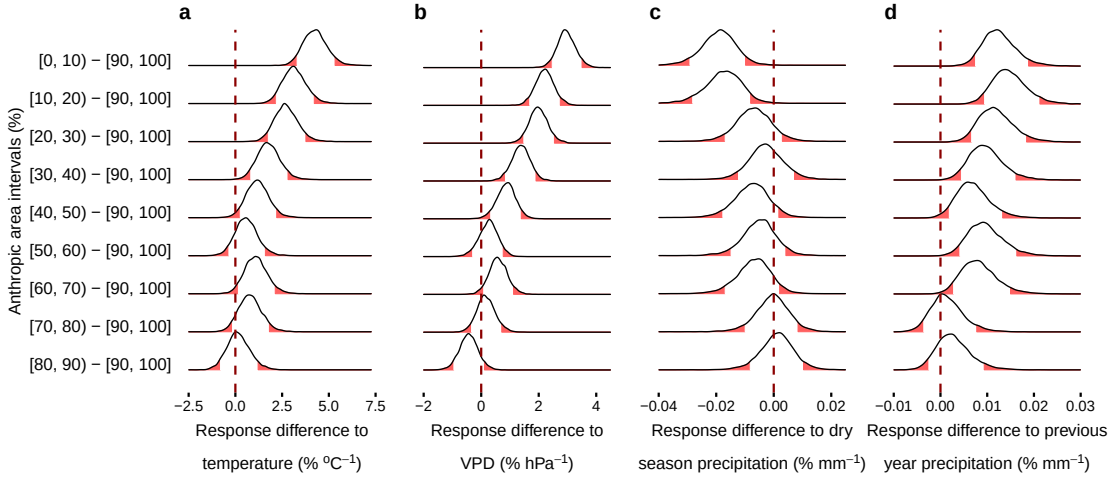

Figure S3.7: **Pairwise posterior distribution contrasts (counterfactual plots) showing the difference in the effect of each climatic variable between each decile of anthropic area and the case where human land uses occupy most of the landscape (90-100% of the cell's area).** We used this decile as a reference because no climatic variables show an effect on burned natural area in this extreme case (Main Fig. 1). Plots show the difference in effects of **a** temperature, **b** VPD, **c** dry season precipitation, and **d** previous year precipitation. The y-axis labels indicate explicitly the anthropic area deciles used in each pairwise contrast calculation. That is, for each climatic variable and decile (e. g. the (20, 30] % anthropic area decile), the posterior contrasts (x-axis) were obtained by calculating the difference between the draws from the posterior distribution of the slope coefficients obtained in models M2 or M3 for this decile and the draws obtained for the slope coefficients of the [90, 100]% decile (and hence it is indicated as "[20, 30) - [90, 100]" on the y-axis). Red coloured areas indicate the region of the posterior distributions falling outside the 90% HPDI, which we use as credibility interval. Red dashed lines are drawn as a reference to indicate whether 0 is a likely outcome of the posterior distributions.

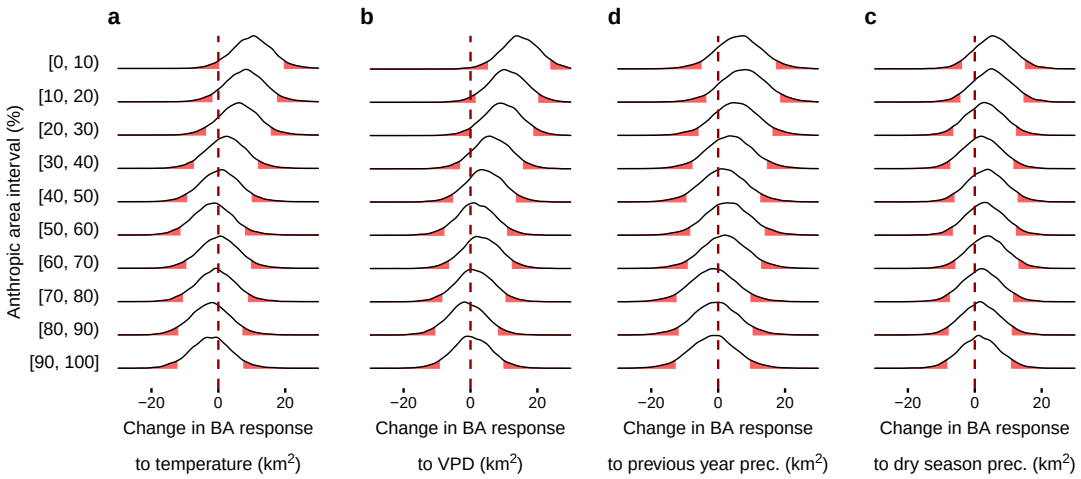

Figure S3.8: **Pairwise posterior distribution contrasts of burned area modelled when each climatic variable is increased (temperature, VPD and previous year precipitation) or decreased (dry season precipitation) by 2 standard deviations from its average value in each anthropic area decile.** Pairwise contrasts for **a** temperature, **b** VPD, **c** previous year precipitation, and **d** dry season precipitation. To obtain these pairwise contrasts, we used models M2 (for temperature and VPD) and M3 (for previous year and dry season precipitation) to model burned natural area for each climatic variable at its average value in each decile, and subtracted it from the modelled burned area at the climatic variable's average value displaced by 1.5 standard deviations. The aim was to ascertain what climatic variable may have a more prominent effect on burned area when their values change by the same standard deviation.

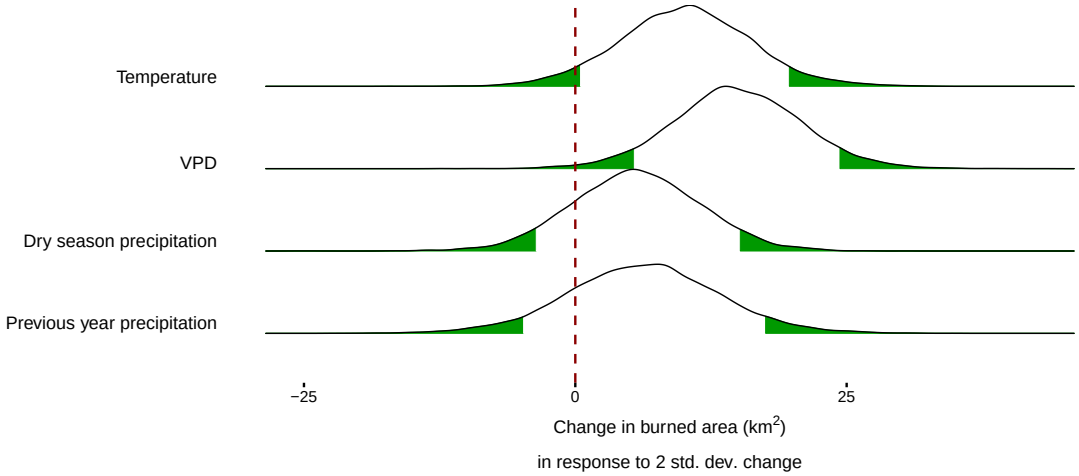

Figure S3.9: **Pairwise posterior distribution contrasts (counterfactual plots) of burned area modelled when each climatic variable increases (temperature, VPD, and previous year precipitation) or decreases (dry season precipitation) by 2 standard deviations from its average value in landscapes with least anthropic presence ([0-10) % anthropic area).** To obtain these pairwise contrasts, we used models M2 (for temperature and VPD) and M3 (for previous year and dry season precipitation) to predict burned natural area for each climatic variable at its average value in this anthropic area decile, and subtracted it from the modelled burned area at the climatic variable's average value displaced by 2 standard deviations. The aim was to ascertain what climatic variable may have a more prominent effect on burned area when their values change by the same amount of standard deviations.

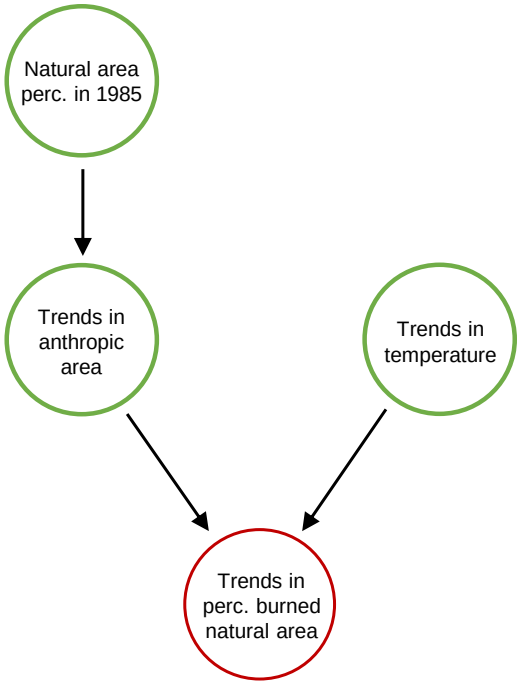

Figure S3.10: **Directed Acyclic Graph, DAG2, describing the set of variables that may influence trends in burned natural area that were included in this study.** We used this DAG to inform the design of model M4. All of the conditional independencies (Laubach et al., 2021) implied by this and alternative DAGs that we considered (comprising the same variables as in DAG2) were tested and validated. Green circles indicate those variables that we have included in the study either directly as covariates or in the calculation of other covariates and the red circle indicates the outcome variable.

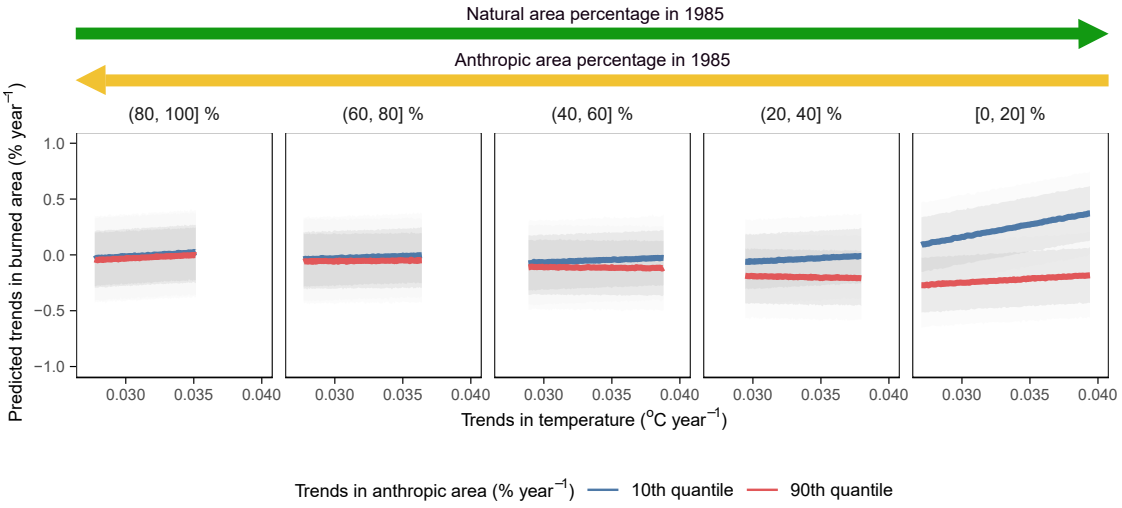

Figure S3.11: **Model predictions of trends in burned area from model M4 using trends in temperature (tT) as the predictor after fixing the value of trends in anthropic area (tA) at the 10th percentile (blue) and the 90th percentile (red) of the range of observed tA values in each group of cells.** Each figure shows the model predictions for the different groups of cells classified on groups of 20 % of their anthropic area percentage in 1985 (mostly anthropic to mostly natural from left to right). Grey shaded area shows the 80% Highest Posterior Density Interval (HPDI).

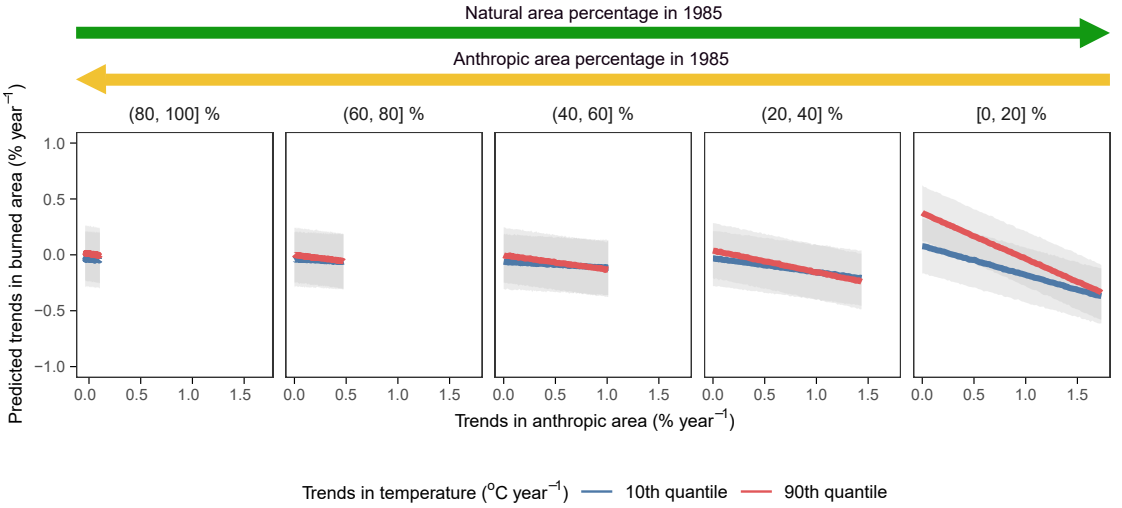

Figure S3.12: **Model predictions of trends in burned area from model M4 using trends in anthropic area (tA) as the predictor after fixing the value of trends in temperature (tT) at the 10th percentile (blue) and the 90th percentile (red) of the range of observed tT values in each group of cells.** Each figure shows the model predictions for the different groups of cells classified on groups of 20 % of their anthropic area percentage in 1985 (mostly anthropic to mostly natural from left to right). Grey shaded area shows the 80% Highest Posterior Density Interval (HPDI).

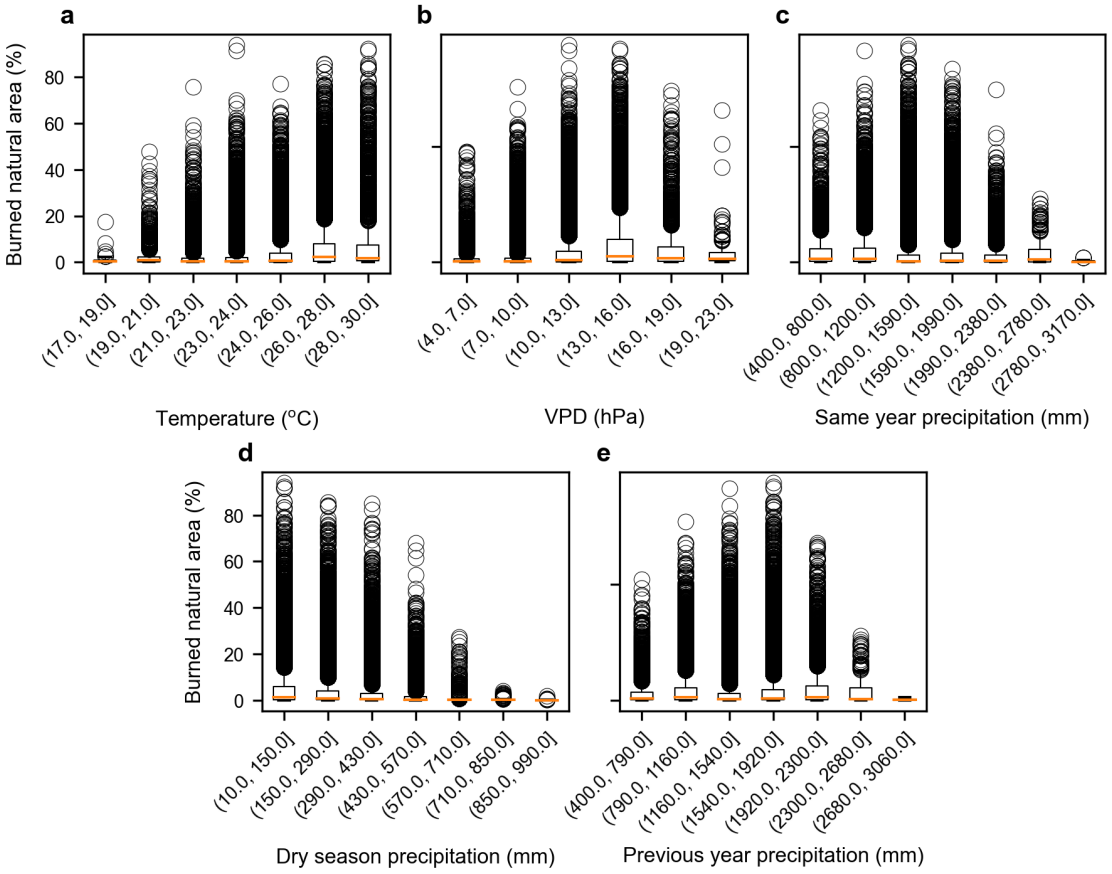

Figure S3.13: **Distribution of natural area burned occurred in the period 1985-2020 for interval of each climatic variable**. **a** Temperature, **b**, VPD, **c** total annual precipitation, **d** dry-season precipitation, and **e** previous year total precipitation. Boxplots represent the distribution of the data points (cell-year pairs) falling in each interval.

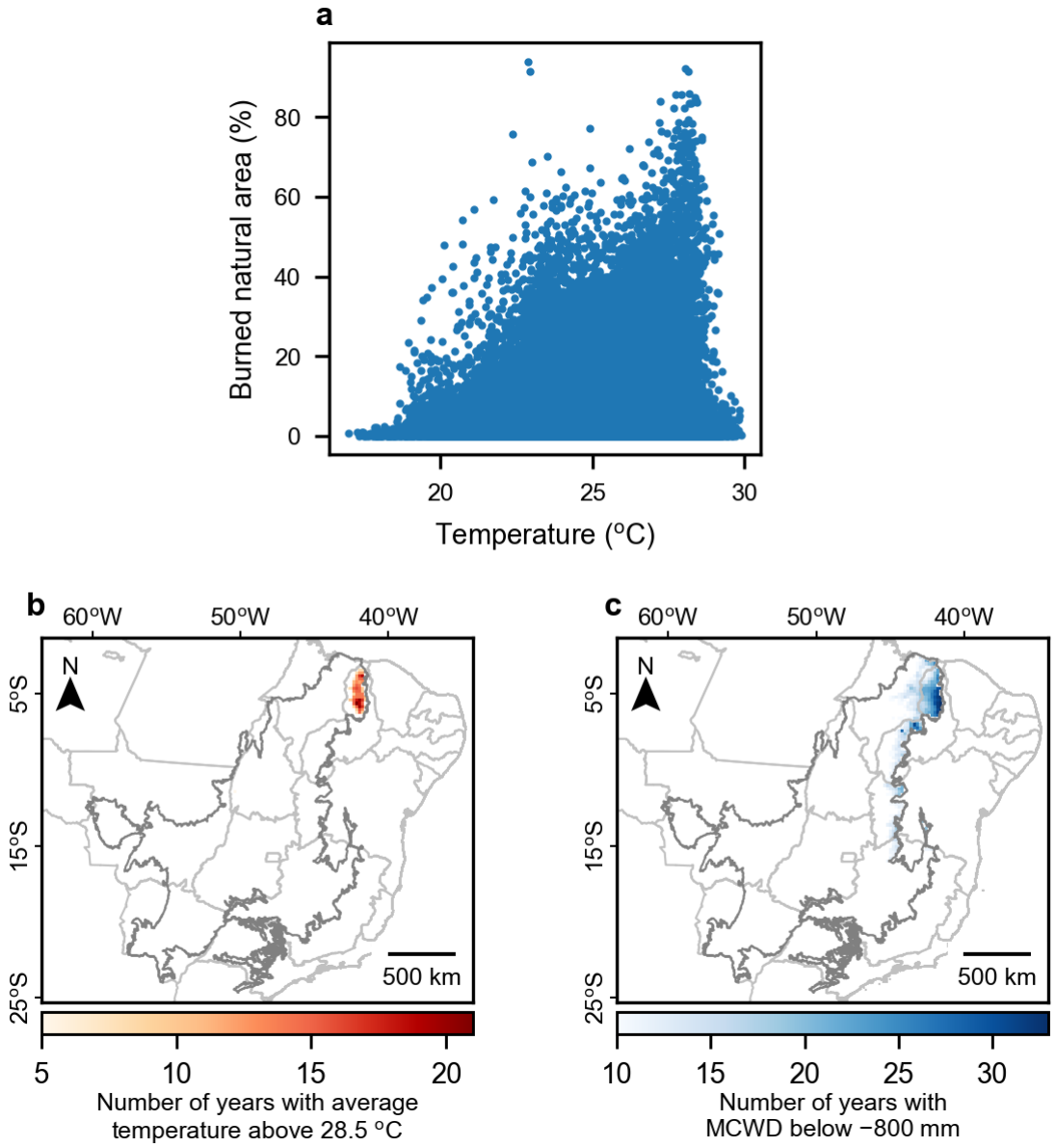

Figure S3.14: **Figures presented to show why a small cluster of cells has been excluded from models M2 and M3. a** Burned natural area against annual average temperature for all the data points, we can observe how the cells experiencing the hottest years do not seem to follow the same behaviour as the rest. **b**, **c** Cells that experienced temperatures equal to or above 28.5 °C five times or more in the period 1985-2020, and those that experienced MCWD values more extreme than -800 mm ten times or more respectively.

Supplementary Tables

Table S3.1: R-squared coefficient adapted for Bayesian inference (Gelman et al., 2019) calculated for model M1 (see Main) with its 95% confidence interval, where anthropic area percentage is the causal predictor of interest.

Anthropic area percentage (Model M1)
0.544 [0.542, 0.547]

Table S3.2: R-squared coefficients adapted for Bayesian inference (Gelman et al., 2019) calculated for models M2 (with temperature and Vapour Pressure Deficit, VPD, as the causal predictors of interest) and M3 (with dry season and previous year precipitation as causal predictors of interest) for each anthropic area decile (see Methods), with their 95% confidence interval.

	Temperature (Model M2)	**VPD (Model M2)**	**Dry season precipitation (Model M3)**	**Previous year precipitation (Model M3)**
[0, 10) %	0.43 [0.41, 0.46]	0.54 [0.52, 0.56]	0.35 [0.32, 0.37]	0.43 [0.40, 0.45]
[10, 20) %	0.39 [0.36, 0.43]	0.47 [0.43, 0.50]	0.29 [0.26, 0.33]	0.43 [0.39, 0.47]
[20, 30) %	0.31 [0.27, 0.36]	0.47 [0.43, 0.51]	0.26 [0.22, 0.30]	0.34 [0.30, 0.38]
[30, 40) %	0.24 [0.21, 0.27]	0.34 [0.30, 0.38]	0.23 [0.20, 0.27]	0.29 [0.26, 0.33]
[40, 50) %	0.24 [0.21, 0.27]	0.29 [0.26, 0.33]	0.27 [0.23, 0.30]	0.27 [0.24, 0.30]
[50, 60) %	0.29 [0.26, 0.33]	0.27 [0.24, 0.31]	0.29 [0.26, 0.33]	0.32 [0.28, 0.36]
[60, 70) %	0.24 [0.21, 0.27]	0.28 [0.24, 0.32]	0.32 [0.28, 0.36]	0.28 [0.25, 0.32]
[70, 80) %	0.29 [0.26, 0.32]	0.29 [0.26, 0.33]	0.34 [0.30, 0.37]	0.35 [0.32, 0.38]
[80, 90) %	0.38 [0.34, 0.41]	0.33 [0.29, 0.37]	0.38 [0.34, 0.42]	0.39 [0.35, 0.42]
[90, 100] %	0.28 [0.17, 0.40]	0.11 [0.05, 0.17]	0.12 [0.07, 0.19]	0.15 [0.08, 0.23]

Table S3.3: R-squared coefficients adapted for Bayesian inference (Gelman et al., 2019) calculated for model M5 - where trends in temperature (tT) and trends in anthropic area (tA) are the causal predictors of interest - for each 20% interval of anthropic area group (see Methods), with their 95% confidence interval.

	Trends in anthropic area percentage and in temperature (Model M5)
[0, 20] %	0.40 [0.37, 0.44]
(20, 40] %	0.17 [0.09, 0.26]
(40, 60] %	0.08 [0.01, 0.18]
(60, 80] %	0.11 [0.01, 0.25]
(80, 100] %	0.32 [0.05, 0.45]

3.12 Supplementary Information References

Bürkner, Paul-Christian (2017). "brms: An R Package for Bayesian Multilevel Models Using Stan". In: *Journal of Statistical Software* 80.1, pp. 1–28.

Durigan, Giselda and James A. Ratter (2016). "The need for a consistent fire policy for Cerrado conservation". In: *Journal of Applied Ecology* 53.1. Ed. by Jeremy James, pp. 11–15.

Elwert, Felix and Christopher Winship (2014). "Endogenous Selection Bias: The Problem of Conditioning on a Collider Variable". In: *Annual Review of Sociology* 40.1, pp. 31–53.

Flannigan, Mike et al. (2013). "Global wildland fire season severity in the 21st century". In: *Forest Ecology and Management* 294, pp. 54–61.

Gelman, Andrew et al. (2019). "R-squared for Bayesian Regression Models". In: *The American Statistician* 73.3, pp. 307–309.

Jepson, Wendy (2005). "A disappearing biome? Reconsidering land-cover change in the Brazilian savanna". In: *The Geographical Journal* 171.2, pp. 99–111.

Laubach, Zachary M. et al. (2021). "A biologist's guide to model selection and causal inference". In: *Proceedings of the Royal Society B: Biological Sciences* 288.1943, p. 20202815.

McElreath, Richard (2018). *Statistical rethinking: A Bayesian course with examples in R and Stan*. Chapman and Hall/CRC.

Pearl, Judea, Madelyn Glymour, and Nicholas P Jewell (2016). *Causal inference in statistics: A primer*. John Wiley & Sons.

Pivello, Vânia R. (2011). "The Use of Fire in the Cerrado and Amazonian Rainforests of Brazil: Past and Present". In: *Fire Ecology* 7.1, pp. 24–39.

Rego, Francisco Castro et al. (2021). *Fire Science: From Chemistry to Landscape Management*. Springer Textbooks in Earth Sciences, Geography and Environment. Cham: Springer International Publishing.

Rosan, Thais M. et al. (2022). "Fragmentation-Driven Divergent Trends in Burned Area in Amazonia and Cerrado". In: *Frontiers in Forests and Global Change* 5, p. 801408.

Schmidt, Isabel Belloni and Ludivine Eloy (2020). "Fire regime in the Brazilian Savanna: Recent changes, policy and management". In: *Flora* 268, p. 151613.

Silva, Patrícia S. et al. (2021). "Putting fire on the map of Brazilian savanna ecoregions". In: *Journal of Environmental Management* 296, p. 113098.

Westerling, A. L. et al. (2006). "Warming and Earlier Spring Increase Western U.S. Forest Wildfire Activity". In: *Science* 313.5789, pp. 940–943.

4 | The fire regimes of the Brazilian Cerrado and their changes through time (Research Paper 2)

By: Carlota Segura-Garcia, Ane A. C. Alencar, Vera L. S. Arruda, David Bauman, Wallace Silva, Dhemerson E. Conciani, Imma Oliveras Menor

Linking statement: This chapter expanded on **Chapter 3 (Research Paper 1)** by quantifying the fire regimes in a more complete manner, that is, including measures of frequency, fire size, and seasonality apart from burned area. This chapter was motivated by the need to understand how the fire regimes of the Brazilian Cerrado have changed over the past few decades, both in their characteristics and in their spatial distribution across this region. This chapter used a clustering algorithm to identify the regions of the Cerrado presenting distinct fire regimes in four consecutive periods (1985-1993, 1994-2002, 2003-2011, and 20129-2020). Then, focusing on the first and last periods, it explored the anthropic and climatic factors that characterise the different fire regime regions, and studied both how these regions and their fire regimes have changed through time.

This chapter was submitted on 29th February, 2024 to a special issue on the topic *Novel fire regimes under climate changes and human influences: impacts, ecosystem responses and feedbacks* in *Philosophical Transactions of the Royal Society of London, Series B: Biological Sciences*, and it is currently on a second round of reviews.

Contribution Statement: I, Carlota Segura-Garcia, conducted the conceptualization, methodology development, data processing and data analysis, investigation, visualization of the results and writing of the manuscript. In addition, I also responded to all review comments during the first round of the peer review process. Dr David Bauman helped in the methodology, analysis and reviewing of the manuscript. Dr Ane Alencar helped in the conceptualization, investigation and reviewing of the manuscript. Vera L. S. Arruda, Dhemerson E. Conciani and Wallace Silva helped in the conceptualization and investigation of this study. Finally, Dr Imma Oliveras Menor supervised and was involved in all steps of this work.

4.1 Abstract

The Brazilian Cerrado is a heterogeneous region of open ecosystems adapted to fire intermingled with patches of woody growth-forms, with high levels of biodiversity and endemism. In recent decades, land conversion and human activities have proliferated across the Cerrado, losing about half of its original area. These changes, coupled with climate change, are altering its fire regimes with uncertain, but possibly adverse, consequences for Cerrado ecosystems. Here, we used burned area data to characterise the fire regimes of each cell on a 30 km grid over the Cerrado, and used a spatially constrained hierarchical clustering approach to delineate the regions with different fire regimes in four consecutive 9-year periods between 1985 and 2020. Comparing the periods 1985-1993 and 2012-2020, we found substantial changes in the number and shape of the fire regime regions, and in their fire characteristics. The main factor differentiating these regions was their level of fire activity: some showed large, numerous and frequent fires, while others showed small, few and infrequent fires. We also identified a region in the north with a later peak of the fire season, characterised by small but numerous fires. Finally, we found that while the fire activity of the southern areas of the Cerrado substantially decreased, fire activity levels in the centre and north increased or remained high over time.

Keywords - fire regimes, open ecosystems, disturbance ecology, land use effects, climate change

4.2 Introduction

Across the world, areas with different types of vegetation, climatic ranges and socio-economic characteristics present different patterns of fire occurrence, referred to as fire regimes (Chuvieco et al., 2008; Archibald, Lehmann, Gómez-Dans, et al., 2013; Cattau et al., 2022). The relations between characteristics of fire like size, frequency, intensity or seasonality, and the factors that affect them are complex, often forming feedbacks by which one factor influences the others and vice versa (Archibald, Lehmann, Belcher, et

al., 2018). Further, the effects of different drivers of fire may become apparent only at certain scales - landscape, regional or global (Krawchuk et al., 2011; Cattau et al., 2022). Fire regimes are a useful framework to study how the characteristics of fire vary geographically in relation to these factors (Cattau et al., 2022), understand how fire may contribute to shaping different landscapes (Bond, Woodward, et al., 2005; Bond and Keeley, 2005), weigh its contribution to carbon emissions and other biogeochemical cycles (Werf, Randerson, Giglio, Collatz, et al., 2010), and foresee how fire may respond to changes in the climate. At regional to local scales, characterising fire regimes can also contribute towards the conceptualisation of fire management strategies and conservation plans that are adequate to specific contexts.

Certain open ecosystems, like savannas and grasslands, are adapted to fire as their vegetation has co-evolved with this phenomenon over millions of years (Pausas and Keeley, 2009; Bond, 2019). Therefore, given a certain vegetation composition, it is argued that there exists an underlying fire regime the vegetation is specifically adapted to (Pausas and Keeley, 2009). However, biomes of open ecosystems are usually very heterogeneous in their vegetation composition, topographic features, and climatic characteristics and, as a consequence, can present different fire regimes across their area (Archibald, Lehmann, Gómez-Dans, et al., 2013). Furthermore, the expansion of modern human land use activities and anthropic climate change are rapidly altering the fire regimes of these regions (Archibald, 2016). Indeed, in tropical savannas, humans shape fire regimes through landscape fragmentation (Rosan et al., 2022), shifting the fire season (Ramos-Neto et al., 2000; Archibald, 2016) by igniting fires for agricultural and land conversion purposes (Klink et al., 2005; Pivello, 2011), or actively preventing or suppressing fires - which may lead to more infrequent but larger and more intense fires as a result of fuel accumulation (Stevens, Lehmann, et al., 2017; Stevens and Bond, 2023). Regarding climate, even though there is established evidence that climate change is altering savannas' fire regimes (Jolly et al., 2015), and that it will continue to do so (Silva, Bastos, DaCamara, et al., 2016; Silva, Bastos, Libonati, et al., 2019), the specific long-term effects are still uncertain. While climate change is associated with surges in the number, size and intensity of

fires in relation to increasing temperatures and the frequency of climate anomalies (Werf, Randerson, Giglio, Gobron, et al., 2008), or the lengthening of the dry season (Jolly et al., 2015); in the long run, the effects on fire regimes will also depend on its effects on vegetation productivity during the growing season, which ultimately influences the amount of available fuel (Pausas and Ribeiro, 2013; Krawchuk et al., 2011). In turn, the alteration of savannas' fire regimes as a result of the expansion of human activities and climate change may further couple with these two processes to affect the vegetation of these open ecosystems (Pivello et al., 2021), as well as having broader effects on the planet's carbon cycle (Beer et al., 2010).

The Brazilian Cerrado is a clear example of large and heterogeneous mosaic of open ecosystems where both its landscape and fire regimes are undergoing rapid and profound changes in their configuration (Silva, Nogueira, et al., 2021; Mataveli et al., 2018). Indeed, despite its high levels of endemism and rich biodiversity (Myers et al., 2000; Klink et al., 2005), around 50% of the Cerrado's 2 million km^2 have been converted to agricultural land uses in recent decades (Alencar, Z. Shimbo, et al., 2020) roughly expanding from the south towards the Matopiba region in the north, the Cerrado's current agricultural frontier (Spera et al., 2016). Simultaneously, this region has also become warmer and drier (Hofmann et al., 2021) under climate change. Apart from its heterogeneous vegetation, the Cerrado presents a diverse topography, climate and soil composition, as well as varying levels of landscape fragmentation and different anthropic land uses, giving rise to different ecoregions (Sano, Rodrigues, et al., 2019). All of these elements influence its fire regimes (Libonati et al., 2015; Bowman, Kolden, et al., 2020; Pausas and Ribeiro, 2013). Indeed, studies across the Cerrado and its ecoregions have observed a great heterogeneity in the patterns of fire, with overall low burned area levels in the south of the Cerrado and higher levels in the centre of this region (Silva, Nogueira, et al., 2021; Mataveli et al., 2018), as well as heterogeneous changes in burned area through time. Decreases in burned area are generally associated with increasing landscape fragmentation as a consequence of agricultural expansion, while increases in burned area are related to both climate change and the growing presence of human activities in the least

converted parts of the Cerrado (Silva, Nogueira, et al., 2021; Silva Arruda et al., 2024; Segura-Garcia et al., 2024), as humans cause ignitions in relation to agricultural practices, accidents, fire management or in the conversion of certain vegetation forms (Pivello, 2011; Ribeiro, Santos, et al., 2024). However, a clear delineation of the different regions of the Cerrado presenting different fire regimes and how these may have changed over time is still lacking.

In this study, we analysed the fire regimes of the Brazilian Cerrado in the period 1985-2020. First, we aimed to identify the different regions of the Cerrado presenting distinct characteristics of fire in four 9-year periods between 1985 and 2020, with a particular focus on the first (1985-1993) and last (2012-2020) periods. For this purpose, we combined monthly burned area data with 30 m spatial resolution with advanced spatially constrained clustering methods to delineate the regions of the Cerrado with different fire regimes based on a 30 km grid. Then, we studied the characteristics of these regions in terms of various factors related to the presence of human activities in the landscape and in terms of various climatic variables that may explain the differences in the fire regimes of the various regions identified. Finally, we analysed how these regions have changed over time, both geographically and in terms of their fire characteristics, with the ultimate aim of understanding how the rapid changes the Cerrado has experienced over the past four decades have shaped its fire regimes.

4.3 Methods

4.3.1 Study area

The Brazilian Cerrado is formed by a range of vegetation growth-forms (Ribeiro and Walter, 2008), predominantly savannas and grasslands. The Cerrado occupies an area over 2 million km^2 spanning eleven Brazilian states, and presents varying levels of anthropic land uses (Alencar, Z. Shimbo, et al., 2020). In the 1970s, large-scale agricultural expansion rapidly converted the Cerrado to anthropic land uses (De Albuquerque Prado et al., 2012; Rocha et al., 2012), affecting around 50% of its native vegetation area (Alencar,

Z. Shimbo, et al., 2020).

The Cerrado presents a latitudinal gradient of temperatures increasing towards the Equator, ranging from around 18°C to 28°C (Nascimento et al., 2020). The climate of this biome is strongly seasonal, with a wet and a dry season (roughly May to October). In addition, there is a gradient of precipitation increasing from east to west varying between 800 mm and over 1,800 mm (Nascimento et al., 2020).

To characterise the fire regimes of these savannas, we used a 30x30 km grid laid over the Cerrado and divided the study period in four 9-year periods: 1985-1993, 1994-2002, 2003-2011, 2012-2020. The size of the cells was chosen to have enough spatial resolution, while being large enough to simultaneously limit the number of fire polygons larger than one cell (see next Section), as well as minimising the number of cells with little to no fire events in a period.

4.3.2 Data sources and processing

Burned area data and fire polygons

We used burned area data from MapBiomas Fogo (Collection 2.0, (Alencar, Arruda, et al., 2022)), a publicly available dataset covering the period 1985-2022 based on Landsat images (30 m spatial resolution with a 16-days interval) and created using machine learning algorithms in the Google Earth Engine platform (Gorelick et al., 2017). This dataset provides annual maps of burned area where pixels identified as burned are labelled with their mapping month. We downloaded the data using the MapBiomas toolkit for the aforementioned Google Earth Engine platform.

We processed this raster data using a custom algorithm to create fire polygons in vector format so that we could have an estimation of the size of the different fire events. Considering the limitations of Landsat data regarding the temporal resolution, as well as those possibly introduced by the mapping methodology, we mapped together as part of the same fire event (i.e. fire polygon) those spatially contiguous pixels belonging to consecutive months, as well as those polygons separated by up to 150 m from border to

border. The reason was three-fold: first, two physically separated fires occurring close to one another in space and time may be part of the same fire event (Martin et al., 1992); second, Landsat's spectral resolution and the mapping algorithm may fail to detect certain burned pixels within a fire event; and third, when simply mapping the polygons without this last condition, we found an excess number of small fires compared to the expected heavy-tail fire size distribution (Hantson, Arneth, et al., 2016). Finally, we kept only those fire polygons larger than 3 ha.

We quantified the fire regimes of a certain 30 km cell in a specific 9-year period by focusing our analyses on six fire variables: (1) **number of fires**, the number of polygons normalised to flammable area (see next Section); (2) the **50th quantile** and (3) **99th quantile** of the polygons' size distribution; (4) **burned area**, the sum of burned pixels in the period normalised to flammable area; (5) **fire frequency** as the 99th quantile of the smoothed Empirical Cumulative Distribution Function (sECDF) of the number of times each cell's pixel burned in the period (between 0 and 9); and (6) **fire seasonality**, as the peak of the fire season using the median value of the sECDF of monthly burned area in a fire-year. We established the fire-year for each cell as the 12-month period centered at the month with highest burned area. This consideration was important given the latitudinal gradient observed in the peak of the fire season . Henceforth, we will refer to the fire regime of a grid cell or region in a period as the combination of these six quantities.

Finally, a few grid cells in each 9-year period presented no burned area, indicating absence of fire. However, the clustering algorithm requires each cell to have a value for each fire variable. Therefore, we assigned these cells the minimum fire size (3 ha) both for the median and 99th percentile fire size and for burned area, and a frequency and number of fires of 1. We used the average peak of the fire season from the immediate 8 neighbouring cells. There were few cells with no fire occurrences, and these were generally spread out across the south of the Cerrado, with the exception of a small group of contiguous cells presenting no fires in the western-most tip of the Cerrado in the period (1985-1993), which were classified as part of cluster wLFA_P1 (see Results and Figure 4.1 for a definition of the clusters and their naming).

Both the creation of fire polygons and the quantification of the six different fire variables in each 30 km grid cell and period were carried out in Python (Python Software Foundation, https://www.python.org/), using the packages GeoPandas (Jordahl et al., 2021), Pandas (team, 2021) and Rasterio (Gillies et al., 2013), as well as the QGIS (QGIS Development Team, 2023) Python API.

Land use area data and fragmentation indices

We used annual maps of land use and land-cover from the MapBiomas project (Collection 8.0, (Souza et al., 2020)). For each grid cell in the first (1985-1993) and last (20120-2020) periods, we calculated the average percentage of anthropic area (comprising "Urban Area", "Mining" and all land use categories under "Farming"), "Forest Formation", "Savanna Formation", "Grassland", and "Wetland". Additionally, we calculated the change in anthropic area within each period as the difference in anthropic area between the last and the first year in the period. Finally, we calculated the average flammable area as the sum of all those categories describing landscapes with enough vegetation to sustain a fire (that is, all categories except "Hypersaline Tidal Flats", "Rocky Outcrops", "Non Vegetated Area" and "Water"). We downloaded the land use and land-cover data using the MapBiomas toolkit for Google Earth Engine, and processed it using various Python packages (Python Software Foundation, https://www.python.org/).

We also calculated different types of landscape fragmentation indices using the Python package "PyLandStats" (Bosch, 2019). However, these indices were not used in the final analysis after inspection of collinearity and variable importance using Random Forests algorithm (see below).

Climate reanalysis data

For each 30 km grid cell in the first (1985-1993) and last (2012-2020) periods, we calculated the average annual and dry season temperature and precipitation, and the peak of the dry season. We used the 2 m temperature variable from ERA5-Land Monthly Averaged climate reanalysis data (Muñoz-Sabater et al., 2021) (9 km spatial resolution) from the

European Centre for Medium-range Weather Forecasts (ECMWF). For precipitation, we used the 5-day precipitation accumulation in mm from the Climate Hazards Group InfraRed Precipitation with Station data (Funk et al., 2015) (CHIRPS, version 2.0), a quasi-global rainfall dataset with 0.05° spatial resolution. We chose the ERA5-Land dataset for temperature because the ECMWF data products have been identified as the most reliable air temperature datasets (Burton et al., 2018). We used CHIRPS v2.0 for precipitation, as it is considered the best data source for precipitation across the tropics (Burton et al., 2018) - along with the Tropical Rainfall Measuring Mission (TRMM) (Liu et al., 2012). Finally, we used the potential evapotranspiration (PET) data provided by TerraClimate (Abatzoglou et al., 2018), a global dataset of climatic data with 0.5° spatial resolution.

First of all, we calculated the average value of each climatic variable - temperature, precipitation and PET - for each 30 km grid cell, year and month as the average of all pixels of the corresponding data products intersecting the cell in the corresponding year and month (weighting each pixel's contribution to the average depending on the pixel's area within the cell, using the R package Exactextractr (Baston, 2020)).

For each period and grid cell, we considered the dry season to be those months in which, on average, PET exceeded precipitation. We identified the peak of the dry season as the month with the most negative Climatological Water Deficit (CWD) on average. We calculated the CWD based on Malhi et al. 2009 (Malhi et al., 2009), as the cumulative difference between precipitation and PET ($\text{CWD}_m = \text{CWD}_{m-1} + \text{Prec.}_m - \text{PET}_m$, $\text{Max}(\text{CWD}_m) = 0$, where m represents a certain month) in every 12-month cycle starting on the wettest month on average of each grid cell and period. Finally, we calculated the average monthly CWD for each period and grid cell, and identified the month with the most negative value.

Finally, for each 30 km grid cell and period, we calculated the average annual temperature as the average temperature across all months in the period, the dry season temperature as the average temperature across dry season months, the annual precipitation as the average total precipitation in a year, and the dry season precipitation as the average total precipitation across dry season months.

We downloaded the climatic data from the Google Earth Engine platform using the Geemap Python package (Wu, 2020) and Jupyter Notebook (Kluyver et al., 2016). In this case, we processed the data in R (R Core Team et al., 2020), using the package Exactextractr (Baston, 2020).

Population and livestock density data

For each grid cell in the first (1985-1993) and last (2012-2020) periods, we calculated the median annual population density and livestock density. The density data were obtained from the Instituto Brasileiro de Geografia e Estatística (IBGE) (*Estimativas da População do Instituto Brasileiro de Geografia e Estatística* n.d.; *Sistema IBGE de Recuperação Automática do Instituto Brasileiro de Geografia e Estatística* n.d.) at municipality level. We resampled these two sets of data from the municipality level to the grid level using various Python packages.

4.3.3 Analysis

Here, we used a combination of ordination and clustering techniques, as well as linear regressions, to address our research questions. As described with more detail below, we first summarised the main axes of variation of the six fire variables (burned area, frequency, largest and median fire sizes, peak of the fire season, and number of fires) using Principal Component Analyses (PCA) to characterise the fire regimes at the grid cell level in each 9-year period. We then used a spatially constrained clustering algorithm to identify the fire regime regions, that is, the geographic areas formed by each cluster of grid cells with similar combinations of fire variables (similar fire regimes). Next, we focused on the first (1985-1993) and last (2012-2020) periods as we were mostly interested in understanding how the fire regime regions and their climatic and anthropic characteristics may have changed between 1985 and 2020. For each of these two periods, we used PCAs and redundancy analysis to investigate the characteristics of the different fire regime regions in terms of the climate and the presence of human activities, and their association with the characteristics of fire. Finally, we explored how these fire regime regions changed

through time geographically and also how their characteristics of fire evolved using linear regression on time series data.

Clustering algorithm

In preparation for the clustering algorithm, we calculated the fire regimes for each cell and 9-year period, transformed seeking normality by taking the natural logarithm of the median and 99th percentile fire size, burned area, number of fires, and fire frequency (after adding a unit). Then, for each 9-year period, we performed a PCA on the correlation matrix of the set of standardised fire variables (Borcard et al., 2011) (henceforth PCA_fire). We ran the clustering algorithm on the first three axes of each period's PCA as they described more than 95% of the variation in the data.

To determine the different fire regime regions of the Cerrado, we used a hierarchical clustering algorithm with a spatial contiguity constraint (Guénard et al., 2022) because we were interested in delineating spatially contiguous regions where fire regimes have similar features in a certain period, and investigate the environmental characteristics that may explain such geographical patterns. As a result of such constraint, areas with similar fire regimes but geographically disconnected would be identified as different clusters - i.e. different fire regime regions. We explored the fire regime characteristics of each cluster using the first two components of the PCA_fire (PC1_fire and PC2_fire, Supplementary Information, Table S1).

Because the algorithm we used is an unsupervised method (Guénard et al., 2022) - that is, the classification does not use any *a priori* knowledge on the clustering of the data -, we explored a few metrics to identify an optimal clustering solution (i.e. the number of clusters) delineating compact and dissimilar clusters. We finally based the decision on the Bayesian Information Criteria (BIC) (Supporting Information, Figure S1), although also consulting the Dunn Index and a Silhouette plot.

Finally, we repeated the clustering procedure on the first (1985-1993) and last (2012-2020) periods excluding the peak of the fire season. The objective was to understand the distinctiveness of certain areas in absence of this fire attribute (see Results and Supple-

mentary Information, Figure S9).

We carried out this part of the analysis using R (R Core Team et al., 2020). In particular, we used the package Vegan (Oksanen et al., 2024) to run the PCA and the function constr.hclust() (Guénard et al., 2022) distributed with the package adespatial (Dray et al., 2023) to run the clustering algorithm.

Environmental characteristics of the clusters

Focusing on the first (1985-1993) and last (2012-2020) periods, we analysed the fire regime regions in terms of two sets of explanatory variables related to the level of anthropic activities in the landscape (percentage of anthropic area, the change in anthropic area percentage within the period, and the population and livestock densities), and to the climatic characteristics (average annual and dry season temperature, average total annual and dry season precipitation, and the peak of the dry season) of each fire regime region. For both groups of variables, we first assessed collinearity between variables and performed transformations as appropriate seeking to improve normality (Supplementary Information, Figures S3 and S4 and Table S8).

For each group of explanatory variables separately and together, we first ran a Random Forests algorithm (Breiman, 2001) to assess the classification power of each set and evaluate the variables' predictive importance. Then, we performed a PCA on each set of variables in each of the two periods to analyse the climatic and anthropic characteristics of each region (henceforth PCA_clim and PCA_anth). Finally, we analysed the relation between each of the first components of the anthropic (PC1_ant) and climatic (PC1_clim) variables and the PC1_fire. These post-hoc assessments of PC1 components and environmental variables were further tested using constrained ordinations - redundancy analyses (RDA), a method that allows to use multiple explanatory variables to model simultaneously a set of response variables (Borcard et al., 2011) - to test for the statistical significance and explanatory power of the environmental variables sets to explain the variation in the multivariate space of fire variables.

To run the Random Forests algorithm, we used the R package randomForest (Liaw et al.,

2002). For the various PCAs and RDAs, we again used the package Vegan (Oksanen et al., 2024).

Temporal changes of the fire regimes

We studied temporal changes in each of the six fire variables and the PC1_fire. To make the periods comparable, we projected the PC1_fire of each 9-year period on the PC1_fire of the first period (Figure 4.4). Then, we calculated the temporal changes of PC1_fire and of each fire variable by fitting a linear regression model to each cell using either the time period (for PC1_fire and fire frequency) or the year (for the other fire variables) as the predictor (Figure 4.6 and Supplementary Information, Figure S7). Hence, we fitted

$$\mathrm{x}_f = \alpha + \beta \mathrm{t}, \tag{4.1}$$

where x_f represents PC1_fire or each of the fire variables, t is the time variable, α represents the average value of the grid cell at the beginning of each time series, and β is the rate of change of x_f over time. We fitted the model using Ordinary Least Squares (OLS) in Python with the statsmodels library (Seabold et al., 2010). We used an 80% confidence interval to assess the statistical significance of the trends.

Finally, because the PC1_fire - capturing the largest variation in the data - had a meaning in terms of the characterisation of the fire regimes of the various regions (see Results), we further compared the PC1_fire value of each cell in the first (1985-1993) and last (2012-2020) periods to investigate whether this PCA_fire score had increased or decreased over time.

4.4 Results

4.4.1 The fire regime regions of the Cerrado

Using the hierarchical clustering algorithm with a spatial contiguity constraint and based on the BIC criteria, we identified a different optimal number of fire regime regions (the

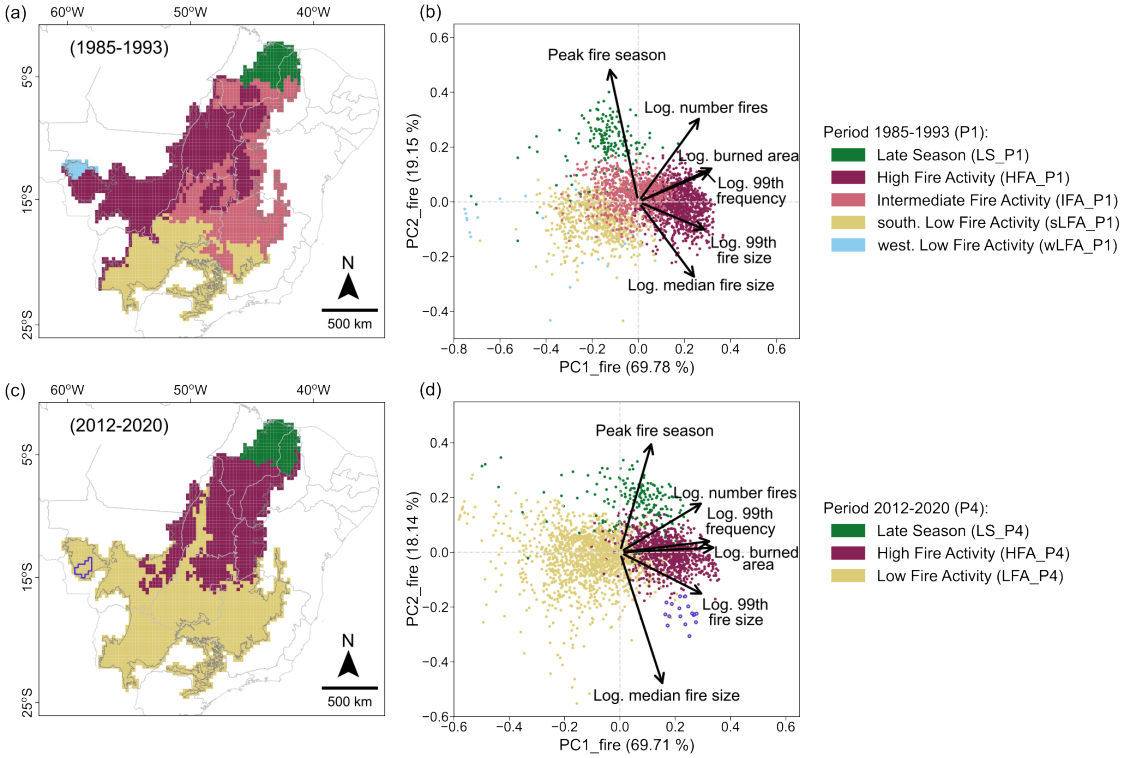

Figure 4.1: Fire regime regions obtained for (a) the first period (1985-1993) and (c) the last period (2012-2020) corresponding to the different clusters identified by the spatially constrained clustering algorithm performed on a 30 km grid over the Cerrado. Plots (b) and (d) present, for each period respectively, the first two axes (PC1_fire and PC2_fire) resulting from the Principal Component Analysis performed on the six fire variables (PCA_fire): the median and 99th percentile fire sizes, the burned area and the number of fires, the 99th percentile of the fire frequency distribution, and the median (peak) of the fire season. Each point in the PCAs represents a 30 km grid cell in the period coloured depending on the fire regime region it was classified into. Overall, in both periods, the PC1_fire captures a gradient of fire activity (see Results) and the fire regime regions appear ordered along this axis. In the first period, five different fire regime regions were identified: one in the north characterised by small numerous fires and a later peak of the fire season (LS_P1), a region in the centre-west with comparatively higher fire activity (HFA_P1), another region in the centre-east with intermediate fire activity (IFA_P1), and two regions with lower fire activity, one in the south (sLFA_P1) and another one in the western-most tip of the Cerrado (wLFA_P1). In the fourth and last period, three regions were identified: one in the north presenting a later peak of the fire season (LS_P4), one in the centre with higher fire activity (HFA_P4), and another one in the south with comparatively lower fire activity (LFA_P4). Note that even though the same colour scheme was used in both periods to denote analogous fire regime regions, neither the geographical limits nor the overall fire characteristics of the equally-coloured fire regime regions between periods are necessarily the same.

different clusters of grid cells located in a certain area of the Cerrado) for each 9-year period: five regions for the first period (1985-1993), and three regions for the following three periods (1994-2002, 2003-2011, 2012-2020) (Figure 4.1 and Supplementary Information, Figure S8).

Focusing on the first (1985-1993) and last (2012-2020) periods, the PCA_fire in these two periods (Figures 4.1 b and d, and Supplementary Information, Table S1) showed a similar composition of the first and second axes (PC1_fire and PC2_fire respectively) in terms of fire variables, and a similar proportion of the variance described (88.9% and 87.9 in the first and last periods respectively). In both periods, burned area, fire frequency, largest fire size, and the number of fires contributed the most, and in the same direction, to PC1_fire. Regarding PC2_fire, it was the peak of the fire season and the number of fires in one direction, and the median fire size in the opposite direction, that contributed the most. Further, even though the contribution of the 99th percentile fire size to PC2_fire was weaker than the three aforementioned variables, it did so in the same direction of the median fire sizes, and opposite direction to the number of fires. This opposite direction between the size and the number of fires indicated a trade-off between these two variables of fires, even though we still observed some cells with simultaneously large and rather numerous fires.

In both periods, the clusters appeared ordered along PC1_fire indicating that, overall, cells with high levels of burned area, also had high levels of fire frequency, fire size or number of fires, and vice versa for cells with low and intermediate values (Figure 4.1). That is, cells with similar overall low, intermediate or high levels of the various variables were generally classified as part of the same fire regime region. Therefore, the PC1_fire captured a gradient of increasing fire activity, and the level of fire activity (PC1_fire) was the main factor differentiating the different clusters.

In the first period (1985-1993), the clustering algorithm delineated a fire regime region whose grid cells presented the highest fire activity levels (henceforth HFA_P1) overall when compared to the other four regions. This HFA_P1 cluster was the largest region delineated in the first period (occupying 38% of the Cerrado), located in the west of the

Cerrado and spanning a large latitudinal range. East of this region, the algorithm identified a fire regime region that also covered a large latitudinal variation and presented intermediate values for all fire characteristics (intermediate fire activity, IFA_P1). The algorithm identified two clusters with low fire activity when compared to the other fire regime regions, one located in the southern-most part of the Cerrado (sLFA_P1) and another located in the western-most tip of the Cerrado (wLFA_P1) - the smallest region identified in the first period. Finally, the last fire regime region delineated was located in the northern-most part of the Cerrado, standing out for presenting small but numerous fires and, particularly, a later peak of the fire season - the month when most fires occur - compared to the other regions (late season region, LS_P1). Particularly, most fires in the LS_P1 fire regime region took place between October and November, while the peak of the fire season for the other clusters took place between August and September (Supplementary Figure S2 f).

In the fourth and last period (2012-2020), the algorithm identified again a fire regime region with overall higher fire activity (HFA_P4) when compared to the other fire regime regions, located in the central part of the Cerrado. In addition, the algorithm identified a region in the south with overall lower levels of fire activity (LFA_P4), except for a set of cells showing some of the largest fires (highlighted in blue in Figures 4.1 c and d). In this last period, however, this low fire activity region was much larger than in the first period, spanning 59.5% of the Cerrado. Finally, there was only one fire regime region that persisted from the first period presenting, again, overall high number of fires and a later peak of the fire season (late season region, LS_P4). In this last period, however, the size of the largest fires observed in LS_P4 were larger than those in LS_P1, and comparable in size to HFA_P4 (Figure 4.1 d). Again, while the peak of the fire season of grid cells in LS_P4 took place in October and November; the peak of the fire season for the other two regions was between August and September (Supplementary Figure S2 f).

Finally, we also explored the relative importance of the peak of the fire season when delineating the fire regime regions by excluding this variable from the clustering. Even when not including the peak of the fire season, the fire regime region in the north was still

delineated in the first period (Supplementary Information, Figure S9 a and b), while in the last period it was classified as part of the high fire activity region but still presented a distinctive combination of fire characteristics in comparison to other grid cells in the same fire regime region (Supplementary Information, Figure S9 c and d).

4.4.2 Environmental characteristics of the fire regime regions

Exploring the climatic characteristics and the level of human activities of the different regions, both PCA_clim and PCA_anth revealed that the fire regime regions obtained independently through the clustering algorithm appeared well separated by each set of explanatory variables in each period (Figure 4.2), indicating that the variation in these variables shared geographical structure with that of the fire variables. Further, we evaluated the ability of the explanatory variables to classify the fire clusters running a Random Forests algorithm. The classification accuracy was very high in both periods for both the sets of anthropic (81.7 [78.1 84.9]% and 82.3 [79.3, 85.9]%, both with 95% confidence interval, CI) and climatic (82.3 [78.7, 85.4]% and 90.0 [87.1, 92.4]%, 95% CI) variables (Supplementary Information, Table S2). This accuracy was even higher when using both sets of variables together (88.7 [85.9, 91.2] % and 94.0 [91.8 and 95.8] % in each period respectively, 95% CI).

Regarding the PCA_anth, in both periods PC1_anth was contributed primarily by the percentage of anthropic area, and the livestock and human population densities, all pointing in the same direction (Figures 4.2 a and b, and Supplementary Information, Table S4). Therefore, this axis seemed to capture the variation in the level of anthropic presence and activities in the landscape. Moreover, the clusters appeared aligned along this gradient. In the first period, region sLFA_P1 in the south presented the highest levels of anthropic activity, followed by regions IFA_P1 in the centre-east, LS_P1 in the north, and part of cluster HFA_P1 in the centre-west; while region wLFA_P1 in the western-most tip of the Cerrado and most of region HFA_P1 presented the lowest levels of anthropic presence (Figure 4.2 a). In the last period, the region LFA_P4 in the south had the highest levels of anthropic presence, followed by regions LS_P4 in the north and HFA_P4 in the centre,

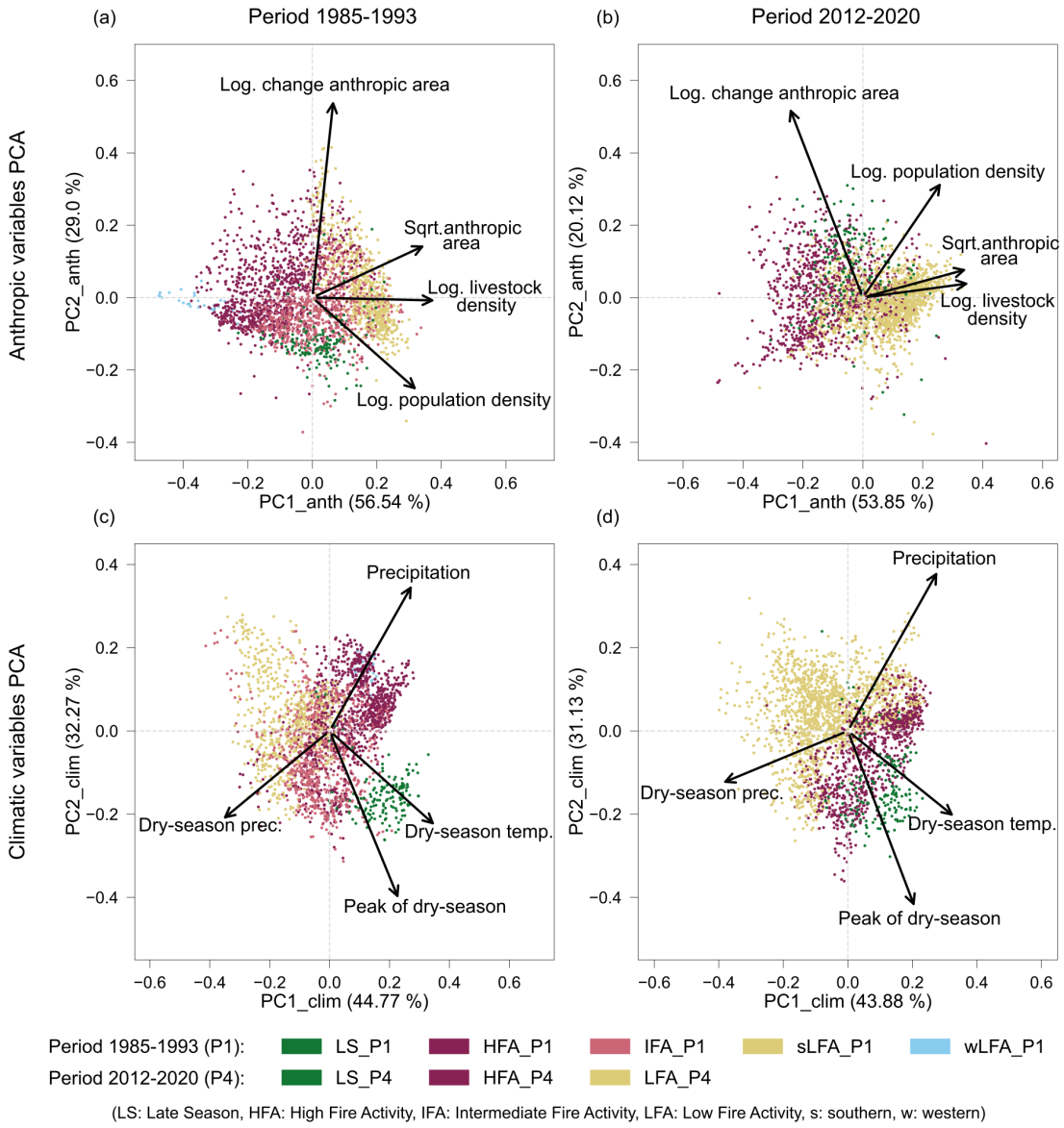

Figure 4.2: The two major axes of variation obtained from the PCA performed on each set of explanatory variables, anthropic and climatic variables. The anthropic variables (PCA_anth) used in the first (a) and last periods (b) were anthropic area percentage, livestock density, population density, and change in anthropic area percentage within the period. The climatic variables (PCA_clim) used in the first (c) and last (d) periods were the total annual precipitation, total precipitation in the dry season, average temperature in the dry season, and peak of the dry season. Points represent a 30 km grid cell in the corresponding period coloured according to the fire regime region they were classified into (see Figure 4.1). Note that even though the same colour scheme was used in both periods to denote analogous fire regime regions, neither the geographical limits nor the overall nor the fire, anthropic or climatic characteristics of the equally-coloured fire regime regions are necessarily the same.

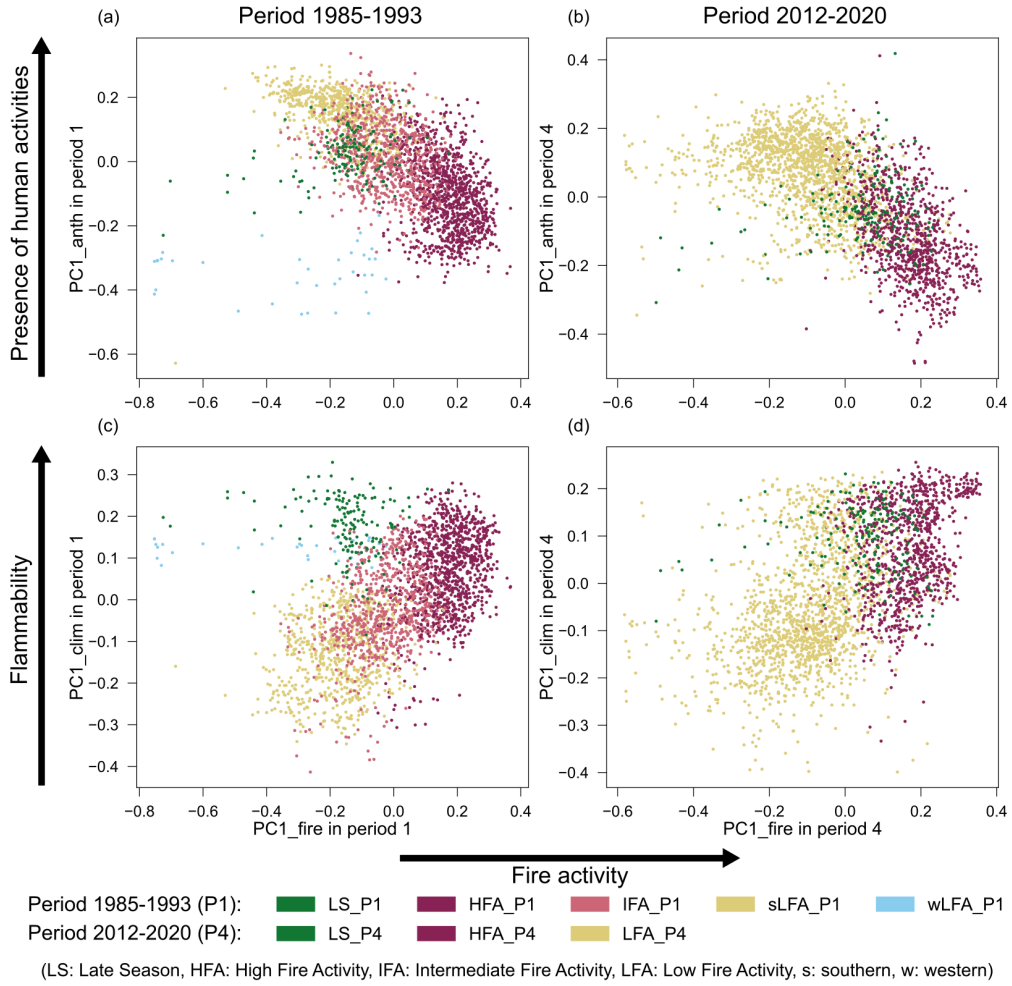

Figure 4.3: Relation between the first component of the PCA performed on the anthropic variables (PC1_anth), (a) and (b) in the first and last periods respectively, or the climatic variables (PC1_clim), (c) and (d) in each period respectively, and the first component of the PCA performed on the fire variables (PC1_fire). PC1_fire in each period represents a gradient of increase in burned area, frequency, and the size and number of fires (Figure 4.1 a, Supplementary Information, Table S1), capturing a gradient of fire activity. PC1_anth in both periods represents a gradient of increase in anthropic area, population and livestock density (Figures 4.2 a and b, Supplementary Information, Table S4), that is, an increase in the presence of human activities and land use area in the landscape. Finally, PC1_clim represents a gradient of flammability conditions, with an increase in dry season temperature and in annual precipitation (contributing to vegetation growth (Krawchuk et al., 2011; Pausas and Ribeiro, 2013)), and a decrease in dry season precipitation, when most fires occur (Silva, Bastos, Libonati, et al., 2019) (Figures 4.2 c and d, Supplementary Information, Table S6). Points represent a 30 km grid cell in the corresponding period coloured according to the fire regime region they were classified into (see Figure 4.1). Note that even though the same colour scheme was used in both periods to denote analogous fire regime regions, neither the geographical limits, nor the fire, anthropic or climatic characteristics of the equally-coloured fire regime regions are necessarily the same.

in opposite order to the gradient of fire activity of these regions (Figure 4.2 b). In both periods, the change in anthropic area within the period was the variable that contributed the most to PC2_anth.

Considering the PCA_clim, both in the first and last periods the dry season temperature and mean annual precipitation in one direction, and the dry season precipitation in the opposite, contributed the most to PC1_clim, while the peak of the dry season contributed the most to PC2_clim (Figures 4.2 c and d, and Supplementary Information, Table S6). In this case, PC1_clim seemed to capture a gradient of availability of fuel and suitability of conditions to burn, that is, the flammability: hotter and drier climate in the dry season, when most of the fires occur (Silva, Bastos, Libonati, et al., 2019); and amount of annual precipitation, which contributes to vegetation growth (Krawchuk et al., 2011; Pausas and Ribeiro, 2013). In this case, however, the clusters aligned along the direction of dry season temperature - hence following the latitudinal gradient -, and less perfectly along the flammability gradient (PC1_clim). Finally, in both periods, the northern regions LS_P1 and LS_P4 presented a later peak of the dry season than the other regions.

Lastly, since the PC1 axes represented environmental gradients, we looked at their relation with the fire activity gradient (Figure 4.3). On the one hand, PC1_anth and PC1_fire were inversely related: as the presence of humans and their activities in the landscape decreased (lower PC1_anth), fire activity increased (higher PC1_fire) for all clusters in both periods (Figures 4.3 a and b). The only exception to this relation were region wLFA_P1 and some cells in the northern region LS_P1 that presented a lower fire activity than other cells with the same level of human presence. On the other hand, PC1_clim and PC1_fire were directly related: as the flammability increased (higher PC1_clim), fire activity also increased in both periods (Figures 4.3 c and d). Again, most cells in regions wLFA_P1 and LS_P1 presented lower fire activity than those cells in region HFA_P1 with similar flammability scores.

These negative and positive correlations with fire activity of human presence and flammability respectively were further confirmed when modelling the correlations of each set of explanatory variables with the fire variables using a redundancy analysis approach

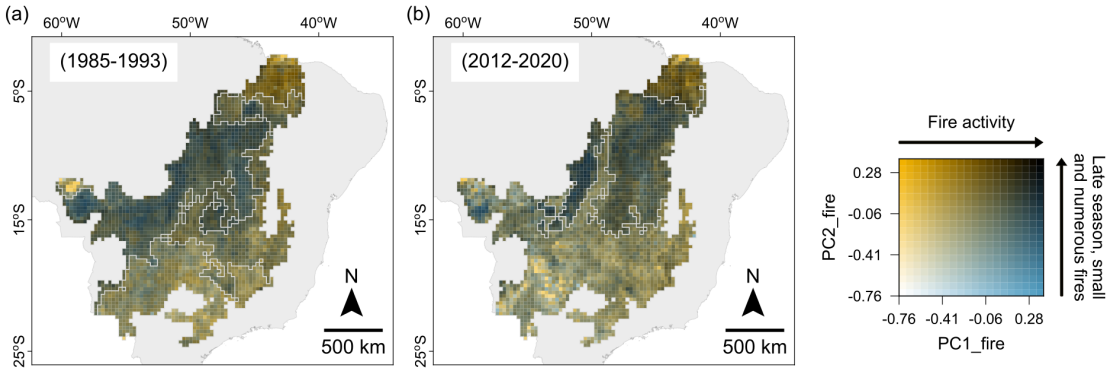

Figure 4.4: Bivariate maps showing the PCA_fire coordinates of each 30 km grid cell in the first and last periods projected on the PCA_fire-space obtained for the first period PCA_fire. Map (a) shows the PCA_fire scores directly obtained from the fire variables in the first period (1985-1993). Map (b) shows the projection of the fire variables of the last period (2012-2020) on the PCA_fire-space of the first period. In this manner, the fire regimes (6-dimensional) are summarised into two dimensions, and the values of the grid cells in each period can be compared. PC1_fire (x-axis of the colour map) represents an increase in fire activity (larger burned area, frequency, and larger fire sizes) from white to blue, while PC2_fire (y-axis) represents the direction of a later fire season, an increase in the number of fires and a decrease in median fire size from white to yellow.

(r^2_{adj}=0.316, 0.305 for anthropic and r^2_{adj}=0.242, 0.305 for climatic variables in each period respectively, and p-value<0.001 for all variables and cases; Supplementary Information, Figure S6 and Tables S5 and S7). These models further revealed that precipitation was only weakly correlated with the fire variables, and that there was a strong correlation between the peak of the dry season and that of the fire season (Supplementary Information, Figures S6 c and d, and Table S7).

4.4.3 Changes of fire regime regions over time

Between the first (1985-1993) and last (2012-2020) periods, there was a reduction in the number and a change in the shape of the fire regime regions (Figures 4.1 and 4.4). Moreover, the last period clusters were formed by grid cells coming from a mix of different first-period regions (Figure 4.4).

Apart from these geographical changes, the fire characteristics of the individual grid cells also changed over time. In particular, there were increases and decreases in fire activ-

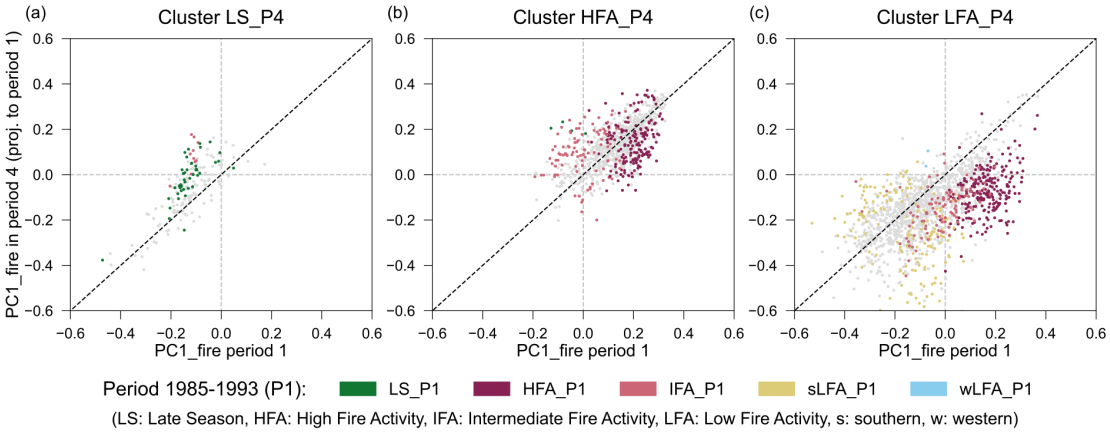

Figure 4.5: Relation between PC1_fire obtained in the first period, 1985-1993, (x-axis), and the projection of PC1_fire obtained for the last period, 2012-2020, projected on the PCA_fire of the first period (y-axis). (a) subset of 30 km grid cells classified into the northern fire regime region in the last period with small numerous fires and a later peak of the fire season, LS_P4; (b) subset of grid cells classified into the high fire activity region of the last period, in the centre of the Cerrado, HFA_P4; and (c) cells classified into the lower fire activity region of the last period, in the south, LFA_P4. Points represent 30 km grid cells and are coloured depending on the fire regime region they were classified into in the first period if they present clear trends in time in PC1_fire (with 80% confidence interval), or coloured in grey if they do not present clear trends in time. The dashed black lines represent the one-on-one correspondence between PC1_fire in the first period and the projection of PC1_fire in the last. Thus, points above the dashed black line represent an increase in fire activity over time, while data points below the line represent a decrease. Dashed gray lines represent the 0 values of PC1_fire and are included for reference.

ity heterogeneously distributed across the Cerrado (the PC1_fire score, Figure 4.5 and Supplementary Information, Figure S7). Thus, even though the fire regime regions were organised along a gradient of fire activity in both periods, the levels of high fire activity of region HFA_P1 and low levels of regions sLFA_P1 and wLFA_P1 in the first period, did not perfectly correspond to the levels of high fire activity of region HFA_P4 and low fire activity of region LFA_P4 in the last period (Figures 4.5 b and c). Furthermore, the last period clusters were not the result of unidirectional changes, but rather the result of changes in different directions of each of the different fire variables (Figure 4.6).

Clusters LS_P1 and LS_P4 in the north comprise the only region whose geographical shape and location did not substantially change between periods, and maintained its unique attribute of a later fire season peak. Regarding fire activity, however, 29% of

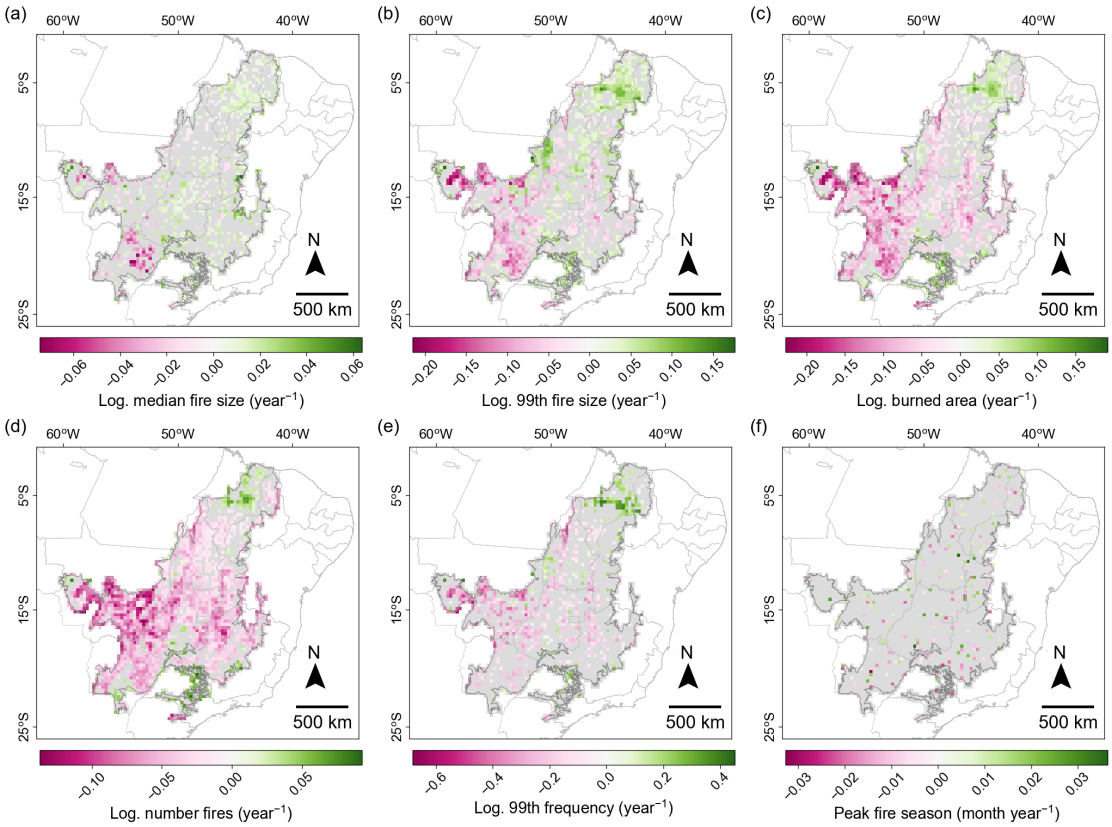

Figure 4.6: Trends in time (slope coefficients) obtained by fitting a linear regression (using Ordinary Least Squares) to the time series of each of the six fire variables, for each 30 km grid cell over the Cerrado. Plots show the median fire size (a), the 99th percentile fire size (b), burned area (c), the number of fires (d), and the median fire season (f). The time series for these five variables comprised the annual values for each year in the period 1985-2020. The time series for the 99th percentile of the fire frequency distribution (e) comprised the frequency value in each of the four periods, since this value expresses the largest number of times the pixels in a cell burned in 9 years. Pink indicates decreases in the fire variable over time, green indicates increases, and grey indicates no clear trends in time with 80% confidence interval.

its area experienced an increase in fire activity over the study period (Figure 4.5 a). On the other hand, region HFA_P4 in the centre of the Cerrado - with the highest levels of fire activity in the last period - was composed of cells showing increases (14.3% of its area) and decreases (15.9%) in fire activity over time (Figure 4.5 b). However, these decreases were limited and remained mostly within the range of activity of cluster HFA_P1 (around a minimum value of 0 in the PC1_fire, Figure 4.5 b). Regarding region LFA_P4 in the south - the cluster with lowest fire activity in the last period -, 27.1% of its cells experienced decreases in fire activity (Figure 4.5 c) over the study period. Most of its cells transitioned from clusters HFA_P1 and IFA_P1 - initially with high and intermediate fire activity - experiencing mild to strong decreases in fire activity (47.9% and 22.8% of each cluster respectively), while 16.9% of the cells transitioning from region sLFA_P1 - already with low levels of fire activity - experienced further reductions.

4.5 Discussion

In this study, we identified the regions of the Cerrado presenting different fire regimes, the fire regime regions, using a hierarchical clustering algorithm with a spatial contiguity constraint in each of four 9-year periods between 1985 and 2020. We identified five fire regime regions in the first period, 1985 to 1993, and three fire regime regions in the last period, 2012 to 2020, and in the two periods in-between (Figure 4.1 and Supplementary Information, Figure S8). These regions reflect the spatial patterns of fire across the Cerrado and allowed us to explore how its fire regimes have changed over time. We found considerable differences in the geographical shape of the fire regime regions between the first and last periods, as well as in the fire characteristics of the individual 30 km grid cells that form the different regions (Figures 4.4 and 4.5).

In each period, the fires regime regions of the Cerrado were primarily differentiated by their level of fire activity, from low fire activity - that is, with overall infrequent, small, and non-numerous fires - to high fire activity - with overall frequent, large, and numerous fires - (Figures 4.1 b and c). This gradient of fire activity was captured by the first component

of the PCA performed on the six fire variables (PCA_fire), along which the fire regime regions appear ordered (Figure 4.1). Therefore, the primary feature differentiating the fire regimes of the Cerrado is their overall level of fire activity, prevailing over other differences in fire characteristics, in agreement with previous studies characterising the fire regimes of the Cerrado (Silva, Nogueira, et al., 2021). Still, we observed a certain trade-off between the size and the number of fires (Figures 4.1 b and d), indicating that the grid cells with the largest fires did not experience the highest numbers of fires, and vice versa. The trade-off between these two variables of fire is related to the fact that when a large fire occurs, it consumes a large portion of the landscape's fuel bed, thus inevitably hampering the occurrence of other fires in the same period and limiting the overall number of fires, as reported in previous studies (Conciani et al., 2021; Batista et al., 2018; Alvarado et al., 2018; Fidelis et al., 2018).

The Cerrado is very heterogeneous in terms of vegetation (Ribeiro and Walter, 2008; Klink et al., 2005), topography and soil composition (Sano, Rodrigues, et al., 2019), climate (Nascimento et al., 2020), hydrology (Oliveira et al., 2014), and land use area (Souza et al., 2020). Based on these factors, different ecoregions have been described in the Cerrado (Sano, Rodrigues, et al., 2019), and their patterns of fire subsequently quantified (Silva, Nogueira, et al., 2021). Because these factors affect the patterns of fire (Archibald, Roy, et al., 2009), we could expect some similarities between the fire regimes of these ecoregions (Silva, Nogueira, et al., 2021) and the fire regime regions identified here. Even though neither the number nor the overall geographical shape of the ecoregions (Supplementary Information, Figure S10) corresponds to those of the fire regime regions identified (Figure 4.1), we did find some similarities. For example, the ecoregions located in the centre of the Cerrado were found to present large burned area and fire sizes overall (Silva, Nogueira, et al., 2021), in agreement with the high and intermediate fire activity regions identified here (Figure 4.1). In particular, the Bananal ecoregion in the centre-west of the Cerrado (Supplementary Information, Figure S10, (Sano, Rodrigues, et al., 2019)) appears clearly delineated as part of the high fire activity region of the last period (HFA_P4), presenting some of the highest levels of fire activity (Figure 4.4), in

accordance with this ecoregion's fire regimes (Silva, Nogueira, et al., 2021; Silva Arruda et al., 2024). Similarly, the ecoregion Chapadão do São Francisco (Supplementary Information, Figure S10, (Sano, Rodrigues, et al., 2019)), characterised with large burned areas and fire sizes (Silva, Nogueira, et al., 2021), can also be recognised as part of the high fire activity region of the first period (HFA_P1).

We did find, however, a remarkable difference between our fire regime regions and the ecoregions located in the south-west of the Cerrado, comprising the states of Mato Grosso and Mato Grosso do Sul (Supplementary Information, Figure S10). The ecoregion covering this area, Paraná Guimarães (Supplementary Information, Figure S10, (Sano, Rodrigues, et al., 2019)), was classified as having intermediate levels of burned area and big fires in the period 2001-2019 (Silva, Nogueira, et al., 2021). However, we observed the lowest levels of fire activity in the period 2012-2020 precisely within this area (LFA_P4, Figure 4.4). This difference in the level of fire activity could be related to the fact that the Paraná Guimarães ecoregion includes part of the high fire activity region (HFA_P4) identified here, which could be contributing to the higher burned area and larger fire sizes reported for the whole ecoregion (Silva, Nogueira, et al., 2021). This highlights the relevance of exploring patterns of fire at different scales, as it can reveal different processes and dynamics (Krawchuk et al., 2011).

The fire regime regions we identified are overall large and somewhat heterogeneous in the fire characteristics of their grid cells (Figure 4.4). For example, we observed the subregion of large fires located within the low fire activity region of the last period (LFA_P4, highlighted in blue in Figures 4.1 c and d). Hierarchical clustering algorithms with a spatial contiguity constraint generate solutions (i.e. classifications for different numbers of clusters) by grouping together grid cells and clusters consecutively only if they are spatially contiguous (Borcard et al., 2011; Guénard et al., 2022). Here, we focused on the first optimal clustering classification of the data, which we found to discriminate generally large fire regime regions primarily in relation to their level of fire activity. However, there could be further statistically relevant clustering solutions delineating clusters at smaller scales (Lambiotte et al., 2014), which could uncover further patterns of fire regimes per-

haps recovering some of the Cerrado's ecoregions, opening an avenue for future studies of the Cerrado's fire regimes.

In terms of the two major drivers of fire, humans and the climate (Archibald, 2016; Archibald, Scholes, et al., 2010; Hantson, Pueyo, et al., 2015), both the anthropic and the climatic variables have high classification accuracy of the fire characteristics (Supplementary Information, Table S2), as expected (Bowman, Balch, et al., 2009; Archibald, Roy, et al., 2009). We found that the fire regime regions appear distributed along the first axis of the PCA performed on the anthropic variables (PC1_anth, Figures 4.2 a and b), which indicates a gradient of increasing presence of human activities. This anthropic presence is particularly associated with agriculture - land use area and livestock density - and, to a lesser extent, with population density (Figure 4.2 a). Importantly, we observe that as anthropic presence increases, fire activity decreases (Figure 4.3), in agreement with previous studies relating the expansion of land use area and fragmentation in savannas with decreases in burned area (Silva, Nogueira, et al., 2021; Segura-Garcia et al., 2024; Silva Arruda et al., 2024; Archibald, Scholes, et al., 2010; Andela, Morton, et al., 2017; Andela and Werf, 2014).

Indeed, both land use area and livestock grazing are associated with smaller fires and reduced burned area as they create fuel discontinuities through landscape fragmentation (Hantson, Pueyo, et al., 2015; Archibald, Roy, et al., 2009) and diminishing fuel loads (Archibald, Staver, et al., 2012; Eloy et al., 2019). Population density, however, has a more intricate relation with fire activity as humans can ignite fires in higher or smaller numbers (Hantson, Pueyo, et al., 2015; Archibald, Roy, et al., 2009), but they can also limit fire activity through fire suppression efforts (Archibald, 2016; Archibald, Staver, et al., 2012) - a widespread practice in the Cerrado (Durigan, 2020; Durigan and Ratter, 2016; Fidelis et al., 2018). On the other hand, we observed the highest level of fire activity in the areas of the Cerrado with larger remnants of native vegetation (Supplementary Information, Figures S2 and S3), in agreement with previous studies (Mataveli et al., 2018; Silva, Nogueira, et al., 2021; Segura-Garcia et al., 2024; Silva Arruda et al., 2024). These dynamics in the more intact areas of the Cerrado may result from a confluence of

factors comprising human-started fires escaping from nearby agricultural lands into native vegetation (Pivello, 2011) and the timing of ignitions in the dry season (Pivello, 2011), when the fuel bed of native vegetation is more flammable and effectively more continuous (Zanzarini et al., 2022).

The western fire regime region in the first period (wLFA_P1) is, however, an exception to the inverse relation between the gradient of human presence and that of fire activity (Figure 4.1 a and b). This fire regime region simultaneously presents both the lowest fire activity levels and the lowest presence of human activities in this period (Figures 4.1 b and 4.2 a). The low fire activity of this region could be the result of a vegetation composition closer to that of the Amazon tropical rainforest, where natural fires are extremely rare (Barlow et al., 2020; Rosan et al., 2022) due to moister conditions and a closed canopy with scant surface fuels, particularly when human presence is low. The contrast in terms of human presence between this region and the other low fire activity region in the same period (sLFA_P1) also shows how areas with different landscape characteristics can present similar fire regimes (Archibald, Lehmann, Gómez-Dans, et al., 2013).

The distribution of the fire regime regions on the PCA_clim seems to reflect their geographical location, as they appear ordered along the latitudinal gradient of temperature (Nascimento et al., 2020), with the northern regions (LS_P1 and LS_P4) presenting the hottest values, and the southern regions (sLFA_P1 and LFA_P4) presenting the lowest values (Figures 4.2 c and d). Perpendicularly, the fire regime regions appear organised along the direction of increase in annual precipitation from east to west (Nascimento et al., 2020). For example, in the first period, the intermediate fire activity (IFA_P1) in the east presents lower annual precipitation than the high fire activity (HFA_P1) and the western low fire activity (wLFA_P1) regions. Still, the first axis of the PCA_clim captures a gradient of climatic flammability conditions (Figures 4.2 c and d), which is positively related with fire activity (Figures 4.3 c and d). That is, fire activity increases with drier and hotter conditions in the dry season as expected - when most fires occur (Mataveli et al., 2018; Silva, Bastos, Libonati, et al., 2019) -(Silva, Rodrigues, et al., 2020; Silva, Bastos, Libonati, et al., 2019; Westerling et al., 2006; Flannigan et al., 2013), as well as

with greater annual precipitation, which contributes to productivity during the growing season (Pausas and Ribeiro, 2013) and fuel load (Krawchuk et al., 2011). However, we observed that, comparing cells with similar high climatic flammability values, some cells with high presence of anthropic activities in the last period (region LFA_P4) have lower fire activity than cells with low anthropic activity levels (region HFA_P4), suggesting an interaction between humans and climate. Indeed, it has been demonstrated that the effect of the climate on fire is subject to the level of anthropic presence in savannas (Conciani et al., 2021; Segura-Garcia et al., 2024; Andela and Werf, 2014).

Only one fire regime region was consistently identified in each period (LS_P1 and LS_P4, Figure 4.1 and Supplementary Information, Figure S8) presenting a later peak of the fire season. In addition, this area presents small but numerous fires, which makes this region stand out even when excluding the peak of the fire season from the clustering analysis (Supplementary Information, Figure S9). That is, this region's fire regimes are distinct from those of the other fire regime regions and not merely shifted in time. A number of factors may explain the particularities of this region's fire regimes. First, this area comprises the Floresta de Cocais and Costeiro ecoregions (Supplementary Information, Figure S10, (Sano, Rodrigues, et al., 2019)), which is noteworthy for being an ecological transition region between tropical dry forest, rainforest and savanna (Sano, Rosa, et al., 2010) composed primarily of broadleaf tree species (Oliveira-Filho, 2017) and palm trees (Sano, Rodrigues, et al., 2019). In fact, in early versions of the Cerrado's geographical limits, this area was not fully included and was classified instead as either a mix of Amazon and Cerrado (IBGE, 1993) or as dry broadleaf forest (Olson et al., 2001). Second, this area also presents unique climatic characteristics as it is affected by the Intertropical Convergence Zone, which carries air moisture from the Atlantic towards the Amazon rainforest (Nascimento et al., 2020), and presents an overall later peak of the dry season (Figure 4.2). Third, in terms of human presence, this area presents a number of municipalities with high densities of *quilombola* population (IBGE, 2023), communities of people with African descent (IBGE, 2023) who traditionally use fire to renew native pastures or as part of shifting cultivation practices, among other uses (Eloy et al., 2019). Finally, this

area is found within the Matopiba region, considered the Cerrado's current agricultural frontier and where land conversion has been more widespread in recent years (Spera et al., 2016; Silva, Rodrigues, et al., 2020; Teixeira Pitta et al., 2017).

We observed opposing trends over time in fire activity across the Cerrado (Figure 4.5), in agreement with previous studies (Silva, Nogueira, et al., 2021; Segura-Garcia et al., 2024). In the northern half of the Cerrado, comprising the Matopiba - encompassing regions LS_P4 and HFA_P4 -, we observed the largest concentration of increases in fire activity. The surges in fire activity of these regions could be the result of the use of fire in land conversion and as part of modern agricultural practices (Klink et al., 2005; Pivello, 2011) alongside large native vegetation remnants with little fuel discontinuities, and in the context of climate change. On the other hand, the southern half of the Cerrado mostly experienced decreases in fire activity. Such reduction was particularly striking in the state of Mato Grosso (Supplementary Information, Figures S7 and S10), in agreement with previous studies (Silva, Nogueira, et al., 2021; Silva Arruda et al., 2024), which has undergone extensive Cerrado vegetation fragmentation due to conversion to pastures and croplands in the 1990s and early 2000s (Rocha et al., 2012; Alencar, Z. Shimbo, et al., 2020). Further, the shape of the low fire activity region in the southern half of the Cerrado in the last period (LFA_P4) clearly reflects the geographical patterns of anthropic land uses (Alencar, Z. Shimbo, et al., 2020), highlighting the depth of the footprint of land use area on the Cerrado's fire regimes.

Finally, between 1985 and 2020, many aspects of the fire management policies across Brazil have changed. Indeed, at the beginning of the study period, the use of fire had been banned by successive laws since colonial times (Pivello et al., 2021), further supported by misunderstandings about the ecology of fire-adapted ecosystems and the occurrence of destructive fires in iconic fire-sensitive ecosystems. In the late 1990s, however, there was a shift in the discussion as fire started to be recognised as a disturbance agent that could promote and sustain Cerrado biodiversity (Durigan, 2020). There was hence a push to (re)introduce fires into protected areas, which eventually translated into fire policy changes (Pivello et al., 2021). Indeed, the 2012 New Forest Code contemplated the use

of fire in fire-adapted ecosystems for ecological and cultural purposes. Therefore, part of the increase in fire activity that we observe in certain areas of the Cerrado could be related to the use of prescribed fires as a management tool. However, prescribed burns are usually performed in the early dry season (Schmidt et al., 2020; Batista et al., 2018), while most Cerrado fires currently occur later in the dry season (Silva Arruda et al., 2024), indicating that other uses of fire may still prevail. In this sense, the recently approved Brazilian National Policy on Integrated Fire Management (IFM) is a promising avenue for Cerrado conservation, as these practices are demonstrating to be an effective tool in Cerrado conservation and preventing more extreme fire behaviour (Schmidt et al., 2020; Fidelis et al., 2018).

4.6 Conclusion

Our findings indicate that the main factor differentiating Cerrado's fire regime regions is the level of fire activity, which is inversely related to the extent of modern human presence in the landscape. On the one hand, we report that recent agricultural expansion and fragmentation have profound effects on the Cerrado's fire regimes by primarily diminishing fire activity. Indeed, high livestock densities, modern mechanised agricultural practices and croplands such as soybean plantations where fire use is limited now occupy large areas of the Cerrado. On the other hand, climate change could be setting the stage for increased fire sizes and frequency in areas where most native vegetation remains. Therefore, both agricultural expansion and climate change could impact Cerrado's vegetation and contribute to its homogenization and loss of biodiversity, highlighting the profound multi-faceted effects of large-scale Cerrado native vegetation loss. Future research efforts should be allocated to decipher the variation in fire patterns at finer spatial scales, as well as establishing in more detail the causal relations between the different drivers and specific fire characteristics. This knowledge about the Cerrado's fire regimes is essential to develop meaningful policies aimed at conserving this unique biome in the context of global change.

4.7 Data and code availability statement

The climate data used in this study are publicly available from ERA5-Land Monthly Averaged at https://doi.org/10.5194/essd-13-4349-2021, the Climate Hazards Group InfraRed Precipitation with Station data version 2.0 at https://doi.org/10.1038/sdata.2015.66, and TerraClimate at https://doi.org/10.1038/sdata.2017.191. The land use data are publicly available from MapBiomas collection 8.0 at https://doi.org/10.3390/rs12172735. The burned area data are publicly available from MapBiomas Fogo Collection 2.0 at https://doi.org/10.3390/rs14112510. Livestock density data for Brazil is available at https://sidra.ibge.gov.br/tabela/3939 and population density of Brazil https://www.ibge.gov.br/estatisticas/sociais/populacao/9103-estimativas-de-populacao.html. The processed data (including the custom fire polygons created from MapBiomas Fogo Collection 8.0) and custom code are available at https://doi.org/10.5281/zenodo.14025420.

4.8 Acknowledgements

We thank the Ecosystems Lab Group at the Environmental Change Institute, School of Geography and the Environment, University of Oxford, and the Science Team at the Instituto de Pesquisa Ambiental da Amazônia (IPAM), Brazil, for helpful feedback during discussions. We thank Prof. Emilio Chuvieco, Dr Blas Kolic and Francisco Navarro-Rosales for their comments and suggestions. We would like to thank the reviewers for providing useful feedback to improve the readability and content of the manuscript.

4.9 References

Abatzoglou, John T. et al. (2018). "TerraClimate, a high-resolution global dataset of monthly climate and climatic water balance from 1958–2015". In: *Scientific Data* 5.1, p. 170191.

Alencar, Ane, Julia Z. Shimbo, et al. (2020). "Mapping Three Decades of Changes in the Brazilian Savanna Native Vegetation Using Landsat Data Processed in the Google Earth Engine Platform". In: *Remote Sensing* 12.6, p. 924.

Alencar, Ane A. C., Vera L. S. Arruda, et al. (2022). “Long-Term Landsat-Based Monthly Burned Area Dataset for the Brazilian Biomes Using Deep Learning”. In: *Remote Sensing* 14.11, p. 2510.

Alvarado, Swanni T., Thiago Sanna Freire Silva, and Sally Archibald (2018). “Management impacts on fire occurrence: A comparison of fire regimes of African and South American tropical savannas in different protected areas”. In: *Journal of Environmental Management* 218, pp. 79–87.

Andela, N., D. C. Morton, et al. (2017). “A human-driven decline in global burned area”. In: *Science* 356.6345, pp. 1356–1362.

Andela, Niels and Guido R. van der Werf (2014). “Recent trends in African fires driven by cropland expansion and El Niño to La Niña transition”. In: *Nature Climate Change* 4.9, pp. 791–795.

Archibald, S, C E R Lehmann, C M Belcher, et al. (2018). “Biological and geophysical feedbacks with fire in the Earth system”. In: *Environmental Research Letters* 13.3, p. 033003.

Archibald, S., R. J. Scholes, et al. (2010). “Southern African fire regimes as revealed by remote sensing”. In: *International Journal of Wildland Fire* 19.7, p. 861.

Archibald, Sally (2016). “Managing the human component of fire regimes: lessons from Africa”. In: *Philosophical Transactions of the Royal Society B: Biological Sciences* 371.1696, p. 20150346.

Archibald, Sally, Caroline E. R. Lehmann, Jose L. Gómez-Dans, et al. (2013). “Defining pyromes and global syndromes of fire regimes”. In: *Proceedings of the National Academy of Sciences* 110.16, pp. 6442–6447.

Archibald, Sally, David P. Roy, et al. (2009). “What limits fire? An examination of drivers of burnt area in Southern Africa”. In: *Global Change Biology* 15.3, pp. 613–630.

Archibald, Sally, A. Carla Staver, and Simon A. Levin (2012). “Evolution of human-driven fire regimes in Africa”. In: *Proceedings of the National Academy of Sciences* 109.3, pp. 847–852.

Barlow, Jos et al. (2020). “Clarifying Amazonia’s burning crisis”. In: *Global Change Biology* 26.2, pp. 319–321.

Baston, Daniel (2020). “exactextractr: Fast extraction from raster datasets using polygons”. In: *R package version 0.5. 0*.

Batista, Eugênia Kelly Luciano et al. (2018). “An evaluation of contemporary savanna fire regimes in the Canastra National Park, Brazil: Outcomes of fire suppression policies”. In: *Journal of Environmental Management* 205, pp. 40–49.

Beer, Christian et al. (2010). “Terrestrial Gross Carbon Dioxide Uptake: Global Distribution and Covariation with Climate”. In: *Science* 329.5993, pp. 834–838.

Bond, W and J Keeley (2005). “Fire as a global ‘herbivore’: the ecology and evolution of flammable ecosystems”. In: *Trends in Ecology & Evolution* 20.7, pp. 387–394.

Bond, W. J., F. I. Woodward, and G. F. Midgley (2005). “The global distribution of ecosystems in a world without fire”. In: *New Phytologist* 165.2, pp. 525–538.

Bond, William J (2019). *Open ecosystems: ecology and evolution beyond the forest edge*. Oxford University Press.

Borcard, Daniel, François Gillet, Pierre Legendre, et al. (2011). *Numerical ecology with R*. Vol. 2. Springer.

Bosch, Martí (2019). "PyLandStats: An open-source Pythonic library to compute landscape metrics". In: *PloS one* 14.12. Publisher: Public Library of Science San Francisco, CA USA, e0225734.

Bowman, David M. J. S., Jennifer K. Balch, et al. (2009). "Fire in the Earth System". In: *Science* 324.5926, pp. 481–484.

Bowman, David M. J. S., Crystal A. Kolden, et al. (2020). "Vegetation fires in the Anthropocene". In: *Nature Reviews Earth & Environment* 1.10, pp. 500–515.

Breiman, L (2001). *Random forests Mach Learn 45 (1): 5–32*.

Burton, Chad, Sami Rifai, and Yadvinder Malhi (2018). "Inter-comparison and assessment of gridded climate products over tropical forests during the 2015/2016 El Niño". In: *Philosophical Transactions of the Royal Society B: Biological Sciences* 373.1760, p. 20170406.

Cattau, Megan et al. (2022). "Modern Pyromes: Biogeographical Patterns of Fire Characteristics across the Contiguous United States". In: *Fire* 5.4, p. 95.

Chuvieco, Emilio, Louis Giglio, and Chris Justice (2008). "Global characterization of fire activity: toward defining fire regimes from Earth observation data". In: *Global Change Biology* 14.7, pp. 1488–1502.

Conciani, Dhemerson E. et al. (2021). "Human-climate interactions shape fire regimes in the Cerrado of São Paulo state, Brazil". In: *Journal for Nature Conservation* 61, p. 126006.

De Albuquerque Prado, Licius, Fausto Miziara, and Manuel Eduardo Ferreira (2012). "Expansão de fronteira agrícola e mudanças no uso do solo na região sul de Goiás: ação antrópica e características naturais do espaço". In: *Boletim Goiano de Geografia* 32.1, pp. 151–165.

Dray, Stéphane et al. (2023). *adespatial: Multivariate Multiscale Spatial Analysis*. R package version 0.3-23.

Durigan, Giselda (2020). "Zero-fire: Not possible nor desirable in the Cerrado of Brazil". In: *Flora* 268, p. 151612.

Durigan, Giselda and James A. Ratter (2016). "The need for a consistent fire policy for Cerrado conservation". In: *Journal of Applied Ecology* 53.1. Ed. by Jeremy James, pp. 11–15.

Eloy, Ludivine et al. (2019). "Seasonal fire management by traditional cattle ranchers prevents the spread of wildfire in the Brazilian Cerrado". In: *Ambio* 48.8, pp. 890–899.

Estimativas da População do Instituto Brasileiro de Geografia e Estatística (n.d.). https://www.ibge.gov.br/estatisticas/sociais/populacao/9103-estimativas-de-populacao.html. Accessed: 2023-09-20.

Fidelis, Alessandra et al. (2018). "The Year 2017: Megafires and Management in the Cerrado". In: *Fire* 1.3, p. 49.

Flannigan, Mike et al. (2013). “Global wildland fire season severity in the 21st century”. In: *Forest Ecology and Management* 294, pp. 54–61.

Funk, Chris et al. (2015). “The climate hazards infrared precipitation with stations—a new environmental record for monitoring extremes”. In: *Scientific Data* 2.1, p. 150066.

Gillies, Sean et al. (2013). *Rasterio: geospatial raster I/O for Python programmers*. Mapbox.

Gorelick, Noel et al. (2017). “Google Earth Engine: Planetary-scale geospatial analysis for everyone”. In: *Remote sensing of Environment* 202. Publisher: Elsevier, pp. 18–27.

Guénard, Guillaume and Pierre Legendre (2022). “Hierarchical Clustering with Contiguity Constraint in *R*”. In: *Journal of Statistical Software* 103.7.

Hantson, Stijn, Almut Arneth, et al. (2016). “The status and challenge of global fire modelling”. In: *Biogeosciences* 13.11, pp. 3359–3375.

Hantson, Stijn, Salvador Pueyo, and Emilio Chuvieco (2015). “Global fire size distribution is driven by human impact and climate”. In: *Global Ecology and Biogeography* 24.1. Publisher: Wiley Online Library, pp. 77–86.

Hofmann, Gabriel S. et al. (2021). “The Brazilian Cerrado is becoming hotter and drier”. In: *Global Change Biology* 27.17, pp. 4060–4073.

IBGE (2023). “Censo Demográfico 2022: Quilombolas: primeiros resultados do universo”. In: *Rio de Janeiro: Instituto Brasileiro de Geografía e Estatística*.

IBGE, USGS (1993). “Mapa de vegetação do Brasil”. In: *Fundação Instituto Brasileiro de Geografia e Estatística-IBGE*. Publisher: Rio de Janeiro Brasil.

Jolly, W. Matt et al. (2015). “Climate-induced variations in global wildfire danger from 1979 to 2013”. In: *Nature Communications* 6.1, p. 7537.

Jordahl, Kelsey et al. (2021). *geopandas/geopandas: v0.9.0*. Version v0.9.0.

Klink, Carlos A. and Ricardo B. Machado (2005). “Conservation of the Brazilian Cerrado”. In: *Conservation Biology* 19.3, pp. 707–713.

Kluyver, Thomas et al. (2016). “Jupyter Notebooks – a publishing format for reproducible computational workflows”. In: *Positioning and Power in Academic Publishing: Players, Agents and Agendas*. Ed. by F. Loizides and B. Schmidt. IOS Press, pp. 87–90.

Krawchuk, Meg A. and Max A. Moritz (2011). “Constraints on global fire activity vary across a resource gradient”. In: *Ecology* 92.1, pp. 121–132.

Lambiotte, Renaud, Jean-Charles Delvenne, and Mauricio Barahona (2014). “Random Walks, Markov Processes and the Multiscale Modular Organization of Complex Networks”. In: *IEEE Transactions on Network Science and Engineering* 1.2, pp. 76–90.

Liaw, Andy and Matthew Wiener (2002). “Classification and Regression by randomForest”. In: *R News* 2.3, pp. 18–22.

Libonati, Renata et al. (2015). “An Algorithm for Burned Area Detection in the Brazilian Cerrado Using 4 μm MODIS Imagery”. In: *Remote Sensing* 7.11, pp. 15782–15803.

Liu, Zhong et al. (2012). “Tropical Rainfall Measuring Mission (TRMM) precipitation data and services for research and applications”. In: *Bulletin of the American Meteorological Society* 93.9, pp. 1317–1325.

Malhi, Yadvinder et al. (2009). “Exploring the likelihood and mechanism of a climate-change-induced dieback of the Amazon rainforest”. In: *Proceedings of the National Academy of Sciences* 106.49, pp. 20610–20615.

Martin, Robert E and David B Sapsis (1992). “Fires as agents of biodiversity: pyrodiversity promotes biodiversity”. In: *Proceedings of the conference on biodiversity of northwest California ecosystems. Cooperative Extension, University of California, Berkeley*, pp. 150–157.

Mataveli, Guilherme Augusto Verola et al. (2018). “Satellite observations for describing fire patterns and climate-related fire drivers in the Brazilian savannas”. In: *Natural Hazards and Earth System Sciences* 18.1, pp. 125–144.

Muñoz-Sabater, Joaquín et al. (2021). “ERA5-Land: a state-of-the-art global reanalysis dataset for land applications”. In: *Earth System Science Data* 13.9, pp. 4349–4383.

Myers, Norman et al. (2000). “Biodiversity hotspots for conservation priorities”. In: *Nature* 403.6772, pp. 853–858.

Nascimento, Diego Tarley Ferreira and Giuliano Tostes Novais (2020). “Clima do Cerrado: dinâmica atmosférica e características, variabilidades e tipologias climáticas”. In.

Oksanen, Jari et al. (2024). *vegan: Community Ecology Package*. R package version 2.6-6.1.

Oliveira, Paulo Tarso S. et al. (2014). “Trends in water balance components across the Brazilian Cerrado”. In: *Water Resources Research* 50.9, pp. 7100–7114.

Oliveira-Filho, AT de (2017). “NeoTropTree, Flora arbórea da Região Neotropical: Um banco de dados envolvendo biogeografia, diversidade e conservação”. In: *Univ. Fed. Minas Gerais. Available online at: http://www. neotroptree. info (Accessed October 1, 2017)*.

Olson, David M et al. (2001). “Terrestrial Ecoregions of the World: A New Map of Life on Earth: A new global map of terrestrial ecoregions provides an innovative tool for conserving biodiversity”. In: *BioScience* 51.11. Publisher: American Institute of Biological Sciences, pp. 933–938.

Pausas, Juli G. and Jon E. Keeley (2009). “A Burning Story: The Role of Fire in the History of Life”. In: *BioScience* 59.7, pp. 593–601.

Pausas, Juli G. and Eloi Ribeiro (2013). “The global fire-productivity relationship: Fire and productivity”. In: *Global Ecology and Biogeography* 22.6, pp. 728–736.

Pivello, Vânia R et al. (2021). “Understanding Brazil’s catastrophic fires: Causes, consequences and policy needed to prevent future tragedies”. In: *Perspectives in Ecology and Conservation* 19.3, pp. 233–255.

Pivello, Vânia R. (2011). “The Use of Fire in the Cerrado and Amazonian Rainforests of Brazil: Past and Present”. In: *Fire Ecology* 7.1, pp. 24–39.

QGIS Development Team (2023). *QGIS Geographic Information System*. QGIS Association.

R Core Team, R et al. (2020). *R: A language and environment for statistical computing*.

Ramos-Neto, Mário Barroso and Vânia Regina Pivello (2000). “Lightning Fires in a Brazilian Savanna National Park: Rethinking Management Strategies”. In: *Environmental Management* 26.6, pp. 675–684.

Ribeiro, Andreia F. S., Lucas Santos, et al. (2024). “The time since land-use transition drives changes in fire activity in the Amazon-Cerrado region”. In: *Communications Earth & Environment* 5.1, p. 96.

Ribeiro, J.F. and B.M.T. Walter (2008). “Cerrado Ecologia e Flora”. In: *As principais fitofisionomias do Bioma Cerrado*. Embrapa, pp. 152–212.

Rocha, Genival Fernandes et al. (2012). “Detecção de desmatamentos no bioma Cerrado entre 2002 e 2009: padrões, tendências e impactos”. In: *Revista Brasileira de Cartografia* 63.3.

Rosan, Thais M. et al. (2022). “Fragmentation-Driven Divergent Trends in Burned Area in Amazonia and Cerrado”. In: *Frontiers in Forests and Global Change* 5, p. 801408.

Sano, Edson E., Ariane A. Rodrigues, et al. (2019). “Cerrado ecoregions: A spatial framework to assess and prioritize Brazilian savanna environmental diversity for conservation”. In: *Journal of Environmental Management* 232, pp. 818–828.

Sano, Edson E., Roberto Rosa, et al. (2010). “Land cover mapping of the tropical savanna region in Brazil”. In: *Environmental Monitoring and Assessment* 166.1, pp. 113–124.

Schmidt, Isabel Belloni and Ludivine Eloy (2020). “Fire regime in the Brazilian Savanna: Recent changes, policy and management”. In: *Flora* 268, p. 151613.

Seabold, Skipper and Josef Perktold (2010). “statsmodels: Econometric and statistical modeling with python”. In: *9th Python in Science Conference*.

Segura-Garcia, Carlota et al. (2024). “Human land occupation regulates the effect of the climate on the burned area of the Brazilian Cerrado”. In: *Communications Earth & Environment* 5.1, p. 361.

Silva, P S, J A Rodrigues, et al. (2020). “Drivers of burned area patterns in Cerrado: the case of MATOPIBA region”. In: *2020 IEEE Latin American GRSS & ISPRS Remote Sensing Conference (LAGIRS)*.

Silva, Patrícia, Ana Bastos, Carlos C. DaCamara, et al. (2016). “Future Projections of Fire Occurrence in Brazil Using EC-Earth Climate Model”. In: *Revista Brasileira de Meteorologia* 31.3, pp. 288–297.

Silva, Patrícia S., Ana Bastos, Renata Libonati, et al. (2019). “Impacts of the 1.5 °C global warming target on future burned area in the Brazilian Cerrado”. In: *Forest Ecology and Management* 446, pp. 193–203.

Silva, Patrícia S., Joana Nogueira, et al. (2021). “Putting fire on the map of Brazilian savanna ecoregions”. In: *Journal of Environmental Management* 296, p. 113098.

Silva Arruda, Vera Laísa da et al. (2024). “Assessing four decades of fire behavior dynamics in the Cerrado biome (1985 to 2022)”. In: *Fire Ecology* 20.1, p. 64.

Sistema IBGE de Recuperação Automática do Instituto Brasileiro de Geografia e Estatística (n.d.). https://sidra.ibge.gov.br/tabela/3939. Accessed: 2023-09-20.

Souza, Carlos M. et al. (2020). “Reconstructing Three Decades of Land Use and Land Cover Changes in Brazilian Biomes with Landsat Archive and Earth Engine”. In: *Remote Sensing* 12.17, p. 2735.

Spera, Stephanie A. et al. (2016). “Land-use change affects water recycling in Brazil’s last agricultural frontier”. In: *Global Change Biology* 22.10, pp. 3405–3413.

Stevens, Nicola and William J. Bond (2023). “A trillion trees: carbon capture or fuelling fires?” In: *Trends in Ecology & Evolution*, S016953472300246X.

Stevens, Nicola, Caroline E. R. Lehmann, et al. (2017). “Savanna woody encroachment is widespread across three continents”. In: *Global Change Biology* 23.1, pp. 235–244.

team, The pandas development (2021). *pandas-dev/pandas: Pandas 1.2.3*. Version v1.2.3.

Teixeira Pitta, Fabio and Gerardo Cerdas Vega (2017). “Impacts of the agribsuiness expansion in teh Matopiba region: communities and the environment”. In: *ActionAid - Rio de Janeiro*.

Werf, G. R. van der, J. T. Randerson, L. Giglio, G. J. Collatz, et al. (2010). “Global fire emissions and the contribution of deforestation, savanna, forest, agricultural, and peat fires (1997–2009)”. In: *Atmospheric Chemistry and Physics* 10.23, pp. 11707–11735.

Werf, Guido R. van der, James T. Randerson, Louis Giglio, Nadine Gobron, et al. (2008). “Climate controls on the variability of fires in the tropics and subtropics”. In: *Global Biogeochemical Cycles* 22.3, 2007GB003122.

Westerling, A. L. et al. (2006). “Warming and Earlier Spring Increase Western U.S. Forest Wildfire Activity”. In: *Science* 313.5789, pp. 940–943.

Wu, Qiusheng (2020). “geemap: A Python package for interactive mapping with Google Earth Engine”. In: *Journal of Open Source Software* 5.51, p. 2305.

Zanzarini, Vagner, Alan N Andersen, and Alessandra Fidelis (2022). “Flammability in tropical savannas: Variation among growth forms and seasons in Cerrado”. In: *Biotropica* 54.4, pp. 979–987.

4.10 Supplementary Information

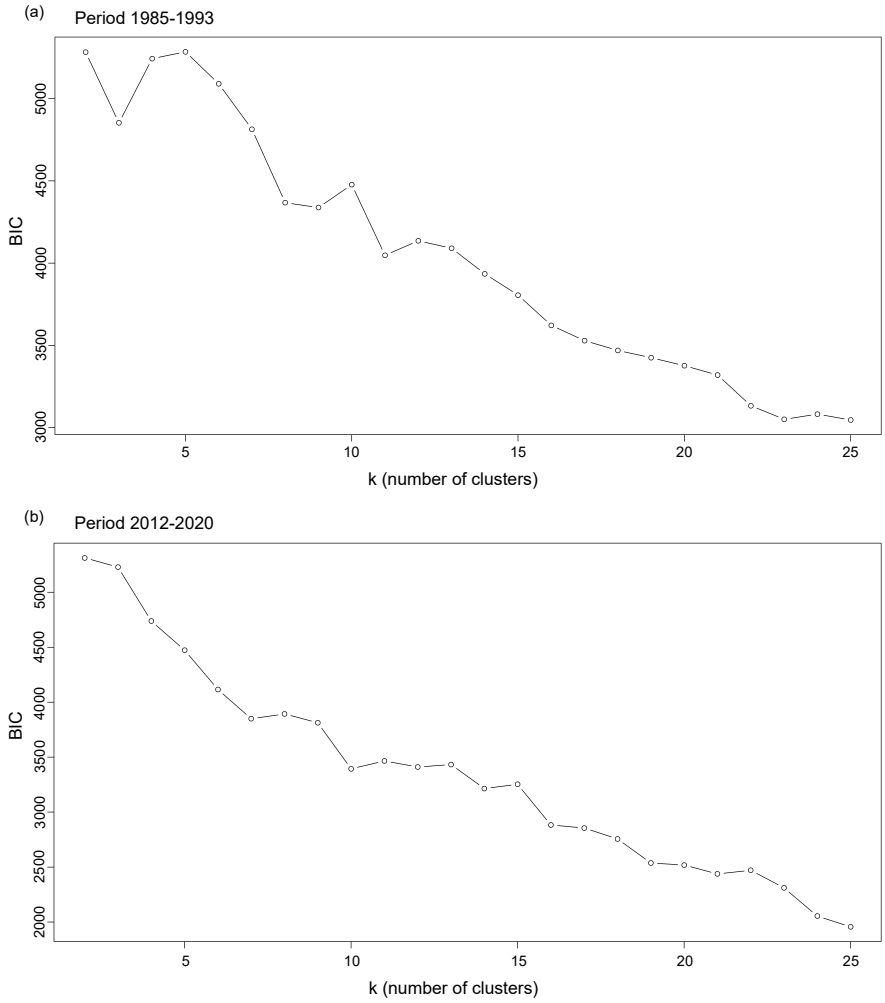

Figure S4.1: Bayesian Information Criteria index calculated for each clustering solution with an increasing number of clusters between 2 and 25 for the first (a) and last (b) periods.

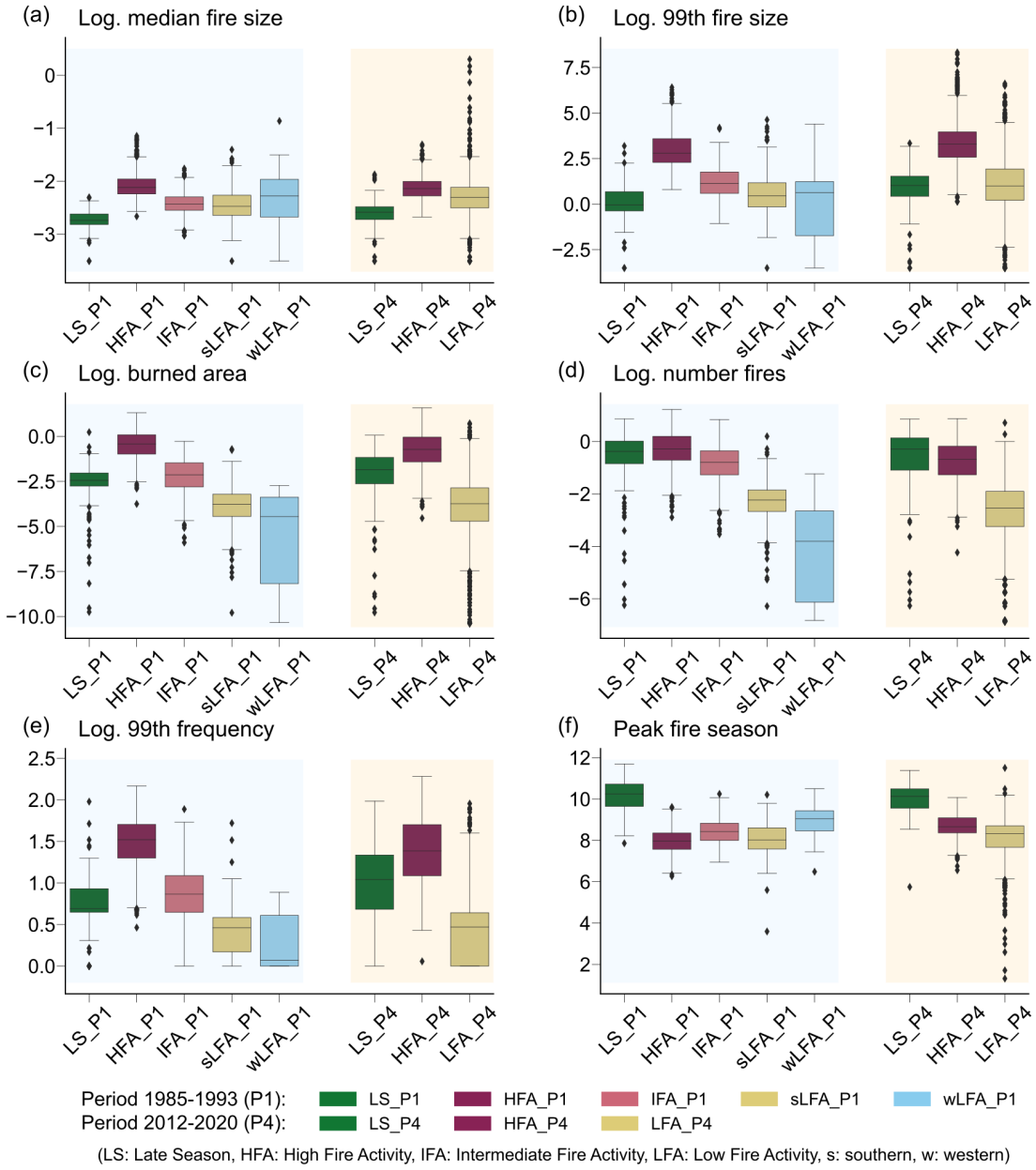

Figure S4.2: Distribution of each of the six fire variables for each fire regime region in the first (1985-1993, shaded in blue) and last (2012-2020, shaded in orange) periods. Plots show the median fire size (a), the 99th percentile fire size (b), the burned area (c), the number of fires (d), the 99th percentile fire frequency (e), and median fire season (f), expressed in months.

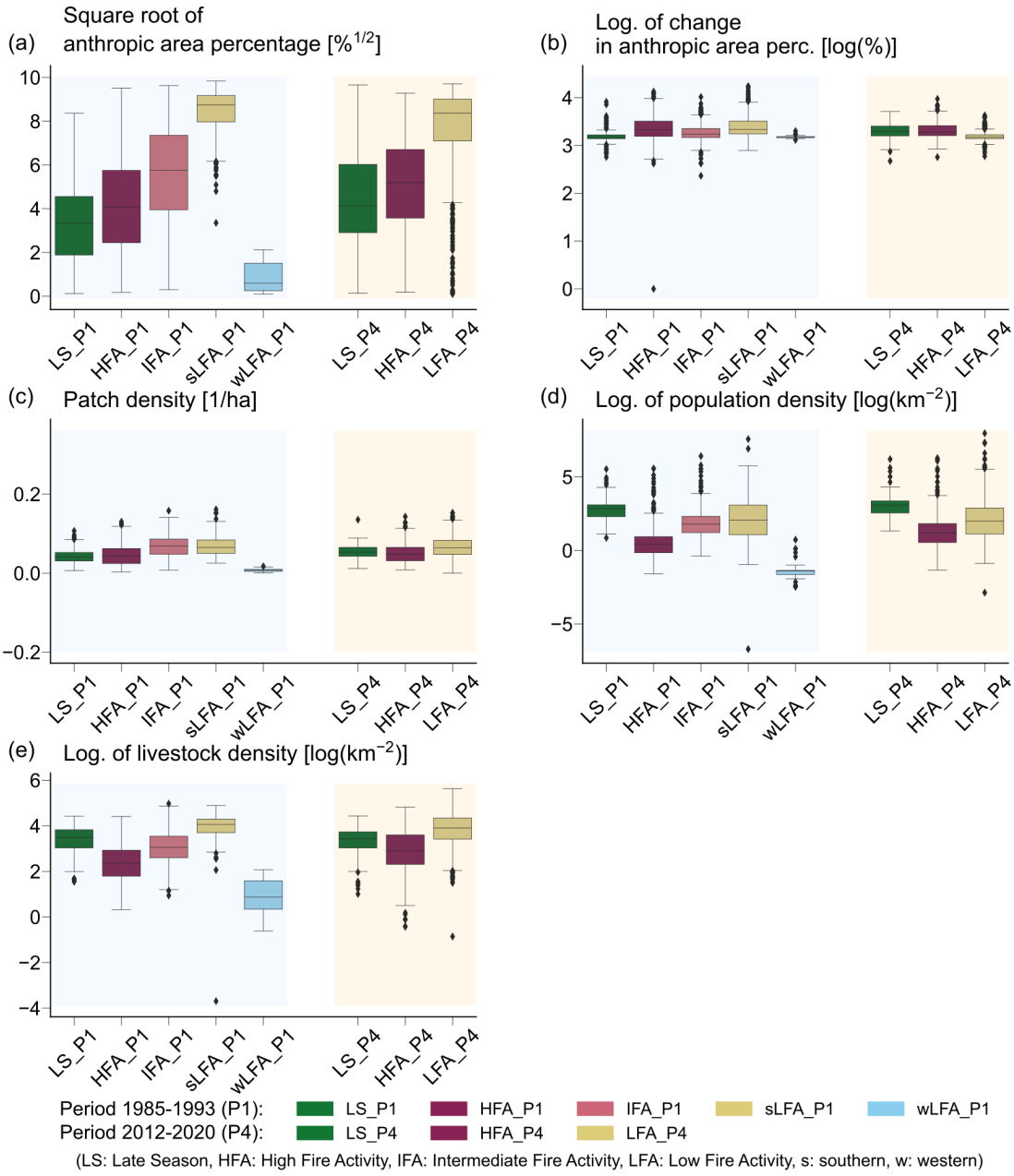

Figure S4.3: Distribution of each anthropic variable for each fire regime region in the first (1985-1993, shaded in blue) and last (2012-2020, shaded in orange) periods. Plots show the anthropic area percentage (a), the change in anthropic area percentage within the period (b), the patch density (c), the population density (d), and the livestock density (e).

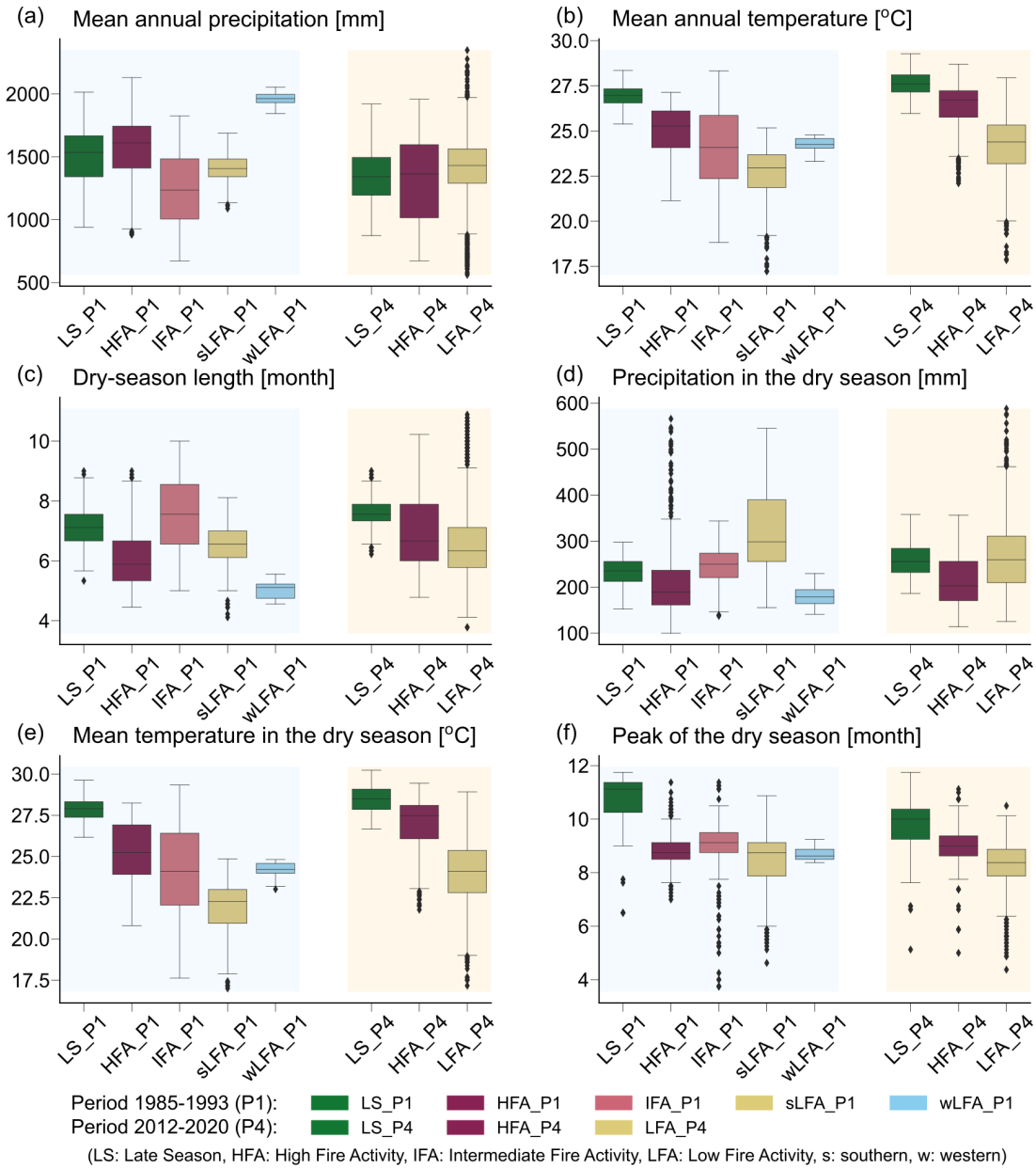

Figure S4.4: Distribution of each climatic variable for each fire regime region in the first (1985-1993, shaded in blue) and last (2012-2020, shaded in orange) periods. Plots show the mean annual precipitation (a), mean annual temperature (b), dry-season length (c), precipitation in the dry season (d), the mean annual temperature in the dry season (e), and the peak of the dry season (f).

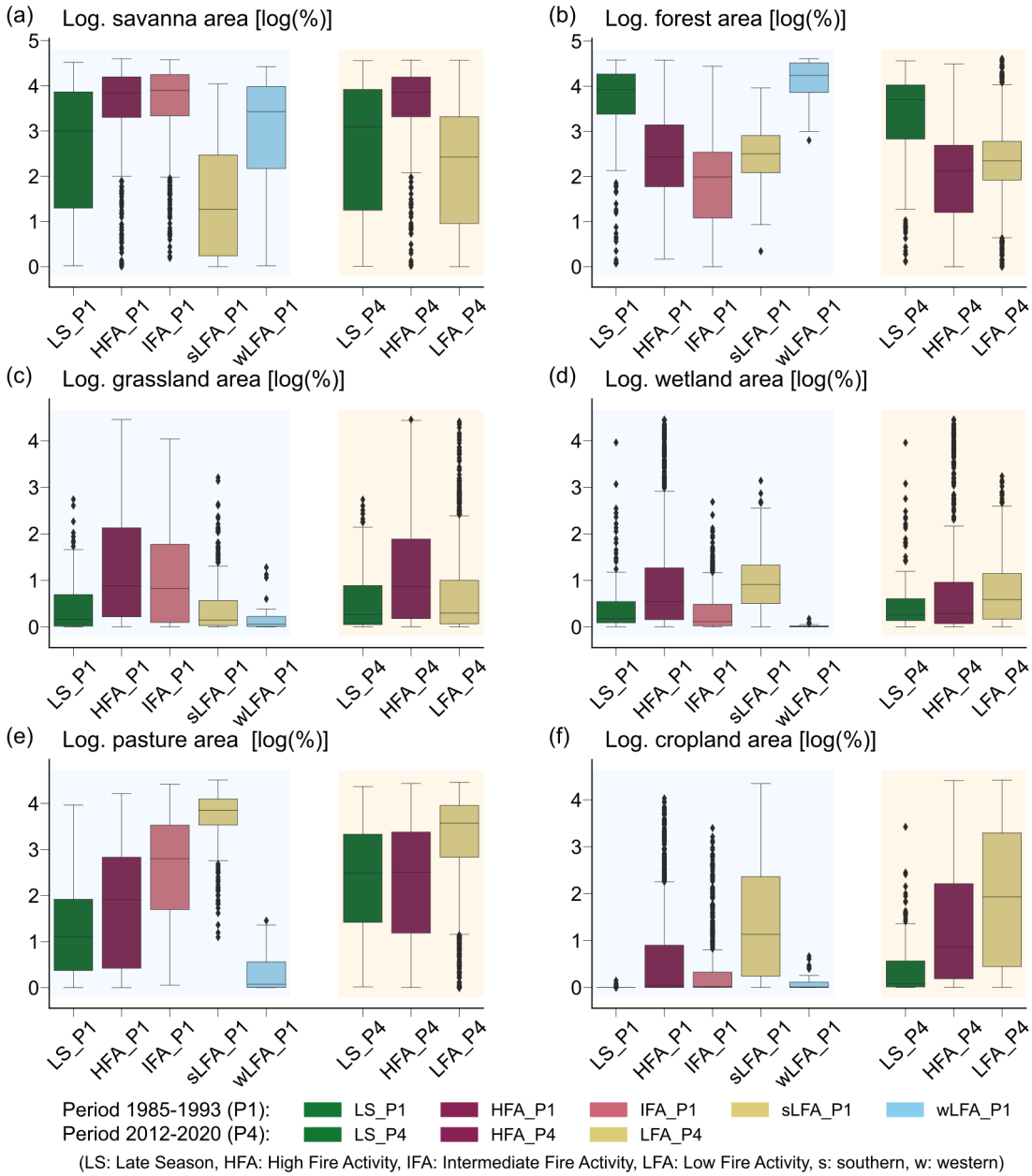

Figure S4.5: Distribution of the percentage area covered by different vegetation and land use categories (as per MapBiomas Collection 8.0 categories, see Methods) for each fire regime region in the first (1985-1993, shaded in blue) and last (2012-2020, shaded in orange) periods. Plots show savanna (a), forest (b), grassland (c), wetland (seasonally flooded savanna) (d), pasture (e), and cropland (f) land use categories.

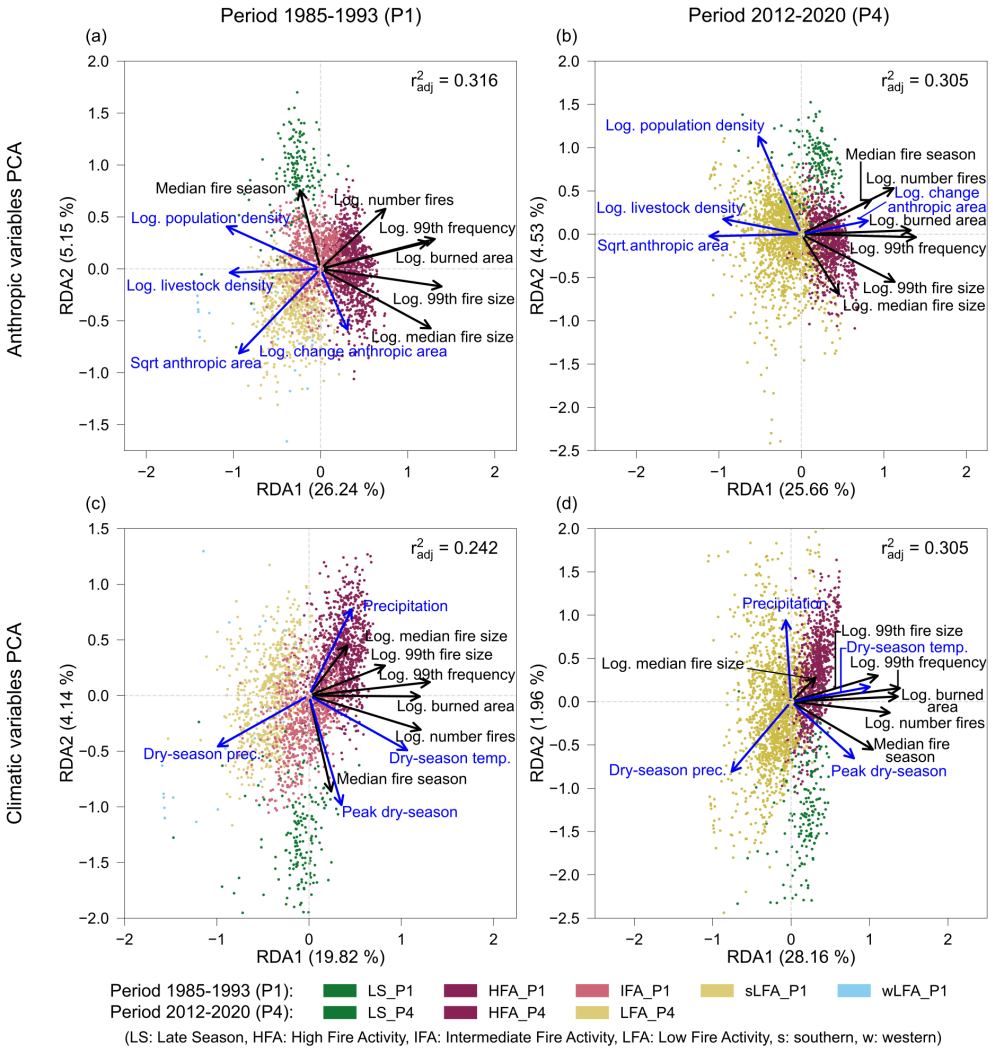

Figure S4.6: Results of the redundancy analysis (RDA) performed using each set of anthropic (top row) and climatic parameters (bottom row) as explanatory variables and the six fire characteristics as response variables, for the first (1985-1993, left column) and last (2012-2020, right column) periods. The anthropic variables comprise anthropic area percentage, livestock density, population density, and change in anthropic area percentage within the period. The climatic variables comprise the total annual precipitation, total precipitation in the dry season, mean temperature in the dry season and the peak of the dry season. The projection used to represent the RDA results is such that the angles between the explanatory and response variables represent the correlation between the variables. The data points are projected in the space of the response variables and coloured according to the fire regime region they were classified in for each period (see Methods). Note that even though the same colour scheme was used in both periods to denote analogous fire regime regions, neither the geographical limits, nor the fire, anthropic or climatic characteristics of the equally-coloured fire regime regions are necessarily the same. All variables in all cases had a p-value < 0.001.

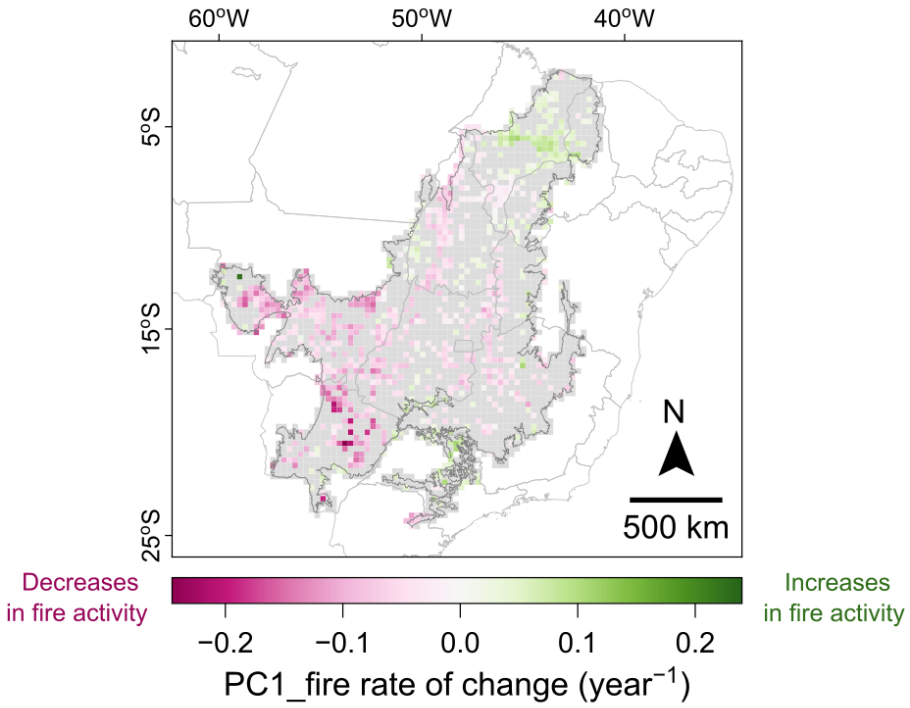

Figure S4.7: Trends in time (slope coefficients) over the four 9-year periods of fire activity (see Methods) for each 30 km grid cell in the Cerrado. The time series of fire activity comprised the PC1_fire values for each period projected on the PCA_fire space of the first period (see main, Figure 1) so that these consecutive values are comparable. The time series was calculated as a linear regression and fitted using Ordinary Least Squares. Pink indicates decreases in fire activity over time, green indicates increases, and grey indicates no clear trends in time with 80% confidence interval.

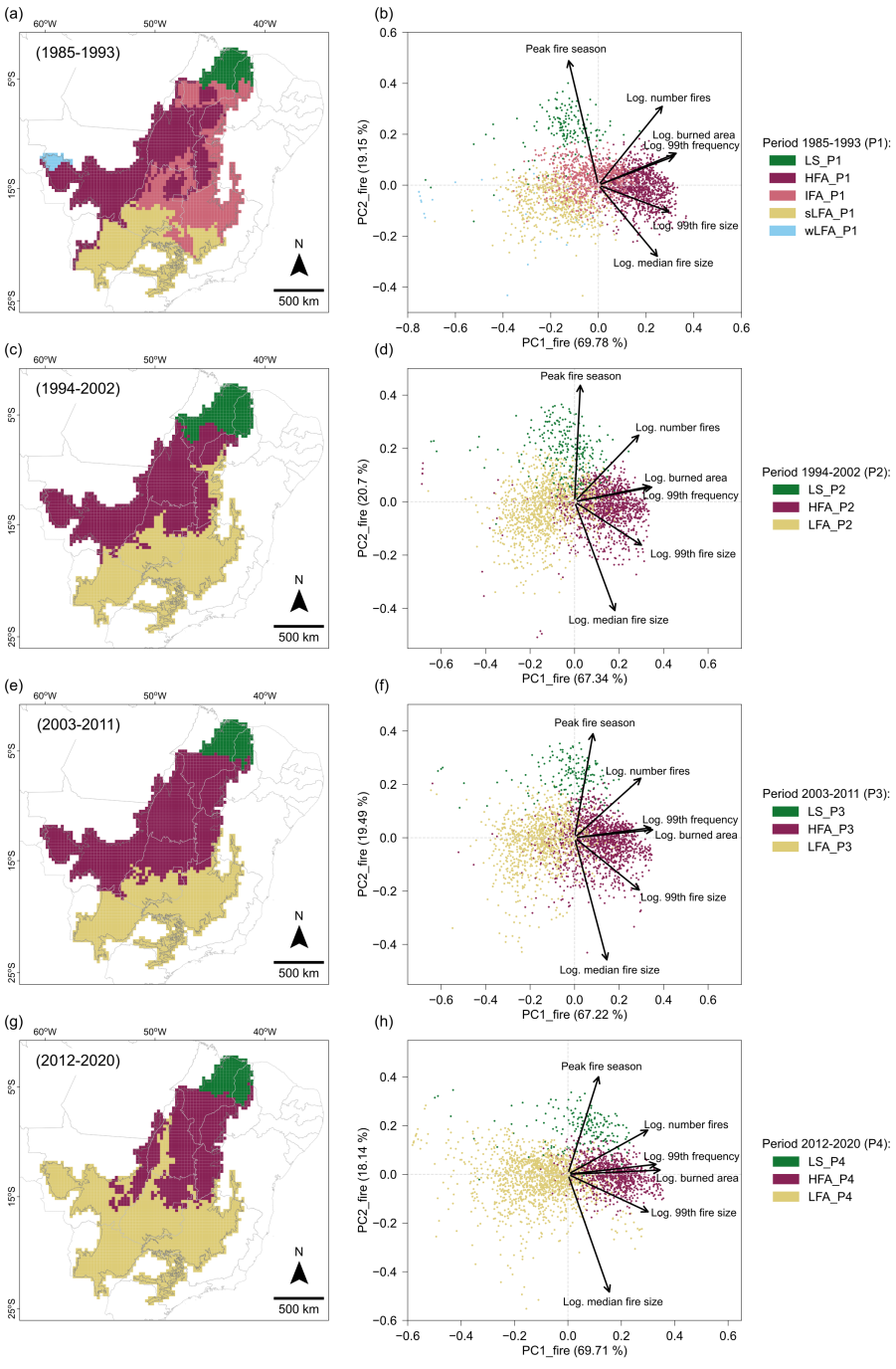

(LS: Late Season, HFA: High Fire Activity, IFA: Intermediate Fire Activity, LFA: Low Fire Activity, s: southern, w: western)

Figure S4.8: Maps showing the fire regime regions identified by the spatially constrained hierarchical algorithm (see Methods) accompanied by plots of the two main axes of variation of the PCA_fire for the period 1985-1993 (a-b), 1994-2002 (c-d), 2003-2011 (e-f), and 2012-2020 (g-h). Percentage values indicate the explanatory power of each PCA axis.

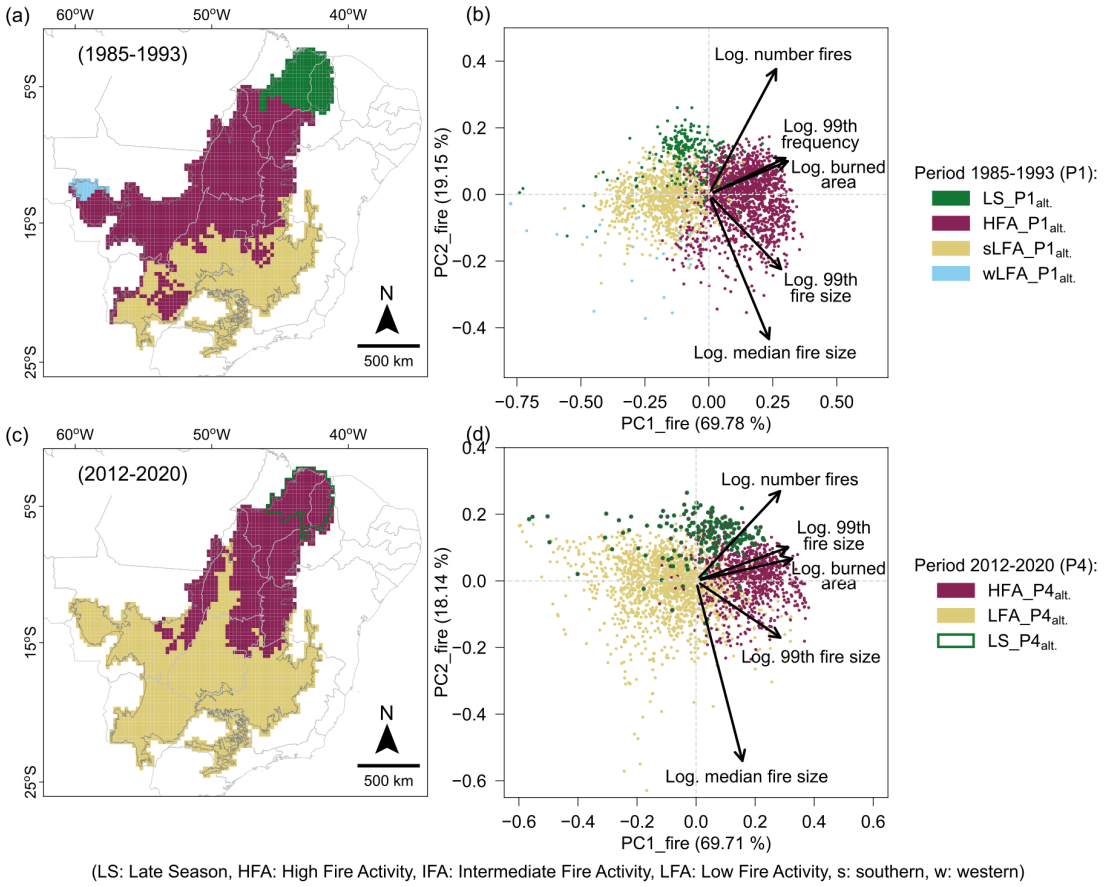

Figure S4.9: Maps (a and c) showing the alternative fire regime regions obtained in the first and last periods respectively when the peak of the fire season is not included as a fire variable when running the spatially constrained clustering algorithm. Figures (b) and (d) show the first two axes of the PCA_fire used to classify the grid cells. These maps and PCAs were generated to explore whether regions LS_P1 and LS_P4 in each period would present any distinct characteristic in addition to the later peak of the fire season, and would hence be delineated when running the clustering algorithm without this variable. In this case, the Bayesian Information Criteria (BIC) suggests that four regions in the first period and two regions in the last period are the clustering solutions optimising data partition. In the first period, the four-clusters solution does identify a region equivalent to LS_P1, confirming the distinct fire regime of this region compared to HFA_P1 (and its HFA_P1$_{alt.}$ equivalent alternative), with an overall lower fire activity and overall small and numerous fires. In the last period, the equivalent LS_P4 region is not identified in the two-cluster solution suggested by the BIC, suggesting that the increases in fire activity experienced by this area over time resulted in fire regimes closer to those of region HFA_P4 (and its HFA_P4$_{alt.}$ equivalent). Nevertheless, this northern area is identified in the four-clusters solution for the last period when leaving the peak of the fire season out (outlined in green in c and d, LS_P4$_{alt.}$), suggesting this area presents characteristics relevant to data classification. Moreover, despite the fire characteristics of the northern region being closer to those of HFA_P4$_{alt.}$, we can observe these cells are still clearly clustered in the PCA_fire with numerous and medium-sized fires.

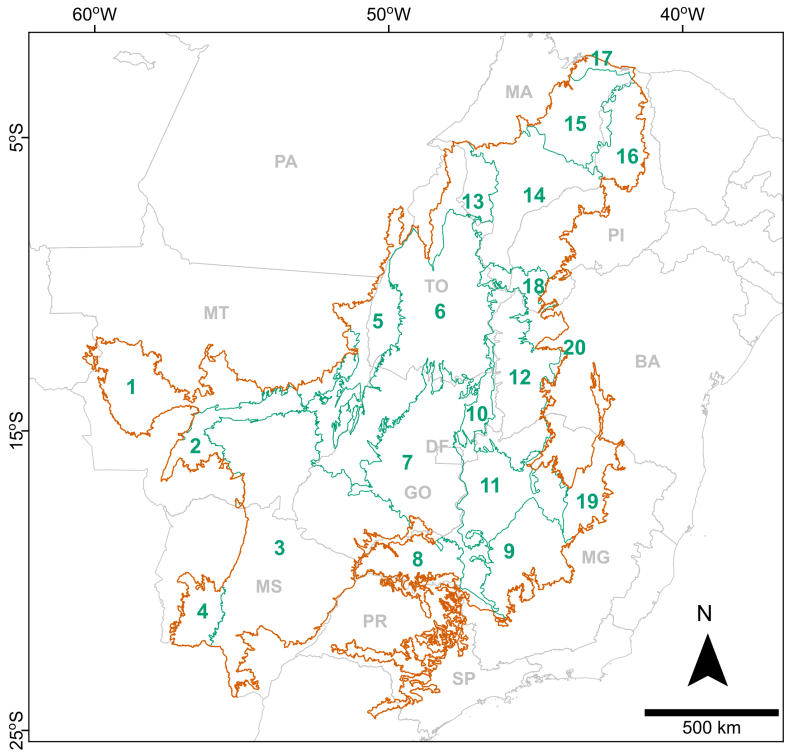

Figure S4.10: Map showing the limits of the Cerrado (orange), the limits of the different Cerrado ecoregions (green), and the different Brazilian states (grey) that intersect the Cerrado. Ecoregions: 1, Chapada dos Parecis; 2, Depressão Cuiabana; 3, Paraná Guimarães; 4, Complexo Bodoquena; 5, Bananal; 6, Araguaia Tocantins; 7, Planalto Central; 8, Basaltos do Paraná; 9, Alto São Francisco; 10, Vão do Paraná; 11, Paracatu; 12, Chapadão do São Francisco; 13, Bico do Papagaio; 14, Alto Parnaíba; 15, Floresta de Cocais; 16, Centro-norte Piauiense; 17, Costeiro; 18, Parnaguá; 19, Jequitinhona; 20, Depressão Cárstica do São Francisco. PA, Pará; MT, Mato Grosso; MS, Mato Grosso do Sul; GO, Goiás; DF, Distrito Federal; PR, Paraná; SP, São Paulo; MG, Minas Gerais; MA, Maranhão; TO, Tocantins; PI, Piauí; BA, Bahía.

Table S4.1: Components of each fire variable on the six axes of the PCA_fire in the first (top) and in the last (bottom) periods.

	Period 1985-1993					
Fire variables	PC1_fire	PC2_fire	PC3_fire	PC4_fire	PC5_fire	PC6_fire
Peak fire season	-2.07	8.11	7.46	-0.33	0.51	-0.03
Median fire size	4.15	-4.70	5.89	-7.12	0.76	-0.89
99th percentile fire size	5.03	-1.77	3.92	7.34	-4.12	-3.40
Log. burned area	5.51	2.12	-0.57	-0.08	-2.45	9.21
Log. number fires	4.48	5.18	-4.33	-4.16	-3.96	-5.23
Log. 99th perc. Frequency	5.37	1.92	-1.15	2.06	9.30	-1.23
	Period 2012-2020					
Fire variables	PC1_fire	PC2_fire	PC3_fire	PC4_fire	PC5_fire	PC6_fire
Peak fire season	-1.92	6.71	-8.71	-1.17	0.38	0.01
Median fire size	-2.58	-8.03	-4.85	-5.52	0.58	0.82
99th percentile fire size	-5.07	-2.60	-2.13	8.09	-3.69	3.18
Log. burned area	-5.81	0.29	1.48	-0.63	-2.36	-9.17
Log. number fires	-5.03	3.06	3.98	-5.24	-4.35	5.41
Log. 99th perc. Frequency	-5.57	0.69	2.04	0.99	9.35	1.41

Table S4.2: Outputs from the Random Forest algorithm, decrease in the GINI index (top) and classification accuracy of the resulting model (bottom). The algorithm was run for each set of variables - anthropic and climatic - separately and together, and per period. Parenthesis next to classification accuracy express the 95% confidence interval. Highlighted in bold are the four most important variables for classification according to the GINI index.

	Each set separately		**All variables together**	
Mean GINI decrease	1985-1993	2012-2020	1985-1993	2012-2020
Log. population density	441.6	247.7	**237.5**	**117.1**
Log. livestock density	338.2	217.1	**225.6**	109.7
Sqrt. anthropic area perc.	403.3	388.2	**215.5**	**170.5**
Log. change in anthropic area perc.	205.5	265.2	89.6	104.6
Average annual precipitation	353.4	214.9	147.5	94.3
Average temperature in the dry season	427.2	503.9	**189.7**	**273.6**
Average precipitation in the dry season	410.7	184.6	164.2	94.9
Peak of the dry season	197.6	214.1	81.5	**123.6**
	Each set separately		**All variables together**	
Classification accuracy (%)	1985-1993	2012-2020	1985-1993	2012-2020
Anthropic variables	81.7 (78.1, 84.9)	82.8 (79.3, 85.9)	88.8 (85.9, 91.2)	94.0 (91.8, 95.8)
Climatic variables	82.3 (78.7, 85.4)	90.0 (87.1, 92.4)		

Table S4.3: Percentage area of each fire regime region in the last period (2012-2020) that experienced increasing (> 0), decreasing (< 0), or no clear trends ($==$) in time for each one of the fire variables and each of the PC1_fire with 80% confidence level. The trends in burned area, number of fires, median fire size, 99th percentile fire size, and median fire size were calculated by fitting a linear regression on the annual data for each variable in the period 1985-2020. The trends in the 99th percentile of fire frequency, PC1_fire and PC2_fire were calculated in the same manner but on a 9-year interval time series, since the frequency was estimated as the number of times a pixel burned in each of the four time intervals (see Methods).

	LS_P4			**HFA_P4**			**LFA_P4**		
Fire variables	<0	==	>0	<0	==	>0	<0	==	>0
Log. 99th frequency	2.2	69.2	28.6	14	74.4	11.6	27.5	69	3.5
Log. burned area	8.2	44	47.8	30.8	53.3	15.9	53.4	36.4	10.2
Log. number fires	15.9	53.3	30.8	62.7	32	5.3	63.8	27.7	8.6
Log. median fire size	3.3	57.7	39	7.5	66.9	25.6	11.4	70.7	17.9
Log. 99th fire size	3.3	37.9	58.8	9.3	55.5	35.2	36.9	50.3	12.8
Median fire season	7.7	88.5	3.8	4.8	89.4	5.8	4.5	91.8	3.7
PC1_fire	2.2	68.7	29.1	15.9	69.8	14.3	27.1	67.7	5.2
PC2_fire	7.7	85.7	6.6	5.7	86.6	7.7	16.8	79.2	4.1

Table S4.4: Components of each anthropic variable on the four axes of the PCA_anth in the first (top) and in the last (bottom) periods.

	Period 1985-1993			
Anthropic variables	PC1_anth	PC2_anth	PC3_anth	PC4_anth
Log. population density	5.34	-4.21	6.01	-4.52
Log. livestock density	6.31	-0.13	0.27	7.94
Sqrt. anthropic area perc.	5.78	2.39	-6.72	-6.72
Log. change in anthropic area perc.	1.06	8.91	4.65	4.65
	Period 2012-2020			
Anthropic variables	PC1_anth	PC2_anth	PC3_anth	PC4_anth
Log. population density	4.32	5.25	7.53	-0.16
Log. livestock density	5.91	0.66	-3.70	7.34
Sqrt. anthropic area perc.	5.78	1.31	-4.38	-6.98
Log. change in anthropic area perc.	-3.99	8.56	-3.66	0.60

Table S4.5: Outputs from the Redundancy Analysis performed on the fire variables and the anthropic variables. Showing the first two components of each fire variable (top) and the first two coefficients of each anthropic variable (bottom) for the first (left) and last (right) periods.

	Period 1985-1993		**Period 2012-2020**	
Fire variable	RDA1_fire	RDA2_fire	RDA1_fire	RDA2_fire
Peak fire season	-0.51	1.64	1.83	0.86
99th percentile fire size	2.93	-0.25	2.40	-1.17
Log. burned area	2.62	0.55	2.81	0.10
Log. number fires	1.60	1.24	2.38	1.13
Median fire size	2.66	-1.21	0.99	-1.52
Log. 99th perc. Frequency	2.77	0.61	2.94	-0.07
	Period 1985-1993		**Period 2012-2020**	
Anthropic variable	RDA1_anth	RDA2_anth	RDA1_anth	RDA2_anth
Log. population density	-0.86	0.33	-0.41	0.90
Log. livestock density	-0.84	-0.03	-0.77	0.14
Sqrt. anthropic area perc.	-0.74	-0.65	-0.910	-0.02
Log. change in anthropic area perc.	0.26	-0.48	0.66	0.13

Table S4.6: Components of each climatic variable on the four axes of the PCA_clim in the first (top) and in the last (bottom) periods.

	Period 1985-1993			
Climatic variables	PC1_clim	PC2_clim	PC3_clim	PC4_clim
Average annual precipitation	4.52	5.75	-6.23	-3.22
Average temperature in the dry season	5.80	-3.74	3.99	-6.27
Average precipitation in the dry season	-5.88	-3.50	-6.11	-6.11
Peak of the dry season	3.77	-6.60	3.99	3.99
	Period 2012-2020			
Climatic variables	PC1_clim	PC2_clim	PC3_clim	PC4_clim
Average annual precipitation	4.56	6.28	-0.63	-6.51
Average temperature in the dry season	5.43	-3.39	7.86	-0.22
Average precipitation in the dry season	-6.41	-2.06	3.35	-6.81
Peak of the dry season	3.39	-6.91	-5.43	-3.77

Table S4.7: Outputs from the Redundancy Analysis performed on the fire variables and the climatic variables. Showing the first two components of each fire variable (top) and the first two coefficients of each climatic variable (bottom) for the first (left) and last (right) periods.

	Period 1985-1993		**Period 2012-2020**	
Fire variables	RDA1_fire	RDA2_fire	RDA1_fire	RDA2_fire
Peak fire season	0.51	-1.84	2.24	-1.18
99th percentile fire size	1.78	0.58	2.38	0.65
Log. burned area	2.55	-0.02	2.89	0.13
Log. number fires	2.56	-0.65	2.69	-0.27
Median fire size	0.92	0.99	0.75	0.67
Log. 99th perc. Frequency	2.76	0.25	2.95	0.33
	Period 1985-1993		**Period 2012-2020**	
Climatic variables	RDA1_clim	RDA2_clim	RDA1_clim	RDA2_clim
Average annual precipitation	0.37	0.62	0.05	0.76
Average temperature in the dry season	0.85	-0.39	-0.82	0.14
Average precipitation in the dry season	-0.79	-0.37	0.61	-0.65
Peak of the dry season	0.28	-0.78	-0.65	-0.53

Table S4.8: Pairwise correlation coefficients between all the explanatory variables used in the study. Coefficients were obtained using together the first and last periods' data.

	(1)	**(2)**	**(3)**	**(4)**	**(5)**	**(6)**	**(7)**	**(8)**
Av. annual precipitation (1)	1.00							
Av. temperature in the dry season (2)	0.01	1.00						
Av. precipitation in the dry season (3)	-0.54	-0.20	1.00					
Peak of the dry season (4)	-0.12	0.32	-0.06	1.00				
Log. population density (5)	-0.31	-0.27	-0.15	0.19	1.00			
Log. livestock density (6)	0.26	0.24	0.26	0.02	0.44	1.00		
Sqrt. anthropic area perc. (7)	0.07	-0.39	0.01	-0.15	-0.01	0.60	1.00	
Log. change in anthropic area perc. (8)	0.16	-0.29	0.08	0.24	-0.17	-0.07	-0.10	1.00

5 | Decoupling natural and human-caused fires in the Brazilian Cerrado (Research Paper 3)

By: Carlota Segura-Garcia, Thomas A. J. Janssen, Renata Libonati, Lucas S. Menezes, Guilherme Mataveli, Sander Veraverbeke, Matthew W. Jones, Imma Oliveras Menor

Linking statement: In **Chapter 3 (Research Paper 1)** and **Chapter 4 (Research Paper 2)**, this thesis explored the effects of humans on the fire regimes of the Brazilian Cerrado through mechanisms primarily related to the fragmentation of the landscape, which alters the continuity of the fuel bed. However, humans also shape fire occurrence and behaviour by altering the number of fire ignition opportunities and shifting the timing of these in comparison to naturally-ignited fires. Thus, this chapter, the last research paper of this thesis, quantified the proportion of fires ignited by humans and by lightning - the main cause of natural fire ignitions -, and analysed the patterns of fire created by each type of ignition. Even though humans are usually assumed to be the main cause of fire ignitions in the Cerrado, the quantification of human to lightning-ignited fires was a major outstanding question that had not yet been addressed for the whole Cerrado.

This paper was submitted to the journal *Global Change Biology* on 10th October 2024.

Contribution Statement: I, Carlota Segura-Garcia, conducted the conceptualization, methodology development, data processing and data analysis, investigation, visualization of the results and writing of the manuscript. Dr Matthew W. Jones, Dr Sander Veraverbeke, Dr Thomas Janssen, Dr Guilherme Mataveli, Dr Renata Libonati and Lucas Menezes helped in the conceptualization, methodology, analysis, investigation, and reviewing of the manuscript. Dr Matthew W. Jones and Dr Sander Veraverbeke provided the Vaisala Global Lightning Detection Network GLD360 dataset on lightning strikes. Dr Renata Libonati provided the ground truth data on lightning-ignited fires in Cerrado's protected areas from Instituto Chico Mendes de Conservação da Biodiversidade (ICMBio). Finally, Dr Imma Oliveras Menor supervised and was involved in all steps of this work.

5.1 Abstract

The Brazilian Cerrado is a mosaic of savanna and grassland ecosystems that have co-evolved with fire as a disturbance agent. Before humans dispersed across the Cerrado, lightning-ignited fires created landscapes with varied fire histories contributing to a patchwork of vegetation successional stages, hosting high levels of biodiversity. In the past few decades, however, most of the Cerrado has been converted to agricultural land uses, altering its fire regimes. Quantifying lightning and human-caused fires is fundamental to understanding to what extent current patterns of fire may be caused by humans and diverge from these natural regimes. Here, we used geospatial data on individual fire events and lightning occurrence in an ignition-cause attribution method to identify lightning and human-caused fires. We show that humans are the overwhelming ignition cause in the Brazilian Cerrado, responsible for 89.1% (95% CI, [86.9, 91.3]%) of fires between 2019 and 2023, while 7.5% (95% confidence interval, CI, [6.7, 8.3]%) of fires were ignited by lightning, and 3.4% (95% CI, [2.7, 4.1]%) did not have a clear ignition cause. While most lightning-caused fires occur during the transition from the dry to the wet season (September and October), humans advance the fire season up to the start of the dry season in May, extending its total length threefold. Regardless of timing, human-caused fires take place in drier and hotter conditions than lightning fires, thus encouraging more extreme fire behaviour. Indeed, we find that the most extreme human-ignited fires are about ten times larger or two times more intense than the most extreme lightning-ignited fires. We conclude that humans have altered the natural fire regimes of the Cerrado, igniting larger and more intense fires that burn over a longer fire season, with important implications for the biodiversity and carbon cycles in these ecosystems.

Keywords - neotropical savannas, fire regimes, fire ignitions, lightning, anthropic fires

5.2 Introduction

Many ecosystems in the world co-evolved with fire (Bond, 2015; Bond and Keeley, 2005; Pausas and Keeley, 2009; Beerling et al., 2006), as their flora developed a range of strategies to co-exist with this disturbance agent. These strategies include resisting fire, quickly resprouting, flowering, or germinating after fire, or even promoting fire occurrence by providing flammable biomass (Hoffmann et al., 2003; Simon and Pennington, 2012; Pausas, Keeley, and Schwilk, 2017). The ancient origins of such adaptations (He, Pausas, et al., 2012; He, Lamont, et al., 2016; Simon and Pennington, 2012) indicate that fires, ignited primarily by lightning and volcanic activity, were common on Earth long before the appearance of hominids (Glasspool et al., 2004). These fires contributed to the spread of ecosystems with sparse tree canopies in seasonally dry climates, giving rise to the savanna biome (Beerling et al., 2006). Consequently, some of the present-day fire-adapted ecosystems rely on a certain fire regime to maintain their open physiognomies (Oliveras et al., 2016; Pausas and Bond, 2020). The appearance of humans, and particularly their acquired ability to use fire, further shaped fire regimes and ecosystems globally (Beerling et al., 2006; Archibald, Staver, et al., 2012). However, despite these early contributions, the fast rate of human transformations of many processes and components of the Earth system particularly over the past century have led to rapid alterations of these fire regimes (Pausas and Keeley, 2009), with profound consequences on many ecosystems (Barlow et al., 2020) and biogeochemical cycles (Bowman et al., 2009; Archibald, Lehmann, et al., 2018).

Fire regimes are directly and indirectly influenced by human activities (Archibald, Roy, et al., 2009) through changes in ignition patterns (Balch et al., 2017; Hantson, Andela, et al., 2022), landscape fragmentation (Archibald, Staver, et al., 2012), active fire suppression (Doerr et al., 2016), and anthropic climate change (Cattau et al., 2020; Jolly et al., 2015). Humans start fires in relation to agriculture and landscape management - both in modern and traditional practices -, deforestation, accidents or arson (Archibald, Roy, et al., 2009), and are the main cause of fires along with lightning (Veraverbeke et al., 2017). Even

though lightning densities over land are highest near the Equator and greatly decrease towards the poles (Christian et al., 2003), lightning is the main cause of fire in the remote boreal regions (Janssen et al., 2023), while humans are considered to be the main cause of fires in the tropics, both in fire-adapted ecosystems like grasslands and savannas (Andela, Morton, et al., 2019; Archibald, Staver, et al., 2012), and fire-sensitive ecosystems like rainforests (Barlow et al., 2020).

Quantifying how much the current patterns of human-ignited fires differ from those started by lightning is fundamental to assessing the pressures on ecosystems adapted to natural fire regimes. In particular, isolating lightning fires and focusing on their impacts can help to reveal more about the fire regimes that these ecosystems evolved with (Archibald, Staver, et al., 2012). Humans can expand the so-called fire niche to seasons and areas where lightning densities are low (Balch et al., 2017), as long as flammability conditions allow. That is, humans can shift the timing of fires towards drier (Menezes et al., 2022; Archibald, Staver, et al., 2012) or wetter (Balch et al., 2017) weather conditions than lightning fires, and broaden the geographical range of fire occurrence to landscapes with different characteristics (e.g. in terms of fragmentation or topography) (Balch et al., 2017). Both these processes can give rise to fires with different behaviour (e.g. in terms of size and intensity) than those naturally occurring (Hantson, Andela, et al., 2022). In fire-adapted ecosystems, humans can increase or decrease fire frequencies, both with potentially degrading effects due to an excess or a lack of fire (Pivello et al., 2021), contributing to changes in vegetation composition over time (Pinheiro et al., 2009).

The balance between lightning and humans as causes of fire ignition is particularly relevant to the Brazilian Cerrado, the world's most biodiverse tropical savanna (Ratter et al., 2003). This region is formed by fire-adapted grasslands and savannas with different levels of canopy cover intermingled with patches of riverine forests where fire-sensitive species are present (Ribeiro and Walter, 2008). Such diversity is argued to stem from nearby ecosystems evolving adaptation strategies to fire (Simon, Grether, et al., 2009; Simon and Pennington, 2012) which, along with the stochastic nature of fire and other factors such as soil composition (Eiten, 1972), contributed to creating the mosaic of vegetation

that characterises the Cerrado (Coutinho, 1982). In addition, studies on the use of fire by indigenous peoples indicate that, over millennia, different communities developed a refined knowledge of fire management (Mistry, Bilbao, et al., 2016; Mistry, Schmidt, et al., 2019; Mistry, Berardi, et al., 2005; Welch et al., 2013) that further contributed to the Cerrado's heterogeneity (Eloy et al., 2019; Durigan et al., 2020; Fidelis et al., 2018). In these traditional patch mosaic burning practices (Mistry, Bilbao, et al., 2016), fire is used with varying frequencies, and at different times throughout the dry season for a range of purposes, including regenerating pastures, clearing vegetation for cultivation, hunting and landscape management (Mistry, Berardi, et al., 2005; Welch et al., 2013; Melo et al., 2011).

Nowadays, however, industrial agriculture is the main economic activity in the Cerrado, producing both livestock and commercial crops like soybean and sugarcane (Rekow, 2019). This economic transformation has been particularly acute over the past few decades, when over 50% of the Cerrado's native vegetation has been lost to land use changes (Alencar et al., 2020). The current patterns of fire in this region clearly reflect this expansion (Silva, Nogueira, et al., 2021; Segura-Garcia et al., 2024; Silva Arruda et al., 2024), with reductions in burned area where fragmentation is extensive, and increases associated with human activities and climate change where the Cerrado has remained more intact (Conciani et al., 2021; Segura-Garcia et al., 2024; Silva, Nogueira, et al., 2021; Silva Arruda et al., 2024). Humans are considered to be the main cause of fire ignitions in the Cerrado based on the widespread presence of modern agricultural activities and their concomitant use of fire (Coutinho, 1982; Pivello, 2011), the high fire frequencies observed in some areas (Silva Arruda et al., 2024), the mismatch between the fire season and the lightning season (Schumacher, 2022), and the disproportionately larger percentage of human fires compared to lightning fires in nearby ecoregions like the Pantanal (Menezes et al., 2022). However, different studies in some protected areas of the Cerrado suggest that lightning strikes are still a prevalent cause of fires (Ramos-Neto et al., 2000; Pereira and França, 2005; Medeiros and Fiedler, 2004). A formal assessment of fire ignition causes across the whole region, however, is still lacking.

Here, we use geospatial data on individual fire perimeters and lightning occurrence, along with an ignition-cause attribution method (Larjavaara et al., 2005), to identify those fire events in the Cerrado most likely caused by a lightning strike or by human activities over the period 2019-2023. First, we aim to quantify the proportion of lightning and human-caused fires and study how these change throughout the year. Then, we quantify the spatial patterns of lightning and human-caused fires to identify areas of the Cerrado potentially dominated by a certain ignition cause. Finally, we compare the fire frequencies of both ignition types, and their fire behaviour in relation to the level of human presence in the landscape and the weather conditions at ignition. We expect current Cerrado's fire regimes to be largely dominated by human-caused fires, and for these fires to present more extreme behaviour than lightning fires, as previously suggested (Ramos-Neto et al., 2000; Medeiros and Fiedler, 2004; Fiedler et al., 2006).

5.3 Methods

5.3.1 The study area

The Brazilian Cerrado (Figure 5.1) extends over more than 2.2 million km^2, and is composed of very heterogeneous vegetation including primarily grasslands and savannas, but also forest patches (Ribeiro and Walter, 2008). The region stands out for its high levels of biodiversity and endemism (Klink et al., 2005), comprising fire-adapted species and, to a lesser extent, fire-sensitive species. This heterogeneity is reflected in the different ecoregions identified within the Cerrado (Sano et al., 2019). The climate of the Cerrado presents a strong seasonality, with well-defined wet and dry seasons. Annual precipitation varies between 800 mm to over 1,800 mm roughly increasing from east to west (Nascimento et al., 2020). Average annual temperatures vary between 18 ^{o}C and 28 ^{o}C increasing along a latitudinal gradient towards the Equator (Nascimento et al., 2020).

Currently, most of the Cerrado's original native vegetation has been converted to agricultural land uses, and ongoing conversion is still occurring in its northern half, the Matopiba region - comprising the Cerrado of the Brazilian states of Maranhão, Tocantins, Piauí and

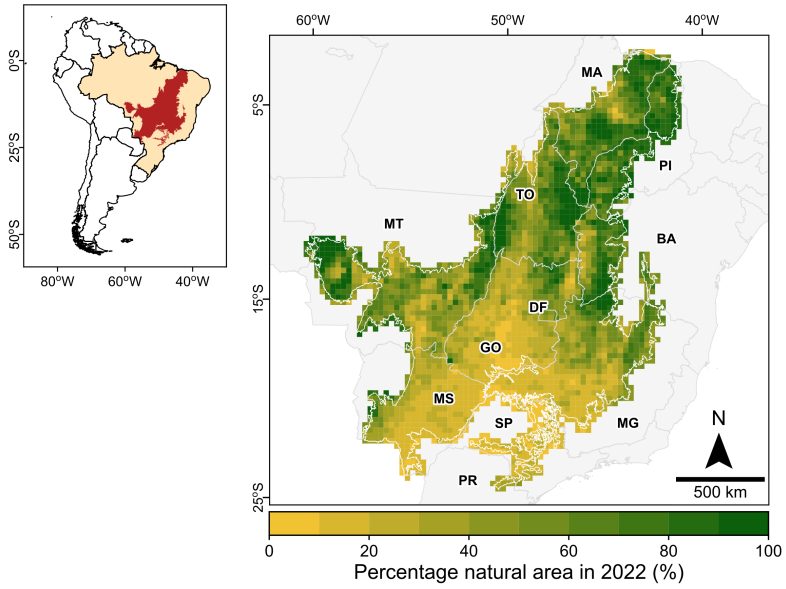

Figure 5.1: Location of the study area (left panel), the Brazilian Cerrado (red), within Brazil (yellow) in South America. The Brazilian Cerrado is coloured according to the natural area percentage of each 30 km grid cell in the year 2022 (right panel). We used the land use data from the MapBiomas Collection 8.0 (Souza et al., 2020) dataset, considering as natural all MapBiomas subcategories under "Forest" (which includes savannas) along with "Wetlands" and "Grassland". Values range from 0-10% natural area (orange), indicating cells mostly converted to human land uses, to 90-100% natural area (green), indicating mostly unconverted landscapes. Grey lines represent the limits of the Brazilian states, and the labels refer to those states with some area within the Cerrado: MT, Mato Grosso; MS, Mato Grosso do Sul; GO, Goiás; DF, Distrito Federal; SP, São Paulo; PR, Paraná; MG, Minas Gerais; MA, Maranhão; TO, Toncantins; PI, Piauí; BA, Bahía.

Bahía (Teixeira Pitta et al., 2017). This ongoing large-scale conversion process in such a biodiverse region makes the Cerrado one of the world's biodiversity hotspots for conservation (Myers et al., 2000).

5.3.2 Data sources

Individual fire data

We used data on individual fire events from the Global Fire Atlas (GFA) (Andela and Jones, 2024), a global dataset derived from the Moderate-resolution Imaging Spectroradiometer (MODIS) MCD64A1 Collection 6.1 (Giglio et al., 2016) burned area data with a daily frequency and 500 m spatial resolution. For the period 2002-present, the GFA

provides information at the individual fire level in the form of georeferenced polygons representing the fire scar and the estimated coordinates of the ignition point, as well as the start and end dates of the fires, their duration, size, perimeter, average length of the daily fire line, and the rate and direction of spread (Andela, Morton, et al., 2019; Andela and Jones, 2024).

To compare the fire behaviour of lightning and human-caused fires, we focused on the size of the fires and on their intensity. The fire size was readily available from the GFA dataset, with a minimum fire size of 0.21 km^2 because of the MODIS spatial resolution. To study the intensity of fires, we combined the GFA data with active fire (AF) observations from the Visible Infrared Imaging Radiometer Suite (VIIRS) (Schroeder et al., 2014). This instrument detects sub-pixel fire activity based on thermal anomalies with a daily overpass frequency and 375 m resolution (Schroeder et al., 2014), and provides fire radiative power (FRP), a measure of the radiative energy of the fire. As such, we restricted our analysis to those GFA polygons overlapping with at least one VIIRS AF within a 500 m distance from the GFA perimeter and within the duration period of the fire indicated by the GFA. Then, we calculated the median FRP of each fire out of all the VIIRS AF overlapping the polygon in space and time.

We used the coordinates of the ignition point and the estimated date of ignition to determine the plausibility that each fire perimeter was ignited by lightning (see Section 5.3.3). To estimate the date and location of the ignition point, the GFA uses an algorithm that searches for local minima of the mapped burned dates of the MCD64A1 pixels within each fire perimeter (Andela, Morton, et al., 2019). As a consequence, the estimated date of ignition has an associated uncertainty between ± 1 day and ± 2 days (Andela, Morton, et al., 2019; Pinto et al., 2020). In addition, we estimated an upper bound for the uncertainty of the location of the ignition point to be around 2.2 km (Supplementary Figure S5.1 a). We estimated this uncertainty by calculating, for each GFA polygon, the maximum distance between the coordinates of the ignition point and the edge of the fire's sub-polygon formed by all pixels with the same burned date contiguous to that of the ignition point. The burned date raster data was also provided by the GFA dataset (Andela

and Jones, 2024).

Lightning data

We used lightning data from the Vaisala Global Lightning Detection Network GLD360, a global dataset on lightning strikes based on a network of lightning sensors. This network records the occurrence of lightning strikes, both cloud-to-ground and cloud-to-cloud, and provides information for each lightning strike: location, timing of occurrence and intensity. For the spatial uncertainty on the lightning ignition location, the dataset provides the angle and lengths of the semi-major and semi-minor axes of the confidence ellipse.

In this study, we used the GLD360 cloud-to-ground data on lightning strikes over the Cerrado for the period January 2019 to December 2023. Based on the information provided by the GLD360 dataset, we estimated that, over the Cerrado, the uncertainty on the location of a lightning strike - which we considered as the median length of the semi-major axis of the 95% confidence ellipse - was around 3.4 km (95% confidence interval, CI, [2.3, 7.8] km) (Supplementary Figure S5.1 b). The uncertainty associated with the time of the lightning strike is the order of seconds - and hence negligible when compared to the temporal uncertainty of GFA ignition points.

Ground truth data on lightning-caused fires

To assess the effectiveness of the fire cause attribution method, we used reference data on observations of fires caused by lightning recorded by the Instituto Chico Mendes de Conservação da Biodiversidade (ICMBio), which is responsible for managing, protecting, monitoring and inspecting the 340 Federal Conservation Units across Brazil. The data provided consisted of two types of datasets recording lightning fires observed in several protected areas across the Cerrado for the period 2020-2023: (a) a georeferenced dataset providing manually drawn polygons of lightning fires with the date of ignition (Supplementary Table S5.1), and (b) a non-georeferenced tabular dataset containing records on the detection of lightning fires (Supplementary Table S5.2). This non-georeferenced dataset (b) contained information on the protected area where the fire occurred, the es-

timated date of ignition, and the type of management intervention (e.g. if the fire was suppressed or no action was taken). The tabular dataset (b) included all the fire events recorded in the georeferenced data (a), in addition to other lightning fire occurrences.

Land use data

To quantify the level of landscape fragmentation across the Cerrado, and hence the level of agricultural presence, we used land use and land cover data from the MapBiomas project (Collection 8.0 (Souza et al., 2020)), which uses the random forest algorithm to classify annual mosaics of Landsat images (30 m spatial resolution). MapBiomas is an open source and open data project that uses Google Earth Engine (Gorelick et al., 2017) to develop their products.

We divided the Cerrado into a 30 km grid, and calculated for each grid cell and year the percentage area occupied by non-converted vegetation - as opposed to human land use area. We simplified MapBiomas Collection 8.0 land use and land cover classes into "anthropic" and "natural" groups, the first comprising "Urban Area", "Mining" and all subcategories under "Farming"; the second comprising all subcategories under "Forest", as well as "Wetland" and "Grassland". Hence, the percentage of natural area was calculated as the percentage of pixels classified as "natural" out of the union of "natural" and "anthropic". Because the MapBiomas Collection 8.0 (Souza et al., 2020) was the last available version at the time of the study and it went only up to the year 2022, we used the land use and land cover data from this year for all those fires in the year 2023.

Climate data

We used climate data to characterise the weather conditions in which the fires took place. We used daily precipitation data from the Climate Hazards Group InfraRed Precipitation with Station data (CHIRPS, version 2.0), a quasi-global rainfall dataset with 0.05^{o} spatial resolution for the period 1981-present (Funk et al., 2015). We used the CHIRPS data product for precipitation as it has been identified as the most reliable dataset for precipitation in tropical climates (Burton et al., 2018). For each ignition point, we calculated the

accumulated precipitation over the 10 days prior to the ignition day.

We used the 2-metre temperature and 2-metre dewpoint temperature from the climate re-analysis dataset ERA5-Land Daily Aggregated product (Muñoz-Sabater et al., 2021), with a 9 km resolution, to calculate the vapour pressure deficit (VPD) - the difference between saturation pressure (e_s) and actual vapour pressure (e_a) (Allen et al., 1998). We calculated the VPD on the day of ignition. We used temperature data from ERA5-Land dataset because it is one of the most reliable data products for temperature for tropical climates (Burton et al., 2018).

Infrastructure data

We used data on two types of infrastructure, roads and urban areas (Supplementary Figure S5.8). We obtained the road data as georeferenced files from the MapBiomas website (https://brasil.mapbiomas.org/dados-de-infraestrutura/, last accessed 27/07/2024), which in turn compiled this data from various sources, including the Geographic and Statistics Institute of Brazil (Instituto Brasileiro de Geografia e Estatística, IBGE). We used the MapBiomas Collection 8.0 (Souza et al., 2020) classifications to create georeferenced polygons of urban areas by drawing polygons of all "Urban Area" pixels for each year.

5.3.3 Data analysis

All data processing and analysis in this study were carried out using Python (Python Software Foundation, https://www.python.org/) and Jupyter Notebook (Kluyver et al., 2016).

Ignition cause attribution method

To identify those fires most likely ignited by lightning, we searched for those GFA polygons that co-occur in space and time with a lightning strike. However, because of the uncertainties in the spatial and temporal location of the fire events and lightning strikes of the datasets used, any attribution method had to allow a certain time lag and spatial gap between the time and location of the observed lightning strikes and those of the ignition

points.

Here, we followed the method of Larjavaara et al. (2005) that assigns an attribution score, B, to every fire quantifying how likely each one is to have been ignited by lightning (Larjavaara et al., 2005), and which has been previously applied to the Pantanal savanna-like wetland (Menezes et al., 2022) in Brazil. Following this method, all lightning strikes within certain spatial and temporal windows from the ignition point are considered to be ignition candidates, but their contribution to the attribution score depends on how far in space and time they are from the ignition point.

This method is implemented in four steps. First, the temporal, Δt_{max}, and spatial, Δx_{max}, windows are selected. Then, every lightning strike, i, and fire, j, pair is assigned a proximity index, $A_{i,j}$, that weights their spatial and temporal separation,

$$A_{i,j} = \begin{cases} \left(1 - \dfrac{\Delta t_{i,j}}{\Delta t_{\text{max}}}\right)\left(1 - \dfrac{\Delta x_{i,j}}{\Delta x_{\text{max}}}\right) & \text{if } \Delta t_{i,j} < \Delta t_{\text{max}}, \Delta x_{i,j} < \Delta x_{\text{max}} \\ 0 & \text{otherwise,} \end{cases} \tag{5.1}$$

where $\Delta t_{i,j}$ expresses the time lag and $\Delta x_{i,j}$ the spatial distance between the lightning strike and the ignition point. This proximity index ranges between 1 (perfect co-occurrence) and 0 (the lightning strike falls outside the temporal or the spatial windows).

Once the lightning strike candidates are identified and their proximity index quantified, the attribution scores, B_j, for a fire j are calculated as

$$B_j = 1 - \prod_{i=1}^{n_j}(1 - A_{i,j}), \tag{5.2}$$

where n_j is the number of lightning candidates for fire j. Finally, all those fires with an attribution score larger or equal than some threshold, B_{thresh}, are considered to be ignited by lightning.

Hence, this attribution method requires making a number of decisions concerning the values of Δt_{max}, Δx_{max}, and B_{thresh}. The choice of these values should aim to balance

omission and commission errors.

Attribution score thresholds, B

Following Menezes et al. (2022), we used a rather high attribution score threshold, $B_{\text{thresh}} = 0.8$, so that, once the temporal and spatial windows were chosen, only those fires with higher attribution scores would be identified as likely caused by lightning. Then, we carried out a preliminary sensitivity analysis (Supplementary Figure S5.2) to understand how the proportion of lightning fires varied with different temporal and spatial windows considering a wide range of values, $\Delta t_{\text{max}} \in [1, 10]$ days and $\Delta x_{\text{max}} \in [2, 25]$ km.

To diminish confusion when comparing lightning and human-caused fires, we imposed a second attribution score threshold to identify those fires most likely caused by humans. Using again a conservative score, only those fires with $B \leq 0.2$ were identified as caused by humans. Consequently, fires with attribution scores between 0.2 and 0.8 were considered as not having a clear ignition cause.

Attribution method windows and uncertainty

Instead of selecting a unique value for the spatial (Δx_{max}) and temporal (Δt_{max}) windows, as has been done before (Dorph et al., 2022; Moris, Conedera, et al., 2020; Pérez-Invernón, Huntrieser, Soler, et al., 2021; Pérez-Invernón, Huntrieser, and Moris, 2022), we selected a set of plausible combinations, $\{(\Delta t_{\text{max}}, \Delta x_{\text{max}}), \Delta t_{\text{max}} \in [3, 7]$ days and $\Delta x_{\text{max}} \in [6, 12]$ km$\}$. For each $(\Delta t_{\text{max}}, \Delta x_{\text{max}})$ pair, we identified those fires with $B \geq 0.8$ as caused by lightning, those with $B \leq 0.2$ as caused by humans, and the remaining fires (B between 0.2 and 0.8) as having no clear ignition cause. Then, we quantified the number of fires per ignition category (lightning, humans or not clear) and calculated the percentage of fires and the percentage of total burned area corresponding to each ignition category. Then, we estimated the final percentages for each ignition category as the average values obtained from all temporal and spatial window pairs, $\{(\Delta t_{\text{max}}, \Delta x_{\text{max}})\}$. Finally, we assessed how much these percentages varied when using different $(\Delta t_{\text{max}}, \Delta x_{\text{max}})$ values, which we expressed as a 95% CI around the mean using the bootstrapping algorithm

(Mokhtar et al., 2023).

The time elapsed between the lightning strike and the moment in which the fire is first detected by an observer or detection device is commonly referred to as holdover time (Moris, Álvarez-Álvarez, et al., 2023). In this case, the detection time corresponds to the day of ignition provided by the GFA dataset, so the holdover time depends on when the Terra and Aqua satellites overpass the fire, the presence of clouds (Moris, Álvarez-Álvarez, et al., 2023) - particularly in the Cerrado (Pereira, Pereira, et al., 2017; Libonati, DaCamara, et al., 2015) -, when the spectral signal from the burn scar becomes detectable to the MODIS instrument, and the uncertainties on the day of burn from the MCD64A1 burned area algorithm (Giglio et al., 2016) and from the GFA dataset (around 2 to 4 days (Andela, Morton, et al., 2019)).

Considering these sources of uncertainties, most studies identifying lightning-caused fires use a Δt_{max} around 5 days (Menezes et al., 2022). In this study, we considered a range of values, $\Delta t_{\text{max}} \in [3, 7]$ day, because the MODIS uncertainty on the day of burn can reach up to 6 days in the Cerrado (Pinto et al., 2020). In addition, because MODIS' uncertainty on the day of burn is ± 1 day in 45% of the cases (Pinto et al., 2020), the GFA dataset could be reporting ignition dates around one day or more earlier than the actual start of the fire. Therefore, when running the attribution method algorithm, we included as candidates all lightning strikes falling from Δt_{max} days before the GFA day of ignition to one day after.

Regarding Δx_{max}, the mismatch between the lightning strike location and that of the ignition point depends on the uncertainty of these two locations, as well as spatial mismatches derived from delays in the detection of the fire. As indicated earlier, the uncertainty on the location of the lightning strike could go up to 8 km, and that of the GFA ignition point up to 2.2 km (Supplementary Figure S5.1). Therefore, we considered $\Delta x_{\text{max}} \in [6, 12]$ km to identify fire-igniting lightning candidates. Again, this range is also in accordance with other studies, which usually consider spatial windows around 8-10 km (Moris, Conedera, et al., 2020; Dorph et al., 2022; Pérez-Invernón, Huntrieser, Soler, et al., 2021).

Validation of the attribution method with ground truth data

Next, we used both the georeferenced dataset (with fire polygons) and the non-georeferenced dataset (in tabular format) provided by ICMBio containing observed lightning-caused fires as ground truth data for our attribution method. Even though the number of records in the ICMBio dataset on lightning fires was too small to allow a full statistical validation, we used the two datasets to verify whether the attribution method was able to identify any of the ground truth records as caused by lightning. Therefore, although we could not use the ground truth data to select the Δt_{max} and Δx_{max} values that balanced commission and omission errors of identification, at least we could have an indication of whether it was able to identify any lightning fires at all.

Regarding the georeferenced vector dataset, a total of 11 fire polygons were selected after inspection of the data (Supplementary Table S5.1). Out of these, we found that 6 events had been mapped by the GFA dataset (i.e. GFA polygons overlapping in time and space with the corresponding ICMBio ground truth records). Next, we evaluated whether any of these 6 fires were identified as caused by lightning by the attribution method and found that 5 of these had an attribution score $B > 0.8$ for at least one of the $(\Delta t_{\text{max}}, \Delta x_{\text{max}})$ combinations considered. The remaining fire had a score B between 0.7 and 0.8 for $\Delta x_{\text{max}} = 12$ km and all Δt_{max} considered (Supplementary Figure S5.3).

Even though the non-georeferenced tabular dataset did not provide the exact location of fires, it indicated that in specific protected areas of the Cerrado and in specific dates some lightning-caused fires had occurred. Hence, as a further check to the attribution method, we explored whether there were any fire polygons in the GFA dataset overlapping these protected areas within a period up to five days before and one day after the ignition date recorded in the tabular ICMBio data, and whether any of these records had $B \geq 0.8$. In the non-georeferenced tabular data, there were 20 records reporting lightning-caused fires in different protected areas and dates (Supplementary Table S5.2). The GFA dataset detected 14 fire polygons corresponding to 7 out of these 20 tabular records. Out of these 14 fire polygons, we identified 13 polygons as likely caused by lightning ($B \geq 0.8$)

(Supplementary Figure S5.3). The remaining polygon had, again, an attribution score B between 0.7 and 0.8. We also noted that these 13 fire polygons included the 6 fire polygons contained in the ICMBio georeferenced data.

Characterising the spatial patterns of fires and lightning strikes

Next, we explored how the lightning and human-caused fires were distributed across the landscape. For each 30 km grid cell, year, and combination of spatial and temporal windows, we obtained the number of fires in each ignition category (lightning, human or not clear). Then, for each cell and year, we calculated the average number and percentage of fires in each ignition category out of all the $\{(\Delta t_{\text{max}}, \Delta x_{\text{max}})\}$ combinations, and the corresponding 95% CI using bootstrapping. Finally, for each cell, we calculated the average annual number of fires of each ignition category, along with the 95% CI of the mean. Even though we took into account that a number of fires had no clear ignition cause when calculating the percentages, we focused the spatial analysis only on the lightning and human-caused fires.

Regarding lightning densities, we counted the number of strikes per grid cell and year and calculated the annual average number of lightning densities. Again, we also calculated the 95% CI around the mean.

Characterising the fire frequencies of lightning and human fires

We then quantified the fire frequencies of humans ($B \leq 0.2$) and lightning ($B \geq 0.8$) ignited fires. In this case, we used $\Delta t_{\text{max}} = 5$ days and $\Delta x_{\text{max}} = 9$ km, the middle values out of all temporal and spatial window combinations considered earlier, to identify the ignition causes of each GFA polygon. Then, to calculate the fire frequencies, we counted how many times each pixel had burned in the period for each ignition cause. Therefore, fire frequencies would range from 1 year to 5 consecutive years in the period 2019 to 2023. Finally, to compare the fire frequencies between lightning and human-caused fires, we normalised the pixel count (equivalent to burned area) of each frequency and ignition cause by the corresponding total number of affected pixels (the total area that burned at

least once for that type of ignition).

Characterising the climatic and the landscape fragmentation conditions of fires

Next, we compared the conditions in which the human-caused ($B \leq 0.2$) and the lightning-caused ($B \geq 0.8$) fires took place, both in terms of the weather and fuel conditions at ignition, and in terms of the level of fragmentation of the landscapes where the fires happened. Both weather and fragmentation are known to affect fire behaviour (Archibald, Roy, et al., 2009). Again, we used $\Delta t_{\text{max}} = 5$ days and $\Delta x_{\text{max}} = 9$ km to calculate the attribution scores B.

Regarding the weather conditions, we compared the distribution of the precipitation accumulated over the ten days prior to the ignition of the fire and the VPD on the ignition day, which we used as proxies of fuel flammability. We did so for all fires in the study period and per month.

Then, each GFA fire polygon was assigned to the grid cell containing the fire ignition point. In this manner, the landscape characteristics where the fire took place were assessed in terms of the natural area percentage of the cell and year where the fire started. We did the same for each lightning strike in the study period. Then, we classified the occurrences of each type of event (lightning-caused fires, human-caused fires and lightning strikes) according to the decile of natural area percentage - a proxy for the level of fragmentation. To understand how each type of event was distributed across landscapes with different levels of natural area percentage, we divided the number of occurrences in a decile by the total area occupied by that decile.

Finally, for each GFA polygon, we calculated the distance from the ignition point to the closest road and to the closest urban area. Because the distance distributions we obtained for lightning-caused fires were very skewed towards small values for both types of infrastructure, we also calculated the shortest distances for all lightning strikes in the period. In this manner, we could interpret whether the skewness of the distance distribution could be related to lightning strikes also being more likely to fall close to these two types of infrastructure.

Comparing fire behaviour between lightning and human fires

We compared the fire behaviour of lightning and human-caused fires focusing on two measures of fire behaviour: fire size and median FRP. We compared the distributions of each of these two variables for lightning ($B \geq 0.8$) and human ($B \leq 0.2$) ignitions for the whole study period and by month. We also explored the distribution of these two variables per decile of natural area percentage because the level of landscape fragmentation can also affect fire behaviour. Again, we used $\Delta t_{\text{max}} = 5$ days and $\Delta x_{\text{max}} = 9$ km.

Finally, we compared the largest (fire size $\geq$ 150 km^2) and the most intense (median FRP $\geq$ 100 MW) fires separately by ignition cause. For each of these two variables, we explored the weather conditions at ignition against the level of natural area percentage of the landscape where they took place.

5.4 Results

5.4.1 Quantifying lightning fires

Using the attribution method for a set of temporal and spatial windows, $\{(\Delta t_{\text{max}}, \Delta x_{\text{max}}),\ \Delta t_{\text{max}} \in [3, 7]$ days and $\Delta x_{\text{max}} \in [6, 12]$ km$\}$, we estimated that, in the period 2019-2023, 7.5% (95% CI, [6.0, 9.0]%) of all fires in the Brazilian Cerrado were ignited by lightning, 89.1 % (95% CI, [86.9, 91.3]%) were ignited by humans, and a remaining 3.4% (95% CI, [2.7, 4.1]) had no clear ignition cause. Similarly, around 7.9% (95% CI, [5.6, 10.4]%) of the annual burned area was caused by lightning fires, 88.7% (95% CI, [85.3, 92.0]%) was caused by humans, and 3.4% (95% CI, [2.4, 4.4]%) had no clear ignition cause.

Exploring these percentages by year, we observed some inter-annual variability both in the number of lightning fires and in the burned area associated with this type of fires (Figure 5.2). In both cases, 2021 was the year with the lowest percentage of lightning fires, 6.5 [6.0, 7.0]%, and burned area caused by lightning, 5.8% (95% CI, [5.2, 6.4]%); while 2023 was the year with the highest values, 10.1% (95% CI, [9.3, 11.1]%) and 11.7%

(95% CI, [10.7, 12.8]%) respectively.

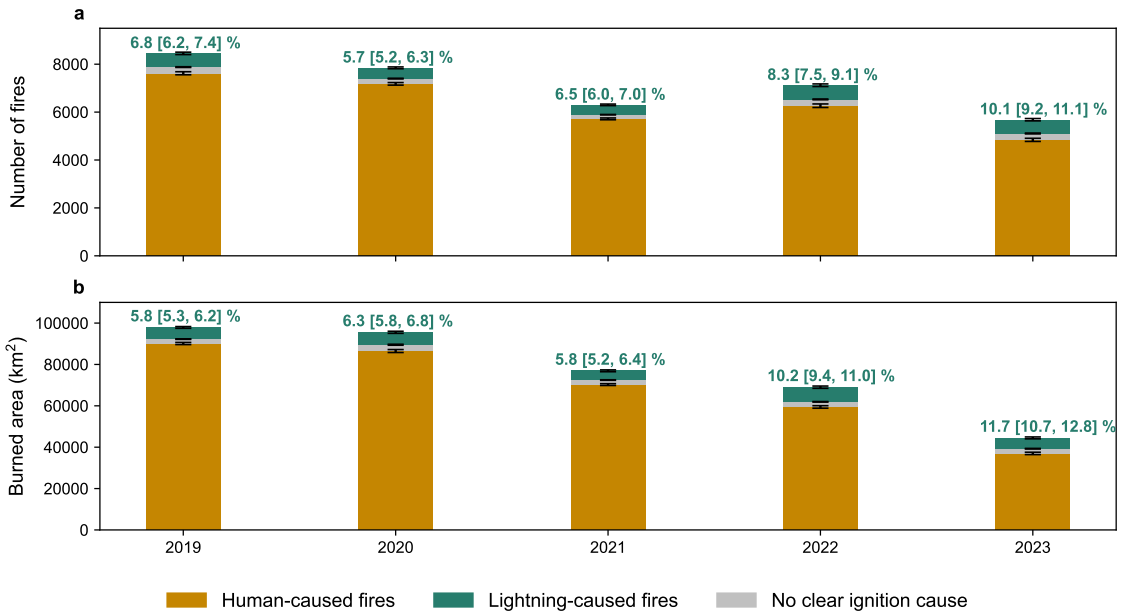

Figure 5.2: Inter-annual variability throughout the study period (2019-2023) of the number of fires, **a**, caused by humans (brown) and lightning (green), or with no clear cause of ignition (grey), and the corresponding annual burned areas, **b**. Numbers indicate the percentage of fires ignited by lightning in the year (**a**), and the percentage of burned area from lightning fires (**b**). Fires were considered to be ignited by lightning if their attribution score was $B \geq 0.8$, ignited by humans if $B \leq 0.2$, and the remaining fires were not considered to have a clear ignition cause. Given these attribution score thresholds, the different values shown by the coloured bars were obtained as the average out of those numbers of fires, or average burned areas, obtained when using different combinations of spatial and temporal windows in the attribution method, $\{(\Delta t_{\max}, \Delta x_{\max}),\ \Delta t_{\max} \in [3, 7]$ days and $\Delta x_{\max} \in [6, 12]$ km$\}$ (see Methods). Error bars indicate the 95% confidence interval (CI) around these averages when using the different window combinations and were obtained using bootstrapping.

Most lightning fires occurred in the transition from the dry to the wet season, in September and October (Figure 5.3 a). While the lightning-fire season was concentrated in these two months - and to a lesser extent in November -, the human-caused fire season commenced notably earlier, spanning from May to October, and peaking in August and September (Figure 5.3 a).

Quantifying the balance between lightning and human-caused fires in each month, we observed that the dry season was clearly dominated by human fires, as they caused more

than 80% of fires from May to October (Figure 5.3 b). In contrast, during the wettest months of the period, December to February, the percentage of lightning fires was similar or even larger than those of human fires, albeit in remarkably smaller numbers than during the dry season (Figures 5.3 a and b). Interestingly, in October, the month with the highest number of lightning fires, these accounted for 20.9% (95% CI, [13.9, 27.7]%) of fires, while in September this percentage was only 8.1% (95% CI, [2.6, 13.6]%). Finally, July was the month with the lowest percentage of lightning fires, causing less than 1% of fires.

5.4.2 Spatial patterns of lightning-caused and human-caused fires across the Cerrado

Next, we looked at the spatial distribution of lightning and human-caused fires across the Cerrado in the period 2019-2023 (Figures 5.4 a and b respectively). Here, we excluded those cells that experienced less than 10 fires in total over the period to prevent results that may not be representative of ignition dynamics but rather capturing noise. The excluded cells were concentrated in the south of the Cerrado (Figure 5.4 d) where landscapes are highly fragmented (Figure 5.1) and usually present fewer and smaller fires associated with longer human occupation (Silva, Nogueira, et al., 2021), and are also prone to larger omission errors (Rodrigues et al., 2019).

We found considerable overlap between the areas where most lightning and most human fires occur (Figure 5.4 a and b). However, there was a notable exception to these overlapping patterns in the northern ecoregion of Alto Parnaíba (Sano et al., 2019), where fires were predominantly caused by human ignitions, which caused more than 90% of fires (Figure 5.4 d). Nonetheless, in general, the Cerrado's fire regimes were dominated by anthropic fires, as humans were the main ignition cause of fires ($\geq$ 50%) in 94.5% of the grid cells with more than 10 fires on average in the period (Figure 5.4 d).

The percentage of lightning fires across grid cells ranged from 0 to around 60%, and only less than 2% of the Cerrado's area presented percentages above 40%. In general, the average number of lightning fires per year was small, around 4 fires in the grid cells with the

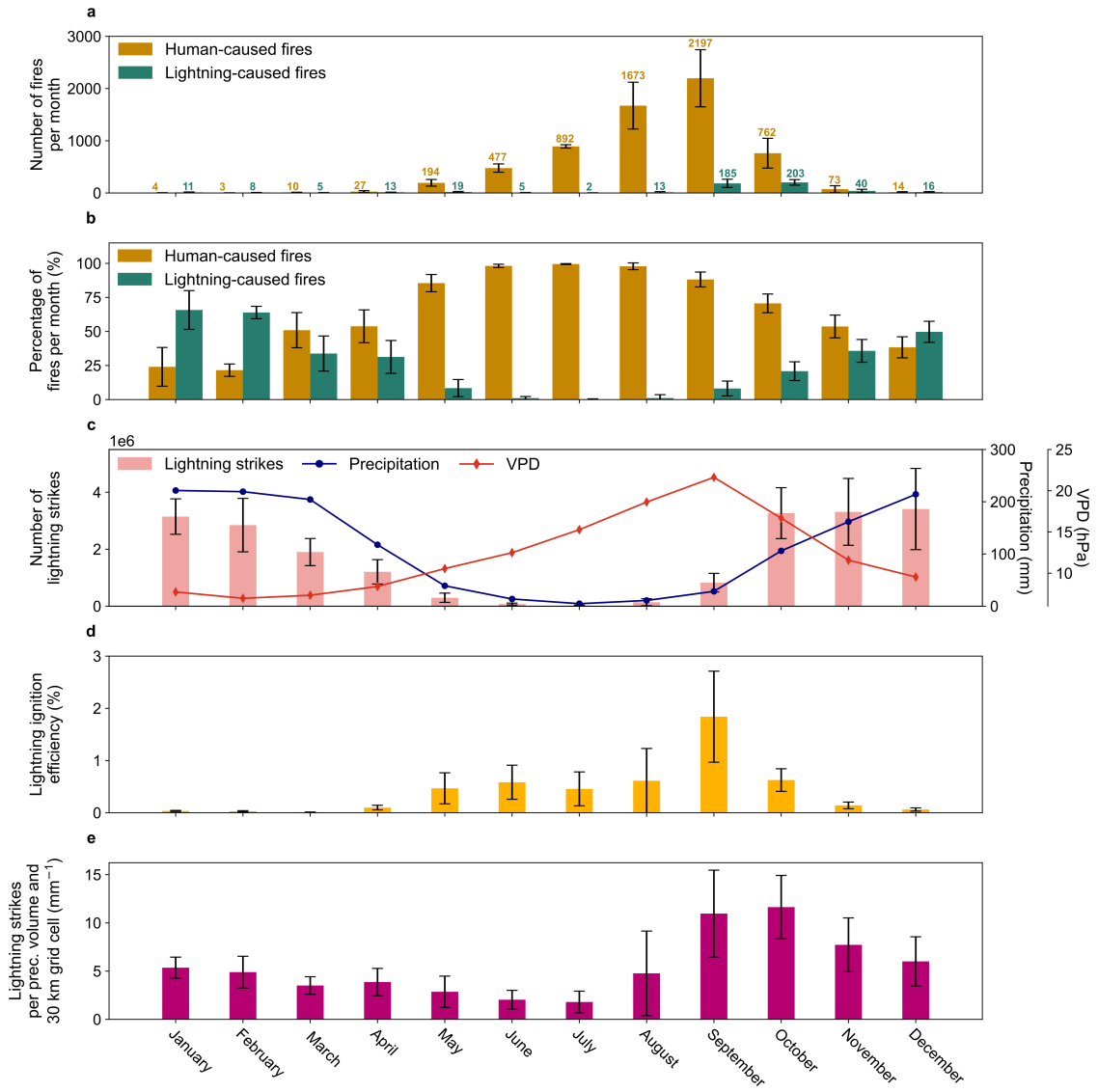

Figure 5.3: **a** Average number of human-caused (brown) and lightning-caused (green) fires per month in the study period, 2019-2023. The numbers indicate the average number of fires per month and type of ignition and are included for reference. In each year and month, a number of fires may have no clear ignition cause (not represented in this figure). **b** Average monthly percentage of fires for each type of ignition. Lightning and human-caused fire percentages in each month do not necessarily add up to 100% as there can be fires with no clear ignition cause (see Methods). **c** Average number of lightning strikes per month (pink), average monthly precipitation (blue) and vapour pressure deficit (VPD, red). **d** Lightning ignition efficiency, the number of lightning strikes igniting fires divided by the total number of lightning strikes. **e** Ratio of the number of total lightning strikes to precipitation per month and grid cell. Error bars were obtained from the standard deviation and represent the 95% confidence interval (CI).

highest occurrences. Lightning fires were concentrated in the ecoregions of the Bananal, the west of the Araguaia Tocantins, and the northwest of Planalto Central (Sano et al., 2019) (Figure 5.4 a). The southern parts of these areas presented the largest percentages of lightning fires (Figure 5.4 d).

5.4.3 The spatiotemporal patterns of lightning

We also characterised the seasonality of lightning and its spatial patterns across the Cerrado. First, as expected, we observed a strong temporal co-occurrence of precipitation and lightning (Figure 5.3 c). Accordingly, in the middle of the dry season, from June to August, the number of lightning strikes was lowest, while they were highest during the wet season, December to February. In fact, there were 100 times more lightning strikes during the later period than the former. However, the lightning ignition efficiency was highest from May to October (between 0.5 and 1.8%, Figure 5.3 d), while from December to March only about 0.04% of lightning strikes ignited fires.

Interestingly, September and October were the months with the largest numbers of lightning strikes per unit volume of precipitation (Figure 5.3 e), exactly those months in which the number of lightning-caused fires peaked. Hence, during the transition from the dry to the wet season, when the first rains begin but the monthly precipitation has not yet reached its peak, there is a higher number of lightning strikes per precipitation volume compared to the rest of the year.

Lightning strikes were not uniformly distributed across the Cerrado (Figure 5.4 c). In particular, the state of Tocantins presented the highest levels of lightning density, along with the northern parts of Mato Grosso and the north of Goiás, in the centre-west of the Cerrado. The state of Mato Grosso in the south-west, and the north-eastern tip of the Cerrado experienced intermediate levels of lightning activity. In contrast, the south-eastern regions of the Cerrado along with an area roughly corresponding to the Alto Parnaíba ecoregion (Sano et al., 2019) in the north presented the lowest levels of lightning densities, about ten times fewer strikes than the grid cells with highest levels. Finally, during the dry season and particularly in June, many areas of the Cerrado experienced no lightning strikes

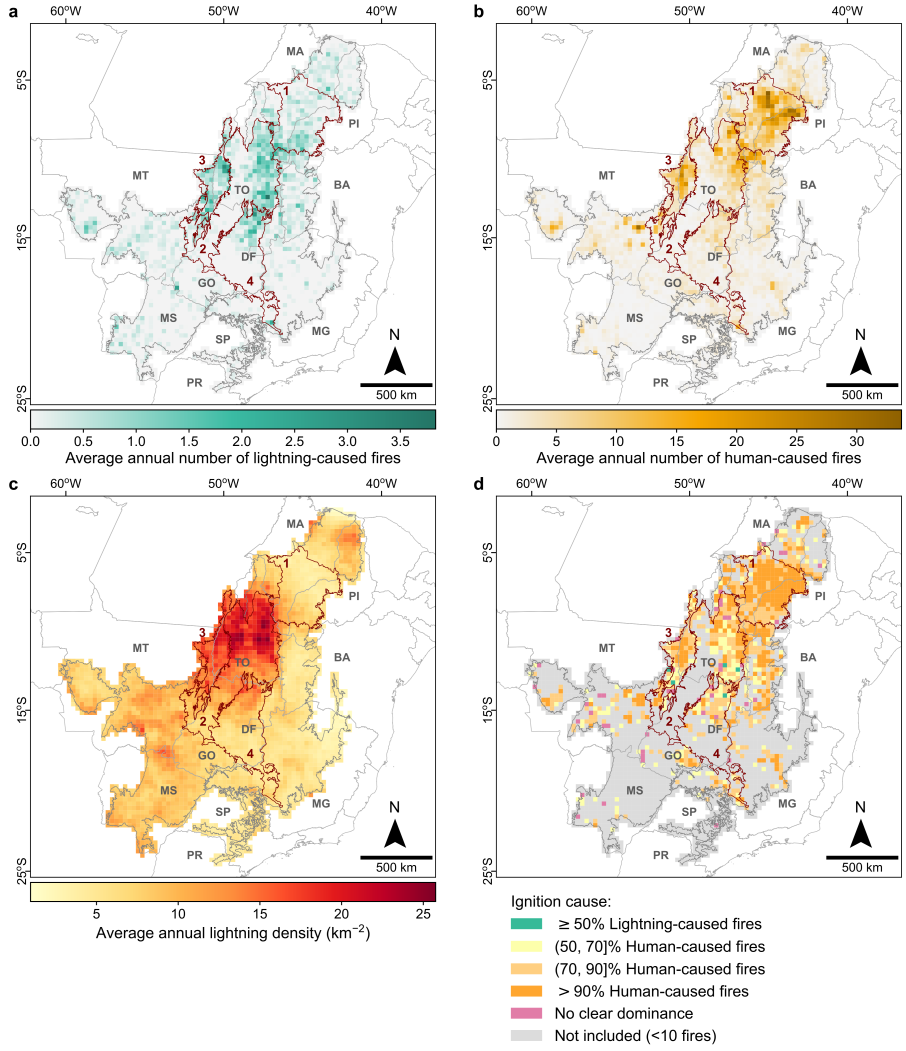

Figure 5.4: Average annual number of **a** lightning and **b** human-caused fires, and **c** lightning density in each 30 km cell over the Cerrado in the period 2019-2023. Note that maps **a** and **b** have different scales so that the spatial variation in the number of lightning-caused fires is visible despite its numbers being overall much smaller than those of human-caused fires. **d** map showing the grid cells dominated by lightning (green) or human ignitions (yellow and oranges), that is, where one of the two causes of ignitions accounts for 50% or more of the ignitions in a grid cell. Grid cells coloured in pink do not have an ignition cause accounting for more than 50% of fires (as there are fires with no clear ignition cause). Cells with less than 10 fires on average in the period appear in grey. Areas and numeric labels highlighted in red correspond to the Cerrado ecoregions referred to in the text: 1, Alto Parnaíba; 2, Araguaia Tocantins; 3, Bananal; 4, Planalto Central. Grey labels indicated the Brazilian states intersecting the Cerrado: MT, Mato Grosso; MS, Mato Grosso do Sul; GO, Goiás; DF, Distrito Federal; SP, São Paulo; PR, Paraná; MG, Minas Gerais; MA, Maranhão; TO, Tocantins; PI, Piauí; BA, Bahía.

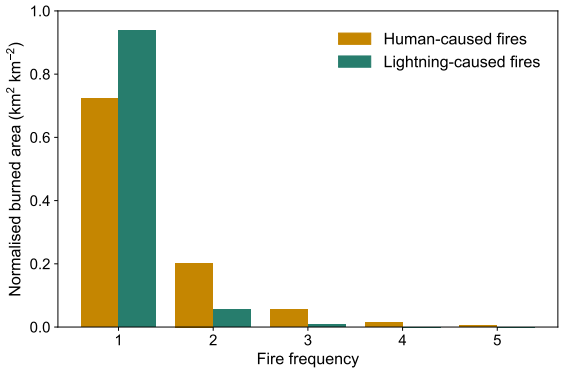

Figure 5.5: Fire frequency distributions for lightning-caused (green) and human-caused (brown) fires in the period 2019-2023. Bars represent the areas burned by each type of ignition a certain number of times in the study period divided by the total area affected at least once by that ignition cause. Here, we identified lightning ($B \geq 0.8$) and human ($B \leq 0.2$) caused fires using $\Delta t_{\text{max}} = 5$ days and $\Delta x_{\text{max}} = 9$ km. The fires with intermediate attribution scores, B between 0.2 and 0.8, were considered as having no clear cause of ignition and were excluded from this analysis.

- especially in the centre, while the southern- and northern-most parts of the Cerrado did experience some level of lightning activity throughout the year (Supplementary Figure S5.4).

5.4.4 The fire frequencies of lightning and human-caused fires

We also quantified the fire frequencies of lightning and human-caused fires (Figure 5.5). Comparing the fire frequency distributions, we found that most of the area affected by fire over the 5 years of the study period burned only once for both types of ignition. However, around 28% of the areas affected by human-caused fires burned two times or more, while only about 6% of the areas affected by lightning burned more than once in 5 years. Furthermore, the lightning-affected area that burned four times was very small (3 km^2, $\simeq 0.01\%$) and none burned five times. In contrast, around 3,550 km^2 were affected by human-caused fires four times ($\simeq 1.4\%$ of the human-affected area), and 1,190 km^2 ($\simeq 0.5\%$) burned every year between 2019 and 2023.

5.4.5 Comparing weather conditions and landscape characteristics

Next, we explored the weather conditions at the time of each fire occurrence and the landscape characteristics where fires took place, as both these factors can affect fire behaviour. We measured the landscape characteristics in terms of the natural area percentage of the grid cell where each ignition happened, and the distance to the nearest road and urban area.

Regarding weather conditions, we explored the amount of precipitation accumulated over the ten days prior to the ignition on the location where the fire started, as well as the VPD on the day of ignition. We found that lightning-ignited fires took place in more humid conditions than human-started fires, with overall larger accumulated precipitation and lower VPD values (Figure 5.6 c and d). Importantly, we observed these same patterns when comparing by month (Figure 5.6 a and b), with particularly acute differences from August to October.

Then, we explored how the fire density (number of fires per unit area) for both ignition causes and the lightning strikes density changed with the level of natural area percentage (Supplementary Figure S5.5). We found that, even though the lightning density was similar across levels of natural area - meaning there was a similar number of lightning ignition opportunities across fragmentation levels -, the number of lightning-caused fires detected increased with the percentage of natural area (Supplementary Figure S5.5 b). Similarly, the number of human-caused fires detected increased towards less converted landscapes (Supplementary Figure S5.5 a). Hence, most fires occurred in landscapes with $\geq 60\%$ of natural area for both ignition causes.

Finally, we also explored the distances from each ignition point to the nearest road and urban area, as well as for a subset of 500,000 lightning strikes selected at random (in the interest of computational time). We found that the distance distributions for these three types of events were skewed towards small values (Supplementary Figures S5.6 a and c). That is, the proportion of fires (both lightning and human) and lightning strikes happening at shorter distances was larger than the number of fires and strikes occurring

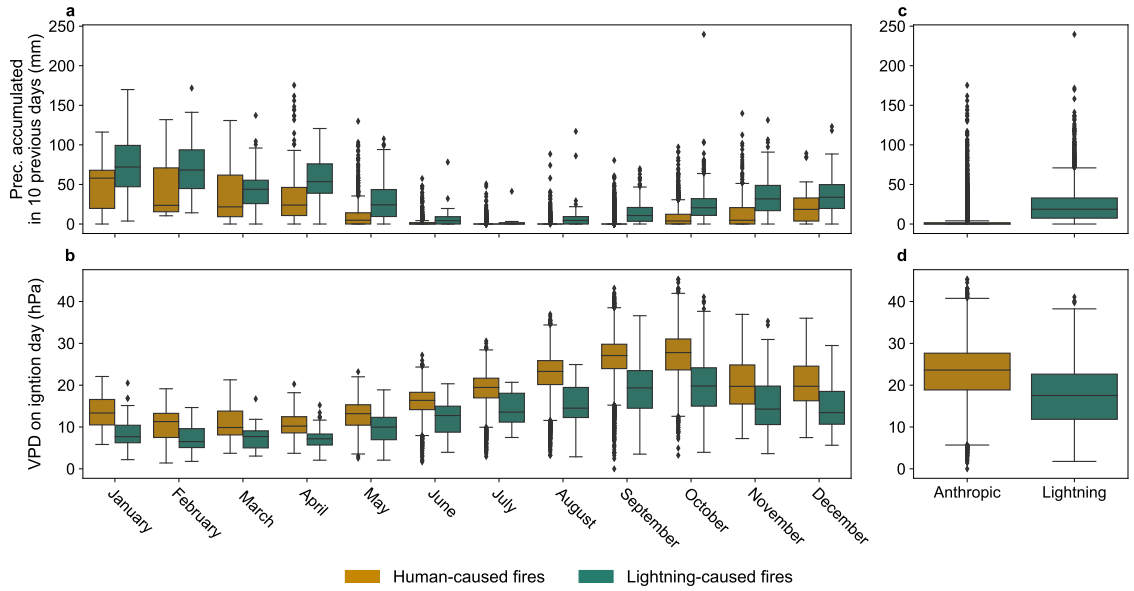

Figure 5.6: **a**, distribution of the precipitation accumulated over the 10 days prior to the fire start per month for lightning (green) and human-caused (brown) fires, and, **b**, over the study period 2019-2023. **c**, distribution of vapour pressure deficit (VPD) values on the day of ignition per month, and, **d**, over the whole period, per ignition cause. Here, we identified lightning ($B \geq 0.8$) and human ($B \leq 0.2$) caused fires using $\Delta t_{\max} = 5$ days and $\Delta x_{\max} = 9$ km. The fires with intermediate attribution scores, B between 0.2 and 0.8, were considered as having no clear cause of ignition and were excluded from this analysis.

further away. Still, we did observe that the distribution of distances for human-caused fires seemed slightly more skewed towards small values than that of lightning-caused fires (Supplementary Figure S5.6). In addition, however, the most remote human-caused fires started at similar distances from roads to those of the most remote lightning-caused fires (Supplementary Figure S5.6).

5.4.6 Comparing fire behaviour in relation to ignition cause

Finally, we compared the behaviour of lightning and human-ignited fires examining the distributions of fire size and median FRP (Figure 5.7 and Supplementary Figure S5.7). While we did not observe apparent differences in the medians (Figure 5.7), there were remarkable differences in the largest values of the fire size and median FRP distributions (Figure 5.7). For example, the largest human-caused fires were about one order of magni-

tude larger than the largest lightning-caused fires (Figures 5.7 b), and the largest median FRP values were about two times larger (Figure 5.7 d).

Differences in fire properties between lightning and human-caused fires were conditional on the timing of fire ignition. The largest human-ignited fires occurred in August (Figure 5.7 a), when the difference between largest sizes was also greatest; followed by September, when the largest lightning fires were closer in size to the human-caused ones. In contrast, we did not observe remarkable differences between the largest sizes of the two types of fires in October nor during the wet season (Figure 5.7 a).

Regarding FRP, we observed similar seasonality patterns (Figure 5.7 b), with generally small values during the wet season for both types of fire. The most intense human-caused fires took place in the dry season, while the most intense lightning fires occurred in the dry-wet transition period. Again, human-caused fires had higher FRP values than lightning ones during these periods, while they were overall similar during the wet season.

Lastly, we explored the weather conditions and landscape characteristics of the largest ($\geq$ 150 km^2) and most intense ($\geq$ 100 MW) fires (Figure 5.8). We found that the largest human-caused fires took place in the less fragmented landscapes ($\geq$ 80 %) and in the driest conditions (Figures 5.8 a and b, and Supplementary Figure S5.7 a). In contrast, the largest lightning-fires were more spread out across landscapes ($\geq$ 50 % natural area) and practically all of them occurred in areas that had experienced some rainfall in the days before the fire (Figure 5.8 a). In addition, the largest lightning fires occurred overall in lower VPD conditions than human ones (Figure 5.8 b). Regarding FRP values, the most intense fires were spread out across all levels of fragmentation (Figures 5.8 c and d, and Supplementary Figure S5.7 b), and the most intense human-caused fires took place in drier and hotter conditions than the most intense lightning fires.

5.5 Discussion

Across the Brazilian Cerrado, we estimated that 7.5% (95% CI, [6.0, 9.0]%) of all fire ignitions are caused by lightning, while human activities were attributed 89.1% (95%

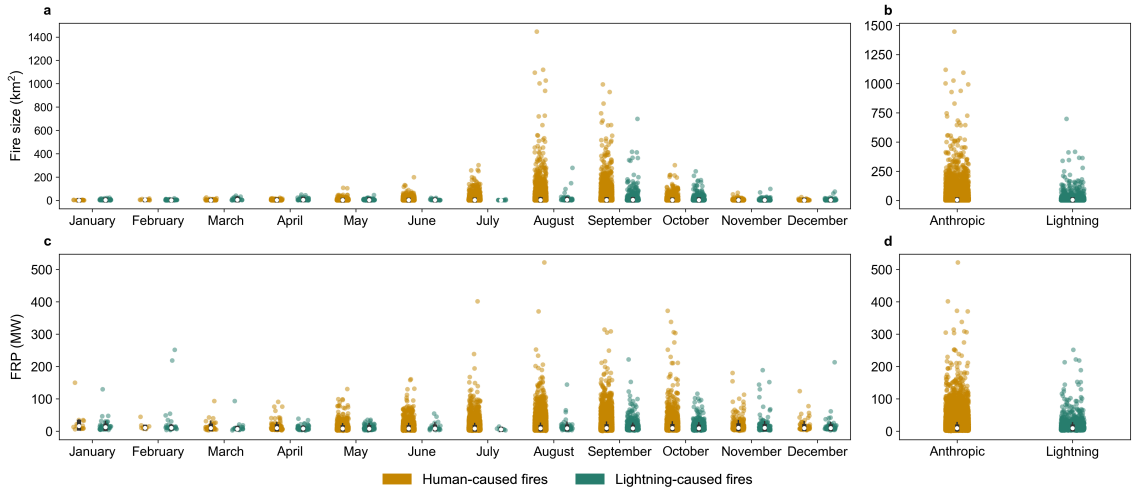

Figure 5.7: Distribution of the fire sizes and median fire radiative power (FRP) of lightning (green) and human-caused (brown) fires. The distributions are shown as a stripplot of the observations - that is, each brown or green dot in the graph represents a fire event. The white dots represent the median value of each distribution, and the black box-and-whisker show the quartiles of the distributions. **a** and **c** show the distributions per month for fire size and median FRP respectively. **b** and **d** show the fire size and median FRP distributions over the period 2019-2023 respectively. We identified lightning ($B \geq 0.8$) and human ($B \leq 0.2$) caused fires using $\Delta t_{\text{max}} = 5$ days and $\Delta x_{\text{max}} = 9$ km. The fires with intermediate attribution scores, B between 0.2 and 0.8, were considered as having no clear cause of ignition and were excluded from this analysis.

CI, [86.9, 91.3]%) of fire ignitions - be it for agricultural purposes, for native vegetation conversion, as part of fire management practices or accidentally -, and 3.4% (95% CI, [2.7, 4.1]%) did not have a clear ignition cause. Our findings highlight the extent of the human footprint on the Cerrado's current fire regimes, and how these substantially differ compared to lightning-caused fire regimes. Indeed, we found that human ignitions dominate across the Cerrado, as they account for more than 50% of fires (Balch et al., 2017) in over 90% of its area (Figure 5.4 d). Apart from increasing the number of ignitions, humans lengthen three-fold the fire season and shift it towards months with drier weather conditions (Figure 5.3 a and c). Moreover, we found that humans are the cause of the largest and most intense fires (Figure 5.8), with extreme fire behaviour that is not observed amongst the fires ignited by lightning. We found that these differences may be attributed to lightning often being accompanied by rainfall and moist weather conditions that prevent extreme fire behaviour, which is not the case for human ignitions (Figures 5.6

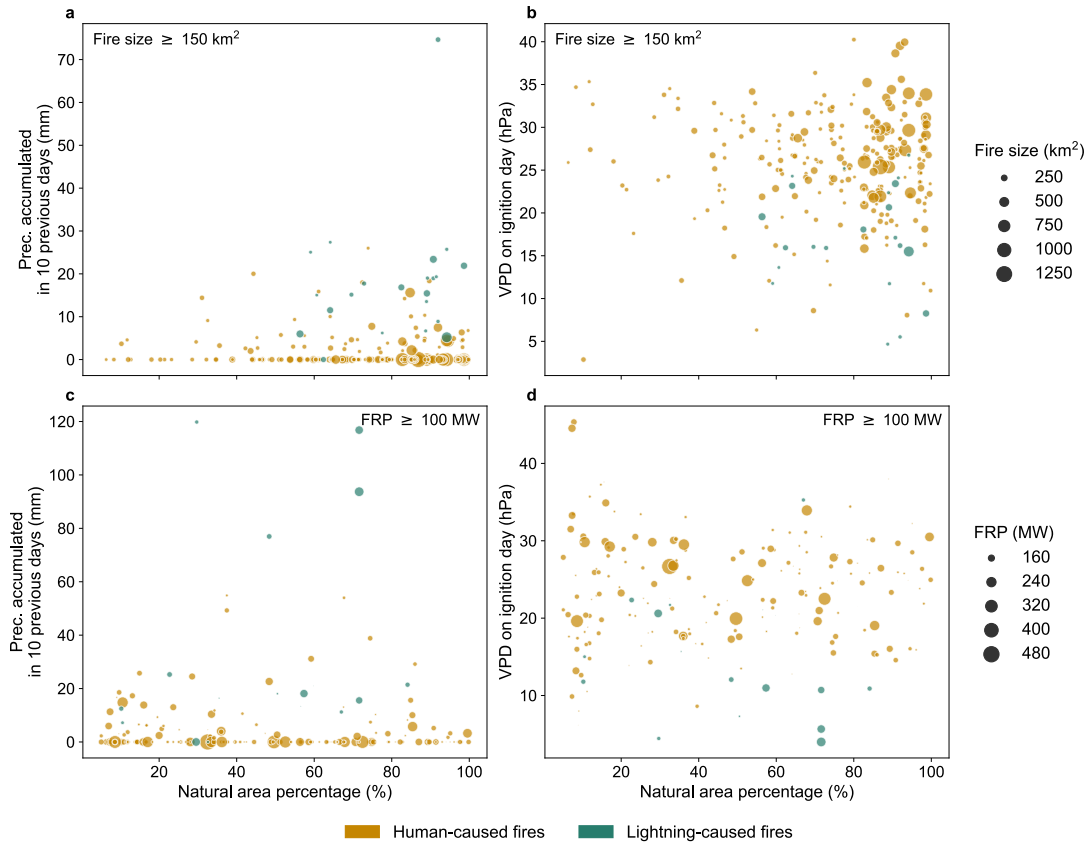

Figure 5.8: Weather conditions (y-axis) and natural area percentage (x-axis) of the ignition points of the largest ($\geq$ 150 km^2) fires (top row) and for those with the highest median fire radiative power (FRP) values ($\geq$ 100 MW) (bottom row). Each dot represents a fire observation coloured by the type of ignition, either human-caused (brown) or lightning-caused (green). The size of the dot represents the size (top row) or the median FRP value (bottom row) of the fire. **a** and **c**, show the relation between the precipitation accumulated in the 10 days prior to ignition and the percentage of natural area of the cell where the fire took place for the largest and most intense fires respectively. **b** and **d**, show the relation between the VPD conditions on the day of ignition and the percentage of natural area for the largest fires and most intense fires respectively. We identified lightning ($B \geq 0.8$) and human ($B \leq 0.2$) caused fires using $\Delta t_{\text{max}} = 5$ days and $\Delta x_{\text{max}} = 9$ km. The fires with intermediate attribution scores, B between 0.2 and 0.8, were considered as having no clear cause of ignition and were excluded from this analysis.

and 5.8).

We estimated that most lightning-caused fires, around 75%, took place in the transition period from the dry to the wet seasons (September and October, Figure 5.3 a), in agreement with previous studies in different areas of the Cerrado (Schumacher, 2022; Ramos-Neto

et al., 2000; Medeiros and Fiedler, 2004; Fiedler et al., 2006; Souza Neves et al., 2018), while they were much lower during the core months of the dry and wet seasons (June to August and December to March). The trade-off between vegetation dryness and the occurrence of sufficient ignition opportunities enabling the fire seasons (Bond and Keeley, 2005) may explain these temporal patterns. The moisture content of the vegetation diminishes throughout the dry season and larger ratios of biomass become flammable (Zanzarini et al., 2022), explaining the higher lightning-ignition efficiency observed during the dry season (Figure 5.3 d), as noted in other ecosystems (Hessilt et al., 2022). However, the density of lightning strikes from June to August is very low (Figure 5.3 c) - precisely due to the lack of atmospheric events leading to cloud formation -, possibly acting as a limiting factor to the occurrence of lightning-ignited fires. Conversely, during the wet season, lightning density is not limited (Supplementary Figure S5.4), but high precipitation and low VPD impair fuel flammability, thus limiting fire occurrence regardless of ignition cause (Figure 5.3 a). However, the quantification of fires during this period must be considered with care because wet-season fires tend to be small, patchy and of low intensity (Ramos-Neto et al., 2000; Medeiros and Fiedler, 2004; Fiedler et al., 2006), and the cloud cover much denser, making them less likely to be identified in satellite-based burned area products (Rodrigues et al., 2019; Prudente et al., 2020). Therefore, our results seemingly underestimate the amount of fires occurring during the wet season, a period during which studies in different Cerrado protected areas and other savanna-like ecosystems have observed numerous lightning fires (Ramos-Neto et al., 2000; Medeiros and Fiedler, 2004; Fiedler et al., 2006; Menezes et al., 2022). In the dry-to-wet transition periods, however, we observed that lightning density increases as rainfall restarts, while precipitation has not yet reached maximum levels and VPD is still high (Figure 5.3 c), so large amounts of fuel may still have low moisture content. In addition, we find a larger ratio of lightning strikes per precipitation volume in September and October (Figure 5.3 e). This confluence of factors can explain the higher incidence of lightning fires in this period.

The majority of fires, however, are caused by humans and take place over a longer period (May to October), precisely during drier months (Figure 5.3 a and c), as suggested in pre-

vious studies (Pivello, 2011; Mataveli et al., 2018; Mataveli et al., 2017; Silva, Nogueira, et al., 2021). This shift in the fire seasonality implies that Cerrado vegetation could be experiencing fires in a phase of the phenological cycle that may not correspond to the timing of fire it co-evolved with (Fontenele et al., 2023). Such mismatch, combined with the drier and hotter conditions in which most fires now happen, could have negative impacts on native vegetation, even if adapted to fire (Pivello et al., 2021). Further, human-caused fires present higher fire frequencies when compared to lightning-ignited fires (Figure 5.5), possibly as a result of the use of fire in modern agricultural practices to burn residues or renew pastures carried out regularly in the same areas (Pivello, 2011). The stochastic nature of lightning strikes and the necessary co-occurrence with appropriate flammability conditions, however, may limit the probability of high frequencies associated with lightning-caused fires.

Moreover, using accumulated precipitation and the VPD on the day of ignition as proxies for fuel moisture content (Spessa et al., 2005; Russell-Smith et al., 2007), we found that even when happening in the same month, human-caused fires tend to take place in drier and hotter conditions than lightning-caused fires (Figure 5.6). These differences emphasise the fact that, as long as fuels are sufficiently flammable and continuous, human ignitions are less constrained than lightning ignitions, which tend to co-occur with rainfall events even during the dry season (Schumacher, 2022). In addition, the remarkable differences in weather conditions during the transition period also suggest that human ignitions may have a tendency to target drier weather, especially when set to fulfill a purpose (Pivello, 2011). By elongating and shifting the fire season, humans expand the climatic niche of fires (Balch et al., 2017) in Cerrado to weather conditions that would otherwise be rare if solely ignited by lightning, a process that may have been occurring since the first humans arrived in the Cerrado (Miranda et al., 2002).

We found that both lightning and human-caused fires are concentrated in regions of the Cerrado with larger native vegetation remnants, while the incidence of both types of fires is low in highly fragmented areas (Supplementary Figure S5.5). Such patterns indicate that the distribution of fires in the Cerrado may be more dependent on bioclimatic and

landscape factors, as previously suggested (Mataveli et al., 2018; Silva, Nogueira, et al., 2021; Silva Arruda et al., 2024; Segura-Garcia et al., 2024), than on the type of ignition. Therefore, while humans modify the rates of fire ignition above natural levels across the Cerrado, they also exert strong controls on fire spread through fragmentation and active fire suppression (Silva, Nogueira, et al., 2021; Archibald, 2016; Archibald, Roy, et al., 2009) on both lightning and human-caused fires.

Still, satellite burned area products with coarse resolution, such as MCD64A1 from which the GFA is derived, can only capture fires larger than a certain size (around 0.21 km^2 in the GFA) and have high omission errors in agricultural landscapes of Cerrado where fires tend to be small and their spectral signal can be confounded (Rodrigues et al., 2019; Campagnolo et al., 2021). Using a higher spatial resolution (20 m) burned area product, Ramo et al., 2021 found that in sub-Saharan Africa, small fires ($<$ 100 ha) make up 41% of total burned area, but only 5% of these were mapped in the MCD64A1 product (Ramo et al., 2021). Hence, we are probably underestimating the number of small fires in the Cerrado as well (Rodrigues et al., 2019; Campagnolo et al., 2021). Additionally, the lightning strikes dataset may also contain omission errors, thus contributing to the underestimation of lightning-ignited fires.

We observed human-ignited fires at large distances from roads and urban areas (Supplementary Figure S5.6), indicating some human presence in the less fragmented areas of the Cerrado. In addition, many large patches of Cerrado vegetation limit with agricultural lands (Medeiros and Fiedler, 2004), and the use of fires to renew pastures that escape human control has been documented in some of these areas (Marimon et al., 2012; Souza Neves et al., 2018). Such ignition dynamics may be coupling with climate change contributing to the increasing fire frequency and burned area observed in the more intact parts of the Cerrado (Silva, Libonati, et al., 2024; Segura-Garcia et al., 2024), exerting further pressures on native vegetation.

Importantly, we found a continuous region in the north of the Cerrado strongly dominated by human ignitions (causing $\geq$90% of fires, Figure 5.4 d). This area corresponds to the ecoregion of Alto Parnaíba (Sano et al., 2019), within the so-called Matopiba region.

Matopiba is considered to be the Cerrado's last agricultural frontier and has experienced large-scale native vegetation conversion over the past two decades (Teixeira Pitta et al., 2017; Rekow, 2019), where fire may be used in relation to agri-business activities (Silva, Rodrigues, et al., 2020; Ribeiro, Santos, et al., 2024). Interestingly, this area presents a lower density of lightning strikes than other parts of the Cerrado (Figure 5.4 c), which could explain the lower number of lightning-caused fires.

Comparing the fire behaviour of lightning and human fires, we found the most remarkable differences in the largest values of fire size and FRP distributions rather than in the medians, as observed in previous studies comparing fire behaviour for different fire categories (Libonati, Pereira, et al., 2021). For both types of ignitions, the largest and most intense fires are concentrated in the dry season (Figure 5.7) as expected (Ramos-Neto et al., 2000), as this is the period when the vegetation is more flammable, giving rise to higher fire intensities and effectively extending the fuel bed continuity (Archibald, Roy, et al., 2009). However, the largest ($\geq$150 km^2) and most intense ($\geq$ 100 MW) human-ignited fires occurred in overall drier conditions than the lightning fires counterparts (Figure 5.8). In both cases, the largest fires occurred in the least converted landscapes (>80% natural area, Figure 5.8), also as expected because land use fragmentation exerts a strong control on fire size (Archibald, Roy, et al., 2009; Hantson, Pueyo, et al., 2015; Haas et al., 2022). Therefore, given similar levels of landscape fragmentation, the different weather conditions at the time of the fire start appear as a determining factor explaining the more extreme behaviour of human fires, even though the weather conditions over the duration of fires will also contribute to their size and intensity.

Throughout this study, we have focused on lightning and human ignitions. However, there is a fundamental distinction that must be made between small-scale traditional uses of fires, the use of prescribed fires in integrated fire management (IFM) practices (Santos et al., 2021; Andrade et al., 2021), and those uses associated with modern agricultural activities (Pivello, 2011; Medeiros, 2002). Indigenous peoples and pastoral communities in the first case, and environmental agencies and other organisations in the second, use mosaic burning practices where fire is planned and managed (Mistry, Berardi, et al.,

2005; Pivello, 2011). These practices intend to create landscapes of patches with different fire histories, which can contribute to shaping and maintaining Cerrado's heterogeneous vegetation (Eloy et al., 2019; Durigan et al., 2020; Fidelis et al., 2018). In modern agricultural uses, however, fire occurrence in native vegetation is usually a by-product of its use in the cultivation of commercial crops and cattle-ranching fields (Pivello, 2011) or in native vegetation conversion (Pivello, 2011) and arson (Medeiros and Fiedler, 2004). In these cases, fire is used with high frequencies, concentrated in the dry and late-dry season, and with little control on fire escape into adjacent native vegetation (Pivello, 2011). Future studies could further discriminate ignition cause amongst IFM, traditional practices, modern agricultural activities and lightning, to deepen our understanding about the fire regimes created in each case and how they may be impacted by climate change.

5.6 Conclusions

Our results highlighted the profound differences between the Cerrado's fire regimes caused by lightning and by human ignitions. We provided quantitative evidence that humans are the main cause of fires across the Brazilian Cerrado, creating an excessive number of ignitions and higher fire frequencies in comparison to lightning. Still, we also showed that lightning ignites a small but relevant fraction of fires, particularly in the transition period from the dry to the wet season, when adequate flammability conditions and high lightning densities concur. In contrast, humans lengthen threefold the fire season by starting fires throughout the drier months of the year and in generally more flammable conditions than lightning, leading to more extreme fire behaviour. Further, we found that both types of fires are primarily concentrated in the least converted areas of the Cerrado, seemingly constrained by the level of landscape fragmentation (Silva, Nogueira, et al., 2021; Silva Arruda et al., 2024; Segura-Garcia et al., 2024). Therefore, our results indicate that, through fire ignitions, humans are altering the fire regimes of the largest remnants of Cerrado native vegetation towards more frequent fires and extreme behaviour than would naturally occur. Even though most Cerrado ecosystems are adapted to fire, these patterns of human ignitions can have negative impacts affecting the structure of the

vegetation and lead to biodiversity losses (Pivello et al., 2021). In this sense, the recently adopted Brazilian National Policy on IFM (Lei n. 14,944) that regulates the use of fire for agricultural practices - apart from recognising the role of fire in Cerrado ecosystems and promoting its use for conservation (Schmidt et al., 2020) - is a promising way forward in light of the findings presented in this study. However, the extent to which Cerrado has been converted and its fire regimes altered stress the urgency and scale of conservation needed to protect this region.

5.7 Data and code availability statement

The climate data used in this study are publicly available from ERA5-Land Monthly Averaged at https://www.ecmwf.int/en/forecasts/dataset/ecmwf-reanalysis-v5-land, and Climate Hazards Group InfraRed Precipitation with Station data version 2.0 at https://data.chc.ucsb.edu/products/CHIRPS-2.0/. The land use data are publicly available from MapBiomas collection 8.0 at https://brasil.mapbiomas.org/en/colecoes-mapbiomas/. The Global Fire Atlas data are publicly available from https://zenodo.org/records/11400062. The lightning strikes data from the Vaisala Global Lightning Detection Network GLD360 will be made publicly available (and a link to the repository provided) upon acceptance or if requested during review process in a coarsened format as it is subject to contractual agreement. The code supporting this study will also be made available through a repository and a link will be provided.

5.8 Acknowledgements

We thank Esther Brambleby for subsetting and formatting the lightning data. We thank the Ecosystems Lab Group at the Environmental Change Institute, School of Geography and the Environment, University of Oxford, for helpful feedback during discussions. We also thank the Instituto Chico Mendes de Conservação da Biodiversidade (ICMBio) for the ground truth data on lightning-ignited fires in Cerrado's protected areas. C.S.G. was supported by the UK Natural Environment Research Council under grant number

NE/S007474/1.

5.9 References

Alencar, Ane et al. (2020). “Mapping Three Decades of Changes in the Brazilian Savanna Native Vegetation Using Landsat Data Processed in the Google Earth Engine Platform”. In: *Remote Sensing* 12.6, p. 924.

Allen, Richard G. et al. (1998). *Crop evapotranspiration - Guidelines for computing crop water requirements*. FAO - Food and Agriculture Organization of the United Nations.

Andela, Niels and Matthew William Jones (2024). *Update of: The Global Fire Atlas of individual fire size, duration, speed and direction*. Version v20240409. Zenodo.

Andela, Niels, Douglas C Morton, et al. (2019). “The Global Fire Atlas of individual fire size, duration, speed and direction”. In.

Andrade, Ananda Santa Rosa de et al. (2021). “Implementation of Fire Policies in Brazil: An Assessment of Fire Dynamics in Brazilian Savanna”. In: *Sustainability* 13.20, p. 11532.

Archibald, S, C E R Lehmann, et al. (2018). “Biological and geophysical feedbacks with fire in the Earth system”. In: *Environmental Research Letters* 13.3, p. 033003.

Archibald, Sally (2016). “Managing the human component of fire regimes: lessons from Africa”. In: *Philosophical Transactions of the Royal Society B: Biological Sciences* 371.1696, p. 20150346.

Archibald, Sally, David P. Roy, et al. (2009). “What limits fire? An examination of drivers of burnt area in Southern Africa”. In: *Global Change Biology* 15.3, pp. 613–630.

Archibald, Sally, A. Carla Staver, and Simon A. Levin (2012). “Evolution of human-driven fire regimes in Africa”. In: *Proceedings of the National Academy of Sciences* 109.3, pp. 847–852.

Balch, Jennifer K. et al. (2017). “Human-started wildfires expand the fire niche across the United States”. In: *Proceedings of the National Academy of Sciences* 114.11, pp. 2946–2951.

Barlow, Jos et al. (2020). “Clarifying Amazonia’s burning crisis”. In: *Global Change Biology* 26.2, pp. 319–321.

Beerling, David J. and Colin P. Osborne (2006). “The origin of the savanna biome”. In: *Global Change Biology* 12.11, pp. 2023–2031.

Bond, W and J Keeley (2005). “Fire as a global ‘herbivore’: the ecology and evolution of flammable ecosystems”. In: *Trends in Ecology & Evolution* 20.7, pp. 387–394.

Bond, William J. (2015). “Fires in the Cenozoic: a late flowering of flammable ecosystems”. In: *Frontiers in Plant Science* 5.

Bowman, David M. J. S. et al. (2009). “Fire in the Earth System”. In: *Science* 324.5926, pp. 481–484.

Burton, C., S. Rifai, and Y. Malhi (2018). “Inter-comparison and assessment of gridded climate products over tropical forests during the 2015/2016 El Niño”. In: *Philosophical Transactions of the Royal Society B: Biological Sciences* 373.1760, p. 20170406.

Campagnolo, M.L. et al. (2021). “A comprehensive characterization of MODIS daily burned area mapping accuracy across fire sizes in tropical savannas”. In: *Remote Sensing of Environment* 252, p. 112115.

Cattau, Megan E et al. (2020). “Anthropogenic and lightning-started fires are becoming larger and more frequent over a longer season length in the USA”. In: *Global Ecology and Biogeography* 29.4. Publisher: Wiley Online Library, pp. 668–681.

Christian, Hugh J. et al. (2003). “Global frequency and distribution of lightning as observed from space by the Optical Transient Detector”. In: *Journal of Geophysical Research: Atmospheres* 108 (D1).

Conciani, Dhemerson E. et al. (2021). “Human-climate interactions shape fire regimes in the Cerrado of São Paulo state, Brazil”. In: *Journal for Nature Conservation* 61, p. 126006.

Coutinho, L. M. (1982). “Ecological Effects of Fire in Brazilian Cerrado”. In: *Ecology of Tropical Savannas*. Ed. by Brian J. Huntley and Brian H. Walker. Red. by W. D. Billings et al. Vol. 42. Series Title: Ecological Studies. Berlin, Heidelberg: Springer Berlin Heidelberg, pp. 273–291.

Doerr, Stefan H. and Cristina Santín (2016). “Global trends in wildfire and its impacts: perceptions versus realities in a changing world”. In: *Philosophical Transactions of the Royal Society B: Biological Sciences* 371.1696, p. 20150345.

Dorph, Annalie et al. (2022). “Modelling ignition probability for human- and lightning-caused wildfires in Victoria, Australia”. In: *Natural Hazards and Earth System Sciences* 22.10, pp. 3487–3499.

Durigan, Giselda et al. (2020). “No Net Loss of Species Diversity After Prescribed Fires in the Brazilian Savanna”. In: *Frontiers in Forests and Global Change* 3, p. 13.

Eiten, George (1972). “The cerrado vegetation of Brazil”. In: *The Botanical Review* 38.2, pp. 201–341.

Eloy, Ludivine et al. (2019). “Seasonal fire management by traditional cattle ranchers prevents the spread of wildfire in the Brazilian Cerrado”. In: *Ambio* 48.8, pp. 890–899.

Fidelis, Alessandra et al. (2018). “The Year 2017: Megafires and Management in the Cerrado”. In: *Fire* 1.3, p. 49.

Fiedler, Nilton César, Daniela Araújo Merlo, and Marcelo Brilhante de Medeiros (2006). “Ocorrência de incêndios florestais no Parque Nacional da Chapada dos Veadeiros, Goiás.” In: *Ciência Florestal* 16.2, pp. 153–161.

Fontenele, Hudson GV and Heloisa S Miranda (2023). “What happens when fire is too early? Observations of fire-stimulated fruit opening releasing underdeveloped seeds for an endemic Cerrado shrub”. In: *Austral Ecology* 48.8. Publisher: Wiley Online Library, pp. 2246–2252.

Funk, Chris et al. (2015). “The climate hazards infrared precipitation with stations—a new environmental record for monitoring extremes”. In: *Scientific Data* 2.1, p. 150066.

Giglio, Louis, Wilfrid Schroeder, and Christopher O. Justice (2016). “The collection 6 MODIS active fire detection algorithm and fire products”. In: *Remote Sensing of Environment* 178, pp. 31–41.

Glasspool, I.J., D. Edwards, and L. Axe (2004). “Charcoal in the Silurian as evidence for the earliest wildfire”. In: *Geology* 32.5, p. 381.

Gorelick, Noel et al. (2017). “Google Earth Engine: Planetary-scale geospatial analysis for everyone”. In: *Remote sensing of Environment* 202. Publisher: Elsevier, pp. 18–27.

Haas, Olivia, Iain Colin Prentice, and Sandy P Harrison (2022). “Global environmental controls on wildfire burnt area, size, and intensity”. In: *Environmental Research Letters* 17.6, p. 065004.

Hantson, Stijn, Niels Andela, et al. (2022). “Human-ignited fires result in more extreme fire behavior and ecosystem impacts”. In: *Nature Communications* 13.1, p. 2717.

Hantson, Stijn, Salvador Pueyo, and Emilio Chuvieco (2015). “Global fire size distribution is driven by human impact and climate”. In: *Global Ecology and Biogeography* 24.1. Publisher: Wiley Online Library, pp. 77–86.

He, Tianhua, Byron B Lamont, and John Manning (2016). “A Cretaceous origin for fire adaptations in the Cape flora”. In: *Scientific Reports* 6.1. Publisher: Nature Publishing Group UK London, p. 34880.

He, Tianhua, Juli G Pausas, et al. (2012). “Fire-adapted traits of Pinus arose in the fiery Cretaceous”. In: *New Phytologist* 194.3. Publisher: Wiley Online Library, pp. 751–759.

Hessilt, Thomas D et al. (2022). “Future increases in lightning ignition efficiency and wildfire occurrence expected from drier fuels in boreal forest ecosystems of western North America”. In: *Environ. Res. Lett.*

Hoffmann, William A., Birgit Orthen, and Paula Kielse Vargas do Nascimento (2003). “Comparative fire ecology of tropical savanna and forest trees: *Fire traits of savanna and forest trees*”. In: *Functional Ecology* 17.6, pp. 720–726.

Janssen, Thomas A. J. et al. (2023). “Extratropical forests increasingly at risk due to lightning fires”. In: *Nature Geoscience*.

Jolly, W. Matt et al. (2015). “Climate-induced variations in global wildfire danger from 1979 to 2013”. In: *Nature Communications* 6.1, p. 7537.

Klink, Carlos A. and Ricardo B. Machado (2005). “Conservation of the Brazilian Cerrado”. In: *Conservation Biology* 19.3, pp. 707–713.

Kluyver, Thomas et al. (2016). “Jupyter Notebooks – a publishing format for reproducible computational workflows”. In: *Positioning and Power in Academic Publishing: Players, Agents and Agendas*. Ed. by F. Loizides and B. Schmidt. IOS Press, pp. 87–90.

Larjavaara, M., J. Pennanen, and T.J. Tuomi (2005). “Lightning that ignites forest fires in Finland”. In: *Agricultural and Forest Meteorology* 132.3, pp. 171–180.

Libonati, R., J. M. C. Pereira, et al. (2021). “Twenty-first century droughts have not increasingly exacerbated fire season severity in the Brazilian Amazon”. In: *Scientific Reports* 11.1, p. 4400.

Libonati, Renata, Carlos DaCamara, et al. (2015). “An Algorithm for Burned Area Detection in the Brazilian Cerrado Using 4 μm MODIS Imagery”. In: *Remote Sensing* 7.11, pp. 15782–15803.

Marimon, Beatriz Schwantes et al. (2012). “Florística dos campos de murundus do Pantanal do Araguaia, Mato Grosso, Brasil”. In: *Acta Botanica Brasilica* 26.1, pp. 181–196.

Mataveli, Guilherme Augusto Verola et al. (2017). *Analysis of fire dynamics in the Brazilian savannas*. preprint. Other Hazards (e.g., Glacial, Snow Hazards, Karst, Wildfires Hazards, and Medical Geo-Hazards).

– (2018). "Satellite observations for describing fire patterns and climate-related fire drivers in the Brazilian savannas". In: *Natural Hazards and Earth System Sciences* 18.1, pp. 125–144.

Medeiros, Marcelo Brilhante de (2002). "Manejo do fogo em unidades de conservação do cerrado". In: *Boletim do Herbário Ezechias Paulo Heringer* 10.

Medeiros, Marcelo Brilhante de and Nilton Cezar Fiedler (2004). "Incêndios florestais no parque nacional da Serra da Canastra: desafios para a conservação da biodiversidade." In: *Ciência Florestal* 14.2, pp. 157–168.

Melo, Mônica Martins and Carlos Hiroo Saito (2011). "Regime de queima das caçadas com uso do fogo realizadas pelos Xavante no Cerrado". In: *Biodiversidade Brasileira* 1.2, pp. 97–109.

Menezes, Lucas S et al. (2022). "Lightning patterns in the Pantanal: Untangling natural and anthropogenic-induced wildfires". In: *Science of the Total Environment*.

Miranda, Heloisa S, Mercedes MC Bustamante, and Antonio C Miranda (2002). "The fire factor". In: *The cerrados of Brazil: ecology and natural history of a neotropical savanna*. Columbia University Press, pp. 51–68.

Mistry, Jayalaxshmi, Andrea Berardi, et al. (2005). "Indigenous Fire Management in the cerrado of Brazil: The Case of the Krahô of Tocantíns". In: *Human Ecology* 33.3, pp. 365–386.

Mistry, Jayalaxshmi, Bibiana A. Bilbao, and Andrea Berardi (2016). "Community owned solutions for fire management in tropical ecosystems: case studies from Indigenous communities of South America". In: *Philosophical Transactions of the Royal Society B: Biological Sciences* 371.1696, p. 20150174.

Mistry, Jayalaxshmi, Isabel Belloni Schmidt, et al. (2019). "New perspectives in fire management in South American savannas: The importance of intercultural governance". In: *Ambio* 48.2, pp. 172–179.

Mokhtar, Siti Fairus, Zahayu Md Yusof, and Hasimah Sapiri (2023). "Confidence intervals by bootstrapping approach: a significance review". In: *Malaysian Journal of Fundamental and Applied Sciences* 19.1, pp. 30–42.

Moris, Jose V., Pedro Álvarez-Álvarez, et al. (2023). "A global database on holdover time of lightning-ignited wildfires". In: *Earth System Science Data* 15.3, pp. 1151–1163.

Moris, Jose V., Marco Conedera, et al. (2020). "Lightning-caused fires in the Alps: Identifying the igniting strokes". In: *Agricultural and Forest Meteorology* 290, p. 107990.

Muñoz-Sabater, Joaquín et al. (2021). "ERA5-Land: a state-of-the-art global reanalysis dataset for land applications". In: *Earth System Science Data* 13.9, pp. 4349–4383.

Myers, Norman et al. (2000). "Biodiversity hotspots for conservation priorities". In: *Nature* 403.6772, pp. 853–858.

Nascimento, Diego Tarley Ferreira and Giuliano Tostes Novais (2020). "Clima do Cerrado: dinâmica atmosférica e características, variabilidades e tipologias climáticas". In.

Oliveras, Immaculada and Yadvinder Malhi (2016). “Many shades of green: the dynamic tropical forest–savannah transition zones”. In: *Philosophical Transactions of the Royal Society B: Biological Sciences* 371.1703, p. 20150308.

Pausas, Juli G. and William J. Bond (2020). “Alternative Biome States in Terrestrial Ecosystems”. In: *Trends in Plant Science* 25.3, pp. 250–263.

Pausas, Juli G. and Jon E. Keeley (2009). “A Burning Story: The Role of Fire in the History of Life”. In: *BioScience* 59.7, pp. 593–601.

Pausas, Juli G., Jon E. Keeley, and Dylan W. Schwilk (2017). “Flammability as an ecological and evolutionary driver”. In: *Journal of Ecology* 105.2. Ed. by Mark Rees, pp. 289–297.

Pereira, Alfredo and Helena França (2005). “Identificação de queimadas naturais ocorridas no período chuvoso de 2003-2004 no Parque Nacional das Emas, Brasil, por meio de imagens dos sensores do satélite CBERS-2”. In: *Anais XII Simpósio Brasileiro de Sensoriamento Remoto, Goiânia, Brasil, INPE*, pp. 3245–3252.

Pereira, Allan, José Pereira, et al. (2017). “Burned Area Mapping in the Brazilian Savanna Using a One-Class Support Vector Machine Trained by Active Fires”. In: *Remote Sensing* 9.11, p. 1161.

Pérez-Invernón, Francisco J., Heidi Huntrieser, and Jose V. Moris (2022). “Meteorological Conditions Associated with Lightning Ignited Fires and Long-Continuing-Current Lightning in Arizona, New Mexico and Florida”. In: *Fire* 5.4, p. 96.

Pérez-Invernón, Francisco J., Heidi Huntrieser, Sergio Soler, et al. (2021). “Lightning-ignited wildfires and long continuing current lightning in the Mediterranean Basin: preferential meteorological conditions”. In: *Atmospheric Chemistry and Physics* 21.23, pp. 17529–17557.

Pinheiro, Eduardo Da Silva and Giselda Durigan (2009). “Dinâmica espaço-temporal (1962-2006) das fitofisionomias em unidade de conservação do Cerrado no sudeste do Brasil”. In: *Revista Brasileira de Botânica* 32.3, pp. 441–454.

Pinto, Miguel M. et al. (2020). “A deep learning approach for mapping and dating burned areas using temporal sequences of satellite images”. In: *ISPRS Journal of Photogrammetry and Remote Sensing* 160, pp. 260–274.

Pivello, Vânia R. (2011). “The Use of Fire in the Cerrado and Amazonian Rainforests of Brazil: Past and Present”. In: *Fire Ecology* 7.1, pp. 24–39.

Pivello, Vânia R. et al. (2021). “Understanding Brazil’s catastrophic fires: Causes, consequences and policy needed to prevent future tragedies”. In: *Perspectives in Ecology and Conservation* 19.3, pp. 233–255.

Prudente, Victor Hugo Rohden et al. (2020). “Limitations of cloud cover for optical remote sensing of agricultural areas across South America”. In: *Remote Sensing Applications: Society and Environment* 20, p. 100414.

Ramo, Ruben et al. (2021). “African burned area and fire carbon emissions are strongly impacted by small fires undetected by coarse resolution satellite data”. In: *Proceedings of the National Academy of Sciences* 118.9, e2011160118.

Ramos-Neto, Mário Barroso and Vânia Regina Pivello (2000). “Lightning Fires in a Brazilian Savanna National Park: Rethinking Management Strategies”. In: *Environmental Management* 26.6, pp. 675–684.

Ratter, J. A., S. Bridgewater, and J. F. Ribeiro (2003). “Analysis of the floristic composition of the Brazilian Cerrado vegetation III: comparison of the woody vegetation of 376 areas”. In: *Edinburgh Journal of Botany* 60.1, pp. 57–109.

Rekow, Lea (2019). “Socio-Ecological Implications of Soy in the Brazilian Cerrado”. In: *Challenges in Sustainability* 7.1, pp. 7–29.

Ribeiro, Andreia F. S., Lucas Santos, et al. (2024). “The time since land-use transition drives changes in fire activity in the Amazon-Cerrado region”. In: *Communications Earth & Environment* 5.1, p. 96.

Ribeiro, J.F. and B.M.T. Walter (2008). “Cerrado Ecologia e Flora”. In: *As principais fitofisionomias do Bioma Cerrado*. Embrapa, pp. 152–212.

Rodrigues, Julia A. et al. (2019). “How well do global burned area products represent fire patterns in the Brazilian Savannas biome? An accuracy assessment of the MCD64 collections”. In: *International Journal of Applied Earth Observation and Geoinformation* 78, pp. 318–331.

Russell-Smith, Jeremy et al. (2007). “Bushfires ’down under’: patterns and implications of contemporary Australian landscape burning”. In: *International Journal of Wildland Fire* 16.4, p. 361.

Sano, Edson E. et al. (2019). “Cerrado ecoregions: A spatial framework to assess and prioritize Brazilian savanna environmental diversity for conservation”. In: *Journal of Environmental Management* 232, pp. 818–828.

Santos, Filippe L.M. et al. (2021). “Prescribed Burning Reduces Large, High-Intensity Wildfires and Emissions in the Brazilian Savanna”. In: *Fire* 4.3, p. 56.

Schmidt, Isabel Belloni and Ludivine Eloy (2020). “Fire regime in the Brazilian Savanna: Recent changes, policy and management”. In: *Flora* 268, p. 151613.

Schroeder, Wilfrid et al. (2014). “The New VIIRS 375 m active fire detection data product: Algorithm description and initial assessment”. In: *Remote Sensing of Environment* 143. Publisher: Elsevier, pp. 85–96.

Schumacher, Vanúcia (2022). “Characteristics of lightning-caused wildfires in central Brazil in relation to cloud-ground and dry lightning”. In: *Agricultural and Forest Meteorology*.

Segura-Garcia, Carlota et al. (2024). “Human land occupation regulates the effect of the climate on the burned area of the Brazilian Cerrado”. In: *Communications Earth & Environment* 5.1, p. 361.

Silva, P S, J A Rodrigues, et al. (2020). “Drivers of burned area patterns in Cerrado: the case of MATOPIBA region”. In: *2020 IEEE Latin American GRSS & ISPRS Remote Sensing Conference (LAGIRS)*.

Silva, Patrícia S, Renata Libonati, et al. (2024). “Climate Change and Fire: The Case of Cerrado, the Brazilian Savanna”. In: *Climate Change and Regional Socio-Economic Systems in the Global South: Resilience Strategies for Sustainable Development*, pp. 87–105.

Silva, Patrícia S., Joana Nogueira, et al. (2021). “Putting fire on the map of Brazilian savanna ecoregions”. In: *Journal of Environmental Management* 296, p. 113098.

Silva Arruda, Vera Laísa da et al. (2024). “Assessing four decades of fire behavior dynamics in the Cerrado biome (1985 to 2022)”. In: *Fire Ecology* 20.1, p. 64.

Simon, Marcelo F., Rosaura Grether, et al. (2009). “Recent assembly of the Cerrado, a neotropical plant diversity hotspot, by in situ evolution of adaptations to fire”. In: *Proceedings of the National Academy of Sciences* 106.48, pp. 20359–20364.

Simon, Marcelo F. and Toby Pennington (2012). “Evidence for Adaptation to Fire Regimes in the Tropical Savannas of the Brazilian Cerrado”. In: *International Journal of Plant Sciences* 173.6, pp. 711–723.

Souza, Carlos M. et al. (2020). “Reconstructing Three Decades of Land Use and Land Cover Changes in Brazilian Biomes with Landsat Archive and Earth Engine”. In: *Remote Sensing* 12.17, p. 2735.

Souza Neves, Laís Fernandes de et al. (2018). “Dinâmica do fogo no Parque Estadual do Araguaia, zona de transição Amazônia-Cerrado”. In: *Ra’e Ga* 44.

Spessa, Allan, Bevan McBeth, and Colin Prentice (2005). “Relationships among fire frequency, rainfall and vegetation patterns in the wet–dry tropics of northern Australia: an analysis based on NOAA-AVHRR data”. In: *Global Ecology and Biogeography* 14.5, pp. 439–454.

Teixeira Pitta, Fabio and Gerardo Cerdas Vega (2017). “Impacts of the agribsuiness expansion in teh Matopiba region: communities and the environment”. In: *ActionAid - Rio de Janeiro*.

Veraverbeke, Sander et al. (2017). “Lightning as a major driver of recent large fire years in North American boreal forests”. In: *Nature Climate Change* 7.7, pp. 529–534.

Welch, James R. et al. (2013). “Indigenous Burning as Conservation Practice: Neotropical Savanna Recovery amid Agribusiness Deforestation in Central Brazil”. In: *PLoS ONE* 8.12. Ed. by Brock Fenton, e81226.

Zanzarini, Vagner, Alan N. Andersen, and Alessandra Fidelis (2022). “Flammability in tropical savannas: Variation among growth forms and seasons in Cerrado”. In: *Biotropica* 54.4, pp. 979–987.

5.10 Supplementary Information

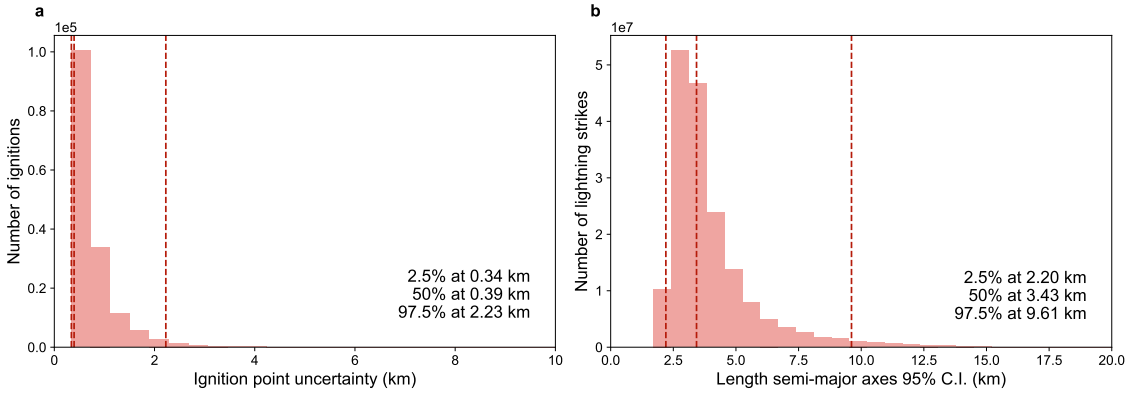

Figure S5.1: **a** distribution of uncertainties around the ignition point of each Global Fire Atlas (GFA) fire polygon. These uncertainties were calculated as the maximum distances between the ignition point and the border of the sub-polygon formed by all pixels in the GFA perimeter with the same burn date as the ignition point contiguous to it. **b**, distribution of the lengths of the semi-major axis of the 95% confidence ellipse for the location of the lightning strikes in the Vaisala Global Lightning Detection Network GLD360 dataset in the period 2019 to 2023. Dashed red lines show, from left to right, the 2.5th, the 50th and the 97.5th quantiles of the distributions.

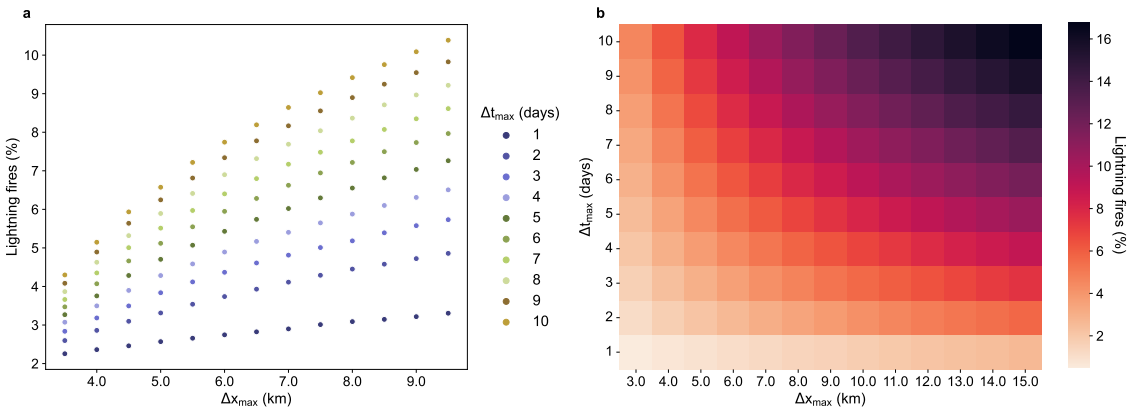

Figure S5.2: Percentage of lightning-caused fires identified when using different temporal and spatial windows with an attribution score threshold of 0.8 (see Methods). **a**, shows the percentage of lightning-caused fires only for those temporal and spatial distances within the set considered in the study, $\{(\Delta t_{\max}, \Delta x_{\max}), \Delta t_{\max} \in [3, 7]$ days and $\Delta x_{\max} \in [6, 12]$ km$\}$. **b**, for reference, this plot shows the percentage of lightning fires for a larger set of spatial and temporal window combinations.

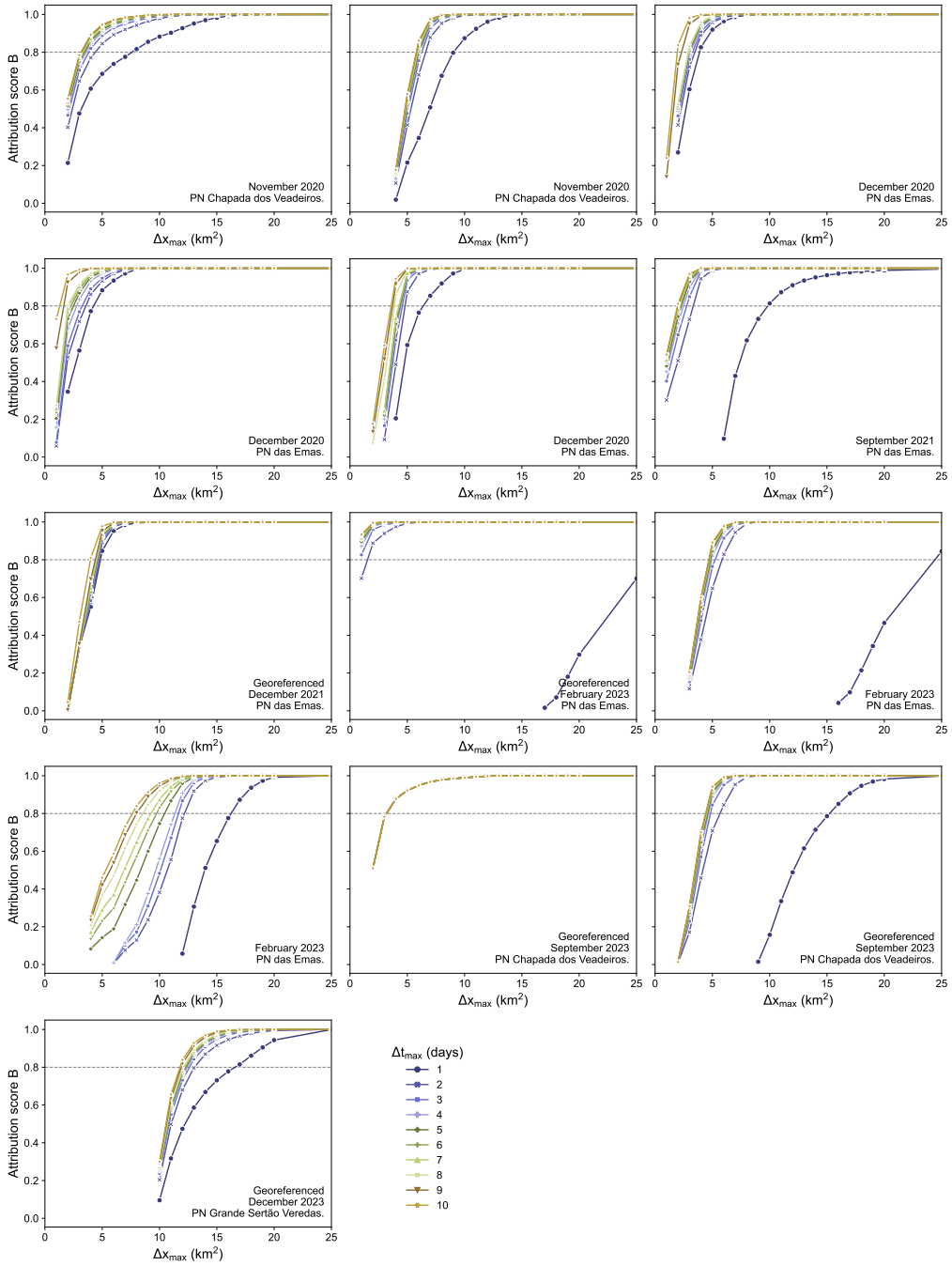

Figure S5.3: Attribution scores for different combinations of temporal and spatial windows for the different Global Fire Atlas (GFA) polygons identified as corresponding to a protected area, year and period where lightning fires were observed by the Instituto Chico Mendes de Conservação de Biodiversidade (ICMBio) in the non-georeferenced dataset. Each plot corresponds to a single GFA polygon out of all the records in the ICMBio (Supplementary Table 2). Those GFA polygons that were recorded in the georeferenced data from ICMBio are identified as such in the bottom right label of the plots along with month, year and the national park (PN) where the fire took place.

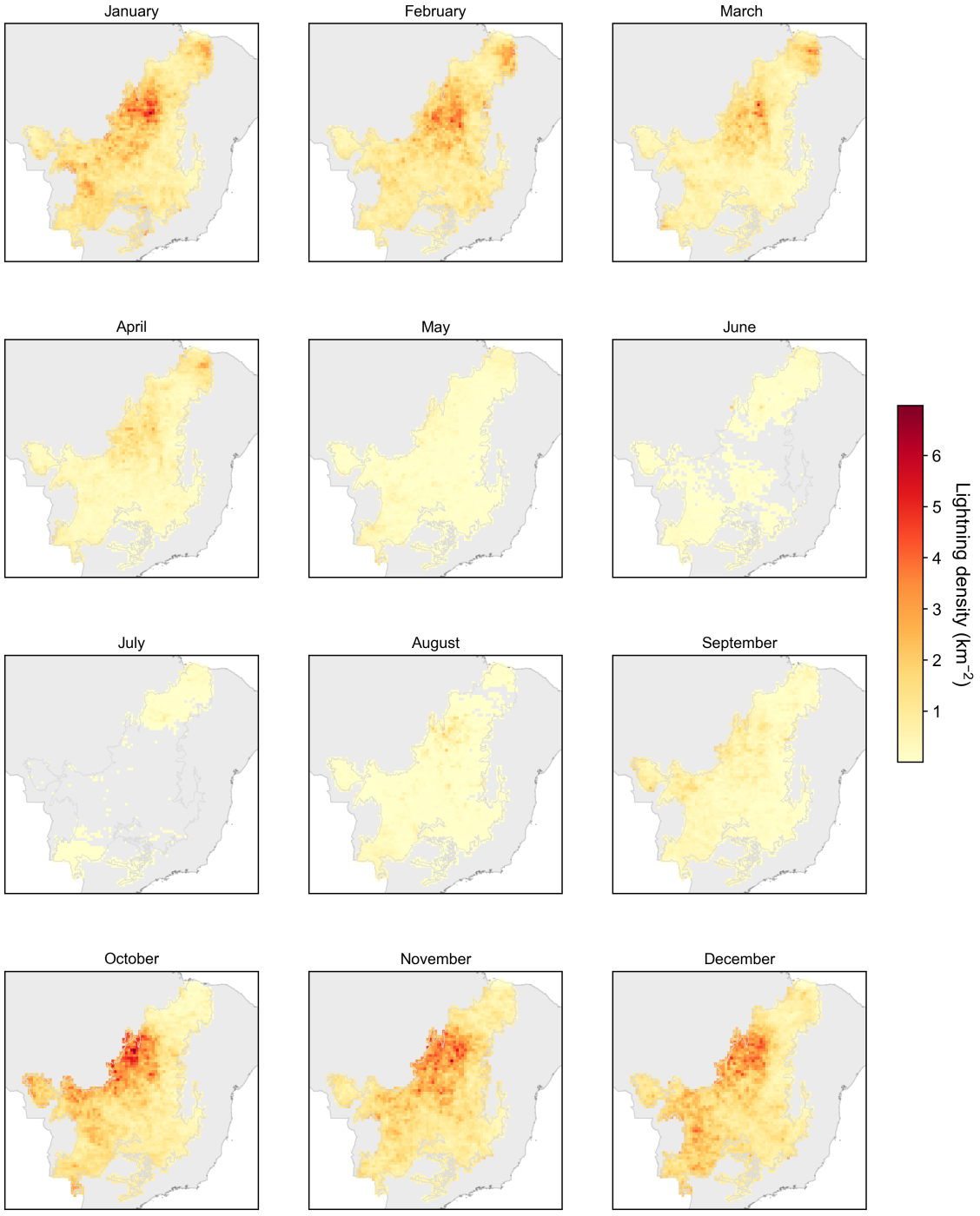

Figure S5.4: Average annual lightning density (number of lightning strikes per unit area) for each 30 km grid and month over the Cerrado in the period 2019-2023.

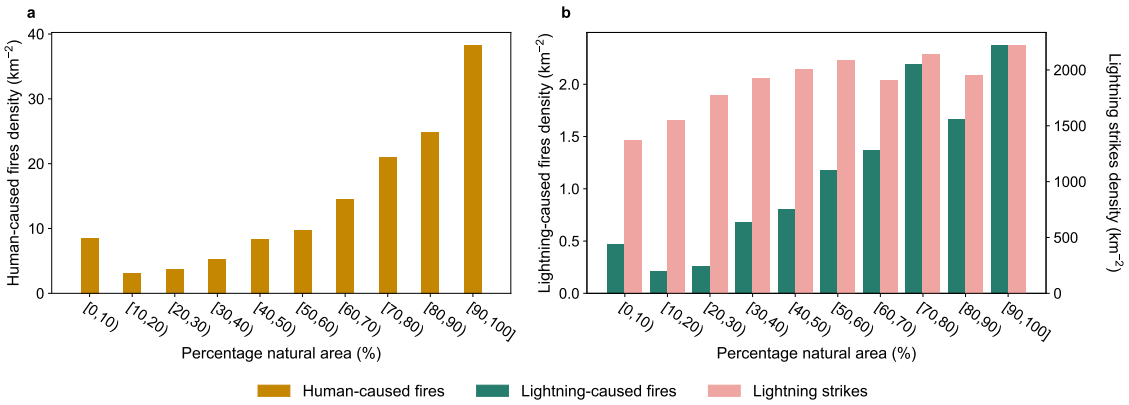

Figure S5.5: Density of fires and lightning strikes falling in different types of landscapes classified in deciles of natural area percentage (see Methods). Densities are obtained dividing per unit area of the total extension occupied by each type of landscape (i.e. by the number of cells with the same decile of natural area percentage). **a**, density of human-caused fires per unit area of each type of landscape. **b** density of lightning-caused fires per unit area (green, left y-axis), and density of lightning strikes per unit area (pink, right y-axis) of each type of landscape. Here, we identified lightning ($B \geq 0.8$) and human ($B \leq 0.2$) caused fires using $\Delta t_{\max} = 5$ days and $\Delta x_{\max} = 9$ km. The fires with intermediate attribution scores, B between 0.2 and 0.8, were considered as having no clear cause of ignition and were excluded from this analysis.

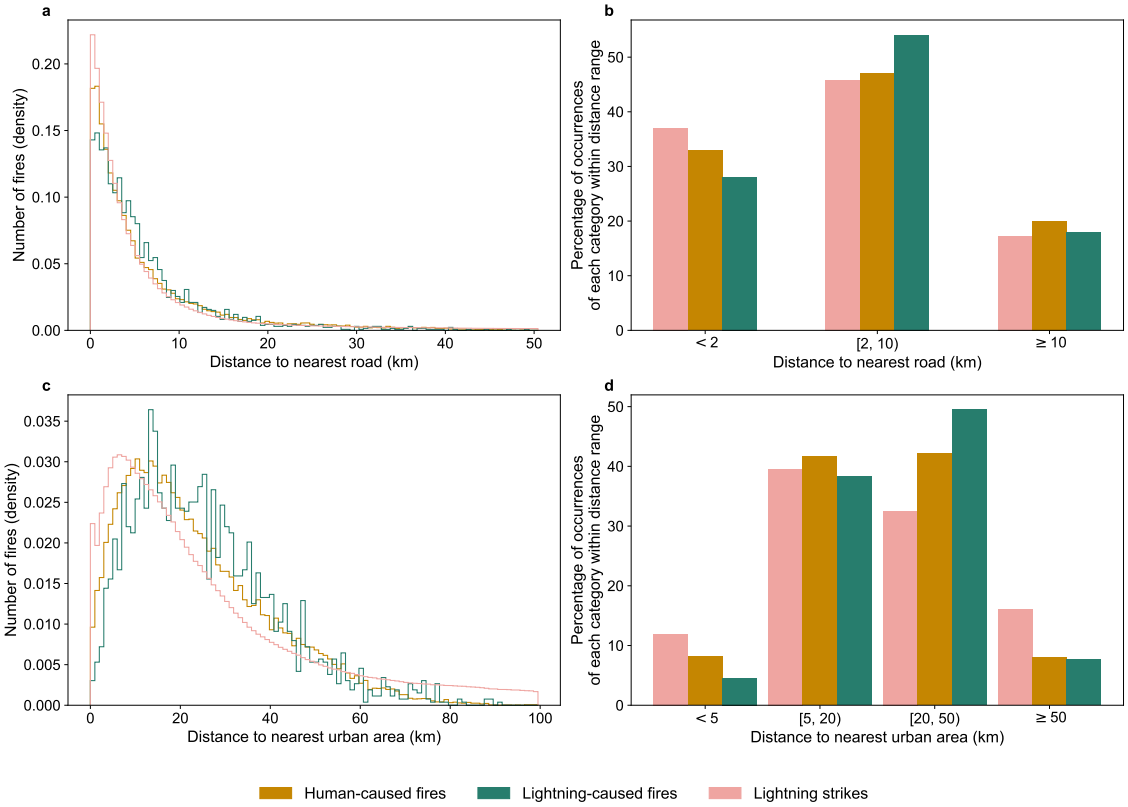

Figure S5.6: Distances from the ignition points of human-caused (brown) and lightning-caused (green) fires, and from the location of lightning strikes (pink) to the nearest roads (top row) and urban areas (bottom row). **a**, normalised histogram distribution of distances to nearest roads for each type of event (ignition point or lightning strike). **b**, percentage of each type of event taking place in each of three different ranges of distances to nearest roads, less than 2 km, between 2 and 10 km, and more than 10 km. **c**, normalised histogram distribution of distances to nearest urban area for each type of event. **d**, percentage of each type of event (ignition point or lightning strike) within four different ranges of distances to urban areas, less than 5 km, between 5 and 20 km, between 20 and 50 km, and more than 50 km. Here, we identified lightning ($B \geq 0.8$) and human ($B \leq 0.2$) caused fires using $\Delta t_{\text{max}} = 5$ days and $\Delta x_{\text{max}} = 9$ km. The fires with intermediate attribution scores, B between 0.2 and 0.8, were considered as having no clear cause of ignition and were excluded from this analysis.

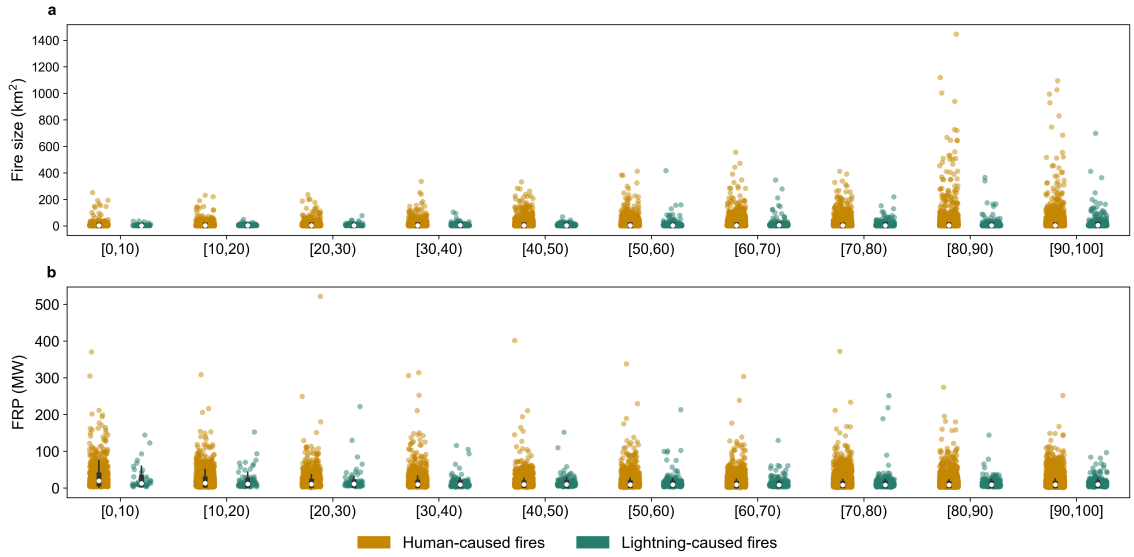

Figure S5.7: Distribution of fire sizes, **a**, and median FRP values, **b**, for lightning (green) and human (brown) caused fires classified per decile of natural area percentage of the landscape where the fire started. In this figure, we identified lightning ($B \geq 0.8$) and human ($B \leq 0.2$) caused fires using $\Delta t_{\text{max}} = 5$ days and $\Delta x_{\text{max}} = 9$ km. The fires with intermediate attribution scores, B between 0.2 and 0.8, were considered as having no clear cause of ignition and were excluded from this analysis.

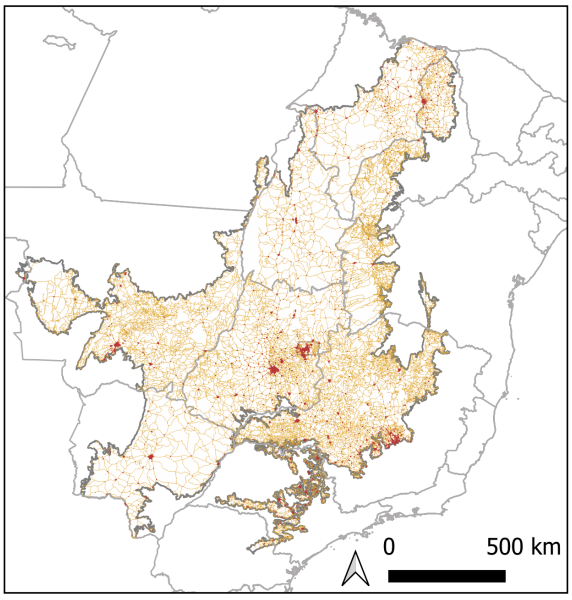

Figure S5.8: Map of road infrastructure (brown lines) as obtained from the MapBiomas project, including the categories "federal highway", "state highway" and "other roads". The map also shows the urban areas (red polygons), obtained from the MapBiomas Collection 8.0 land use and land cover product.

Table S5.1: Lightning-caused fires registered in the field record provided by the Instituto Chico Mendes de Conservação da Biodiversidade (ICMBio) in georeferenced vector format. Record includes the year, protected area, area burned by the fire, the estimated date of ignition of the fire, and the corresponding date expressed as day-of-year (DOY). Out of the 11 records, 6 were also mapped in the GFA dataset. The table also shows the starting and ending DOY date for each fire record that appears in the Global Fire Atlas (GFA), as well as whether the attribution method identified the fire as lightning for some combination of spatial and temporal windows (see Methods). PARNA stands for National Park.

Year	**Protected area**	**Burned area (ha)**	**Estimated ignition date**	**Est. DOY**	**Registered in GFA**	**Start DOY GFA**	**End DOY GFA**	**Identified as lightning fire**
2021	PARNA das Emas	7216.9	10/12/2021	344	Yes	336	346	Yes
2022	PARNA da Serra da Canastra	947.7	24/01/2022	20	No	-	-	-
2022	PARNA da Serra da Canastra	286.7	16/02/2022	46	No	-	-	-
2022	PARNA da Chapada dos Veadeiros	1414.9	17/11/2022	314	No	-	-	-
2022	PARNA Grande Sertão Veredas	117.5	20/01/2021	20	No	-	-	-
2023	PARNA das Emas	1332.5	05/03/2023	57	Yes	56	62	Yes
2023	Sertão Veredas	68.1	18/03/2023	64	No	-	-	-
2023	PARNA da Chapada dos Veadeiros	826.0	30/05/2023	148	Yes	146	148	No
2023	PARNA da Chapada dos Veadeiros	462.6	19/09/2023	259	Yes	259	263	Yes
2023	PARNA da Chapada dos Veadeiros	594.9	01/10/2023	273	Yes	272	285	Yes
2023	PARNA Grande Sertão Veredas	717.7	05/12/2023	336	Yes	336	336	Yes

Table S5.2: The protected areas in Brazil and the period of the year in which lightning fire observations were recorded by the Instituto Chico Mendes de Conservação da Biodiversidade (ICMBio) in the non-geoereferenced tabular format. Out of the 20 records of protected areas and months when lightning fires were recorded, we found that the Global Fire Atlas (GFA) had identified at least one fire for 7 of them, totalling 14 polygons. Out of these 14 records, the attribution method identified 13 as caused by lightning for some combination of spatial and temporal windows (see Methods). PARNA stands for National Park.

Year	**Month**	**Protected area**	**Containing GFA fires**	**Num. GFA polygons**	**Num. lightning fires**
2020	January	PARNA das Nascentes do Rio Parnaíba	No	-	-
2020	October	PARNA da Chapada dos Veadeiros	No	-	-
2020	November	PARNA da Chapada dos Veadeiros	Yes	2	2
2020	December	PARNA das Emas	Yes	3	3
2021	February	PARNA da Serra da Canastra	No	-	-
2021	September	PARNA das Emas	Yes	1	1
2021	November	PARNA da Chapada dos Guimarães	No	-	-
2021	December	PARNA das Emas	Yes	1	1
2022	January	PARNA Grande Sertão Veredas	No	-	-
2022	January	PARNA da Serra da Canastra	No	-	-
2022	February	PARNA da Serra da Canastra	No	-	-
2022	September	Floresta Nacional de Carajás	No	-	-
2022	November	PARNA da Chapada dos Veadeiros	No	-	-
2022	December	PARNA da Chapada dos Veadeiros	No	-	-
2023	February	PARNA das Emas	Yes	3	3
2023	April	PARNA da Chapada dos Veadeiros	No	-	-
2023	August	PARNA da Chapada dos Guimarães	No	-	-
2023	September	PARNA da Chapada dos Veadeiros	Yes	3	2
2023	October	PARNA da Chapada dos Veadeiros	No	-	-
2023	December	PARNA Grande Sertão Veredas	Yes	1	1
Total			**7 out of 20**	**14 GFA polygons**	**13 out of 14**

6 | Synthesis and Conclusions

In this chapter, I first provide a summary of the main findings, their significance and the novelty of the research undertaken to address each of the three objectives of this thesis. Then, I provide an overall synthesis elaborating on the main takeaway messages about the dynamics of fire in the Cerrado uncovered by this thesis. Finally, I conclude by outlining future avenues for research in light of the findings and limitations of the present work.

6.1 Summary of key findings

6.1.1 Objective 1: Determine how land use area and the climate interact to affect the burned area of the Cerrado

What is the causal effect of land use area on the amount of burned area? How does land use area interact with the climate to affect Cerrado's burned area? What are the burned area trends across the Cerrado and how are these related to anthropic expansion and climate change?

This objective was addressed in **Chapter 3 (Research Paper 1)**.

Findings - We showed that land use area reduces the fraction of burned area in Cerrado native vegetation - i.e. burned natural area. In addition, we demonstrated that human controls through land use area limit the responsiveness of burned area to climatic effects in landscapes with $\geq 40\%$ of anthropic area. Therefore, it is only in the least converted regions of the Cerrado that burned area increases in response to warm and dry conditions. Finally, regarding changes over time between 1985 and 2020, we found that burned area remained low and did not show clear changes in time in those landscapes that were already mostly converted in 1985; while the largest changes in burned area were concentrated in those landscapes that were mostly intact at the beginning of the study period. In these regions, we found that climate change caused increases in burned area where the landscapes remained mostly unconverted, while agricultural expansion brought about

decreases in burned area.

Significance - This study addressed a knowledge gap in the literature studying the dynamics of fire in the Cerrado, as the interaction between land use area and the climate had not been previously quantified for this region. Our results contribute to the increasing literature identifying landscape fragmentation as a stronger control than climate on the burned area of savanna ecosystems (Archibald, Nickless, et al., 2010; Andela et al., 2014; Conciani et al., 2021). These findings indicate that current predictions of generalised increases in Cerrado burned area under different scenarios of climate change (Silva, Bastos, et al., 2019) may be overestimating the climate forcing when not accounting for current, nor future, patterns of land use area. Finally, this study identified the largest remnants of Cerrado native vegetation as being the most vulnerable to changing patterns of burned area in relation to climate change. Therefore, these are priority areas for Cerrado conservation where the implementation of prescribed burns as fire management practices may be particularly beneficial to diminish the occurrence of large burned area events (Santos et al., 2021; Andrade et al., 2021), helping to maintain biodiversity levels.

Novelty - This is the first study to explicitly quantify the interaction between land use area and the climate as drivers of burned area in the Brazilian Cerrado. Further, the novelty of this study also stems from the statistical methods used. First, the use of causal inference in this study is part of a growing and relatively recent trend in environmental sciences to construct statistical models that allow the interpretation of relationships between variables as causal rather than merely correlational. In addition, a rather simple but novel methodological aspect that ultimately allowed to disentangle land use area and climate effects, either when considering the full study period or the trends in time, was precisely investigating these effects conditioning on (pre)existing levels of land use area. In this study, the conditioning was done using Bayesian multilevel models, equivalent to modelling effects by level of anthropic area. Previous studies in the Cerrado did not consider this aspect, reporting as a consequence both increasing and decreasing effects of land use expansion on burned area, and not resolving the interaction with climatic effects (Rosan et al., 2022; Silva, Rodrigues, et al., 2020).

6.1.2 Objective 2: Characterising the fire regime regions of the Cerrado and their changes through time

What are the regions of the Cerrado presenting different fire regimes? What are the environmental characteristics of these regions? How have these fire regime regions changed through time?

This objective was addressed in **Chapter 4 (Research Paper 2)**.

Findings - This study delineated the fire regime regions of the Cerrado in four consecutive periods between 1985 and 2020, finding that the fire regime regions of the Cerrado have profoundly changed over the past almost forty years, both geographically and in terms of fire characteristics. Only two aspects seem to have remained constant between 1985-1993 and 2012-2020: a) the identified fire regime regions in each period were organised along a gradient of fire activity, which was the main feature differentiating them (i.e. regions with large fires also had a tendency to have numerous and frequent fires, and vice versa); and b) the identification of a region in the north of the Cerrado characterised by rather large numbers of small fires and a later peak of the fire season. Further, we found that the gradient of fire activity was opposed to a gradient of increase in the presence of human activities. This seemed a general pattern across the Cerrado, except for one fire regime region near the Amazon rainforest and a few forest areas in the north of the Cerrado in the period 1985-1993, and some scattered areas in the period 2012-2020, pointing at the importance of other factors like vegetation type influencing fire regimes. Finally, most of the southern parts of the Cerrado experienced losses in fire activity concomitant to land use expansion, while other areas either experienced gains in, or maintained high levels of, fire activity.

Significance - This study clearly revealed the profound changes experienced by the Cerrado's fire regimes over the past four decades. Importantly, it showed how the fire regimes of the Cerrado are increasingly portraying the land use footprint on this region, highlighting the large-scale loss of Cerrado native vegetation and the wider impacts disrupting ecosystem processes and their disturbance regimes. Further, it underscored the impor-

tance of landscape fragmentation as a major determinant, and driver of change, of savannas fire regimes. **Chapter 4 (Research Paper 2)** expanded on the findings of **Chapter 3 (Research Paper 1)** showing opposing temporal changes in fire activity. These processes emphasise the double-sided pressures on these tropical savannas: while part of the Cerrado is being lost to agricultural land uses and experiencing decreases in fire activity, other areas are experiencing increases in the size and frequency of fires. Since only about 3% of the Cerrado is under strict protection, these findings underscore the urgent need to expand the protected areas of the Cerrado, as well as the need to implement fire management strategies that contribute to Cerrado conservation within protected areas but also in private lands.

Novelty - This is the first study delineating the regions of the Cerrado with different fire regimes without assuming geographical boundaries *a priori*. In addition, it delineates the fire regime regions in different periods, analysing how both the regions and their fire characteristics have changed through time, which is not a common approach in the literature, and the first time this has been done for the Cerrado. Further, this study uses a hierarchical clustering algorithm with a spatially contiguity constraint to identify the fire regime regions, unlike the unconstrained clustering methods commonly used in the literature that can lead to very fragmented fire regime regions (Archibald, Lehmann, et al., 2013), which can hamper the interpretation of patterns at regional scales.

6.1.3 Objective 3: Quantifying and comparing the fire regimes ignited by lightning and humans

What is the proportion of lightning to human-ignited fires? How does it change throughout the year and across the Cerrado? How do these two types of fires compare?

This objective was addressed in **Chapter 5 (Research Paper 3)**.

Findings - This study estimated that, in the period 2019-2023, 7.5% (95% confidence interval, CI, [6.7, 8.3]%) of fires were ignited annually by lightning, while 89.1% (95% CI, [86.9, 91.3]%) were ignited by humans, and 3.4% (95% CI, [2.7, 4.1]%) did not have

a clear cause of ignition. Therefore, humans are the major cause of fires in the Brazilian Cerrado, creating an excessive number of ignitions in comparison to lightning. Further, we found that humans lengthen the fire season threefold starting fires throughout the dry season (May to October), while most lightning-caused fires took place in the transition period from the dry to the wet season (September and October). In addition, we found that humans create higher fire frequencies and ignite fires in more flammable conditions than lightning, even when comparing fires starting in the same month. Finally, our results indicate that these differences in flammability at ignition led to the more extreme fire behaviours observed in some human-caused fires. Indeed, the most extreme human-caused fires were about ten times larger, or two times more intense, than their lightning-caused counterparts, and took place in generally drier and hotter weather conditions.

Significance - This study fills a clear gap in the literature addressing how current human-caused fires differ from naturally ignited ones, and providing numerical evidence that humans ignite a much larger number of fires than lightning, something that was previously assumed but had not yet been quantified (Pivello, 2011). Still, this study also demonstrated that lightning ignites a considerable percentage of fires, as had been previously suggested in some Cerrado protected areas (Ramos-Neto et al., 2000), indicating that global models estimating low numbers of lightning ignitions in tropical savannas and grasslands (Janssen et al., 2023) may be underestimating the amount of fires caused by lightning in this biome. Crucially, it also demonstrated that most fires in the larger remnants of Cerrado native vegetation are ignited by humans, and that these fires are generally larger and more intense than lightning-ignited ones. These findings are important in relation to the results from **Chapter 3 (Research Paper 1)** showing the relation between increasing trends in burned area and climate change, as they indicate that humans also contribute to these increases by causing the fires. Finally, the excess number of ignitions and more extreme behaviour of fires caused by humans highlights the need to address the regulations on the use of fire as part of non-conservation human activities that either cause fires directly on native vegetation, or cause fires that escape into these areas.

Novelty - This is the first study providing a quantification of the proportion of lightning

and human-ignited fires for the whole Brazilian Cerrado, and comparing the characteristics of fires ignited naturally and by humans in this region. In addition, to the best of my knowledge, this study went further than previous studies using the same well-established ignition-cause attribution method (Larjavaara et al., 2005) in two aspects. First, we used two attribution score thresholds, one threshold to identify those fires most likely caused by lightning and another one to identify those fires most likely caused by humans. In this manner, those fires with intermediate attribution score thresholds were classified as not having a clear ignition cause and were excluded from the comparison between lightning and human fires. Further, we also assessed the uncertainty on the estimated proportion of each type of fire, which has not been done before (e.g. Menezes et al. (2022)).

6.2 Thesis synthesis and conclusions

This thesis has investigated how the patterns of fire of the Brazilian Cerrado have changed over the past few decades shaped by agricultural land use expansion and climate change. In particular, it has explored different aspects of fire in relation to the two main mechanisms by which humans influence fire regimes, namely altering fuel - primarily through landscape fragmentation resulting from land use activities - and ignitions, and how these two interact or combine with climatic effects.

This work began by understanding how land use area and the climate interact to affect the Cerrado's burned area, a key aspect to disentangle the current spatiotemporal dynamics of fire of tropical savannas and grasslands. **Chapter 3 (Research Paper 1)** showed that human controls on fire through land use area lead to low burned areas in native vegetation. Further, it provided a clear demonstration of the landscape fragmentation controls on the climatic effects on burned natural area, suggested by previous research in the Cerrado (Conciani et al., 2021) and observed in African savannas (Archibald, Nickless, et al., 2010; Andela et al., 2014). Crucially, this first study illustrated that there is a clear difference between the fire dynamics of the highly converted areas of the Cerrado and those of the mostly intact landscapes, precisely as a result of the different level of landscape

fragmentation. This distinction provides a fundamental basis to interpret the current patterns of fire of the Cerrado, and it was recurrently observed in subsequent chapters of this thesis.

Results from **Chapter 3 (Research Paper 1)** also showed that declines in burned natural area over time occurred as a result of large-scale land use expansion, while increases in burned natural area were related to climate change and restricted to areas of the Cerrado that had remained largely unconverted over the past four decades. This relation between decreases in burned area and agricultural expansion is in agreement with recent research indicating that fire is not commonly used in the conversion of Cerrado's native savannas and grasslands to agricultural lands, except in the conversion of Cerrado's forest vegetation, and that fire activity reduces gradually over time in all cases after the conversion event (Ribeiro et al., 2024). Together, these findings indicate that the observed increases in burned area in the Cerrado's most intact regions, as reported in **Chapter 3 (Research Paper 1)**, may not necessarily be attributed to the limited native vegetation conversion they experienced, but rather to climate change and, possibly, other anthropic uses of fire.

In **Chapter 4 (Research Paper 2)**, we expanded the study of the dynamics of fire in the Cerrado by characterizing fire regimes in a more complete way, and identified the different fire regime regions in consecutive periods. This study showed the nuances in the spatiotemporal patterns of fire uncovered when more fire characteristics in addition to burned area are considered. Overall, the main aspect differentiating the fire regime regions at a certain moment in time was their level of fire activity, which varied inversely to the level of human impact on the landscape. In a similar fashion to the results of **Chapter 3 (Research Paper 1)**, **Chapter 4 (Research Paper 2)** found opposing trends in fire activity, and a clear distinction between highly converted areas with overall low fire activity levels, and the more intact areas presenting high levels of fire activity. Therefore, we encountered again the dichotomy in the patterns of fire of the Cerrado, which seems to have deepened throughout the past four decades. However, **Chapter 4 (Research Paper 2)** also highlighted some exceptions to the relation between increases in land use area and decreases in fire activity. Indeed, in some areas in the western-most border with

the Amazon rainforest and in the north of the Cerrado, predominantly formed of forests, increases in fire activity could be related to land use expansion as a result of the use of fire in forest vegetation conversion (Ribeiro et al., 2024).

Considering the findings from **Chapter 3 (Research Paper 1)** and **Chapter 4 (Research Paper 2)**, we can conclude that agricultural activities and the extent of land use area are the dominant driver of the current fire regimes of the Cerrado. These studies contribute to the wider literature indicating that human socioeconomic activities linked to land uses limit the extent of fires in savannas primarily through the introduction of fuel discontinuities and through active fire suppression (Archibald, Roy, et al., 2009; Archibald, Nickless, et al., 2010). Nonetheless, it is important to underline that the land use imprint on the spatiotemporal patterns of fire of the Cerrado is a symptom of the main process threatening this region's ecosystems: the large-scale loss of native vegetation to croplands and pastures.

Finally, this thesis addressed the cause of fire ignitions, one of the major outstanding questions in the study of Cerrado's fire regimes. The results of **Chapter 5 (Research Paper 3)** demonstrated that humans are the main cause of fire ignitions across the Cerrado, and showed that human activities extend the occurrence of fires to the full dry season, increase fire frequency, and create more extreme fire behaviour than lightning. Still, the spatial patterns of fire observed both for lightning and human-caused fires were, once more, mostly influenced by the patterns of land uses, with few and small fires observed in highly converted landscapes.

Interestingly, **Chapter 5 (Research Paper 3)** demonstrated that humans are the main cause of fire ignitions in the least fragmented areas of the Cerrado. This finding links back to **Chapter 3 (Research Paper 1)** and the question on whether the increases in burned natural area observed in these intact regions in relation to climate change were also mediated by human intervention. Findings in **Chapter 5 (Research Paper 3)** indicated that, indeed, the excess of human ignitions and their timing during the dry season could be coupling with climate change to explain the increasing trends in burned area observed over the most intact areas of the Cerrado. Accordingly, these investigations suggest that

while climate change is setting the stage for larger and more intense fires to occur in these areas, it is humans who start these fires in flammable conditions and with high frequencies.

Findings in **Chapter 5 (Research Paper 3)** suggested that naturally occurring fire regimes would consist of far lower numbers of fires than is currently observed in the Cerrado, and that these would take place in generally less flammable conditions. Still, results from this study also indicated that lightning does ignite a substantial amount of fires and that, occasionally, these fires occur in climatic conditions enabling considerably large or intense fires. Based on these observations, we can speculate that the structure of Cerrado vegetation would be less open than at present if lightning was the only source of fire ignitions, as suggested in other subtropical savannas (Van Wilgen et al., 2000), but also that some large lightning-caused fires could take place with a certain frequency causing larger openings in the vegetation. However, our findings also demonstrated that the current patterns of lightning-caused fires are deeply influenced by humans, either through landscape fragmentation or by shaping the fire histories of the landscape, as both these processes create fuel discontinuities, which in turn affect the occurrence and fire behaviour of subsequent fires (Fidelis et al., 2018). Therefore, the patterns of lightning-caused fires reported in **Chapter 5 (Research Paper 3)** should not be considered as strictly natural.

Overall, we can expect the changes in fire regimes reported in this thesis to bring about ecological changes to Cerrado's ecosystems, particularly to the structure and composition of their vegetation (Pivello et al., 2021; Abreu et al., 2017; Pinheiro et al., 2009). In the areas with larger remnants of native vegetation, burned area and fire sizes have increased over the past few decades and, crucially, fires have taken place with elevated frequencies and with exacerbated behaviour. Because fire favours grasses and herbaceous vegetation (Medeiros et al., 2008), we can expect a further retreat of forest patches and a further opening of the vegetation in these areas (Pivello et al., 2021). These ecological effects may be stronger at the transition with tropical rainforest and in the northern parts of the Cerrado where tree canopy is denser. Still, even though savanna and grassland species present adaptations to fire, vegetation can eventually lose its capacity to resist fire and to recover from its effects when fires are too frequent or when they are particularly intense

(Pinheiro et al., 2009; Pivello et al., 2021). One of the main concerns resulting from these processes is the loss of biodiversity, both among tree species (Abreu et al., 2017) and among grasses, herbs and shrubs (Pivello et al., 2021).

Concomitantly to the large-scale agricultural conversion and to the increases in fire activity in unconverted areas of Cerrado, there have been other processes linked to humans and fires over the past decades. In particular, active fire suppression in certain protected areas of the Cerrado has been a major conservation strategy for several decades, as signaled repeatedly in the literature (Durigan, 2020; Mistry et al., 2016; Pivello et al., 2021; Fidelis et al., 2018). These suppression practices have brought about woody encroachment in these areas and generalised biodiversity losses among light-demanding species but also among Cerrado tree specialists (Abreu et al., 2017). These processes have also caused fuel accumulation contributing to the occurrence of fires with unprecedented sizes and behaviour (Fidelis et al., 2018), which have more chances of causing vegetation mortality as their high temperatures and residence times can surpass fire protections (Medeiros et al., 2008).

The vegetation composition and the extent of savannas and grasslands in South America has dynamically changed over the past few thousands of years responding to several episodes of climate change (Araujo et al., 2025), as well as to other events such as the extinction of mega-herbivores and the arrival of humans (Dantas et al., 2020; Araujo et al., 2025). Therefore, similarly to what happened with these environmental changes, we can expect Cerrado vegetation to change in response to ongoing climate change and to human-caused changes in fire regimes. As such, Cerrado vegetation may further open in some areas in response to drying conditions and exacerbated fire activity; or it may evolve towards closed ecosystems if fire is reduced and favoured by increasing atmospheric carbon concentrations (Stevens et al., 2017) - a process of woody encroachment that may have been ongoing throughout the Holocene since megafauna extinction (Doughty et al., 2016).

Still, recent transformations of the Cerrado have taken place at an extraordinary fast pace, which contrasts with Holocene transformations - even if some may have been rather fast

for geological time scales (Dantas et al., 2020). Indeed, as shown in this thesis and in other studies, the fire regimes of the Cerrado have changed at an unprecedented large scale in just about five to six decades in relation with human activities (Silva, Nogueira, et al., 2021; Mataveli et al., 2017; Silva Arruda et al., 2024). Such fast-paced processes have been simultaneous to - and also caused by - the widespread conversion of Cerrado native vegetation and to the anthropic climate change taken place during the same period. The combination of these processes are impacting Cerrado's ecosystems, with particularly harmful effects on their rich biodiversity (Klink et al., 2005). Therefore, the conservation of Cerrado at scale is absolutely urgent to stop the loss of native vegetation. Further, conservation needs to address the fire regimes that affect the remnants of Cerrado, particularly to preserve and enhance this region's biodiversity.

In conclusion, this thesis has highlighted the high and increasing level of anthropisation of the Cerrado's fire regimes. We have shown that humans are altering the Cerrado's fire regimes through the two main mechanisms of fire control: modifying the vegetation continuity through land use activities and fragmentation, and through ignitions. Further, we have repeatedly highlighted that the spatial patterns of fire of the Cerrado primarily reflect the patterns of land use area, independently of the fire ignition cause. In fact, we have demonstrated that controls on fire through landscape fragmentation are so strong that limit the climatic effects on Cerrado's burned natural area. Finally, we also conclude that humans are directly responsible for both the increases and decreases in fire activity observed across the Cerrado, the two main directions of change of this region's fire regimes over the past four decades: agricultural expansion brings about decreases in fire activity, while humans facilitate increases in fire activity in the larger remnants of native vegetation by creating ignitions throughout the dry season in the context of climate change.

6.3 Future research directions

This thesis has addressed key aspects to understanding how, and in relation to what, the fire regimes of the Brazilian Cerrado have changed over the past few decades, regard-

ing the interaction between anthropic land uses and the climate **(Chapter 3, Research Paper 1)**, the identification of the Cerrado's fire regimes and their changes through time **(Chapter 4, Research Paper 2)**, and the characterisation of fires depending on their ignition cause **(Chapter 5, Research Paper 3)**. These findings, along with the statistical and geospatial analysis methods employed in this thesis, open new avenues for future research, which are summarised in the following list:

1. One of the unexplored aspects of this thesis, and generally in the literature studying spatiotemporal patterns of fires in Cerrado using spaceborne data, is related to the characterisation of fire severity. This is primarily due to a lack of sufficient research across the Cerrado linking measurements of fire severity on the field to vegetation indices obtained from satellite data. Thus, future research could focus on addressing this research gap for the different vegetation forms of the Cerrado.

2. Further, future research could be directed at identifying and monitoring, through field-based studies, the ecosystem processes and characteristics that are being impacted by different fire regimes. This would imply going beyond studying the effects of single fires, but rather considering the effects of the overall fire histories of a region. Findings could then complement the larger-scale characterisation of Cerrado's fire regimes to identify those areas of the Cerrado that are already experiencing harmful patterns of fire.

3. A clear gap in the study of fires in tropical savannas and grasslands, and more generally across the world, are the small fires missed by satellite-based products (Jones et al., 2024; Ramo et al., 2021), particularly over agricultural areas (Rodrigues et al., 2019). Thus, further efforts devoted to improving the mapping of small fires would enable a more complete characterisation of fire regimes, as well as improving the estimation of the contributions of different ecosystems to carbon emissions (Werf et al., 2017).

4. Future studies could conduct more tailored research to further differentiate the fires created by different human communities (e.g. indigenous peoples, traditional pas-

toral communities, or activities related to industrial agriculture) as well as by lightning. This would improve our understanding about how the various human fire regimes differ among them and in comparison to naturally-ignited fires, but also whether any of these groups - for example, industrial agriculture - may be the predominant cause of human fires across the Cerrado.

5. Future studies could focus on understanding the climatic conditions in which lightning strikes are conducive to fires on different types of savanna vegetation. This could be used to model lightning-caused fire regimes in different climate and vegetation scenarios to investigate questions regarding how the Cerrado, and savannas in general, may have expanded in the past.

6. Future studies could replicate similar approaches to the methods applied in **Chapter 3 (Research Paper 1)** to quantify the interaction between land use area and climate in other savannas of the world. Understanding whether the shape of the interaction or the extent of land use controls on climate effects change depending on the region in relation to differences in vegetation or socioeconomic factors could inform more nuanced projections of burned area in tropical savannas and grasslands.

7. Causal inference offers a very powerful approach to understanding relations between different factors and processes in nature. **Chapter 3 (Research Paper 1)** opens the stage to use causal inference to explore the factors affecting other fire characteristics (e.g. fire size or frequency), as well as to explore the use of more sophisticated statistical analyses for cause-effects relations (e.g. convergent cross mapping that allows causality analysis of dynamical systems (Setty et al., 2023)).

8. Currently, there is no established common way of calculating fire variables (like frequency, seasonality, or length of the fire season), and different studies use different methodologies. Future research could be devoted to comparing methods and identifying optimal ways of calculating or measuring some of these variables. Standardising these methods would facilitate comparison between studies.

9. The methods used in **Chapter 4 (Research Paper 2)** to assess the number of fire

regime regions in which to divide the Cerrado are designed to identify a unique, most optimal, number of clusters. However, there are other methods (e.g. Lambiotte et al. (2014)) that allow to identify meaningful partitions of the data (i.e. number of clusters) at different levels. Future studies could use these methods to investigate whether, apart from the few and generally large fire regime regions identified in this thesis, there could be other partitions of the Cerrado into smaller regions that would also capture meaningful patterns of fire. These approaches could be used to investigate the level at which different drivers of fire may become relevant (Lambiotte et al., 2014). For example, findings of **Chapter 4 (Research Paper 2)** point at landscape fragmentation as a determining factor distinguishing fire regimes, but there could be other factors becoming important at smaller scales.

10. Given the depth of changes in the fire regimes of the Cerrado observed in **Chapter 4 (Research Paper 2)**, future studies could explore methodologies to allow the fire regime regions to evolve dynamically over time (e.g. Lughofer (2012)). That is, instead of generating independent clustering solutions for each consecutive time period, the clusters obtained at the beginning of the time series could be updated in subsequent time steps as fire characteristics change. Developing these methods could provide a relevant science advance in the study of changing fire regimes in different areas of the world.

11. The statistical methods used in the literature to quantify fire regimes, like the ones used in **Chapter 4 (Research Paper 2)**, are generally reductionist. For example, to characterise the fire sizes of a certain region, usually the median or a high percentile of the distribution are used. But, perhaps, there could be ways of harnessing more completely the information of the full probability distributions of the fire variables. For example, instead of characterising the fire regimes of a region as a vector of fire variables, the fire regimes could be expressed as an envelope of probability distributions. Potentially, this type of approach could allow more nuanced characterisation of fire regimes and comparisons between regions.

6.4 References

Abreu, Rodolfo C. R. et al. (2017). "The biodiversity cost of carbon sequestration in tropical savanna". In: *Science Advances* 3.8, e1701284.

Andela, Niels and Guido R. van der Werf (2014). "Recent trends in African fires driven by cropland expansion and El Niño to La Niña transition". In: *Nature Climate Change* 4.9, pp. 791–795.

Andrade, Ananda Santa Rosa de et al. (2021). "Implementation of Fire Policies in Brazil: An Assessment of Fire Dynamics in Brazilian Savanna". In: *Sustainability* 13.20, p. 11532.

Araujo, Astolfo GM et al. (2025). "Human-environment interaction during the Holocene in Eastern South America: Rapid climate changes and population dynamics". In: *PloS one* 20.2, e0315747.

Archibald, S., A. Nickless, et al. (2010). "Climate and the inter-annual variability of fire in southern Africa: a meta-analysis using long-term field data and satellite-derived burnt area data: Fire-climate interactions". In: *Global Ecology and Biogeography* 19.6, pp. 794–809.

Archibald, Sally, Caroline E. R. Lehmann, et al. (2013). "Defining pyromes and global syndromes of fire regimes". In: *Proceedings of the National Academy of Sciences* 110.16, pp. 6442–6447.

Archibald, Sally, David P. Roy, et al. (2009). "What limits fire? An examination of drivers of burnt area in Southern Africa". In: *Global Change Biology* 15.3, pp. 613–630.

Conciani, Dhemerson E. et al. (2021). "Human-climate interactions shape fire regimes in the Cerrado of São Paulo state, Brazil". In: *Journal for Nature Conservation* 61, p. 126006.

Dantas, Vinicius L and Juli G Pausas (2020). "Megafauna biogeography explains plant functional trait variability in the tropics". In: *Global Ecology and Biogeography* 29.8, pp. 1288–1298.

Doughty, Christopher E, Søren Faurby, and Jens-Christian Svenning (2016). "The impact of the megafauna extinctions on savanna woody cover in South America". In: *Ecography* 39.2, pp. 213–222.

Durigan, Giselda (2020). "Zero-fire: Not possible nor desirable in the Cerrado of Brazil". In: *Flora* 268, p. 151612.

Fidelis, Alessandra et al. (2018). "The Year 2017: Megafires and Management in the Cerrado". In: *Fire* 1.3, p. 49.

Janssen, Thomas A. J. et al. (2023). "Extratropical forests increasingly at risk due to lightning fires". In: *Nature Geoscience*.

Jones, Matthew W et al. (2024). "State of Wildfires 2023–2024". In: *Earth System Science Data* 16.8. Publisher: Copernicus Publications Göttingen, Germany, pp. 3601–3685.

Klink, Carlos A. and Ricardo B. Machado (2005). "Conservation of the Brazilian Cerrado". In: *Conservation Biology* 19.3, pp. 707–713.

Lambiotte, Renaud, Jean-Charles Delvenne, and Mauricio Barahona (2014). "Random Walks, Markov Processes and the Multiscale Modular Organization of Complex Networks". In: *IEEE Transactions on Network Science and Engineering* 1.2, pp. 76–90.

Larjavaara, M., J. Pennanen, and T.J. Tuomi (2005). "Lightning that ignites forest fires in Finland". In: *Agricultural and Forest Meteorology* 132.3, pp. 171–180.

Lughofer, Edwin (2012). “A dynamic split-and-merge approach for evolving cluster models”. In: *Evolving Systems* 3.3, pp. 135–151.

Mataveli, Guilherme Augusto Verola et al. (2017). *Analysis of fire dynamics in the Brazilian savannas*. preprint. Other Hazards (e.g., Glacial, Snow Hazards, Karst, Wildfires Hazards, and Medical Geo-Hazards).

Medeiros, MB and HS Miranda (2008). “Post-fire resprouting and mortality in cerrado woody plant species over a three-year period”. In: *Edinburgh Journal of Botany* 65.1, pp. 53–68.

Menezes, Lucas S et al. (2022). “Lightning patterns in the Pantanal: Untangling natural and anthropogenic-induced wildfires”. In: *Science of the Total Environment*.

Mistry, Jayalaxshmi, Bibiana A. Bilbao, and Andrea Berardi (2016). “Community owned solutions for fire management in tropical ecosystems: case studies from Indigenous communities of South America”. In: *Philosophical Transactions of the Royal Society B: Biological Sciences* 371.1696, p. 20150174.

Pinheiro, Eduardo Da Silva and Giselda Durigan (2009). “Dinâmica espaço-temporal (1962-2006) das fitofisionomias em unidade de conservação do Cerrado no sudeste do Brasil”. In: *Revista Brasileira de Botânica* 32.3, pp. 441–454.

Pivello, Vânia R. (2011). “The Use of Fire in the Cerrado and Amazonian Rainforests of Brazil: Past and Present”. In: *Fire Ecology* 7.1, pp. 24–39.

Pivello, Vânia R. et al. (2021). “Understanding Brazil’s catastrophic fires: Causes, consequences and policy needed to prevent future tragedies”. In: *Perspectives in Ecology and Conservation* 19.3, pp. 233–255.

Ramo, Ruben et al. (2021). “African burned area and fire carbon emissions are strongly impacted by small fires undetected by coarse resolution satellite data”. In: *Proceedings of the National Academy of Sciences* 118.9, e2011160118.

Ramos-Neto, Mário Barroso and Vânia Regina Pivello (2000). “Lightning Fires in a Brazilian Savanna National Park: Rethinking Management Strategies”. In: *Environmental Management* 26.6, pp. 675–684.

Ribeiro, Andreia F. S. et al. (2024). “The time since land-use transition drives changes in fire activity in the Amazon-Cerrado region”. In: *Communications Earth & Environment* 5.1, p. 96.

Rodrigues, Julia A. et al. (2019). “How well do global burned area products represent fire patterns in the Brazilian Savannas biome? An accuracy assessment of the MCD64 collections”. In: *International Journal of Applied Earth Observation and Geoinformation* 78, pp. 318–331.

Rosan, Thais M. et al. (2022). “Fragmentation-Driven Divergent Trends in Burned Area in Amazonia and Cerrado”. In: *Frontiers in Forests and Global Change* 5, p. 801408.

Santos, Filippe L.M. et al. (2021). “Prescribed Burning Reduces Large, High-Intensity Wildfires and Emissions in the Brazilian Savanna”. In: *Fire* 4.3, p. 56.

Setty, Shruti et al. (2023). “Loss of Earth system resilience during early Eocene transient global warming events”. In: *Science Advances* 9.14, eade5466.

Silva, P S, J A Rodrigues, et al. (2020). “Drivers of burned area patterns in Cerrado: the case of MATOPIBA region”. In: *2020 IEEE Latin American GRSS & ISPRS Remote Sensing Conference (LAGIRS)*.

Silva, Patrícia S., Ana Bastos, et al. (2019). “Impacts of the 1.5 °C global warming target on future burned area in the Brazilian Cerrado”. In: *Forest Ecology and Management* 446, pp. 193–203.

Silva, Patrícia S., Joana Nogueira, et al. (2021). “Putting fire on the map of Brazilian savanna ecoregions”. In: *Journal of Environmental Management* 296, p. 113098.

Silva Arruda, Vera Laísa da et al. (2024). “Assessing four decades of fire behavior dynamics in the Cerrado biome (1985 to 2022)”. In: *Fire Ecology* 20.1, p. 64.

Stevens, Nicola et al. (2017). “Savanna woody encroachment is widespread across three continents”. In: *Global Change Biology* 23.1, pp. 235–244.

Van Wilgen, BW et al. (2000). “A fire history of the savanna ecosystems in the Kruger National Park, South Africa, between 1941 and 1996”. In: *South African Journal of Science* 96.4. Publisher: Academy of Science for South Africa (ASSAf), pp. 167–178.

Werf, G. R. van der et al. (2017). “Global fire emissions estimates during 1997–2016”. In: *Earth System Science Data* 9.2, pp. 697–720.